ROLE OF UBIQUITIN-MODIFYING ENZYMES IN REGULATING THE ENDOTHELIAL RESPONSE TO VEGF-A

Gina Anne Smith

The University of Leeds

Faculty of Biological Sciences

2016

Submitted in accordance with the requirements for the degree of

Doctor of Philosophy

The candidate confirms that the work submitted is her own, except where work which has formed part of jointly-authored publications has been included. The contribution of the candidate and the other authors to this work has been explicitly indicated below. The candidate confirms that appropriate credit has been given within the thesis where reference has been made to the work of others.

A full list of publications arising from work within this thesis is provided in Appendix A. Copies of publications are provided as separate documents.

Specific contributions from others are as follows:

Dr. Gareth Fearnley (University of Leeds, UK) performed specific tubulogenesis assays relevant to this study (Chapter 3 and 5).

Izma Abdul Zani (University of Leeds, UK) performed specific immunofluorescence microscopy relevant to this study (Chapter 5).

This copy has been supplied on the understanding that it is copyright material and that no quotation from the thesis may be published without proper acknowledgement.

© 2015 The University of Leeds and Gina Anne Smith

ACKNOWLEDGEMENTS

ABSTRACT

Cell surface receptors undergo degradation but the biochemical basis for such control remains poorly defined. Endothelial cells express vascular endothelial growth factor receptor 2 (VEGFR2) which binds to circulating VEGF-A, stimulating signal transduction and new blood vessel sprouting i.e. angiogenesis. A central hypothesis is that ubiquitin-modifying enzymes play a key role(s) in the endothelial response to VEGF-A. Work presented in this thesis provides evidence for a novel pathway requiring the E1 ubiquitin-activating enzyme, UBA1, in controlling basal plasma membrane VEGFR2 levels. Evidence suggests that this ubiquitin-linked regulatory pathway controls VEGFR2 levels by modulating constitutive receptor recycling and degradation. Programming basal plasma membrane VEGFR2 levels influences the intensity and duration of the endothelial response to circulating ligands such as VEGF-A. After identification of an UBA1-dependent pathway for modulating VEGFR2 ubiquitination, the UBA1-interacting E2 ubiquitin-conjugating enzymes were screened. The E2 enzymes, UBE2D1 and UBE2D2, regulate basal VEGFR2 turnover downstream of UBA1. Another feature of regulating VEGFR2 ubiquitination involves a potential role for de-ubiquitinating enzymes (DUBs). There is evidence that a specific DUB enzyme, USP8, regulates VEGFR2 de-ubiquitination, trafficking, signal transduction and proteolysis. Depletion of USP8 caused VEGFR2 accumulation in early endosomes, perturbed VEGFR2 ubiquitination and impaired VEGF-A-stimulated signal transduction. In addition, de-ubiquitination is linked to production of a previously unidentified VEGFR2 cleavage product. Thus, controlling VEGFR2 de-ubiquitination has important consequences for the endothelial cell response and vascular physiology. VEGFR2 is the predominant receptor through which VEGF-A regulates pro-angiogenic signal transduction. Conversely, the role of VEGFR1 in endothelial cells is considered anti-angiogenic. Novel synthetic protein scaffolds called Adhirons were screened for interaction with VEGFR1 or VEGFR2. Adhirons to VEGFR2 inhibited VEGF-A-stimulated signal transduction and endothelial tube formation. In contrast, Adhirons to VEGFR1 increased VEGF-A-stimulated signal transduction, thus promoting increased tubulogenesis. These findings suggest that inhibition of VEGFR1 can stimulate pro-angiogenic responses. Adhirons represent a new class of synthetic tools with potential applications in medical diagnostics, disease therapy and biomarker profiling.

TABLE OF CONTENTS

LIST OF TABLES

LIST OF FIGURES

CHAPTER 4

CHAPTER 7

ABBREVIATIONS

AGE	Advanced glycation end-products
ALL	Acute lymphocytic leukaemia
AMD	Age-related macular degeneration
AML	Acute myeloid leukaemia
AMPK	AMP-activated protein kinase
AMSH	Associated molecule with the SH3 domain of STAM
ANG	Angiopoietin
AP-2	Adaptor protein 2
Apo	Apolipoprotein
ARF6	ADP ribosylation factor 6
ATF-2	Activating transcription factor 2
β_2AR	β_2-adrenergic receptor
BAD	Bcl-2-associated agonist of cell death
BCA	Bicinchoninic acid
Bcl-2	B-cell lymphoma-2
β-TrCP1	β-transducin repeat containing E3 ubiquitin protein ligase
BrdU	Bromodeoxyuridine
CAD	Coronary artery disease
CB1	Cannabinoid receptor
Cbl	Cas-Br-M murine ecotropic retroviral transforming sequence homologue
CCD	Catalytic cysteine domain
CCP	Clathrin-coated pit
CD2AP	CD2-associated protein
Cdc42	Cell division cycle 42
CDK1	Cyclin-dependent kinase 1

CHD	Coronary heart disease
CHX	Cycloheximide
CIN85	Cbl-interacting protein 85
COPD	Chronic obstructive pulmonary disease
CUE	Cue-1-homologous
DAB2	Disabled 2
DAG	Diacylglycerol
DAPI	4',6-diamidino-2-phenylindole
DARPin	Artificial ankyrin repeat protein
DAT	Dopamine transporter
DIUM	Di-ubiquitin motif
DLL4	Delta-like 4
DM	Diabetes mellitus
DUB	De-ubiquitinating enzyme
E6AP	E6-associated protein
ECM	Extracellular matrix
ECGM	Endothelial cell growth medium
EEA1	Early endosome antigen 1
EGF	Epidermal growth factor
EGFL7	EGF-like domain protein 7
EGFR	Epidermal growth factor receptor
eNOS	Endothelial nitric oxide synthase
Eps15	EGFR substrate 15
ERK1/2	Extracellular signal-regulated kinase 1/2
ESCRT	Endosomal sorting complex required for transport
FABP4	Fatty acid-binding protein 4
FAK	Focal adhesion kinase
FAO	Fatty acid oxidation

FAS	Fatty acid synthase
FATP	Fatty acid transporter proteins
FGF	Fibroblast growth factor
FGFR	Fibroblast growth factor receptor
G6PD	Glucose-6-phosphate dehydrogenase
GAP	GTPase-activating protein
GEF	Guanine nucleotide exchange factor
GLUT	Glucose transporter
GM-CSF	Granulocyte-macrophage colony-stimulating factor
GPCR	G-protein coupled receptor
Grb2	Growth factor receptor-bound protein 2
GSH	Reduced glutathione
HBP	Hexosamine biosynthesis pathway
HDAC	Histone deacetylase
HDMEC	Human dermal microvascular endothelial cell
HECT	Homologous to E6-AP C-terminus
HGF	Hepatocyte growth factor
HIF	Hypoxia-inducible factor
Hrs	Hepatocyte growth factor-regulated tyrosine kinase substrate
HSP	Heat shock protein
HSPG	Heparan sulphate glycoproteins
HUVEC	Human umbilical vein endothelial cell
ICAM	Intercellular adhesion molecule
Ig	Immunoglobulin
IP	Immunoprecipitate
IP_3	Inositol-1,4,5-trisphosphate
IP_3R	IP_3 receptor
$JAMM/MPN^+$	Jab1/MPN domain-associated metalloisopeptidase

KIF13B	Kinesin family member 13B
LDH-A	Lactate dehydrogenase-A
LDL	Low density lipoprotein
MAPK	Mitogen-activated protein kinase
MMP	Matrix metalloproteinase
MVB	Multivesicular bodies
NFκB	Nuclear factor κ B
NFAT	Nuclear factor of activated T-cells
NGF	Nerve growth factor
NK1R	Neurokinin-1 receptor
NO	Nitric oxide
NRARP	NOTCH-regulated ankyrin repeat protein
NRP	Neuropilin
oxPPP	Oxidative PPP
OTU	Ovarian tumour proteases
PAD	Peripheral arterial disease
PAI-1	Plasminogen activator inhibitor-1
PAK2	p21-activated protein kinase 2
PBS	Phosphate buffered saline
PDCL3	Phosducin-like 3
PDGF	Platelet-derived growth factor
PDGFR	Platelet-derived growth factor receptor
PDK1	Phosphoinositide-dependent protein kinase 1
PECAM1	Platelet/Endothelial Cell Adhesion Molecule 1
PFKFB3	Phosphofructokinase-2/fructose-2,6-bisphosphate
PGC	Peroxisome proliferator-activated receptor gamma co-activator
PHD	Prolyl hydroxylase
PI3K	Phosphoinositide-3-kinase

PIP$_2$	Phosphatidylinositol-4,5-bisphosphate
PKA	Protein kinase A
PKC	Protein kinase C
PLCγ1	Phospholipase Cγ1
PlGF	Placental growth factor
PPP	Pentose phosphate pathway
PSG	Pig skin gelatin
PTPN11	Protein tyrosine phosphatase non-receptor type 11
PTP	Protein tyrosine phosphatase
RAC1	Ras-related C3 botulinum toxin substrate 1
RACK	Receptor for activated C kinase 1
RAGE	Receptor for advanced glycation end-products
RBR	RING between RING
RCC	Renal cell carcinoma
RING	Really Interesting New Gene
ROS	Reactive oxygen species
RTK	Receptor tyrosine kinase
SH3	Src homology 3
Shb	SH2-domain-containing adaptor protein B
SHP2	SH2 domain-containing tyrosine phosphatase 2
SNARE	Soluble NSF attachment protein receptor
SOS	Son of Sevenless
STAM	Signal transducing adaptor molecule
SUMO	Small ubiquitin modifier
sVEGFR1	Soluble VEGFR1
sVEGFR2	Soluble VEGFR2
T2DM	Type II diabetes mellitus
TACE	TNFα converting enzyme

TfR	Transferrin receptor
TGF	Transforming growth factor
TIMPs	Tissue inhibitors of metalloproteinases
TKI	Tyrosine kinase inhibitor
TNFα	Tumour necrosis factor α
TrkA	Tropomyosin receptor kinase A
TSAd	T-cell-specific adaptor molecule
TSG101	Tumour susceptibility gene 101
UBA	Ubiquitin-associated domain
UBC	Ubiquitin-conjugating enzyme-like domain
UBD	Ubiquitin-binding domain
UBL	Ubiquitin-like proteins
UBP	Ubiquitin-specific protease
UCH	Ubiquitin C-terminal hydrolases
UEV	Ubiquitin E2 variant
Ufd	Ubiquitin-fold domain
UIM	Ubiquitin-interacting motif
uPA	Urinary-type plasminogen activator
USP	Ubiquitin-specific protease
USP8	Ubiquitin-specific protease Y
VCAM-1	Vascular endothelial cell adhesion molecule 1
VE-cadherin	Vascular endothelial cadherin
VEGF	Vascular endothelial growth factor
VEGFR	Vascular endothelial growth factor receptor
VE-PTP	Vascular endothelial protein tyrosine phosphatase
VHL	Von-Hippel Lindau
WCL	Whole cell lysate

CHAPTER 1

INTRODUCTION

1.1. Angiogenesis and the vascular endothelium

1.1.1. A brief history of angiogenesis

Ancient Egyptian and Greek medicine acknowledged the existence of a vascular network in humans. The Greek physician, Galen, identified differences between venous and arterial blood in the 2nd century AD (Aird, 2011). Not until 1628 did the British physician William Harvey propose that the heart pumps blood through a circulatory system with direct connections between arteries and veins (Aird, 2011). The capillary network was discovered in 1661 by Italian physician Marcello Malpighi and the endothelial cell component of the vascular system identified in 1865 by Wilhelm His Sr. (Aird, 2011, Loukas et al., 2008).

Angiogenesis as a contributing factor to malignant tumour growth was first proposed by Judah Folkman in the 1970's (Folkman, 1971). His work led to the development of angiogenesis inhibitors for cancer treatment. Over a decade later, Napoleone Ferrara cloned and characterised vascular endothelial growth factor (VEGF) for its ability to induce *in vivo* angiogenesis (Leung et al., 1989). In 1996, the first clinical trial using VEGF for the treatment of critical limb ischaemia was published by Jeffery Isner (Isner et al., 1996). Today, researchers are actively developing therapeutic agents to stimulate angiogenesis in the brain, heart and peripheral vasculature.

1.1.2. Building a vascular network

In the developing mammalian embryo, blood vessels provide oxygen and the trophic signals required to instruct organ morphogenesis (Coultas et al., 2005). Endothelial precursors (angioblasts) differentiate into endothelial cells and assemble into a primitive vascular plexus of small capillaries in a process known as vasculogenesis. These cells already have a genetically pre-programmed arterial or venous cell fate. The earliest marker for endothelial and haematopoietic progenitors is VEGF receptor 2 (VEGFR2),

the major receptor for VEGF-A (Coultas et al., 2005). VEGFR2 is essential for healthy mammalian development as homozygous $VEGFR2^{-/-}$ knockout mice die at embryonic day E8.5, exhibiting impaired haematopoietic and endothelial cell development and formation of an insufficient vascular network (Shalaby et al., 1995). This mimics the $VEGFA^{-/-}$ knockout mouse phenotype suggesting that VEGF-A signal transduction is also essential for development of both systems (Carmeliet et al., 1996) (Table 1.1). In addition, correct $VEGFA$ gene dosage is essential for normal mammalian health and development. Heterozygous $VEGFA^{+/-}$ knockout mice die between embryonic days E11 and E12 due to a deformed vascular network (Carmeliet et al., 1996, Ferrara et al., 1996).

Vessel sprouting, migration and remodelling progressively expand the vascular plexus into a highly organised vascular network of larger vessels, creating functional circulation in a process known as angiogenesis. Recruited pericytes and vascular smooth muscle cells cover nascent endothelial cell channels during arteriogenesis to regulate vessel perfusion and provide vessel strength. Genetic studies have revealed insights into the key regulators and mechanisms of embryonic angiogenesis. For example, the receptor COUP-TFII regulates venous specification whilst NOTCH family members drive the arterial gene programme. VEGF is a key regulator of vascular endothelial cell sprouting, whilst angiopoietin (ANG)-1 and platelet-derived growth factor (PDGF)-BB recruit mural cells to cover endothelial channels (Carmeliet, 2005). The requirement for a precise balance of stimulatory and inhibitory signals, such as angiopoietins, chemokines, integrins, oxygen sensors, junctional molecules and endogenous inhibitors highlights the complexity of angiogenesis.

1.1.3. Vascular development

The characterisation of vascular-mutant phenotypes in mice has advanced our understanding of normal vascular development. Embryonic phenotypes that fail to develop different aspects of normal vasculature have been reported for defective VEGF/VEGFR, ANG/Tie, PDGF, transforming growth factor-β (TGF-β), ephrin and NOTCH systems (Coultas et al., 2005). During neoangiogenesis in tumour tissue, many of these signalling pathways are re-activated (Bikfalvi and Bicknell, 2002). A healthy adult vasculature contains quiescent endothelial cells that are arrested in G_0 of the cell

Genotype	Phenotype
VEGF-A$^{+/-}$	Die at E11/12 – impaired angiogenesis & blood-island formation/deformed vascular network
VEGF-A$^{-/-}$	Die at E8.5 – impaired haematopoietic and endothelial cell development and formation of an insufficient vascular network
VEGF-B$^{-/-}$	No overt vascular defects – smaller hearts, abnormal cardiac contraction
VEGF-C$^{-/-}$	Embryonically lethal - absence of lymphatic vessel formation, no vascular defects
VEGF-D$^{-/-}$	Same as VEGF-C$^{-/-}$
VEGFR1$^{-/-}$	Die at E8.5-E9.5 – vessel obstruction due to endothelial cell hyperproliferation
VEGFR1-TK$^{-/-}$	Normal blood vessel formation however defects in VEGF-A-dependent macrophage migration
VEGFR2$^{-/-}$	Die at E8.5 – impaired haematopoietic and endothelial cell development and formation of an insufficient vascular network
VEGFR2-Y1173 → F	Same as VEGFR2$^{-/-}$
VEGFR2-Y1214 → F	No obvious phenotype
VEGFR3$^{-/-}$	Die at E10.5 - impaired hierarchical formation of peripheral blood vasculature
VEGFR3-TK$^{-/-}$	Normal blood vessel development but impaired lymphatic development

Table 1.1. VEGFR-VEGF murine models and phenotypes. Information taken from Fong et al., 1995, Carmeliet et al., 1996, Dumont et al., 1998, Zhang et al., 2010, Shibuya, 2014.

cycle, have long half-lives and are protected against overexposure to the autocrine action of maintenance signals such as NOTCH, VEGF, fibroblast growth factors (FGFs) and ANG-1 (Carmeliet and Jain, 2011, Lampugnani and Dejana, 2007). Endothelial cells are equipped with oxygen sensors and hypoxia-inducible factors (HIFs). These enable vessels to fulfil their role as oxygen suppliers, allowing adjustments in vessel shape to optimise blood flow. Quiescent endothelial cells form a monolayer of phalanx cells interconnected by junctional molecules such as claudins and vascular endothelial-cadherin (VE-cadherin). Pericytes coat the endothelial cell layer to supress cell proliferation whilst secreting survival signals such as ANG-1 and VEGF to form a common basement membrane and promote vessel tightness. In the confluent endothelium, ANG-1 binds to its receptor, TIE-2, and induces TIE-2 clustering at cell-cell junctions to maintain quiescence (Saharinen et al., 2008) (Fig. 1.1). Contrastingly, ANG-2 binds TIE-2 to competitively antagonise ANG-1 signalling, enhancing mural cell detachment, vascular permeability and tubulogenesis. Upon sensing an angiogenic signal such as ANG-2, secreted by hypoxic, inflammatory or tumour cells, pericytes detach from the quiescent vessel wall and become liberated from the basement membrane by matrix metalloproteinase (MMP)-mediated proteolysis. Endothelial cell junctions are loosened and the nascent vessel dilates (Carmeliet and Jain, 2011) (Fig. 1.1).

Permeability of the endothelial cell layer is increased by VEGF-induced loosening of adherens junctions (endothelial cadherin complexes and cell adhesion molecules such as platelet/endothelial cell adhesion molecule-1 (PECAM-1)), causing plasma proteins to extravasate and lay down a provisional extracellular matrix (ECM) scaffold. Integrin signalling promotes endothelial cell migration onto the ECM. Angiogenic molecules such as VEGF and FGF are liberated from the ECM by proteases, creating a pro-angiogenic environment. To prevent excess endothelial cell chemotaxis towards the angiogenic signal and to build a perfuse tube, one endothelial cell i.e. the tip cell is selected to lead the vascular sprout upon expression of VEGFRs, neuropilins (NRPs) and the NOTCH ligands (delta-like 4 (DLL4) and Jagged1). Following VEGF-A stimulation, VEGFR2 upregulates DLL4 expression to dictate tip cell specification. DLL4 activates NOTCH in neighbouring stalk cells to down-regulate VEGFR2 and upregulate VEGFR1 levels (Fig. 1.2). Thus, these stalk cells become less responsive to VEGF-A but more sensitive to placental growth factor (PlGF) (Carmeliet and Jain,

2011). As cells meet new neighbours these signalling pathways are constantly re-evaluated - endothelial cells continuously compete for tip cell selection by fine tuning VEGFR1 versus VEGFR2 expression (Jakobsson et al., 2010). Another NOTCH ligand, Jagged1, is pro-angiogenic and opposes DLL4 activity. Jagged1 is expressed by stalk cells and promotes tip cell specification by down-regulating reciprocal NOTCH-DLL4 signalling in the adjacent tip cell (Benedito et al., 2009) (Fig. 1.2). Jagged1 also antagonises NOTCH-DLL4 signalling between stalk cells, facilitating sufficient VEGFR expression in the immature vascular plexus and sustaining responsiveness to VEGF, promoting proliferation and the dynamic emergence of new tip cells (Benedito et al., 2009) (Fig. 1.1). Furthermore, NOTCH signalling in stalk cells upregulates a NOTCH inhibitor, NOTCH-regulated ankyrin repeat protein (NRARP), in a negative feedback cycle (Phng et al., 2009). NOTCH, Wnts, FGF and PlGF stimulate neighbouring stalk cells to divide and elongate the stalk. A lumen is established through VEGF, VE-cadherin, CD34 and Hedgehog signalling. Filopodia on tip cells sense environmental guidance cues such as ephrins and semaphorins. In addition, release of EGF-like domain protein 7 (EGFL7) by stalk cells into the ECM conveys positional information about neighbouring cells so that the stalk elongates correctly (Carmeliet and Jain, 2011) (Fig. 1.1). Myeloid bridge cells assist fusion with an adjacent vessel branch, initiating blood flow in a process termed anastomosis. The vessel matures when endothelial cells resume there quiescent phalanx state i.e. when oxygen levels are sufficient to reduce expression of pro-angiogenic factors. Signals such as PDGF-B, ANG-1, ephrin-B2, NOTCH and TGF-β promote pericyte coverage. Protease inhibitors such as tissue inhibitors of metalloproteinases (TIMPs) and plasminogen activator inhibitor-1 (PAI-1) promote basement membrane deposition and re-establishment of junctions for optimal flow (Carmeliet and Jain, 2011).

HIF-1α drives a hypoxia-inducible program that renders endothelial cells responsive to angiogenic signals. Prolyl hydroxylase domain (PHD) proteins are oxygen sensors that hydroxylate HIF proteins when sufficient oxygen is available. Hydroxylated HIFs are targeted for proteasomal degradation (Majmundar et al., 2010). During hypoxia, PHDs are inactive and HIFs initiate transcriptional responses including upregulation of angiogenic factors such as VEGF (Fraisl et al., 2009). In pathophysiological conditions such as cancer, HIFs can be activated under normoxia by oncogenes and growth factors,

protecting tumour cells from oxygen deprivation. Whereas HIF-1α activity promotes vessel sprouting, HIF-2α regulates vascular maintenance (Fraisl et al., 2009). Interestingly, hypoxia-induced upregulation of VEGF can occur independently of HIF-1α. Under these circumstances, the metabolic regulator, peroxisome proliferator-activated receptor gamma co-activator (PGC)-1α, upregulates VEGF levels in preparation for oxidative metabolism after revascularisation of ischaemic tissues (Arany et al., 2008).

1.1.4. The vascular endothelium

An endothelial cell monolayer forms the vascular endothelium and lines the lumen of all blood vessels. This layer is both exposed to the bloodstream and in contact with the basement membrane and underlying tissue. Thus, the endothelium is vital for regulating blood pressure, thrombosis, permeability, immune function and haemostasis. The endothelium performs such a diverse array of functions by expressing a range of growth factors, hormones, regulatory molecules and their cognate receptors (Onat et al., 2011). The quiescent endothelial cell monolayer remains contact-inhibited due to the unique presence of VE-cadherin-enriched adherens junctions between cells (Dejana et al., 2008). In addition, capillaries in regions of strict transcellular control such as those forming the blood-brain barrier possess 'tight' junctions formed by claudin and cadherin bridges. Together, these adhesive intercellular junctions promote endothelial cell adhesion, contact inhibition, vessel permeability, maintenance of cell polarity, cell growth and survival. Adherens junctions are also essential for correct organisation of new vessels during embryo development and during adult tissue proliferation (Dejana et al., 2008). During angiogenesis or subconfluency, endothelial cells are in a proliferative state which is responsive to growth factor stimulation. Upon reaching confluence, these elongated cells take on characteristic cobblestone morphology. In this state, highly organised cell-cell junctions lose their ability to respond to growth factor and switch to a survival over proliferative phenotype. Vascular damage disrupts cell junctions, causing a switch to an active phenotype which promotes cell proliferation and migration in the wound (Odell et al., 2012). By regulating cell permeability, adherens junctions respond to endogenous growth factors such as VEGF. Upon exposure to VEGF, tyrosine phosphorylation of VE-cadherin increases vascular permeability and leukocyte diapedesis (Dejana et al., 2008).
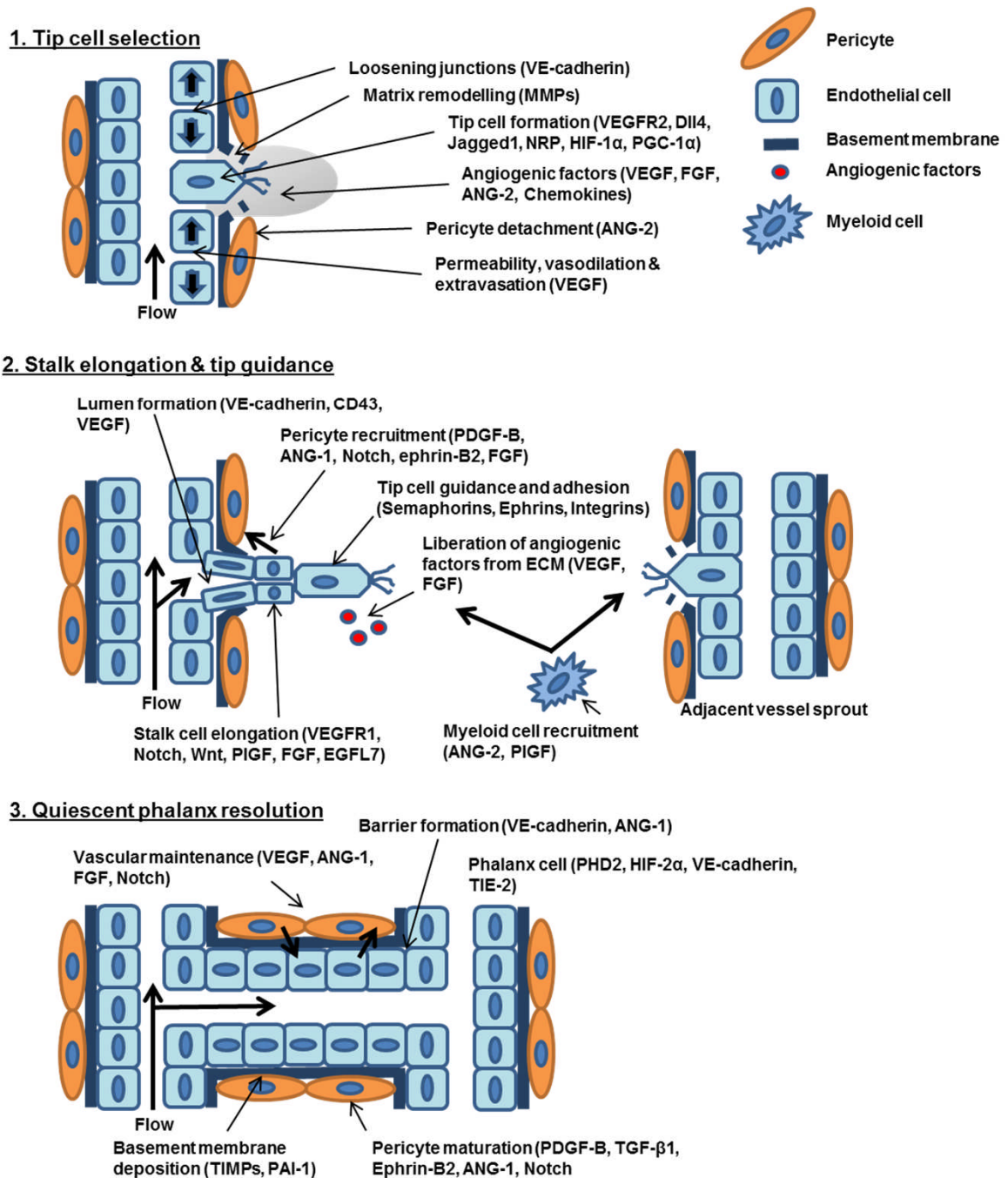
Figure 1.1. Model of angiogenesis. During angiogenesis tip cell selection, vessel branching and vessel quiescence occur consecutively. (1) In the presence of angiogenic factors, endothelial tip cell specification requires breakdown of the basement membrane, loosening of cell-cell junctions and pericyte detachment. (2) Tip cells migrate towards guidance signals, stalk cells proliferate and a lumen is formed. Myeloid cells secrete additional angiogenic factors and provide a bridge to aid fusion with a neighbouring vessel. (3) Lumen formation enables perfusion of the new vessel. Quiescence is resolved by basement membrane deposition, pericyte maturation and re-establishment of adherens junctions. Adapted from Carmeliet and Jain (2011).
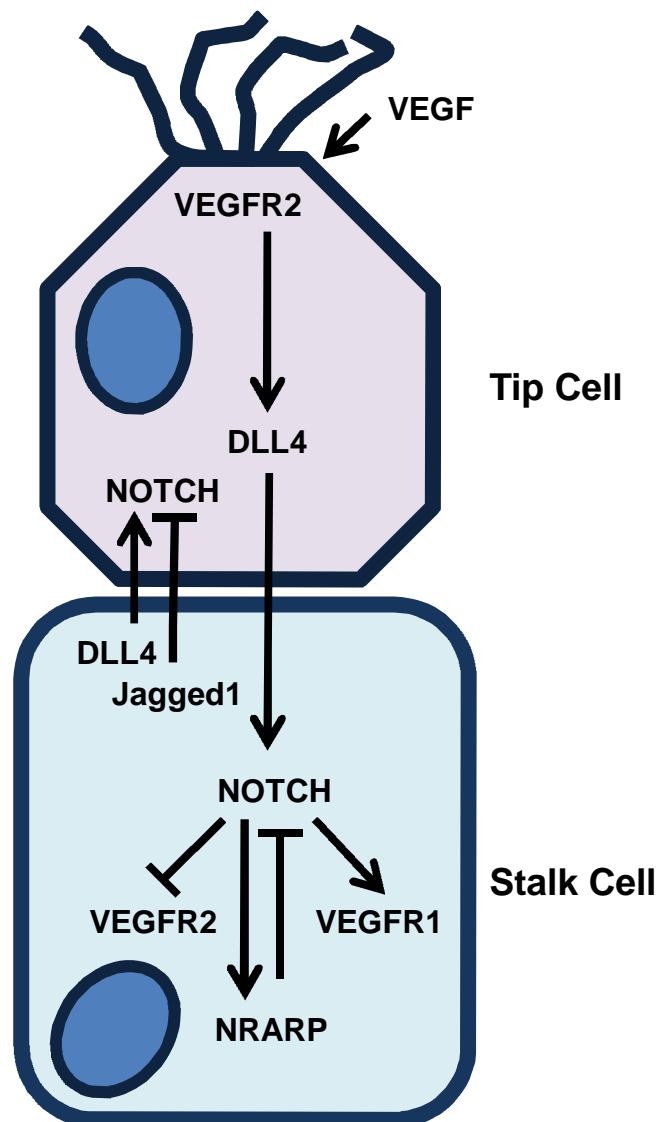
Figure 1.2. NOTCH signalling dictates endothelial tip cell specification. Cells exposed to the highest concentration of VEGF-A elevate expression of the NOTCH ligand, DLL4. In neighbouring stalk cells, DLL4 activates NOTCH to downregulate VEGFR2 expression. These stalk cells also express the DLL4 antagonist, Jagged1, which inhibits DLL4-mediated NOTCH activation in the tip cell, leading to upregulated VEGFR2 expression and increased chemotactic responsiveness to exogenous VEGF-A. The overall effect is reduced branching but generation of perfuse vessels. Adapted from Adams and Eichmann (2010).

1.1.5. Adult blood vessels and disease

Blood vessels evolved for the transport of haematopoietic cells to supply oxygen and nutrients, to dispose of waste and for immune surveillance. Although fundamental for tissue growth and regeneration, angiogenesis is associated with a plethora of diseases.

During adulthood, most blood vessels remain quiescent however endothelial cells retain their ability to rapidly proliferate in response to physiological stimuli such as hypoxia. Neovascularisation in response to tissue damage is a key component of wound healing. In diseases in which this stimulus becomes abnormal, the balance between stimulators and inhibitors is skewed, resulting in an angiogenic switch. Excessive angiogenesis occurs in disorders characterised by abnormal vascular growth and remodelling such as ocular, malignant and inflammatory disorders, obesity, diabetes, multiple sclerosis, asthma and endometriosis (Folkman, 2007). Contrastingly, insufficient angiogenesis is associated with stroke, neurodegeneration, ischaemic heart disease and preeclampsia, linked to vessel regression or malformation, endothelial cell dysfunction and inhibited revascularisation (Carmeliet, 2005). Cardiovascular disease covers all diseases of the heart and circulation, including stroke, heart disease, heart failure, atrial fibrillation and cardiomyopathy and is responsible for more than a quarter of all deaths in the UK (about 425 people per day). Within this category, coronary heart disease (CHD) is the UK's single biggest killer and the leading cause of death worldwide (https://www.bhf.org.uk/.../heart-statistics/cardiovascular-disease-statistics). CHD is characterised by blocked blood supply to the heart caused by atherosclerosis. Thus, it is desirable to develop pro-angiogenic drugs as high impact therapies to promote tissue regeneration in cardiovascular disease. Conversely, anti-angiogenic therapeutic agents could be beneficial for treatment of malignant diseases associated with excessive angiogenesis.

Adult tissues can become vascularised by alternative mechanisms to neovascularisation. In cancer, vessel co-option involves tumour cells hijacking the existing vasculature in a process called vessel mimicry (Carmeliet and Jain, 2011). Additionally, cancer stem-like cells can generate a tumour endothelium (Wang et al., 2010b).

1.2. Vascular endothelial growth factors (VEGFs)

1.2.1 The VEGF family

The VEGF superfamily and its cognate receptors are highly conserved in metazoan species (Ponnambalam and Alberghina, 2011). Many of the VEGF genes play essential roles in animal development and function. However, a recurring theme is the subversion of VEGF ligand and receptor function in a range of pathologies including cancer, atherosclerosis, age-related macular degeneration and pre-eclampsia.

The VEGF superfamily consists of five structurally-related members of angiogenic and lymphangiogenic polypeptides: VEGF-A, VEGF-B, VEGF-C, VEGF-D and PlGF (Fig. 1.3). These growth factors are highly conserved with subtle differences in the distribution of charged residues determining receptor binding specificity (Fig. 1.4). VEGFs regulate blood and lymph vessel development in an isoform-specific manner through activation of receptor tyrosine kinases VEGFR1 (Flt-1), VEGFR2 (KDR) and VEGFR3 (Flt-4) (Roskoski, 2007). VEGF polypeptides form homodimers but heterodimers of VEGF-A and PlGF also occur naturally (DiSalvo et al., 1995). Complexity in the VEGF family is heightened by alternative splicing of VEGF-A, VEGF-B and PlGF and proteolytic processing of VEGF-C and VEGF-D. This allows multiple protein isoforms with distinct receptor and extracellular matrix binding properties to be encoded by a single gene (Ferrara, 2010).

The human *VEGFA* gene encodes a pre-mRNA with at least 8 exons and 7 introns (Robinson and Stringer, 2001). Alternative RNA splicing produces at least 7 pro-angiogenic isoforms of human VEGF-A which encode polypeptides of 121, 145, 148, 165, 183, 189 or 206 residues (a isoforms) and 5 anti-angiogenic isoforms of 121, 145, 165, 183 and 189 residues denoted VEGF-A$_{xxxb}$ (Fig. 1.5). Recent work has shown that *VEGFA* mRNA also undergoes programmed translational read-through to generate an anti-angiogenic VEGF-A$_x$ isoform containing a unique 22 amino acid C-terminal extension (Eswarappa et al., 2014). Each VEGF-A isoform contains exons 1-5 which encode the signal sequence (exon 1), N-terminus dimerisation domain (exon 2), VEGFR1-binding and N-glycosylation site (exon 3), VEGFR2-binding site (exon 4) and a plasmin cleavage site (exon 5) (Fig. 1.5). Exons 6a, 6b, 7a and 7b encode the heparin-
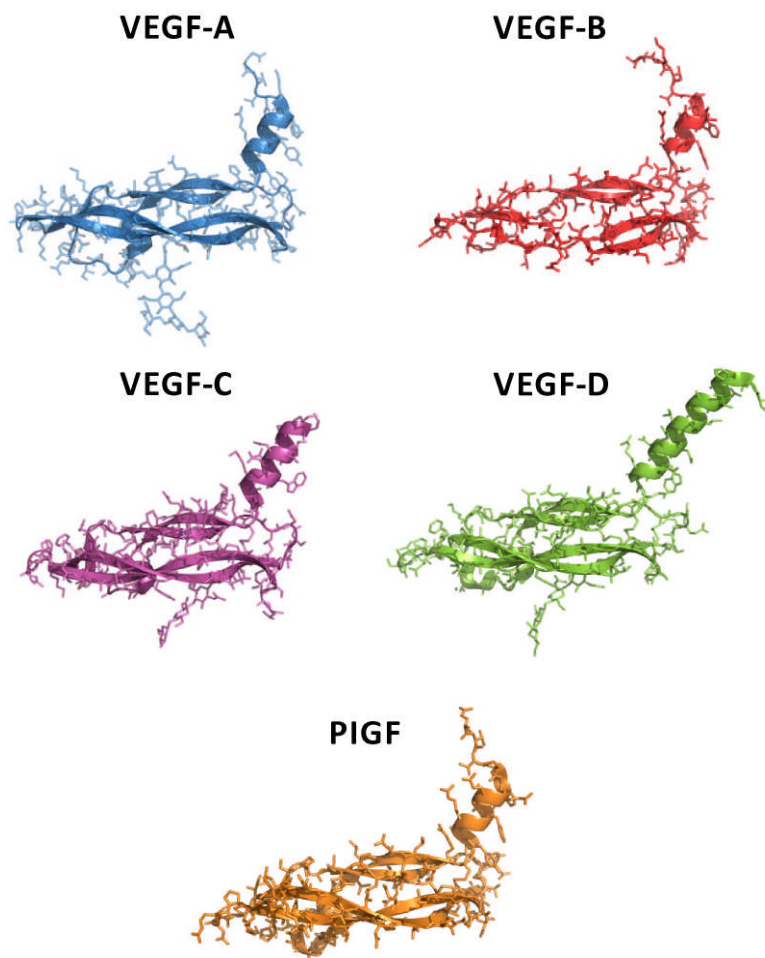
Figure 1.3. *In silico* **modelling of VEGF proteins.** Ribbon and stick diagrams depicting the structure of receptor bound VEGF-A (PDB id: 4KZN), VEGF-B (PDB id: 2XAC), VEGF-C (PDB id: 2X1W), VEGF-D (PDB id: 2XV7) and PlGF (PBD id: 1RV6). Taken from Smith et al. (2015).
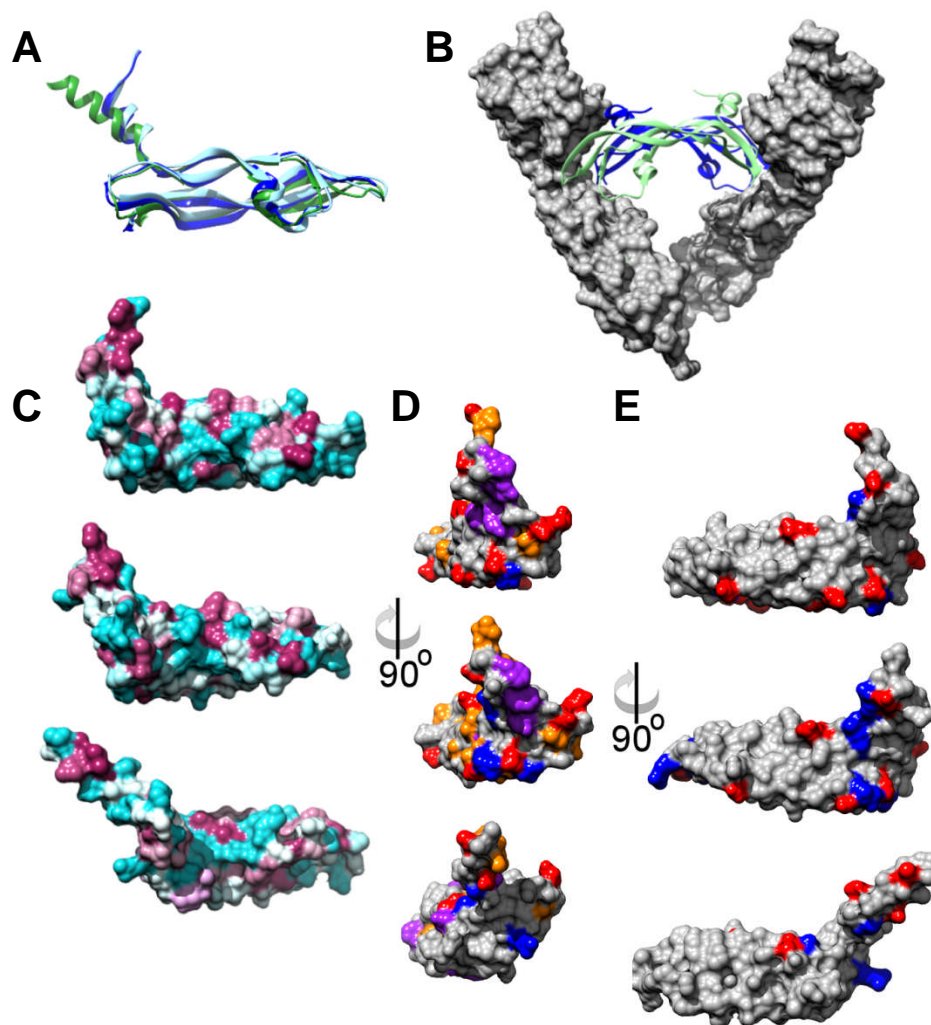
Figure 1.4. Structural differences between VEGF-A, PlGF and VEGF-C influence VEGFR binding. (A) Ribbon diagram depicting the structural similarities between VEGF-A (blue) (PDB id: **3V2A**), PlGF (green) (PDB id: **1RV6**) and VEGF-C (cyan) (PDB id: **4BSK**). (B) A model of VEGF-A binding to VEGFR2 using the PlGF dimer as a template for VEGF-A binding to the Ig-like domains. (C) Structures of VEGF-A (top), PlGF (middle) and VEGF-C (bottom) reveal that although the fundamental fold is similar, the distribution of hydrophobic (purple) and polar (cyan) residues highlights differences between VEGFR1-binding ligands, VEGF-A and PlGF, and VEGFR3-binding ligand, VEGF-C. (D) Structures of VEGF-A (top), PlGF (middle) and VEGF-C (bottom) rotated 90° with positive (blue), negative (red), aliphatic (yellow) and aromatic (purple) residues highlighted. (E) Structures of VEGF-A (top), PlGF (middle) and VEGF-C (bottom) rotated 90° with positive (blue) and negative (red) residues highlighted. Taken from Smith et al. (2015).

12
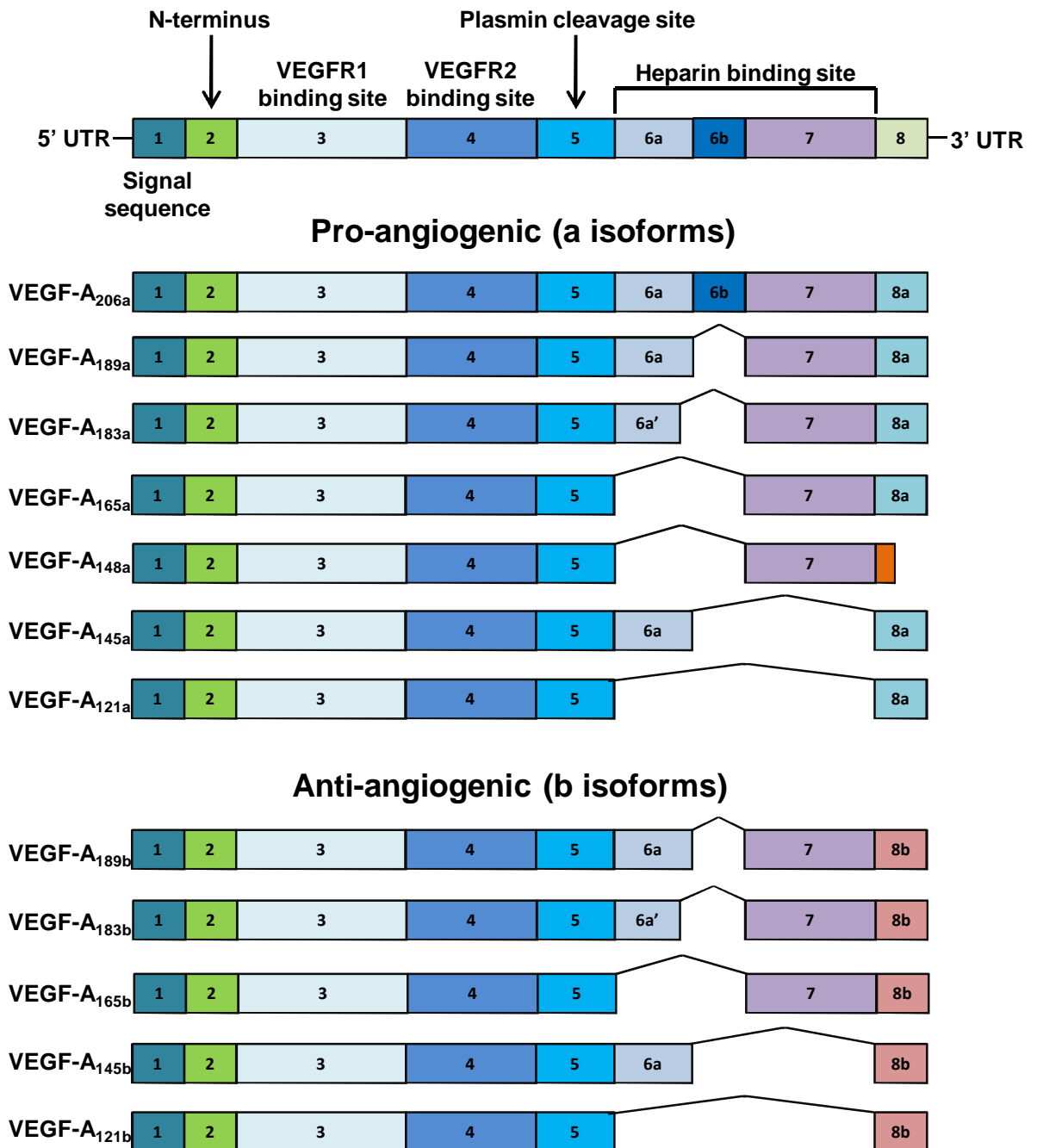
Figure 1.5. Exon arrangement of VEGF-A splice isoforms. The *VEGFA* gene encodes a pre-mRNA with at least 8 exons. Alternative RNA splicing produces at least 7 pro-angiogenic isoforms of human VEGF-A which encode polypeptides of 121, 145, 148, 165, 183, 189 or 206 residues (a isoforms) and 5 anti-angiogenic isoforms of 121, 145, 165, 183 and 189 residues denoted VEGF-A$_{xxxb}$. A premature stop codon causes truncation of VEGF-A$_{148}$ (orange). Exon 6a can also be truncated (6a'). Adapted from Fearnley et al. (2013).

binding domain and their variable inclusion significantly influences the biological properties of each VEGF-A isoform (Fig. 1.5). Those isoforms containing exon 6a such as VEGF-A$_{145}$ and VEGF-A$_{189}$ are weaker chemotactic cytokines and mitogens (Lee et al., 2010, Kawamura et al., 2008, Plouet et al., 1997). Exon 6a has a preponderance of basic amino acids which directly reduce VEGFR2-VEGF-A binding (Jia et al., 2001). Interestingly, exon 6-containing isoforms do not inhibit VEGF-A-stimulated VEGFR1 activity and can promote VEGFR1-mediated vascular permeability (Plouet et al., 1997, Ancelin et al., 2002).

Signal transduction is linked to regulating proximal and distal splice site selection on the primary RNA e.g. specifying the C-terminal 6 amino acids with either the pro-angiogenic CDKPRR (exon 8a) or anti-angiogenic SLTRKD (exon 8b) sequence (Harper and Bates, 2008). Reduced co-receptor binding could explain the anti-angiogenic properties of VEGF-A$_{165b}$ in combination with competition between VEGF-A$_{165b}$ and pro-angiogenic VEGF-A$_{165a}$ for binding to VEGFR2 (Harper and Bates, 2008, Kawamura et al., 2008). The C-terminal SLTRKD sequence in the anti-angiogenic VEGF-A$_{165b}$ isoform cannot bind the co-receptor, NRP1, leading to a VEGFR2 protein complex which exhibits reduced tyrosine kinase activity (Harper and Bates, 2008). Down-regulated VEGF-A$_{165b}$ expression correlates with a switch to a pro-angiogenic phenotype associated with multiple pathologies including diabetic retinopathy and several adult epithelial cancers (Perrin et al., 2005, Varey et al., 2008). Conversely, upregulated VEGF-A$_{165b}$ expression in skin and circulatory tissues of patients with systemic sclerosis or peripheral arterial disease hinders angiogenesis and vascular repair (Manetti et al., 2010).

Human *VEGFB* contains 7 exons and encodes at least 2 isoforms with alternative splice acceptor sites present in exon 6 (Olofsson et al., 1996, Grimmond et al., 1996). The VEGF-B$_{167}$ C-terminus contains the highly basic NRP1/heparin-binding domain whereas the more freely diffusible VEGF-B$_{186}$ isoform has a hydrophobic C-terminus which undergoes *O*-linked glycosylation and proteolytic processing (Olofsson et al., 1996). Within the VEGF family, VEGF-C and VEGF-D are unique in being initially synthesised as precursor proteins containing long N- and C-terminal propeptides (Joukov et al., 1997, Achen et al., 1998). Proteolytic removal of both the N- and C-propeptides releases mature, bioactive VEGF-D containing the central VEGF-homology

domain. Such processing increases VEGF-D affinity for VEGFR3. Furthermore, only mature VEGF-D binds VEGFR2 (Stacker et al., 1999). Although two mouse VEGF-D isoforms have been described, little is known about alternate RNA splicing of human VEGF-C or VEGF-D (Baldwin et al., 2001).

Four PlGF isoforms with distinct properties are encoded by the *PGF* gene. The most commonly expressed isoforms are PlGF-1 (131 amino acids) and PlGF-2 (152 amino acids) (Maglione et al., 1993). The PlGF-2 exon 6 heparin-binding domain facilitates binding to heparin and NRP1. Contrastingly, PlGF-1 and PlGF-3 (203 amino acids) do not contain exon 6 (Maglione et al., 1991). PlGF-3 contains an additional 216 nucleotide insertion between exons 4 and 5. PlGF-4 (224 amino acids) consists of the same sequence as PlGF-3 plus the exon 6-encoded heparin-binding domain (Holmes and Zachary, 2005). These larger PlGF isoforms may function similarly to VEGF-A$_{189}$ and VEGF-A$_{206}$ (Holmes and Zachary, 2005).

1.2.2. VEGF-receptor interactions

VEGFs bind to the extracellular domain of VEGFRs and additional cell surface-expressed co-receptors e.g. heparan sulphate glycoproteins (HSPGs), NRPs, integrins and ephrin B2 (Grunewald et al., 2010, Sawamiphak et al., 2010). PlGF and VEGF-B specifically bind VEGFR1 and NRP1 while VEGF-A binds both VEGFR1 and VEGFR2 (Errico et al., 2004, Olofsson et al., 1998, Makinen et al., 1999). VEGF-C and VEGF-D bind VEGFR2 and VEGFR3 (Takahashi and Shibuya, 2005) (Fig. 1.6). Distinct splice variants of VEGF-A assemble specific receptor/co-receptor complexes. Spatial and temporal aspects of VEGFR signal transduction can be influenced by the restricted diffusion of heparan sulphate (HS)-binding VEGFs and is further modulated by VEGF interactions with the ECM (Koch et al., 2011). Binding of VEGF-A$_{165a}$ and VEGF-A$_{189}$ to HSPGs and NRP1 promotes ternary complex formation and VEGFR2 signal transduction. NRP1 binding to VEGF-A$_{165a}$ enhances VEGFR2-VEGF-A$_{165a}$ complex formation and tyrosine kinase activity. For example, optimal p38 mitogen-activated protein kinase (MAPK) activation is achieved through NRP1-enhanced VEGF-A$_{165a}$ signal transduction (Kawamura et al., 2008). In contrast, VEGF-A$_{121}$ is freely diffusible and NRP1 binding does not promote ternary complex formation with VEGFR2, reducing signal transduction (Pan et al., 2007). Despite PlGF only binding
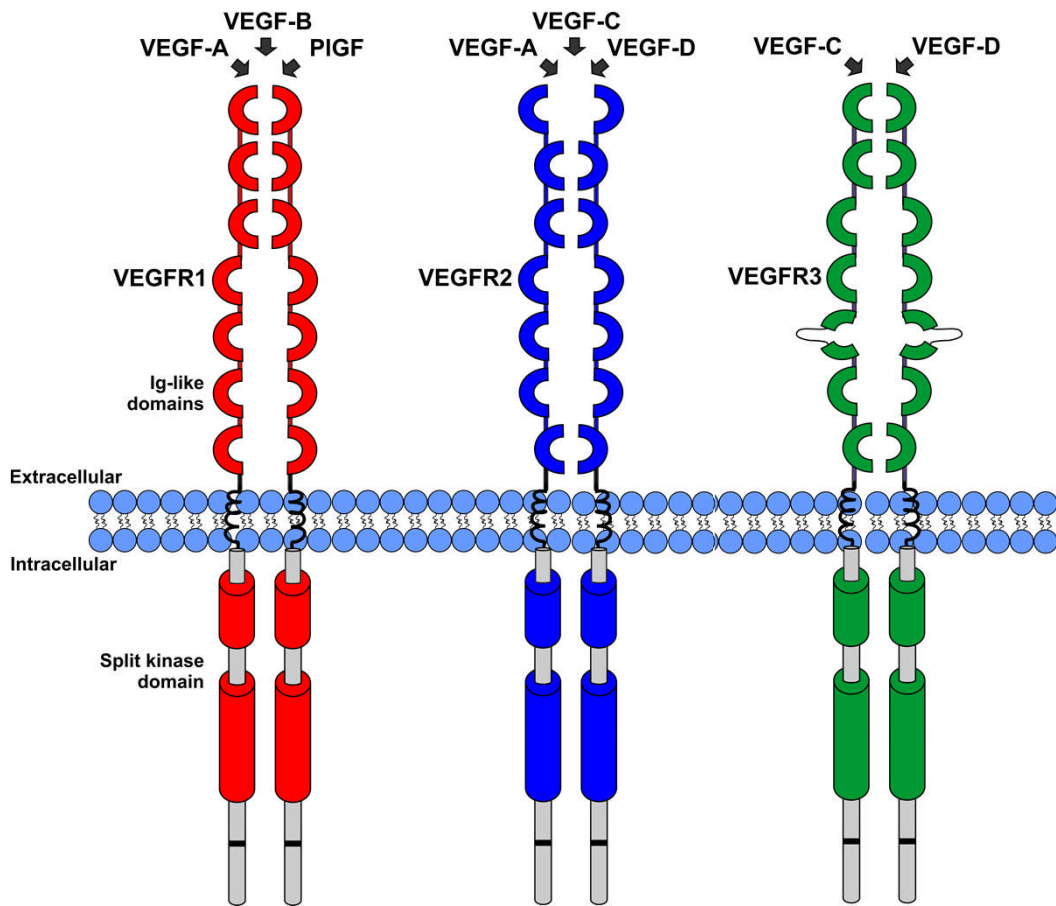
Figure 1.6. The VEGFR receptor tyrosine kinase subfamily. Schematic illustrating VEGFR structure and VEGF ligand specificity. Ig-like domains mediate interaction between VEGFR monomers to promote complex assembly. Adapted from Smith et al. (2015).

VEGFR1, activation of VEGFR2 could occur indirectly through VEGF-A displacement from VEGFR1, thus increasing VEGF-A bioavailability for VEGFR2 (Carmeliet et al., 2001). Interestingly, PlGF/VEGF-A heterodimers can induce VEGFR1/VEGFR2 dimerisation and downstream VEGFR2 activation (Tarallo et al., 2010).

The widely differing function of VEGFR1-specific ligands, VEGF-B and PlGF, raises the possibility that VEGFR1-induced cellular outcomes are regulated by co-receptor recruitment and/or cell-specific intracellular signalling events (Koch and Claesson-Welsh, 2012). VEGF-B-stimulated fatty acid synthesis in endothelial cells is crucial in organs which experience high metabolic stress, such as the heart, and involves both VEGFR1 and NRP1 activation (Hagberg et al., 2010). Therapeutic potential is highlighted in cardiac endothelial cells where VEGF-B promotes physiological angiogenesis and revascularisation of the ischaemic myocardium (Li et al., 2008b). In contrast, PlGF expression is associated with cancer progression and required for inflammation-associated angiogenesis (Carmeliet et al., 2001). PlGF promotes pathological angiogenesis in several inflammatory disease states in which VEGFR1-regulated recruitment of bone marrow-derived monocytes precedes deposition of angiogenic growth factors (Carmeliet et al., 2001). Tumours exhibiting increased PlGF secretion suggest a functional link between VEGFR1 activity and cancer progression.

1.3. Vascular endothelial growth factor receptors (VEGFRs)

The receptor tyrosine kinase (RTK) subfamily containing membrane-bound VEGFRs comprises of VEGFR1, VEGFR2 and VEGFR3. VEGFRs exhibit structural and sequence homologies and comprise an extracellular ligand-binding domain consisting of 7 immunoglobulin (Ig)-like repeats, a transmembrane domain, a juxtamembrane domain, a split tyrosine kinase domain and a C-terminal tail.

1.3.1. VEGFR1

The *VEGFR1* gene contains 30 exons and encodes an estimated 151 kDa transmembrane receptor which undergoes post-translational modification to produce a ~180 kDa mature glycoprotein (Kendall and Thomas, 1993, Devries et al., 1992). VEGF-A has highest affinity for VEGFR1 (Devries et al., 1992) but the activated receptor exhibits relatively weak tyrosine kinase activity and forms a non-productive

signalling complex (Robinson and Stringer, 2001, Waltenberger et al., 1994). The poor tyrosine kinase activity of VEGFR1 arises from structural properties of the activation loop, a repressor sequence in its juxtamembrane domain and a lack of positive regulatory tyrosine residues (Gille et al., 2000, Meyer et al., 2006, Ito et al., 1998). VEGFR1 is expressed in various cell types including both quiescent and actively proliferating endothelial cells, haematopoietic stem cells, monocytes, macrophages and tumour cells (Roskoski, 2007, Koch and Claesson-Welsh, 2012, Robinson and Stringer, 2001). VEGFR1 is essential for mammalian development as homozygous $VEGFR1^{-/-}$ knockout mice die between embryonic days E8.5 and E9.5 after endothelial hyperproliferation leads to blood vessel obstruction (Fong et al., 1995) (Table 1.1). The $VEGFR1$ primary RNA transcript undergoes alternative splicing to generate a soluble VEGFR1 isoform (sFlt-1; sVEGFR1) of ~110 kDa. This soluble isoform comprises Ig-like domains 1-6 of the VEGFR1 ectodomain and a unique 31 residue sequence at the C-terminus (Shibuya, 2001). sVEGFR1 can be a potent inhibitor of VEGF-A, VEGF-B and PlGF signal transduction (Olsson et al., 2006).

In leukaemia cells, PlGF and VEGF-A induce tyrosine phosphorylation of VEGFR1 and increase ectodomain shedding. This occurs via activation of protein kinase C (PKC) and metalloproteases such as tumour necrosis factor α (TNFα) converting enzyme (TACE) (Rahimi et al., 2009). TACE activity generates sVEGFR1 and an intracellular cytoplasmic fragment; detachment of this fragment from the plasma membrane requires γ-secretase/presenilin activity (Cai et al., 2011).

One view is that VEGFR1 has positive or negative regulatory roles in angiogenesis depending on biological conditions. A negative regulatory role arises from sVEGFR1 acting as a decoy receptor to sequester VEGF-A away from VEGFR2 or by formation of non-signalling VEGFR1/VEGFR2 heterodimers (Kendall et al., 1994). A positive regulatory role could occur under pathological conditions of tumour growth where abnormally high expression of VEGFR1-specific ligands leads to elevated VEGFR1 tyrosine kinase activity which promotes angiogenesis (Hiratsuka et al., 2001).

1.3.2. VEGFR2

Immature VEGFR2 has an estimated molecular mass of ~152 kDa and undergoes translocation to the endoplasmic reticulum and N-linked glycosylation along the secretory pathway to produce a mature glycoprotein with a mass of ~200-230 kDa (Waltenberger et al., 1994, Koch et al., 2011). Only mature, fully glycosylated VEGFR2 undergoes efficient trans-autophosphorylation upon VEGF stimulation (Takahashi and Shibuya, 1997). Alternative splicing generates soluble VEGFR2 (sVEGFR2) which is present in plasma and multiple tissues including the heart, spleen, skin, ovary and kidney. This sVEGFR2 can sequester free VEGF-C, thus preventing VEGFR3 activation and inhibiting lymphatic endothelial cell proliferation (Albuquerque et al., 2009). VEGFR2 expression is predominantly restricted to endothelial cells and haematopoietic stem cell precursors, with peaks in expression during embryonic development (Millauer et al., 1993).

VEGF-A binds VEGFR2 with a relatively high affinity (K_d ~150 pM); however, this parameter is ~10-fold lower than that of VEGFR1 (K_d ~15 pM) (Vaisman et al., 1990). Nonetheless, the majority of VEGF-A-regulated angiogenic outcomes are attributed to its interaction with VEGFR2. VEGFR2 is considered a more potent tyrosine kinase which targets numerous substrates including membrane proteins, cytoplasmic enzymes and adaptor proteins (Roskoski, 2007, Quinn et al., 1993). VEGFR2 is thus considered the major pro-angiogenic receptor which regulates blood vessel development and homeostasis in response to circulating VEGFs (Quinn et al., 1993, Roskoski, 2007). VEGFR2 expression is down-regulated in quiescent adult vasculature (Eichmann et al., 1997), likely to reduce the magnitude of VEGFR2-regulated pro-angiogenic responses (Kanno et al., 2000).

1.3.3. VEGFR3

VEGFR3 is an essential regulator of lymphoendothelial function and lymphangiogenesis. Upon co-translational insertion of newly synthesised VEGFR3 into the endoplasmic reticulum this ~195 kDa precursor protein undergoes *N*-linked glycosylation and proteolytic cleavage within the fifth Ig-like domain. This generates an N-terminal polypeptide which forms a stable disulphide linkage with the carboxyl half of the VEGFR3 precursor (Pajusola et al., 1993). VEGFR3 complexity is further

increased by alternative splicing to produce both long and short isoforms (Galland et al., 1993, Pajusola et al., 1992). The VEGFR3 short isoform lacks 65 residues proximal to the C-terminus; this is only present in humans and likely arose through a retroviral integration event during human speciation (Hughes, 2001). Furthermore, the VEGFR3 short isoform lacks two cytoplasmic phosphorylation epitopes which are detected in VEGFR3 homodimers but not in VEGFR2/VEGFR3 heterodimers (Dixelius et al., 2003). *VEGFR3$^{-/-}$* knockout mice die during embryogenesis between E10 to E11 due to impaired hierarchical formation of the peripheral blood vasculature and defects in cardiac remodelling (Dumont et al., 1998) (Table 1.1). The role(s) of VEGFR3 in lymphatic endothelial cell responses is well-studied; however, VEGFR3 expression is also upregulated in vascular endothelial cells during angiogenesis (Carmeliet et al., 2009, Koch and Claesson-Welsh, 2012). VEGFR3 expression is detected in non-endothelial cells such as macrophages, neuronal progenitors and osteoblasts, whilst its functional presence in tumours is much debated (Koch and Claesson-Welsh, 2012). Mice expressing kinase-deficient VEGFR3 maintain normal physiological blood vessel development but exhibit impaired lymphatic development (Zhang et al., 2010) (Table 1.1). VEGFR3 mutations which perturb tyrosine kinase activity are associated with variants of hereditary lymphoedema, reinforcing the pivotal role of VEGFR3 in lymphatic endothelial cell function (Irrthum et al., 2000).

1.4. VEGFR signal transduction

Most parenchymal cells express and secrete growth factors such as VEGF-A. These ligands act in a paracrine manner on neighbouring endothelial cells to regulate VEGFR-mediated signal transduction and influence endothelial, lymphatic, epithelial and neural cell responses (Ruiz de Almodovar et al., 2009, Ponnambalam and Alberghina, 2011, Eichmann and Simons, 2012). Notably, autocrine VEGF-A-induced signal transduction is considered essential for maintaining endothelial cell survival (Lee et al., 2007). VEGF-stimulated signal transduction regulates a host of endothelial cell responses including proliferation, migration, permeability and cell-cell interactions.

Activation of the cytoplasmic tyrosine kinase domain by ligand-induced VEGFR homo- or heterodimerisation causes conformational changes that expose an ATP-binding site (Nilsson et al., 2010). The exchange of ADP for ATP initiates trans-

autophosphorylation of key tyrosine residues on the receptor dimer which create docking sites for SH2-domain-containing adaptor molecules and trigger waves of intracellular signal transduction (Stuttfeld and Ballmer-Hofer, 2009). VEGFR tyrosine kinase activity is tightly regulated by ubiquitination, internalisation and de-phosphorylation by protein tyrosine phosphatases (PTPs) such as PTP1B and vascular endothelial PTP (VE-PTP) (Kappert et al., 2005).

1.4.1. VEGFR1-regulated signal transduction

A highly postulated model is that VEGFR1 acts as a 'VEGF trap' (Kendall et al., 1994). Nonetheless, VEGF-A binding to VEGFR1 Ig-like domains 2 and 3 can trigger low levels of trans-autophosphorylation at specific VEGFR1 cytoplasmic tyrosine residues Y794, Y1169, Y1213, Y1242, Y1309, Y1327, and Y1333 (Cunningham et al., 1997, Yu et al., 2001, Wiesmann et al., 1997) (Fig. 1.7). Patterns of VEGFR1 tyrosine phosphorylation are ligand-dependent e.g. Y1309 phosphorylation is induced by PlGF binding and linked to downstream Akt activation and changes in cell physiology (Autiero et al., 2003).

Computational modelling suggests VEGFR1/VEGFR2 heterodimers comprise 10-50% of activated VEGFR complexes in response to VEGF-A; such modelling predicts low incidence of VEGFR1 homodimers when VEGFR2 levels are relatively high (Mac Gabhann and Popel, 2007). Functional coupling of VEGFR1 and VEGFR2 through heterodimerisation and trans-autophosphorylation could modulate endothelial cell responses (Koch et al., 2011). Surprisingly, *VEGFR1-TK$^{-/-}$* knock out mice expressing truncated VEGFR1 lacking tyrosine kinase activity are viable and exhibit normal blood vessel formation during development; however such mice exhibit defects in VEGF-A-dependent macrophage migration (Shibuya, 2014) (Table 1.1). Other studies on heterozygous *VEGFR1-TK$^{+/-}$* transgenic mice suggest that VEGFR1 tyrosine kinase activity is required for angiogenesis during tumour metastasis, in some inflammatory diseases, stroke, liver repair, gastric ulcer healing and various carcinomas and glioblastomas (Shibuya, 2014). Although VEGFR1 is considered to be a 'poor' tyrosine kinase with limited signalling output, therapeutics aimed at this RTK could be an attractive option for certain diseases (Shibuya, 2006).

VEGFR1 is functionally linked to endothelial cell migration and actin reorganisation through receptor for activated C kinase 1 (RACK1) activation (Wang et al., 2011) (Fig. 1.7). Additionally, activated VEGFR1 upregulates urinary-type plasminogen activator (uPA) and PAI-1 levels which influence p38 MAPK regulation of actin dynamics, extracellular matrix degradation and cell migration (Carmeliet, 2005, Ewan et al., 2006) (Fig. 1.7). VEGFR1-dependent activation of phosphoinositide-3-kinase (PI3K) is linked to endothelial cell proliferation and tubulogenesis (Cai et al., 2003) (Fig. 1.7). Other targets of VEGFR1-mediated signal transduction include phospholipase Cγ1 (PLCγ1), growth factor receptor-bound protein 2 (Grb2) and protein tyrosine phosphatase non-receptor type 11/SH2 domain-containing tyrosine phosphatase 2 (PTPN11/SHP2) (Ito et al., 1998). VEGFR1 activation generates cytoplasmic pY794 and pY1169 epitopes that promote PLCγ1 recruitment, leading to phosphatidylinositol-4,5-bisphosphate (PIP$_2$) cleavage and production of diacylglycerol (DAG) and inositol-1,4,5-trisphosphate (IP$_3$) (Roskoski, 2007, Cunningham et al., 1997) (Fig. 1.7). IP$_3$ binding to the membrane-bound IP$_3$ receptor (IP$_3$R) in the endoplasmic reticulum facilitates Ca^{2+} ion translocation into the cytosol. One consequence of such activity is engagement of the calmodulin-calcineurin pathway which causes de-phosphorylation of nuclear factor of activated T-cell (NFAT) family members leading to their activation, nuclear translocation and stimulation of gene transcription at specific loci (Koch et al., 2011) (Fig. 1.7). This pro-angiogenic pathway promotes an inflammatory response (Jiang and Liu, 2009). VEGFR1-specific ligands, PIGF and VEGF-B, bind to monocytes and stimulate intracellular signalling events including activation of the extracellular signal-regulated kinase 1/2 (ERK1/2), Akt and p38 MAPK pathways (Tchaikovski et al., 2008).

1.4.2. VEGFR2-regulated signal transduction

VEGFR2-specific signal transduction influences endothelial cell proliferation, migration, survival and tubulogenesis. Ligand binding to the VEGFR2 extracellular domain triggers cytoplasmic tyrosine kinase activation and trans-autophosphorylation at residues Y801, Y951, Y1054, Y1059, Y1175, Y1214, Y1223, Y1305, Y1309 and Y1319 (Fig. 1.8). The VEGFR2-pY951 epitope provides a binding site for SH2 domain-containing T-cell-specific adaptor molecule (TSAd) which is functionally linked to endothelial cell migration and vascular permeability (Matsumoto et al., 2005) (Fig. 1.8). Generation of VEGFR2-pY1059 enables recruitment of the proto-oncogene and soluble
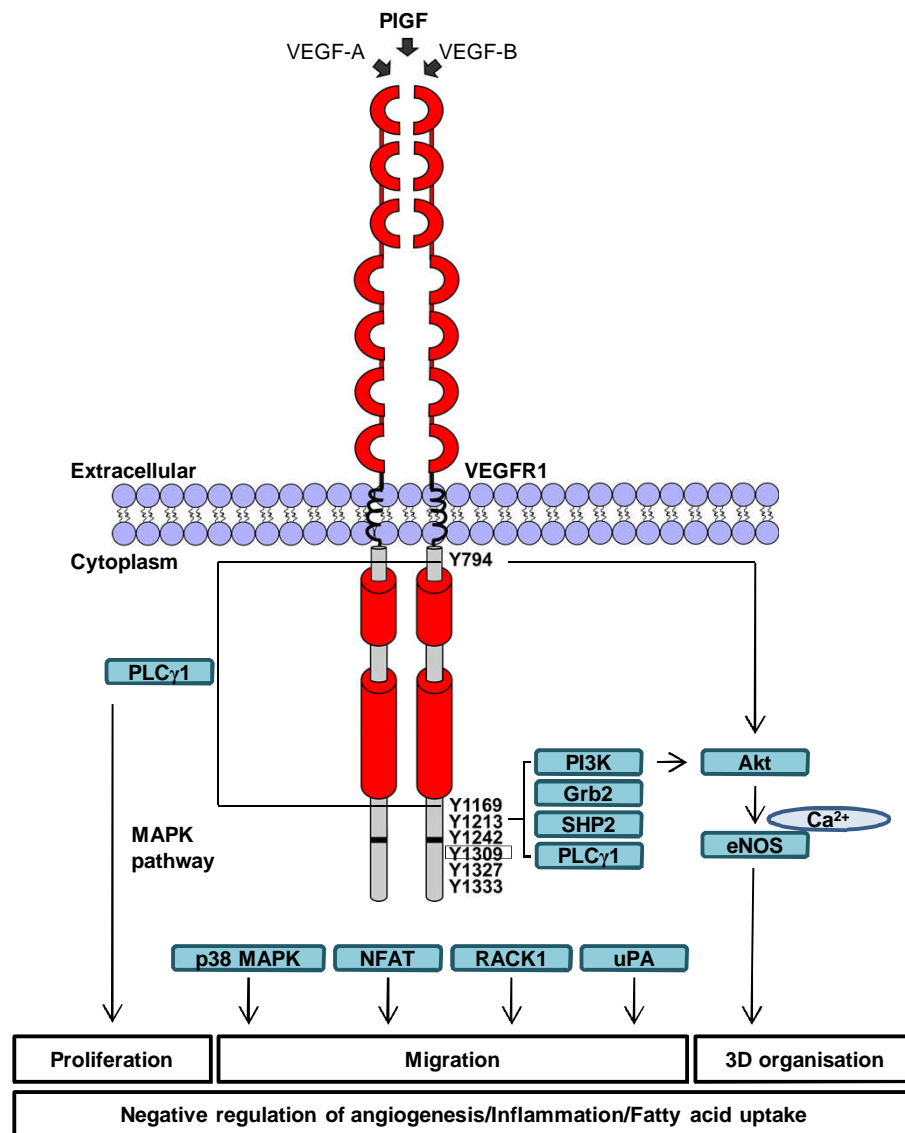
Figure 1.7. VEGFR1-mediated signal transduction. Schematic of the signal transduction cascades activated upon ligand binding to VEGFR1 with tyrosine (Y) phosphorylation sites indicated. Y1309 (boxed) is only phosphorylated by PlGF stimulation. Binding of signalling adaptors to VEGFR1 phospho-tyrosine epitopes initiates activation of downstream signalling proteins and leads to specific biological outcomes. Restricted tyrosine phosphorylation and the presence of a repressor sequence in the juxtamembrane domain are possible mechanisms for the weak kinase activity of VEGFR1. Adapted from Koch et al. (2011).

tyrosine kinase Src which further promotes phosphorylation of residue Y1175 (Fig. 1.8). VEGFR2-pY1175-mediated recruitment of PLCγ1 causes PIP$_2$ hydrolysis, DAG release and subsequent activation of PKC and MAPK enzymes (e.g. ERK1/2) which influence gene expression and cell proliferation (Takahashi et al., 2001) (Fig. 1.8). Furthermore, VEGF-A stimulates both membrane and soluble VEGFR1 expression through VEGFR2 and PKC-dependent pathways (Raikwar et al., 2013). VEGF-A-stimulated ERK1/2 activation leads to the hyperphosphorylation of activating transcription factor 2 (ATF-2), causing elevated expression of vascular endothelial cell adhesion molecule 1 (VCAM-1) and promoting endothelial-leukocyte interactions (Fearnley et al., 2014); this provides a MAPK-regulated gene expression mechanism that links angiogenesis and inflammation.

The VEGFR2-pY1175 epitope can also bind adaptor protein SH2-domain-containing adaptor protein B (Shb) which facilitates interaction with focal adhesion kinase (FAK) and contributes to endothelial cell migration and attachment (Holmqvist et al., 2003) (Fig. 1.8). Shb activation of PI3K results in sequential activation of Akt and endothelial nitric oxide synthase (eNOS) which promote cell survival and nitric oxide (NO)-induced vascular permeability, respectively (Roskoski, 2007, Olsson et al., 2006) (Fig. 1.8). Generation of the VEGFR2-pY1214 epitope enables recruitment of adaptor protein Nck and a cytoplasmic tyrosine kinase, Fyn. Nck-Fyn complex formation regulates phosphorylation of p21-activated protein kinase 2 (PAK2), which in turn activates cell division cycle 42 (Cdc42) and p38 MAPK (Lamalice et al., 2006); impacting on cell migration through increased actin remodelling (Fig. 1.8). VEGF-regulated PI3K activation mediates cell survival through sequential phosphoinositide-dependent protein kinase 1 (PDK1) and Akt activation. Akt is a multifunctional regulator that can inhibit Bcl-2-associated agonist of cell death (BAD) and caspase 9, thus blocking apoptosis (Datta et al., 1999) (Fig. 1.8).

Other post-translational modifications such as methylation are involved in VEGFR2 activation. VEGFR2 methylation takes place at multiple lysine and arginine residues, such as residue L1041 which is proximal to the kinase domain activation loop. Although methylation is ligand-independent, it enhances tyrosine phosphorylation and kinase activity in response to VEGF (Hartsough et al., 2013). In addition, VEGFR2 is
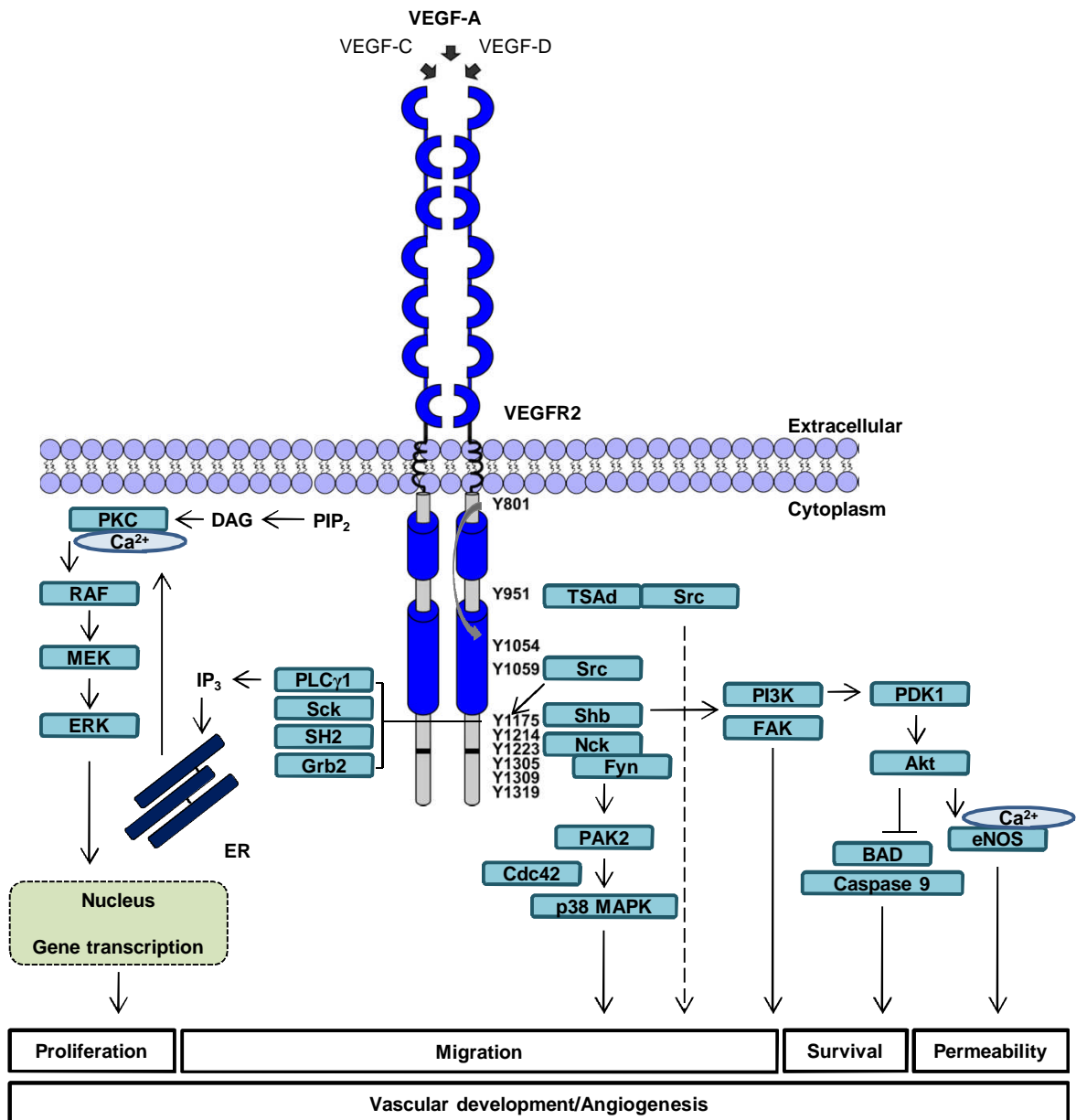
Figure 1.8. VEGFR2-mediated signal transduction. Schematic of the signal transduction cascades activated upon VEGF binding to VEGFR2 with tyrosine (Y) phosphorylation sites indicated. Binding of signalling adaptors to VEGFR2 phospho-tyrosine epitopes initiates activation of downstream signalling proteins and leads to specific biological outcomes. Phosphorylation of Y1054 and Y1059 is essential for VEGFR2 kinase activity. Adapted from Koch et al. (2011).

acetylated at a dense cluster of four lysine residues in the kinase insert domain and at a single lysine within the kinase activation loop (Zecchin et al., 2014). The acetyltransferase p300 and two histone deacetylases, HDAC5 and HDAC6, regulate VEGFR2 acetylation in a process essential for controlling sustained ligand-dependent trans-autophosphorylation and downstream signal transduction (Zecchin et al., 2014).

1.5. VEGF and metabolism

In contrast to other cells and tissues, the endothelium relies heavily on glycolysis to produce ATP as an energy source; the contribution of glucose oxidation or mitochondrial respiration to ATP production is relatively low. This endothelial phenotype is superficially similar to the glycolytic phenotype exhibited by transformed tumour cells i.e. the Warburg effect. The glycolytic flux in endothelial cells is >200-fold higher in comparison to glucose, fatty acid or glutamine oxidation (De Bock et al., 2013a). However, under conditions of stress, mitochondrial respiration can serve as a reserve mechanism for ATP synthesis (Eelen et al., 2013).

1.5.1. VEGF and glycolysis

Different lines of evidence suggest that VEGFs have strong regulatory roles in endothelial cell metabolism. The endothelial glucose transporter 1 (GLUT1) mediates glucose influx in a passive manner (De Bock et al., 2013a). Interestingly, GLUT1 levels are elevated during hypoxia (Ulyatt et al., 2011). VEGF-A stimulation increases the glycolytic rate of endothelial cells through increased PI3K and Akt-stimulated expression of GLUT1, lactate dehydrogenase-A (LDH-A) and phosphofructokinase-2/fructose-2,6-bisphosphate (PFKFB3) (Yeh et al., 2008, De Bock et al., 2013b, Eelen et al., 2013). VEGF-A stimulates PFKFB3-driven glycolysis in endothelial tip cells preferentially to other endothelial cells within the developing vascular sprout (De Bock et al., 2013b). If this upregulation fails due to gene knockdown of PFKFB3, glycolysis, endothelial cell migration, proliferation and vascular sprouting are inhibited (De Bock et al., 2013b). Overexpression of PFKFB3 in endothelial stalk cells confers tip cell-like behaviour, overriding other regulatory signals (Eelen et al., 2013, De Bock et al., 2013b). Thus glucose metabolism regulates angiogenic fate, rather than simply being the engine that drives it (Jang and Arany, 2013).

Compared to glycolysis, oxidative phosphorylation produces ~20-fold more ATP (Locasale and Cantley, 2011). As endothelial cells are exposed to relatively high circulatory blood oxygen levels, the importance of glycolysis in endothelial cell metabolism seems paradoxical (Eelen et al., 2013). One explanation is that the endothelium must maintain high metabolic activity to promote angiogenesis in hypoxic environments thus enabling oxygen-independent ATP synthesis (Eelen et al., 2013). Endothelial glycolysis is increased in pathological conditions such as pulmonary hypertension where oxygen consumption is reduced (Fijalkowska et al., 2010).

1.5.2. VEGF and the pentose phosphate pathway (PPP)

Endothelial cell dependence on glycolysis promotes diversion of glycolytic intermediates into side branches of this pathway, such as the pentose phosphate pathway (PPP) (Fig. 1.9). Oxidation of glucose-6-phosphate to pentose sugars by glucose-6-phosphate dehydrogenase (G6PD) facilitates nucleotide synthesis, NO production, reductive biosynthesis of lipids and production of reduced glutathione (GSH); an important cellular redox buffer (Cairns et al., 2011) (Fig. 1.9). G6PD inhibition decreases VEGF-A-stimulated VEGFR2 tyrosine phosphorylation, eNOS activation and NO production, in addition to inhibiting endothelial cell migration, proliferation and tubulogenesis (Leopold et al., 2003, Pan et al., 2009). The oxidative branch of the PPP (oxPPP) generates NADPH and ribose-5-phosphate. VEGF-A stimulates oxPPP flux (Vizan et al., 2009); increasing both plasma membrane localisation and activity of G6PD (Pan et al., 2009) and creating a positive feedback loop (Fig. 1.9).

Glucose flux through the hexosamine biosynthesis pathway (HBP) facilitates protein glycosylation. Interaction between VEGFR2 N-linked glycans with the N-glycan-binding protein, galectin-3 facilitates plasma membrane retention and receptor activation, thereby promoting VEGF-A-stimulated angiogenesis (Markowska et al., 2011).

1.5.3. VEGF and the polyol pathway

Elevated glucose levels (hyperglycaemia) are characteristic of diabetes-related pathologies and promote vascular dysfunction. The polyol pathway removes excess glucose from the glycolytic pathway by aldose reductase-catalysed reduction of glucose
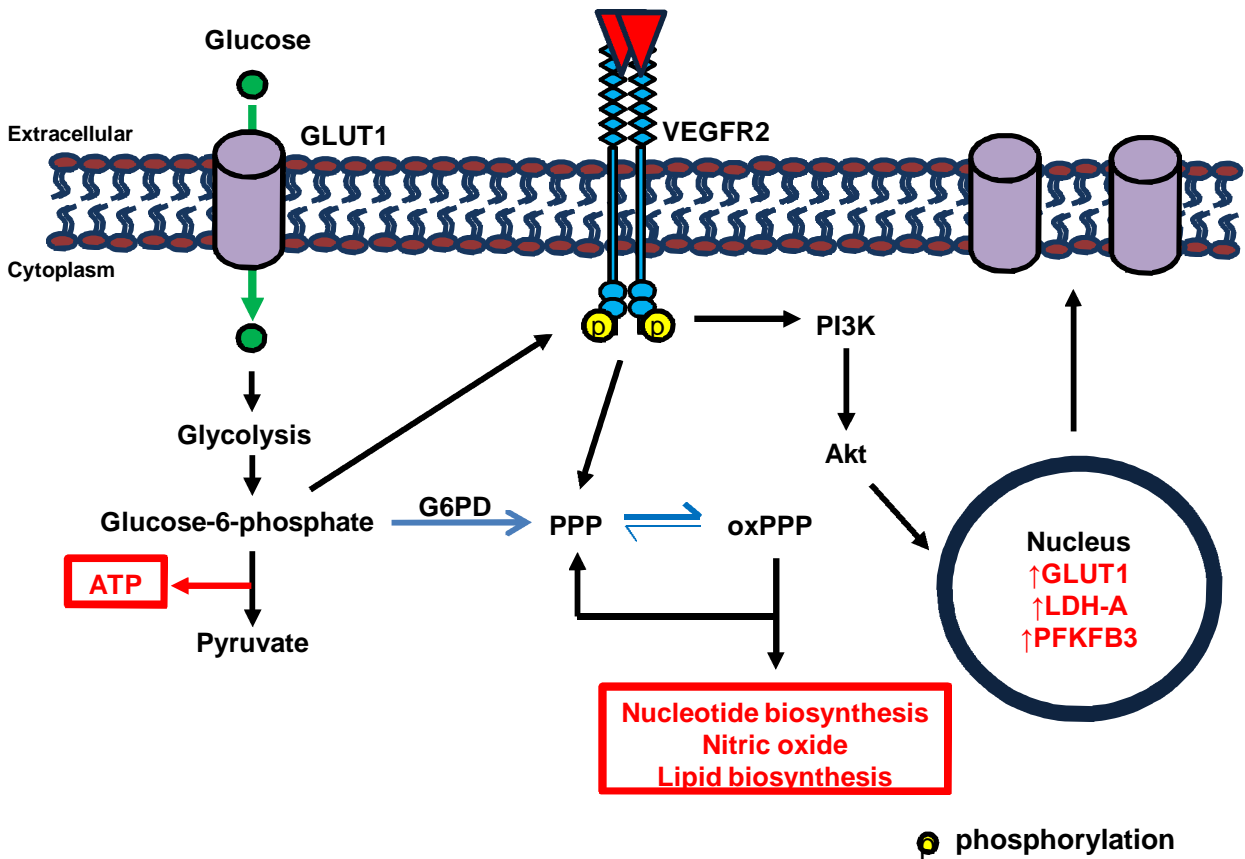
Figure 1.9. VEGF-A endothelial metabolism and glycolysis. Endothelial cell reliance on glycolysis promotes diversion of glycolytic intermediates into side branches of this pathway, such as the pentose phosphate pathway (PPP). VEGF-A stimulation of oxPPP flux increases glucose-6-phosphate dehydrogenase (G6PD) plasma membrane localisation and enzymatic activity, thus creating a positive feedback loop. G6PD also promotes VEGFR2 tyrosine phosphorylation and downstream eNOS activation. VEGF-A-stimulated activation of the PI3K/Akt pathway leads to increased GLUT1, LDH-A and PFKFB3 expression. Taken from Smith et al. (2015).

to sorbitol which is then converted to fructose (Tang et al., 2012). Polyol pathway activity is required for physiological angiogenesis by influencing VEGFR2-regulated signal transduction (Tammali et al., 2011). Inactivation of aldose reductase inhibits PI3K/Akt and nuclear factor κ of activated B cells (NF-κB) signal transduction pathways and down-regulates VEGFR2 levels. Furthermore, downstream VEGF-A-stimulated synthesis and secretion of intercellular adhesion molecule (ICAM), VCAM, interleukin-6, MMP2 and MMP9 is blocked upon aldose reductase depletion (Tammali et al., 2011).

1.5.4. VEGF and fatty acid oxidation (FAO)

Endothelial cells can utilise fatty acid oxidation (FAO) in the absence of glucose to compensate for reduced ATP synthesis (Dagher et al., 2001). VEGF-A-activated VEGFR2 targets fatty acid-binding protein 4 (FABP4) to promote endothelial cell proliferation (Elmasri et al., 2009). VEGF-B stimulates expression of fatty acid transporter proteins 3 and 4 (FATP3, FATP4) in the endothelium. This increases lipid uptake and transport to tissues such as the heart and skeletal muscle (Hagberg et al., 2010). VEGF-B also activates AMP-activated protein kinase (AMPK) which is required for aortic endothelial cell proliferation independently of FAO (Reihill et al., 2011). Neutralising antibodies to VEGF-B restore insulin sensitivity and glucose tolerance by decreasing endothelial-to-tissue lipid transport, indicating that ectopic lipid deposition contributes to type 2 diabetes mellitus (T2DM) disease progression (Carmeliet et al., 2012, Hagberg et al., 2010). Expression of fatty acid synthase (FAS), which catalyses de novo lipid synthesis, is highly upregulated in cancer cells. FAS activity provides additional lipid supply to proliferating cells for membrane biogenesis, conferring a survival and growth advantage (Santos and Schulze, 2012). In contrast, FAS expression is low or undetectable in healthy adult tissues given that diet is the primary lipid source. In the absence of FAS, reduced post-translational palmitoylation of VEGFR2 and eNOS decreases VEGFR2 cell surface levels and downstream eNOS activation, resulting in reduced angiogenesis (Wei et al., 2011).

1.5.5. VEGF and cholesterol efflux

Endothelial cholesterol efflux is essential for angiogenesis (Fang et al., 2013). ATP-binding cassette transporters regulate cellular cholesterol efflux onto apolipoprotein A-1

(ApoA-1) and apoA-1-containing high-density lipoprotein particles which unload excess cholesterol in the liver for metabolism or excretion via the bile pathway. Cholesterol efflux depletes plasma membrane lipid rafts resulting in negative regulatory effects on VEGFR2 activity and thus on VEGF-A-stimulated angiogenesis (Fang et al., 2013). In contrast, apolipoprotein B (ApoB) upregulates VEGFR1 levels which impairs angiogenesis by reducing VEGFR2-VEGF-A binding (Avraham-Davidi et al., 2012).

1.6. VEGF and disease

1.6.1. VEGF and cancer

VEGF expression and activity is associated with many pathological conditions. Lactate inhibition of the oxygen-sensing PHD2 promotes activation of HIF-1α which in turn upregulates VEGF expression in cancer cells (De Saedeleer et al., 2012). Additionally, lactate activates VEGFR2 in a ligand-independent manner (Ruan and Kazlauskas, 2013). Germline mutations in the *VHL* tumour suppressor gene result in Von-Hippel Lindau (VHL) disease, an autosomal dominant inherited disorder which predisposes to a variety of tumours including ocular hemangioblastomas. HIF-1 and -2 play a significant role in angiogenesis, cellular growth, proliferation and metabolism in response to tissue hypoxia. When VHL is inactivated HIF-1 and -2 induce a hypoxic gene response that includes upregulation of VEGF-A (Maher et al., 2011). The development and advancement of vascular tumours characteristically found in VHL patients is driven by the constitutive upregulation of HIF activity (Maher et al., 2011).

High cellular VEGF levels have been associated with advanced disease stages, drug resistance and poor prognosis in several leukaemias, myelomas and lymphomas (Paesler et al., 2012). Many lymphomas and leukaemias secrete a mixture of VEGFs and express at least one VEGFR (Paesler et al., 2012). Leukaemia-derived VEGF-A promotes normal endothelial cells to secrete pro-leukaemic factors such as granulocyte-macrophage colony-stimulating factor (GM-CSF), thus highlighting the existence of a positive feedback loop. This phenomenon strongly increases the likelihood of disease relapse (Trujillo et al., 2012). Interestingly, VEGFR2 is constitutively phosphorylated in acute myeloid leukaemia (AML) cells (Santos and Dias, 2004). Elevated VEGF-A levels are also associated with acute lymphocytic leukaemia (ALL) (Koomagi et al.,

2001). VEGF-A expression promotes ALL cell survival and growth in an autocrine manner (Aguayo et al., 2003). VEGF-A-stimulated phosphorylation of B-cell lymphoma-2 (Bcl-2) and diminished cytochrome c release blocks ALL cell apoptosis (Wang et al., 2005).

1.6.2. VEGF and diabetes mellitus

Abnormal VEGF-A levels are strongly associated with endothelial dysfunction in multiple cardiovascular risk factors including T2DM, hyperglycaemia (Feener and King, 1997), hypertension, hypercholesterolaemia (Zeiher et al., 1993) and smoking (Heitzer et al., 2001). Likewise, VEGF-A levels are perturbed in coronary arterial disease (Heitzer et al., 2001) and heart failure (Hornig et al., 1998). VEGF-A resistance is associated with increased circulating VEGF-A levels in metabolic syndrome. Moreover, insulin-resistant states such as T2DM correlate with VEGF-A resistance (Waltenberger, 2009). Monocytes from DM patients exhibit defects in VEGF-A-stimulated and VEGFR1-dependent signalling pathways, causing reduced chemotaxis (Tchaikovski et al., 2009, Tchaikovski et al., 2008). Other secondary effects of the chronic DM disease state and examples of pre-activated intracellular pathways include reactive oxygen species (ROS) production, PTP inhibition, activation and upregulation of receptor for advanced glycation end-products (RAGE) and hyperglycaemia-induced production of advanced glycation end-products (AGE) (Waltenberger, 2009) (Fig. 1.10). This wide spectrum of biochemical dysfunction leads to constitutive activation of downstream protein kinases such as ERK1/2, p38 MAPK and Akt, thus desensitising VEGF-activated signal transduction pathways (Waltenberger, 2009) (Fig. 1.10). During hyperglycaemia, ROS stimulates ligand-independent VEGFR2 phosphorylation and activation within the biosynthetic secretory pathway leading to depleted plasma membrane levels and a deficient endothelial cell response to VEGF-A (Warren et al., 2014) (Fig. 1.10). Chronic DM exemplifies an angiogenic paradox: it correlates with both enhanced (diabetic retinopathy and chronic wounds) and reduced (arteriogenesis and impaired collateral vessel growth) angiogenesis (Simons, 2005a, Werner et al., 2003). VEGF levels are elevated (Sasso et al., 2005) whilst angiogenic responses are reduced (VEGF resistance) (Tchaikovski et al., 2009). It is possible that VEGF resistance diminishes VEGF responses during short-term stimulation of angiogenesis,

whilst long-term stimulation causes a net increase in neovascularisation due to prolonged exposure to VEGF, despite a weaker response (Waltenberger, 2009).

Increased GLUT1 expression precedes elevated VEGF levels in mesangial cells (Wang et al., 2010a). Conversely, treatment of these cells with VEGF promotes increased GLUT1 levels and glucose uptake, indicating that VEGF is a potent stimulus of GLUT1 synthesis and creating a positive feedback cycle. This bidirectional stimulation between GLUT1 and VEGF indicates a pro-sclerotic role for VEGF in diabetic nephropathy (Heilig et al., 2013). Diabetic glomerulosclerosis is characterised by mesangial expansion, accumulation of ECM proteins and tubulointerstitial fibrosis. Disease development is accelerated by hyperglycaemia. Increased cellular glucose availability drives the expression of proteins associated with diabetic nephropathy including ANG-2 and VEGF (Chiarelli et al., 2009). Similarly, diabetes is induced in NO knockout mice which show elevated VEGF expression and develop diabetic glomerulosclerosis. Under normal circumstances, VEGF triggers NO release. Endothelial cell-derived NO acts with VEGF as a trophic factor for the endothelium and prevents smooth muscle and endothelial cell proliferation and macrophage infiltration (Nakagawa, 2007). A model for diabetic glomerulosclerosis is proposed in which VEGF and NO 'uncoupling' promotes diabetic nephropathy (Nakagawa, 2007). Importantly, a VEGF neutralising antibody prevents diabetes-induced increase in glomerular volume (Flyvbjerg et al., 2002).

1.6.3. VEGF and hypercholesterolaemia

Stimulation of angiogenesis is desirable under conditions of hypoxia and ischaemia. Hypercholesterolaemia provides a link between angiogenesis and ischaemic vascular disease (Jin et al., 2013). Increased VEGFR2 degradation in endothelial cells exposed to low-density lipoprotein (LDL) attenuates VEGF-induced signal transduction through Akt and ERK1/2. Decreased VEGFR1 and VEGFR2 levels following LDL exposure inhibits endothelial cell migration, proliferation and tubulogenesis (Jin et al., 2013). Thus, hypercholesterolaemia compromises pro-angiogenic responses to VEGF in ischaemic vascular disease (Jin et al., 2013).
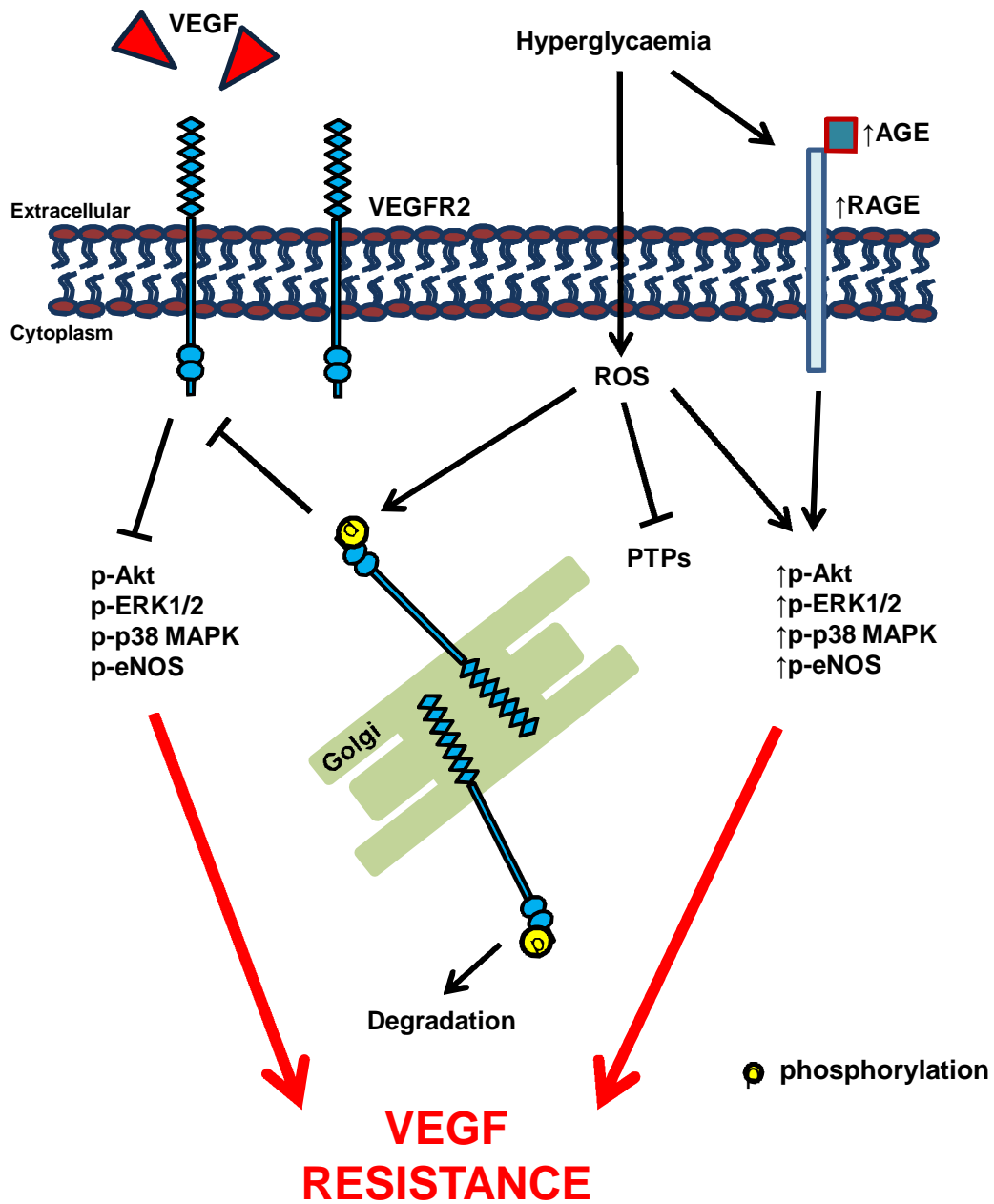
Figure 1.10. Diabetes-associated ROS attenuates VEGF-A-stimulated endothelial cell responses. During hyperglycaemia, ROS stimulates ligand-independent VEGFR2 phosphorylation and activation within the biosynthetic secretory pathway leading to depleted plasma membrane levels and a deficient response to VEGF-A. Secondary effects of the chronic DM disease state and examples of pre-activated intracellular pathways include ROS production, PTP inhibition, activation and upregulation of RAGE and hyperglycaemia-induced production of AGE. This wide spectrum of biochemical dysfunction leads to constitutive activation of downstream ERK1/2, p38 MAPK and Akt, thus desensitising VEGF-stimulated signal transduction pathways.

Adverse effects of cholesterol metabolism and its oxidised products are associated with expression of angiogenic proteins, such as VEGF, in retinal pigment epithelial cells. In age-related macular degeneration (AMD), deposition of 7-ketocholesterol and oxidised cholesterol increases expression of VEGF and induces a pro-angiogenic environment for neovascularisation (Sharma et al., 2014). Impaired cholesterol transport and accumulation in macrophages further increases the number of cells that secrete pro-angiogenic VEGF, thus accelerating the disease phenotype (Sharma et al., 2014).

1.7. VEGF as a drug target

Pathological angiogenesis is associated with multiple diseases. Strategies to promote revascularisation of ischaemic tissues or to inhibit angiogenesis in cancer, ocular, skin or joint disorders are potential therapeutic targets. Clinical trials testing the pro-angiogenic capability of VEGF have produced suboptimal results (Simons, 2005b). Angiogenic complexity underlies the failure of these trials to stimulate growth of functional vessels. Angiogenesis does not cause malignancy but promotes tumour growth and metastasis. Unlike tumour cells, endothelial cells are genomically stable and therefore considered ideal therapeutic targets that would not develop resistance to anti-angiogenic therapy (Carmeliet, 2005).

1.7.1. Anti-VEGF drugs

Anti-angiogenic therapy has been targeted towards members of the VEGF family and associated VEGFRs due to their essential role in angiogenesis (Tugues et al., 2011). Bevacizumab (Avastin) is a humanised monoclonal antibody to VEGF-A approved to treat renal cell carcinoma (RCC), metastatic colorectal cancer, metastatic breast cancer, advanced non-squamous, non-small cell lung cancer and recurrent multiforme glioblastoma (Tarallo and De Falco, 2015). Aflibercept (Zaltrap, VEGF Trap-Eye) is a recombinant fusion protein consisting of the extracellular VEGF-A-binding domains of VEGFR1 and VEGFR2 fused to an Fc domain (Fig. 1.11). This new anti-angiogenic molecule acts as a decoy receptor to block VEGF-A, VEGF-B and PlGF activity and has been approved for the treatment of metastatic RCC (Ciombor et al., 2013).

High levels of VEGF-A in ocular fluid are associated with AMD, diabetes and ischaemic central retinal vein occlusion (Sennino and McDonald, 2012). Current

treatments that directly target circulating VEGF-A in diseases such as wet AMD include Pegaptanib (Macugen), a pegylated 28-base ribonucleic aptamer that selectively binds the herparin-binding domain of VEGF-A_{165} (Fig. 1.11). Ranibizumab (Lucentis) is a recombinant pan-VEGF-A antibody fragment derived from Bevacizumab also approved to treat AMD (Fig. 1.11). Ranibizumab is smaller than Bevacizumab to deliver more effective retinal penetration (Sennino and McDonald, 2012). The use of anti-VEGF drugs as monotherapy for treatment of AMD has proved successful with increased visual acuity experienced by 30% of patients (Sennino and McDonald, 2012).

1.7.2. Tyrosine kinase inhibitors (TKIs)

Tyrosine kinase inhibitors (TKIs) constitute another class of anti-angiogenic drugs approved for cancer therapy. These inhibitors disrupt VEGFR1 and/or VEGFR2 signal transduction and often interfere with the activity of other receptor tyrosine kinases such as fibroblast growth factor receptor (FGFR) and platelet-derived growth factor receptor (PDGFR) (Mendel et al., 2003, Hasinoff and Patel, 2010). The most successful VEGF-related therapies which provide the greatest improvement in progression-free survival in cancer patients are Sorafenib and Sunitinib (Jain et al., 2006) (Fig. 1.11). Sorafenib (Nexavar) is a TKI approved for the treatment of metastatic RCC and hepatocellular carcinoma (Fontanella et al., 2014). The anti-cancer drug Sunitinib (Sutent) is a member of the indolinone family of compounds and is approved to treat RCC and gastrointestinal stromal tumours (Fontanella et al., 2014). Although providing short-term benefits, the activity of these drugs is limited by introduction of compensatory pathways or resistance mechanisms (Hasinoff and Patel, 2010, Zhang et al., 2011). For example, VEGF-A inhibition increases hypoxia which in turn upregulates pro-angiogenic factors such as FGF and PlGF, promoting recruitment of pro-angiogenic bone marrow-derived cells to induce tumour revascularisation (Sennino and McDonald, 2012). Maintaining the correct balance of inhibition between a select group of RTKs including VEGFRs and FGFRs thus appears clinically relevant (Hasinoff and Patel, 2010, Zhang et al., 2011). One strategy to combat drug resistance to VEGF inhibitors is development of multi-targeted TKIs. For example, Nintedanib (Vargatef) is a small molecule multi-target TKI of FGFR, PDGFR and VEGFR used in the treatment of non-small-cell lung cancer (Caglevic et al., 2015). JK-31 is a multi-kinase inhibitor that targets VEGFR2 and cyclin-dependent kinase 1 (CDK1) to simultaneously inhibit pro-

angiogenic signal transduction and cell cycle progression in endothelial cells (Latham et al., 2014) (Fig. 1.11). Another multi-targeted tyrosine kinase inhibitor JK-P3 inhibits the intrinsic catalytic activity of VEGFR2, FGFR1 and FGFR3 (Latham et al., 2012). The ability of multi-targeted TKIs to simultaneously inhibit multiple signalling pathways enables them to overcome redundant angiogenic factors considered to be a key mechanism underlying resistance to anti-VEGF therapy (Huang and Carbone, 2015). Emerging anti-angiogenic agents that selectively inhibit VEGFR2 activity include Ramucirumab, a fully humanised monoclonal antibody targeting the extracellular domain of VEGFR2, and Apatinib, a small molecule inhibitor of the intracellular domain (Fontanella et al., 2014) (Fig. 1.11). Advancement in anti-angiogenic therapies is needed to prolong progression-free survival of responsive patients by years rather than months with most only effective in combination with chemotherapy (Sennino and McDonald, 2012).

Current VEGF therapies target cancer or AMD however future research directions are emerging for VEGF-targeted therapeutics. VEGF plays a crucial protective role in the nervous system. Reduced levels of VEGF and other growth factors are associated with neurodegenerative diseases. Additionally, VEGF has been identified as a causative factor in several motor neuron degenerative diseases and epilepsy (Morin-Brureau et al., 2012). VEGF is of particular interest due to its role in cross-talk between the nervous and vascular systems.

1.8. VEGFR trafficking

1.8.1 Ubiquitin-linked protein modification

A key feature of cellular regulation is the reversible modification of protein substrates to influence protein function e.g. enzymatic activity, multiprotein assemblies, etc. One such modification is protein ubiquitination (Herrmann et al., 2007). In humans, ubiquitin is a 76 amino acid highly conserved polypeptide encoded by 4 genes. The *UbB* and *UbC* genes consist of head to tail repeats of 3 or 9 ubiquitin units, respectively. *UBA52* and *RPS27A/UBA80* encode ribosomal subunits which fuse to the C-terminus of a single copy of ubiquitin (Clague et al., 2015). Polypeptides comprising ubiquitin
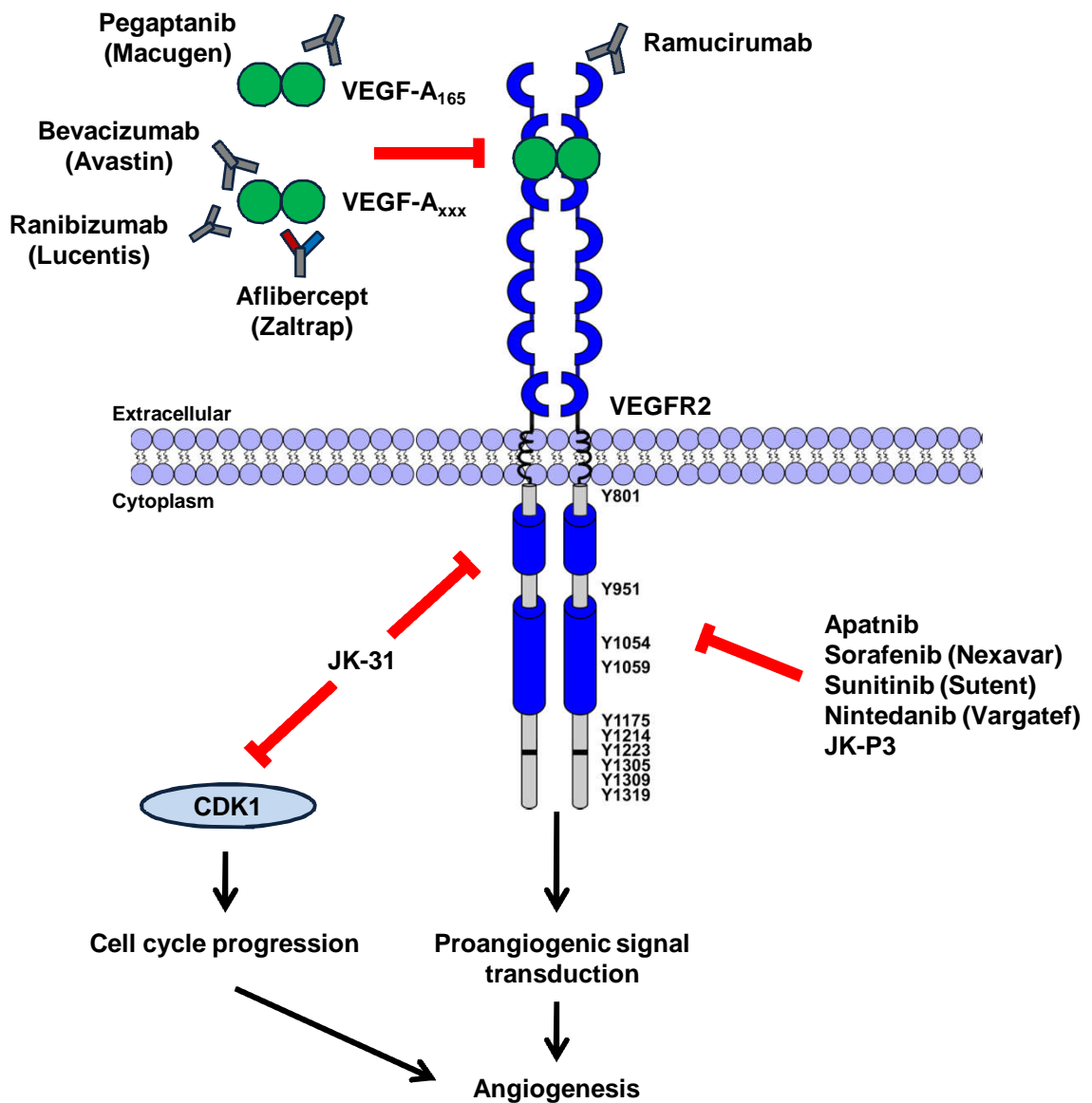
Figure 1.11. Therapeutic inhibitors of VEGFR2 signal transduction.
Schematic depicting target sites of anti-angiogenic agents that inhibit VEGFR2-mediated signal transduction. VEGF-Axxx; non-specific VEGF-A isoform. Adapted from Smith et al. (2015)

repeats are rapidly processed by peptidases belonging to the de-ubiquitinase (DUB) family of enzymes to generate free ubiquitin (Monia et al., 1989). Early work carried out by Varshavsky and colleagues using murine ts85 cells with temperature-sensitive mutations in the *UBA1* gene showed reduced ubiquitin conjugation, decreased protein turnover and cell cycle arrest at non-permissive temperature, demonstrating that ubiquitin mediates proteolysis and lysosomal degradation of the vast majority of short-lived proteins (Ciechanover et al., 1984, Zacksenhaus and Sheinin, 1990, Ciechanover, 2006). It has since been discovered that ubiquitination also regulates intracellular signalling and trafficking pathways. Specific ubiquitination of target substrates leads to proteolysis and/or intracellular redistribution, thus affecting cellular outputs. Many RTKs undergo ligand-dependent ubiquitination including epidermal growth factor receptor (EGFR), PDGFR, c-Met, VEGFR1 and VEGFR2 (Carter et al., 2004, Petrelli et al., 2002, Soubeyran et al., 2002). Ubiquitin conjugation to target proteins involves three sequential steps of an E1-E2-E3 cascade. The ratio of E1:E2:E3 in terms of gene number is 2:35:>300 although this is not reflected in terms of total copy number which is estimated to be 1:3:2 in HeLa cells (Clague 2015).

E1 enzymes consist of 3 domains and initiate the activation and conjugation of a number of ubiquitin-like proteins (UBLs), including ubiquitin, small ubiquitin modifier (SUMO) and NEDD8 to target proteins. An adenylation domain of two ThiF-homology motifs binds ATP and the appropriate UBL (Duda et al., 2005). A catalytic cysteine domain (CCD) is the acyl carrier for ubiquitin, and the C-terminal ubiquitin-fold domain (Ufd) recruits specific E2s (Walden et al., 2003).

It was originally thought that UBA1 was the sole E1 enzyme in humans, as is the case in the yeast *Saccharomyces cerevisiae* where a single E1 mediates ubiquitin presentation to all E2 enzymes (Dohmen et al., 1995). Subsequent studies have identified another E1 enzyme which activates ubiquitin (UBA6) and 6 E1 enzymes that activate ubiquitin-like proteins (UBA2, UBA3, UBA5, UBA7, ATG7 and NAE1). E1 ubiquitin activation is initiated by Mg^{2+}-ATP binding to the carboxyl-terminal glycine of ubiquitin. Formation of an ubiquitin adenylate intermediate facilitates ubiquitin donation to a cysteine residue in the E1 active site and formation of a thiol ester bond (Fig. 1.12). UBA1 catalyses ATP-AMP exchange, from ATP binding to thiol ester formation, at a maximum turnover number of 1-2 s^{-1} making it an efficient enzyme

(Haas and Rose, 1982). However, the catalytic rate (k_{cat}) of substrate ubiquitination is reported as 10-100 fold slower (Mastrandrea et al., 1999). High E1 efficiency accounts for the ability of 8 human E1s to activate ubiquitin or ubiquitin-like proteins for the 600-700 downstream E3 ligases (Li et al., 2008a).

Each E1 enzyme carries two molecules of activated ubiquitin, one as an adenylate and the other as a thiol ester. The thiol-linked ubiquitin is transferred down the conjugation cascade to an active site cysteine in one of 35 E2 (ubiquitin-conjugating) enzymes (Pickart, 2001). An additional 4 E2s receive ubiquitin-like proteins (Clague et al., 2015, Gao et al., 2013). Some E2s are capable of transferring ubiquitin directly to substrate. Alternatively, an E3 ubiquitin ligase forms a complex with the target substrate and catalyses the transfer of ubiquitin from the E2 to the ε-amino group of a lysine residue on the target protein (Pickart, 2001) (Fig. 1.12). The HECT (homologous to E6-AP (E6-associated protein) C-terminus) family and the RING between RING (RBR) families of E3 ligases contain a conserved active site cysteine which accepts ubiquitin from the cognate E2 prior to final substrate transfer (Hochstrasser, 2006). There are 28 HECT E3s and 14 RBR E3s in mammalian cells. The major pool of E3s belongs to the RING/U-box families which do not receive ubiquitin but function as adaptor proteins to ensure proximity of the E2 enzyme and substrate protein (Clague et al., 2015).

The ubiquitin polypeptide contains seven lysines (K6, K11, K27, K29, K33, K48, K63) which can be further conjugated to other ubiquitin monomers to form branched polyubiquitin chains. In mammalian cells, the majority of ubiquitin is conjugated to target proteins as a single unit (monoubiquitin). Monoubiquitination of specific lysine residues in RTKs regulates endocytosis and endosome-lysosome trafficking (Haglund et al., 2003b). Linear ubiquitin chains occur when the C-terminal glycine of one ubiquitin is conjugated to the N-terminal methionine of another (M1-linked) (Walczak et al., 2012). Monoubiquitinated Lys 48 (K48) residues can undergo chain elongation by addition of a pre-formed polyubiquitin oligomer (K48-polyUb); this is associated with targeting the modified protein for degradation (Pickart, 2001). In contrast, Lys63 (K63)-polyUb chains mediate substrate targeting for trafficking through the endosome-lysosome system (Adhikari and Chen, 2009). VEGFR2 undergoes both mono- and polyubiquitination (Meyer et al., 2011).
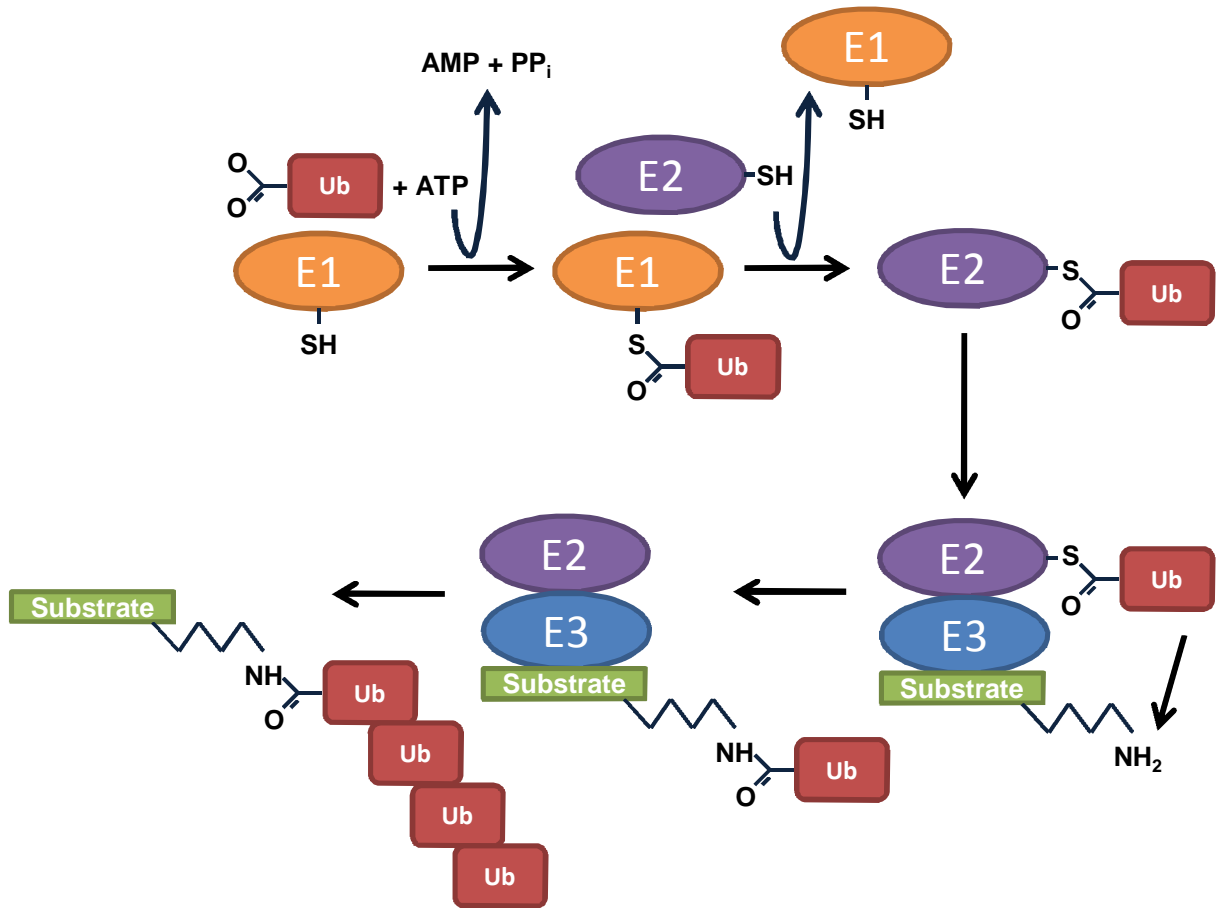
Figure 1.12. The E1-E2-E3 ubiquitin conjugation system. Addition of ubiquitin to a substrate protein is a multi-step process involving a cascade of 3 enzymes; the E1 ubiquitin-activating enzyme, the E2 ubiquitin-conjugating and the E3 ligase. Adapted from Woelk et al. (2007).

The specificity of protein ubiquitination likely depends upon chaperones and scaffold proteins that promote substrate recognition linked to the sequestration of components within the ubiquitin network. Sequential complex assembly based on multiple ubiquitin-ubiquitin-binding domain (UBD) interactions enables the propagation of intracellular signalling events which control the dynamics of receptor trafficking (Grabbe et al., 2011). Ubiquitin signals are recognised by the UBDs of ubiquitin receptors which form non-covalent transient electrostatic interactions with either the ubiquitin moiety or with the linkage region between ubiquitin chains (Ikeda et al., 2010). Monoubiquitination of RTKs stimulates interaction with enzymes or membrane-bound factors which recognise such modifications. Ubiquitin-binding proteins specify the type of ubiquitin modification via their individual UBD; the ubiquitin-interacting motif (UIM) (Polo et al., 2002), ubiquitin-conjugating enzyme-like (UBC)/ubiquitin E2 variant (UEV) (Ponting et al., 1997), ubiquitin-associated (UBA) (Hofmann and Bucher, 1996) and Cue-1-homologous (CUE) (Shih et al., 2003) domain. Many UIMs promote ubiquitination of the proteins that contain them and are frequently found within regulatory proteins which recognise ubiquitinated cargo and regulate membrane trafficking pathways (Bilodeau et al., 2002, Polo et al., 2002, Shih et al., 2003).

DUBs consist of a superfamily of enzymes that can be subdivided into five distinct DUB subsets with differing specificities for the isopeptide bond that links ubiquitin chains. These enzymes play a distinct but crucial role in RTK trafficking and recycling (Clague et al., 2012). Ubiquitin-specific proteases (USPs), ubiquitin C-terminal hydrolases (UCHs), Josephins and ovarian tumour proteases (OTUs) are cysteine-dependent proteases. The fifth family, Jab1/MPN domain-associated metalloisopeptidases (JAMM/MPN$^+$), are zinc-dependent metalloenzymes (Clague et al., 2015). Although it is known that VEGFR2 is recycled from endosomes back to the plasma membrane, it is unknown which DUB prevents its lysosomal degradation. Two DUBs, associated molecule with the Src homology 3 (SH3) domain of STAM (AMSH) and ubiquitin-specific protease Y (USP8), are known to play a role in EGFR recycling and trafficking (McCullough et al., 2004, Mizuno et al., 2005).

1.8.2. Role of ESCRTs in endosomal sorting and trafficking

Endosomal sorting ensures that only ubiquitinated RTK reaches the lysosome for terminal degradation with the remaining receptor recycled from early endosomes back to the plasma membrane. Four individual endosomal sorting complex required for transport (ESCRT) complexes (ESCRT0, I, II and III) are central components of the multivesicular body (MVB) biogenesis machinery. Endocytic proteins and ubiquitin receptors such as hepatocyte growth factor-regulated tyrosine kinase substrate (Hrs), signal transducing adaptor molecule (STAM) and epidermal growth factor receptor substrate 15 (Eps15) provide the initial engagement point between ubiquitinated transmembrane receptor and ESCRT machinery (Fig. 1.13). This enables sorting of membrane-linked cargo into MVBs by forming a multivalent ubiquitin binding complex for trafficking to lysosomes (Bilodeau et al., 2002, de Melker et al., 2001). The adaptor protein, Eps15, is recruited to ubiquitinated RTKs and, via its UIM, facilitates transport along the endocytic pathway (Polo et al., 2002). Hrs endosomal recruitment requires heterodimerisation with its binding partner STAM to form the ESCRT-0 complex; this involves direct interaction with clathrin at regions concentrated in a 'bilayered' clathrin coat (Raiborg et al., 2002). Hrs binds to early endosomal membranes by interaction of its FYVE (Fab1, YOTB, Vac1, EEA1) domain with phosphatidylinositol-3-phosphate. ESCRT-0 can bind several ubiquitin moieties at once through the UIM of STAM and the di-ubiquitin motif (DIUM) of Hrs (Grabbe et al., 2011). Hrs recruits ESCRT-I to endosomes via direct interaction with tumour susceptibility gene 101 (TSG101), facilitating forward movement through the endosome-lysosome system (Urbe et al., 2003).

STAM is constitutively recruited to early endosomes as part of the ESCRT-0 complex and interacts with endosomal DUBs, AMSH and USP8, via the SH3 domain of STAM and their shared STAM binding motif; PX(V/I)(D/N)RXXXKP (Tanaka, 1999, Kato et al., 2000). De-ubiquitination facilitates receptor recycling and is essential for maintaining the free ubiquitin pool upon which receptor trafficking is dependent. Similar to the co-ordinated but opposing effects of kinase and phosphatase activity, ubiquitination is kept in balance by DUB activity (Wing, 2003). USP8 is a cysteine protease and member of the USP family of DUB enzymes. The zinc-dependent ubiquitin isopeptidase, AMSH (McCullough et al., 2004), contains a JAMM motif and

is a member of the isopeptidase family of DUBs (Hochstrasser, 2002). USP8 and AMSH catalyse complete breakdown of polyubiquitin into its component monomers, preferentially generating monoubiquitin (McCullough et al., 2004). In contrast to AMSH, USP8 is able to process both K48- and K63-linked polyubiquitin chains (McCullough et al., 2004, Mizuno et al., 2005, Row et al., 2006).

Once internalised cargo has been committed for degradation, conjugated ubiquitin is recycled and removed by AMSH and USP8 which are recruited to late endosomal compartments by direct interaction with ESCRT-III (Clague and Urbe, 2006). AMSH prevents lysosomal degradation and promotes recycling of substrates such as EGFR by processing K63-linked polyubiquitin chains and is itself ubiquitinated by the E3 ubiquitin ligase, Smurf2. Smurf2-mediated down-regulation of AMSH restricts recycling following receptor activation to promote a return to quiescence. (McCullough et al., 2004, Clague and Urbe, 2006, Li and Seth, 2004).

Ubiquitination of Hrs and STAM inhibits their function by masking ubiquitin-binding sites and interfering with binding to ubiquitinated cargo (Hoeller et al., 2006). Following acute EGF stimulation, USP8 translocates to endosomes where it protects STAM from proteasomal degradation (Mizuno et al., 2005). Hrs and STAM direct ubiquitinated EGFR towards the lysosome for degradation (Clague and Urbe, 2001) and show increased co-distribution with VEGFR2 at early endosomes upon VEGF-A stimulation (Ewan et al., 2006). ESCRT-0 is an integral complex for endosomal sorting and blocking its activity by Hrs depletion stimulates proteasome-mediated VEGFR2 proteolysis (Bruns et al., 2010).

1.8.3. VEGFR trafficking and localisation

VEGFR1 is a plasma membrane resident RTK however ~80% is located within a stable pool in the Golgi apparatus along the secretory pathway (Mittar et al., 2009). VEGF-A-stimulated activation of plasma membrane VEGFR2 is linked to cytosolic Ca^{2+} ion flux, causing transient redistribution of VEGFR1 to the plasma membrane via a *trans*-Golgi network-to-plasma membrane route. This negative feedback model regulates VEGF-A-mediated cellular responses (Mittar et al., 2009). VEGFR1 levels are relatively insensitive to VEGF-A stimulation, unlike VEGFR2 (Ewan et al., 2006, Mittar et al.,

2009). Activated VEGFR1 is internalised through clathrin-mediated endocytosis by ternary complex formation with Cas-Br-M murine ecotropic retroviral transforming sequence homologue E3 ubiquitin protein ligase (Cbl) (Duval et al., 2003) and adaptor protein CD2-associated protein (CD2AP), followed by association with clathrin (Kobayashi et al., 2004).

VEGFR2 is localised to the Golgi, plasma membrane, early endosomes and perinuclear caveolae in non-stimulated endothelial cells (Bruns et al., 2009, Jopling et al., 2011, Manickam et al., 2011, Bhattacharya et al., 2005). Resting VEGFR2 is distributed between the plasma membrane (~40%) and an internal early endosomal pool (~60%), with constitutive recycling between the two compartments (Gampel et al., 2006, Jopling et al., 2011, Jopling et al., 2014). Recent work has revealed requirement for syntaxin 6 and the kinesin motor protein, kinesin family member 13B (KIF13B) in biosynthetic VEGFR2 trafficking through the Golgi apparatus *en route* to the plasma membrane (Manickam et al., 2011, Yamada et al., 2014). Resting VEGFR2 undergoes a relatively fast rate of ligand-independent, constitutive internalisation which does not require tyrosine kinase activity (Gampel et al., 2006, Lampugnani et al., 2006, Jopling et al., 2011). However, phosphorylation of residues Y1054 and Y1059 is required for clathrin-dependent internalisation of activated VEGFR2 (Dougher and Terman, 1999).

Activated VEGFR2 undergoes endocytosis and targeting for recycling or degradation (Miaczynska et al., 2004) (Fig. 1.13). VEGF-A stimulation promotes ~40-60% degradation of plasma membrane and endosomal VEGFR2 pools (Gampel et al., 2006). VEGFR2 redistributes from early to late endosomes depending on VEGF-A concentration and duration of stimulation; nonetheless, a significant early endosomal pool of VEGFR2 is maintained (Gampel et al., 2006).

1.8.4. Receptor tyrosine kinase internalisation

Internalisation of resting VEGFR2 is clathrin-dependent (Lampugnani et al., 2006, Bruns et al., 2010). Upon VEGF-A stimulation, exit of VEGFR2 from lipid rafts/caveolae facilitates clathrin-dependent endocytosis (Jopling et al., 2011). Limited EGF stimulation results in almost exclusive clathrin-dependent internalisation of non-ubiquitinated EGFR and promotes onwards recycling (Fig. 1.14). Higher concentrations

of EGF saturate clathrin-dependent endocytosis, causing ubiquitinated EGFR to preferentially internalise by a clathrin-independent, lipid raft-dependent pathway that promotes lysosomal degradation (Sigismund et al., 2005, Sigismund et al., 2013) (Fig. 1.14). Similarly, the chosen method of VEGFR2 internalisation could depend upon receptor fate. Nonetheless, release of receptors from adherens junctions (Lampugnani et al., 2006) or caveolae (Labrecque et al., 2003) seems to be an indispensable step in receptor internalisation.

Caveolae consist of lipid raft domains enriched in the scaffold protein, caveolin-1, sphingolipids and cholesterol. VEGFR2 is enriched in plasma membrane caveolae and could preferentially internalise via a caveolar pathway when being directed for degradation (Feng et al., 2000). Activated VEGFR2 exits lipid raft/caveolae fractions and associates with ADP ribosylation factor 6 (ARF6) and Ras-related C3 botulinum toxin substrate 1 (RAC1) in focal adhesions, where it interacts with a subpopulation of Tyr14 phosphorylated caveolin before transport to perinuclear caveosomes via a clathrin-independent pathway (Labrecque et al., 2003). Clathrin-dependent versus clathrin-independent internalisation of VEGFR1 and VEGFR2 could imply that receptor homodimers are segregated into discrete regions of the plasma membrane and are internalised by two independent pathways (Mukherjee et al., 2006). Other reports have found no evidence for caveolin-dependent VEGFR2 internalisation (Lampugnani et al., 2006).

Ubiquitination and/or phosphorylation of RTKs provides a sorting signal which adaptor proteins identify to initiate clathrin-dependent endocytosis (Heilker et al., 1999). Adaptor protein complexes select cargo for inclusion into vesicles, recruit soluble clathrin and initiate clathrin polymerisation. Clathrin-coated pits (CCPs) are formed when clathrin polymerisation promotes membrane scission. Detachment from the plasma membrane is controlled by the GTPase, dynamin-2 (Huang et al., 2003, van Delft et al., 1997). The adaptor protein-2 (AP-2) complex is heterotetrameric and mediates clathrin-dependent EGFR endocytosis by binding to dileucine/tyrosine-based cytoplasmic sorting motifs (Huang et al., 2003). AP-2 independent mechanisms of EGFR internalisation have been identified including a pathway involving the SH2 domain-containing protein, Grb2 (Jiang et al., 2003).

EGFR ubiquitination is associated with receptor internalisation, particularly in the presence of high ligand concentrations where UIM-containing adaptor proteins recruit ubiquitinated receptors to CCPs (Sigismund et al., 2005). Internalisation of Tropomyosin receptor kinase A (TrkA) receptor upon nerve growth factor (NGF) binding is also dependent on ubiquitination. Conflicting studies suggest that ubiquitination is dispensable for EGFR internalisation (Huang et al., 2007) whilst G-protein-coupled receptors (GPCRs) internalise through an ubiquitin-independent, clathrin-dependent pathway. (Tanowitz and Von Zastrow, 2002). Additionally, FGFR1 and TGF-β receptor undergo constitutive internalisation independently of tyrosine kinase activity (Reilly et al., 2004).

1.8.5. The role of Rab GTPases

Ubiquitinated VEGFR2 travels through the endosome-lysosome system via a series of targeted fusion steps regulated by decreasing vesicular pH. Following clathrin-dependent endocytosis, the small Rab GTPase family members, Rab5a and Rab7a, have regulatory roles in VEGFR2 trafficking and signal transduction in early and late endosomes respectively (Jopling et al., 2009, Rodman and Wandinger-Ness, 2000) (Fig. 1.13). Rab proteins are members of the Ras superfamily of small GTPases localised to distinct intracellular organelles and perform vital roles in membrane trafficking (Stenmark and Olkkonen, 2001). As molecular switches, Rab GTPases cycle between an inactive GDP-bound state and an active GTP-bound state (Grosshans 2006). Guanine nucleotide exchange factors (GEFs) promote GTP binding whilst GTPase-activating proteins (GAPs) increase GTP to GDP hydrolysis to regulate nucleotide exchange (Mohrmann and van der Sluijs, 1999). Active Rab proteins interact with multiple effector proteins to co-ordinate membrane trafficking through the endocytic pathway (Jordens et al., 2005). Rab localisation within the endosomal membrane is restricted by recruitment of specific effector proteins (de Renzis et al., 2002). Rab proteins fulfil their essential role in membrane transport through interaction with the soluble N-ethylmaleimide-sensitive attachment protein receptors (SNAREs), recruitment of motor proteins and vesicle tethering and fusion (Grosshans et al., 2006, Woodman, 2000).
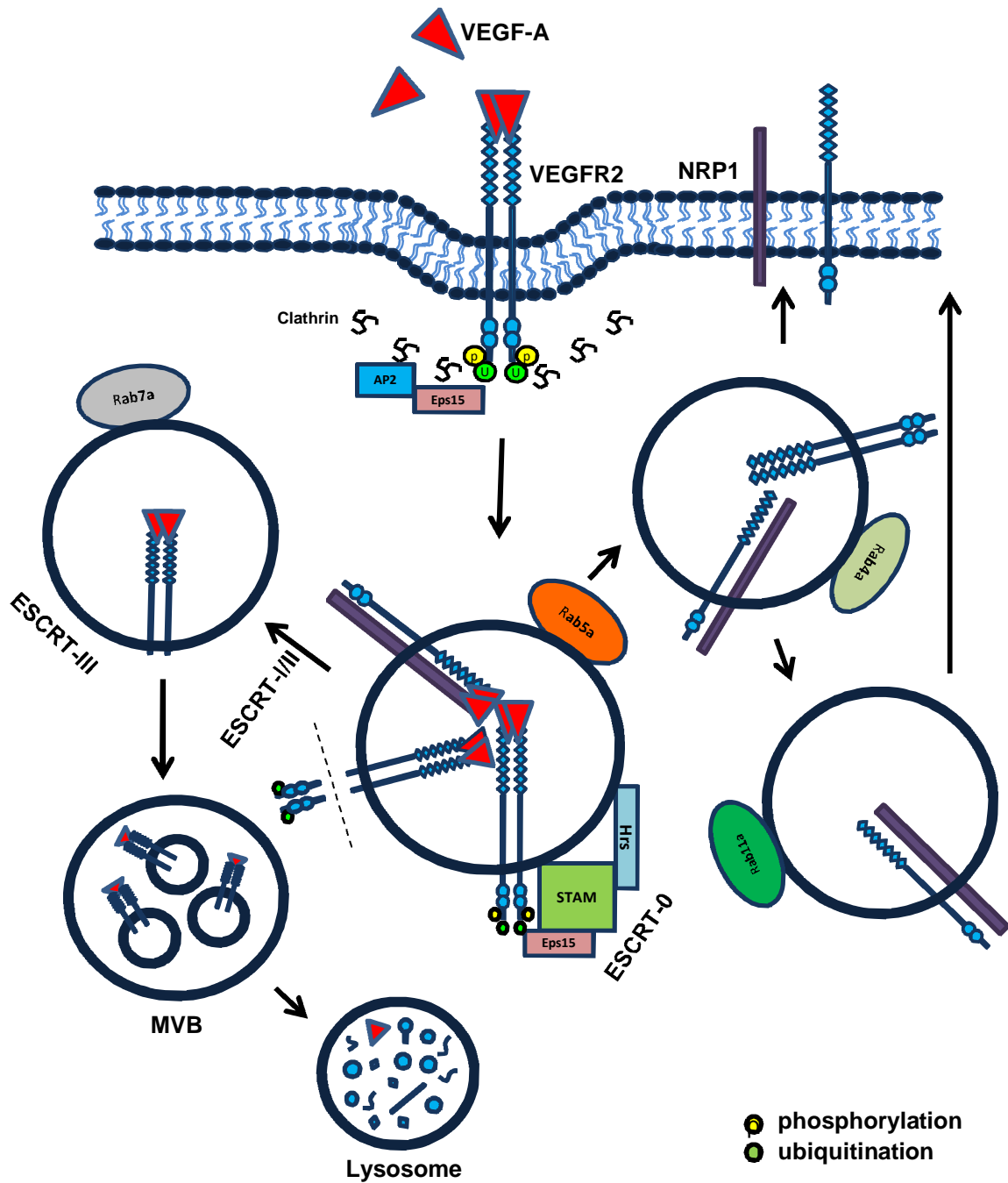
Figure 1.13. VEGFR2 trafficking through the endosome-lysosome system. Activated VEGFR2 undergoes clathrin-dependent endocytosis and delivery to ESCRT-0-positive early endosomes. This endosomal VEGFR2 is recycled back to the plasma membrane or trafficked to late endosomes and multivesicular bodies (MVBs) for terminal lysosomal degradation.
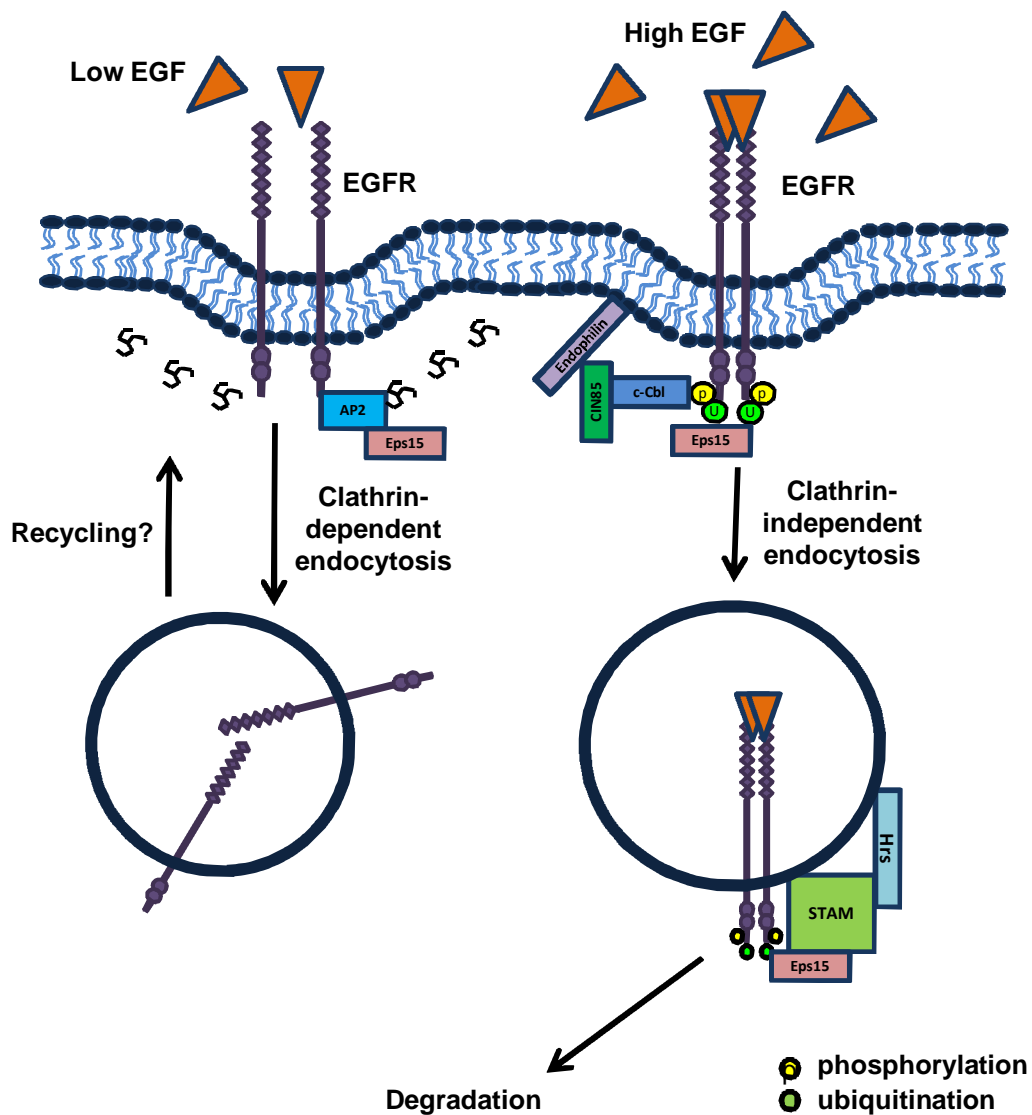
Figure 1.14. Endocytosis of EGFR. During low levels of EGF, an EGFR dileucine/tyrosine cytoplasmic motif is recognised by AP2 resulting in clathrin-dependent endocytosis. High levels of EGF cause saturation of such endocytic routes and EGFR is now internalised through a clathrin-independent, caveolae-linked pathway. Only ubiquitinated EGFR is able to internalise via this pathway after recruitment of the E3 ligase, c-Cbl.

1.8.6. Endosome-linked signal transduction

Following VEGF-A stimulation, phosphorylated and ubiquitinated VEGFR2 is transported to early endosomes after recognition by the ubiquitin-linked receptor complex, ESCRT-0 (Grabbe et al., 2011). Increasing evidence has suggested a link between RTK trafficking and signalling from early endosomes. Early endosomal localisation of VEGFR2 is essential for optimal activation of Akt and ERK1/2 signal transduction pathways (Lanahan et al., 2010, Wang et al., 2010b). In contrast, PLCγ1 and p38 MAPK signalling is linked to cell surface VEGFR2 localisation (Lampugnani et al., 2006, Chen et al., 2010, Sawamiphak et al., 2010). The rate of ligand-induced RTK internalisation is often higher than the rate of lysosomal degradation, resulting in prolonged localisation of signalling receptors in early endosomes (Sorkin and Von Zastrow, 2002). Co-localisation of signalling adaptor proteins Grb2, Shc and Son of Sevenless (SOS) with endosomal EGFR is linked to continued Ras signal transduction (Sorkin et al., 2000, Di Guglielmo et al., 1994, Oksvold et al., 2001). The level of internalisation of a range of plasma membrane receptors dictates MAPK activation, suggesting the existence of a 'signalling endosome' from which activated receptors continue to co-ordinate downstream signal transduction pathways (von Zastrow and Sorkin, 2007). Inhibition of EGFR, GPCR and β_2-adrenergic receptor (β_2AR) endocytosis supresses activation of MAPK and PI3K signalling (Vieira et al., 1996, Daaka et al., 1998). Furthermore, internalisation rate influences temporal regulation of plasma membrane signal transduction, thus the endosome may provide a mechanism to prolong intracellular signalling (von Zastrow and Sorkin, 2007). Interestingly, differential growth factor binding also alters signalling output. For example, EGF and TGF-α dissociate from EGFR at different points along the endocytic pathway as a result of individual sensitivities to endosomal pH (Sorkin and Von Zastrow, 2002).

Endosomes also direct spatial regulation of signalling events. The distinct biochemical composition of endosomal membranes (i.e. enrichment of PtdIns-3-P) enables the selective recruitment of signalling mediators. This could promote a greater level of specificity by preventing unwanted interactions between signalling adaptors, many of which are shared by different pathways (Miaczynska et al., 2004).

1.8.7. VEGFR2 recycling

A primary role of early endosomes is to sort proteins for lysosomal degradation or recycling. RTKs can recycle multiple times to the plasma membrane before commitment to lysosomal degradation. Upon removal of ligand, receptors are free to re-integrate into the plasma membrane and respond to additional growth factor (Sorkin et al., 1991). Constitutive RTK recycling is rare; the majority of RTKs are localised to the plasma membrane and undergo a slow rate of constitutive internalisation (Herbst et al., 1994). However, TGF-β receptor constitutively recycles via a perinuclear compartment with internalisation and recycling rates unaffected by ligand (Mitchell et al., 2004). Constitutive recycling pathways between the plasma membrane and early endosome have also been described for several GPCRs, neurokinin-1 receptor (NK1R) and the cannabinoid receptor, CB1 (Roosterman et al., 2004, Leterrier et al., 2004).

Upregulation of VEGFR2 recycling upon VEGF-A stimulation is evidenced by the clustering of small VEGFR2-positive vesicles beneath the plasma membrane which do not stain with clathrin antibodies but associate with microtubules just below the cell surface (Gampel et al., 2006). Recycling of activated VEGFR2 occurs through Rab4a- or Rab11a-positive endosomes and follows a short loop (Rab4a) or long loop (Rab11a) pathway (Ballmer-Hofer et al., 2011, Jopling et al., 2014) (Fig. 1.13). Long loop recycling occurs in coordination with NRP1 trafficking following transition from Rab4a-postive vesicles. Rab4a-Rab11a transition is co-ordinated by interaction between the C-terminal PDZ-binding motif of synectin, myosin VI and the NRP-1 C-terminal motif, SEA (Ser-Glu-Ala) (Ballmer-Hofer et al., 2011, Cai and Reed, 1999, Wang et al., 2003, Chittenden et al., 2006). Receptor recycling via Rab11a-positive endosomes is VEGF-A isoform-dependent. For example, VEGF-A$_{165b}$ is unable to bind NRP1 and fails to promote Rab11a-dependent recycling (Ballmer-Hofer et al., 2011). In contrast to VEGFR2, EGFR and PDGFR have very low rates of recycling and are instead targeted for immediate lysosomal degradation upon ligand stimulation, providing more permanent signalling down-regulation (Rubin et al., 2005, Marmor and Yarden, 2004).

There is evidence to suggest that VEGFR2 is recycled through a non-conventional pathway in VEGF-stimulated cells (Gampel et al., 2006). Phosphorylated VEGFR2 can undergo VE-cadherin-mediated, clathrin-dependent internalisation into endosomal

compartments where it avoids degradation, retains activation of signalling pathways and promotes sustained cell migration and proliferation (Lampugnani et al., 2006). VEGFR2 is internalised more rapidly when VE-cadherin is absent or not clustered at intercellular contacts (Lampugnani et al., 2006). Interaction between VEGFR2 and VE-cadherin blocks receptor-mediated endocytosis and increases CD148-dependent tyrosine de-phosphorylation (Lampugnani et al., 2006). Activated VEGFR2 recruits adaptor protein TSAd which activates downstream tyrosine kinase, c-Src (Sun et al., 2012). Src activation of PAK2 mediates phosphorylation of serine residues on VE-cadherin at multiple sites located within the binding region for p120-catenin (Weis et al., 2004, Adam et al., 2010). Subsequent dissociation of p120-catenin and VE-cadherin exposes a short endocytic motif (DEE), leading to disruption of adherens junctions and promoting vascular permeability (Nanes et al., 2012). VEGFR2 and VE-cadherin are sorted at the plasma membrane, follow independent endocytic pathways and do not co-localise within endocytic vesicles (Sandilands et al., 2004). c-Src undergoes a novel endocytic recycling pathway and co-localises with peripheral VEGFR2-positive vesicles in VEGF-A-stimulated cells (Gampel et al., 2006, Sandilands et al., 2004). Thus, both VEGFR2 and c-Src are recycled together through the same endocytic recycling pathway. In quiescent endothelial cells, VEGFR2 is stored in intracellular Rab4/Rab11-negative vesicles and delivered to the plasma membrane in a c-Src activation-dependant manner in response to VEGF-A (Gampel et al., 2006); uniquely to other RTKs. Recycling vesicles are targeted towards the leading edge of the cell in migrating fibroblasts to enhance response to chemotactic signals and promote forward movement in response to EGF (Bailly et al., 2000). Similar events may occur to VEGFR2 in endothelial cells to reinforce guidance of the tip cell towards the pro-angiogenic signal (Gerhardt et al., 2003).

1.9. VEGFR2 proteolysis

Intrinsic tyrosine kinase activity of VEGFR2 precedes receptor ubiquitination and is required for VEGF-dependent down-regulation (Ewan et al., 2006, Singh et al., 2005). K48-linked polyubiquitin chains mediate VEGFR2 degradation whilst K63-linked polyubiquitin is associated with receptor trafficking (Meyer et al., 2011). Internalised VEGFR2 continues to signal from multiple cellular compartments until it is committed for recycling or degradation (Murdaca et al., 2004). VEGFR2 is directed for lysosomal

degradation after ubiquitination by E3 ligases c-Cbl or β-transducin repeat containing E3 ubiquitin protein ligase (β-TrCP1) (Bruns et al., 2010, Meyer et al., 2011, Duval et al., 2003).

1.9.1. The role of c-Cbl

VEGF-A stimulates RING domain-containing E3 ubiquitin ligase, c-Cbl, to promote VEGFR2 ubiquitination, signalling down-regulation and lysosomal degradation (Duval et al., 2003). However, contradictory studies suggest that c-Cbl activity is dispensable for VEGFR2 ubiquitination and proteolysis (Singh et al., 2005, Singh et al., 2007). Alternatively, active c-Cbl could process ubiquitin signals for MVB sorting to indirectly down-regulate VEGFR2 activity (Le Roy and Wrana, 2005).

One possibility is that c-Cbl targets PLCγ1 for VEGF-A-stimulated ubiquitination whilst a different E3 enzyme ubiquitinates VEGFR2 (Singh et al., 2007). PLCγ1 is an essential adaptor for c-Cbl binding to pY1054 and pY1057 residues located within the VEGFR2 tyrosine kinase domain. VEGFR2-mediated activation of c-Cbl suppresses phosphorylation and promotes ubiquitination of PLCγ1 without effecting its degradation (Singh et al., 2007, Meyer et al., 2011). c-Cbl-mediated down-regulation of PLCγ1 activity may encourage direct recruitment of other binding partners and intracellular signalling adaptors to shift the balance of signals transmitted from VEGFR2 to favour its degradation.

EGFR undergoes tyrosine phosphorylation-dependent, c-Cbl-mediated ubiquitination and degradation (Lu and Hunter, 2009). c-Cbl mono-ubiquitinates tyrosine phosphorylated EGFR at the plasma membrane and remains associated with the receptor during its transport through the endocytic pathway prior to lysosomal degradation (de Melker et al., 2001, Haglund et al., 2003a) (Fig. 1.14). Grb2 binding to activated EGFR mediates interaction with c-Cbl (Huang and Sorkin, 2005). Limited EGFR ubiquitination could be sufficient to attach activated EGFR-c-Cbl complexes to the UIM of Hrs and facilitate downstream regulatory events, including degradation (Stern et al., 2008, Urbe et al., 2003). At the plasma membrane c-Cbl can ubiquitinate its own negative regulator, Sprouty2, in a ligand-dependent manner, restoring its ability to bind EGFR and promote receptor ubiquitination (Rubin et al., 2003). Cbl-interacting

protein 85 (CIN85) is recruited to endophilin and disabled 2 (DAB2) to promote both clathrin-dependent and clathrin-independent EGFR endocytosis (Soubeyran et al., 2002, Kowanetz et al., 2003a, Kowanetz et al., 2003b, Sigismund et al., 2005) (Fig. 1.14). CIN85 and c-Cbl are mono-ubiquitinated after receptor activation; CIN85 binds multiple molecules of c-Cbl and the resulting oligomer leads to clustering of activated EGFR (Kowanetz et al., 2003a). Ubiquitination of c-Cbl provides binding sites for other UIM-containing endocytic adaptor proteins, such as epsin and Eps15, thus aiding endosomal recruitment of EGFR (Le Roy and Wrana, 2005). Adaptor protein, Alix, interacts with c-Cbl via direct binding to CIN85 and endophilins and decreases EGFR internalisation and ubiquitination in an activation-independent manner (Schmidt et al., 2004). However, phosphorylation by Src kinases antagonises the inhibitory function of Alix on receptor endocytosis (Schmidt et al., 2005). Furthermore, modulation of Hrs ubiquitination, phosphorylation and protein levels by c-Cbl may influence composition of the endocytic sorting machinery to provoke EGFR lysosomal degradation; regulating the fate of both Hrs and EGFR at the level of endosomal sorting (Stern et al., 2007).

1.9.2. The role of Nedd4

The HECT domain-containing E3 enzyme, Nedd4, mediates mono-ubiquitination of ubiquitin receptors such as Hrs, Eps15 and epsins. Hrs is proposed to be involved in endosomal sorting of activated VEGFR2 and displays increased tyrosine phosphorylation following VEGF stimulation (Ewan et al., 2006). As an indirect consequence of the ubiquitination of proteins involved in VEGFR2 endocytosis, Nedd4 has been proposed to play a role in activated VEGFR2 degradation but no role in its ubiquitination. Decreased levels of VEGFR2 following Nedd4 expression imply a role for Nedd4 in VEGFR2 down-regulation (Murdaca et al., 2004). Conversely, Nedd4 can protect EGFR from c-Cbl mediated degradation by ubiquitinating c-Cbl and targeting it for proteasomal degradation, thereby prolonging EGFR signalling (Katz et al., 2002, Magnifico et al., 2003). Interestingly, direct association between Grb10 and Nedd4 blocks VEGFR2 degradation (Murdaca et al., 2004). Excess Grb10 could sequester Nedd4 in the cytoplasm or disrupt the Nedd4-Grb10-Eps15 ternary complex and thereby restrict receptor endocytosis (Murdaca et al., 2004). Similarly, Sprouty-2 sequesters c-Cbl away from activated EGFR to prevent its degradation (Dikic and Giordano, 2003, Haglund et al., 2005, Takayama et al., 2005).

1.9.3. The role of β-TrcP1

The PEST (rich in Pro, Glu, Ser and Thr residues) motif is commonly found in short-lived proteins degraded by the ubiquitin system (Rechsteiner and Rogers, 1996). VEGFR2 has a unique C-terminal PEST domain-like sequence with eight possible serine/threonine phosphorylation sites which promote VEGFR2 ubiquitination and down-regulation. Activation of the protein kinase A (PKA) and p38 MAPK pathways upon Y1175 phosphorylation attenuates VEGFR2 degradation (Meyer et al., 2011). In contrast, pS1188 and pS1191 epitopes promote VEGFR2 ubiquitination and degradation. The phosphodegron motif, pS1188, recruits certain F-box-containing E3 ubiquitin ligases to VEGFR2. Some studies on F-box containing E3 ligase, β-TrcP1, suggest that it targets VEGFR2 for 26S proteasome-mediated degradation (Meyer et al., 2011). Other studies have shown that a related E3 enzyme, β-TrcP2, is not required for VEGFR2 ubiquitination (Bruns et al., 2010).

1.9.4. The role of PKC

VEGF-A-stimulated ubiquitination or activation of non-classical PKC isozymes promotes increased trafficking and proteolysis of VEGFR2 in the endosome-lysosome system (Bruns et al., 2010, Ewan et al., 2006, Jopling et al., 2009, Singh et al., 2005). VEGF-A may promote degradation of VEGFR2 independently of c-Cbl and PLCγ1 by downstream activation of non-classical PKC isozymes (signalling components that negatively regulate VEGFR2 signal transduction at the receptor level). Direct or indirect (by another serine/threonine kinase) PKC-mediated S1188 and S1191 phosphorylation of the VEGFR2 C-terminal domain marks the receptor for PKC-mediated internalisation and proteasomal degradation (Singh et al., 2005). PKC activation is associated with metalloproteinase mediated ectodomain 'shedding' from transmembrane receptors to release biologically active extracellular or cytoplasmic domain fragments. However, inhibition of metalloproteinases and γ-secretases has no effect on VEGFR2 proteolysis (Bruns et al., 2010). It is unknown whether PKC-stimulated internalisation of VEGFR2 follows a caveolae- or clathrin-mediated pathway. In contrast to VEGFR2, PKC-mediated EGFR phosphorylation inhibits tyrosine kinase activation to down-regulate receptor signalling rather than stimulate degradation (Lund et al., 1990).

1.9.5. VEGFR2 proteolytic fragments

VEGFR2 proteolysis is tightly regulated with evidence for at least two distinct proteolytic events associated with the endosome-lysosome system. A 26S proteasome-regulated step, associated with early endosomes and C-terminal domain cleavage, occurs prior to lysosomal processing of the extracellular/luminal domain (Ewan et al., 2006, Bruns et al., 2010) (Fig. 1.13). Post-translational modification and recruitment of signalling proteins bestows the VEGFR2 C-terminal domain with important regulatory roles in VEGFR2 stability and signalling (Meyer et al., 2011). Proteasome-mediated VEGFR2 proteolysis regulates signal transduction through the Akt, eNOS and MAPK pathways (Bruns et al., 2010). VEGF-A stimulation causes degradation of mature VEGFR2 and an associated increase in levels of a 160 kDa VEGFR2-related polypeptide (Ewan et al., 2006, Bruns et al., 2010). Production of the 160 kDa fragment requires VEGF-A-stimulated tyrosine kinase activity and results from cytoplasmic domain removal within an endosomal compartment (Bruns et al., 2010). VEGFR2 monoubiquitination precedes production of the 160 kDa fragment and could provide a sorting signal to mediate proteasome recognition on early endosomes before final degradation in the lysosome (Bruns et al., 2010) (Fig. 1.13). Limited proteolysis of activated, endosomal VEGFR2 alters intracellular signalling outputs and endothelial cell migration (Bruns et al., 2010). The VEGFR2 C-terminal domain appears to control receptor activity by playing a central role in both receptor signalling and degradation (Singh et al., 2005).

1.9.6. The role of chaperone proteins in VEGFR2 degradation

Chaperone proteins such as heat shock protein (HSP) of 70 kDa (HSP70) and related family member, HSP90, are implicated in VEGFR2 ubiquitination, trafficking and turnover (Bruns et al., 2012). HSP70 is associated with VEGFR2 degradation following clathrin-dependent endocytosis whilst HSP90 stabilises VEGFR2 levels (Bruns et al., 2012). Thus, the HSP70-HSP90 axis is essential for regulating VEGFR2 homeostasis. Another chaperone protein involved in VEGFR2 stabilisation is phosducin-like 3 (PDCL3). Receptor ubiquitination and degradation is inhibited by binding of PDCL3 to the juxtamembrane domain of VEGFR2 thus increasing VEGF-A-stimulated tyrosine phosphorylation (Srinivasan et al., 2013).

1.10. Hypothesis and Aims

In heart attack patients there is a clinical need to promote vascular regeneration after angioplasty, stenting or coronary artery bypass surgery. Angiogenesis can stimulate arterial repair after heart attacks. Endothelial cells line all blood vessels and express VEGFR2 to bind soluble VEGF-A, stimulating angiogenesis. VEGF-A-stimulates VEGFR2 ubiquitination and downstream proteolysis but the regulatory factors involved are unclear. This project aims to use RNAi screening as a tool to identify ubiquitinating and DUB enzymes that regulate VEGFR2 turnover in primary human endothelial cells. Such understanding could be used to manipulate VEGFR2 levels, thus altering endothelial function and stimulating vascular regeneration in cardiovascular disease. A central hypothesis is that VEGFR2 ubiquitination is linked to downstream signalling outputs and endothelial function. Such work is also relevant to diseases defined by excessive angiogenesis such as cancer, ocular and inflammatory disorders where ubiquitination enzyme activity or inhibition of DUBs could restrict angiogenesis and be of therapeutic benefit.

VEGF gene therapy or administration of recombinant VEGF-A to stimulate blood vessel repair has proved problematic with side effects such as oedema and tissue swelling (Isner et al., 1996). An alternative, less explored approach is to target VEGFR-associated proteins (effectors) that modulate proteolytic sensitivity, thus promoting a better pro-angiogenic outcome in cardiovascular disease therapy. This work tests the hypothesis that manipulation of VEGFR2 ubiquitination and proteolysis affects vascular outputs such as endothelial cell migration and tubulogenesis, key requirements for vascular repair and regeneration. In the longer term, using gene therapy and/or small molecule inhibitors that target ubiquitin-modifying enzymes could provide improved treatments for damaged arteries. The combined experimental approaches described in this thesis will further our understanding of the role of post-translational VEGFR2 modification on the endothelial response to VEGF-A at a biochemical, cellular and functional level.

CHAPTER 2

MATERIALS AND METHODS

2.1. Materials

2.1.1. General reagents

Recombinant VEGF-A$_{165}$ was gifted from Genentech Inc. (San Francisco, USA). All chemicals were of analytical grade and purchased from Sigma-Aldrich (Poole, UK) unless stated otherwise. Primary and secondary antibodies were used as described in Table 2.1.

2.1.2. Primary cells

Human dermal microvascular endothelial cells (HDMECs) were purchased from PromoCell (Heidelberg, Germany). Human umbilical vein endothelial cells (HUVECs) were isolated from umbilical cords obtained with informed patient consent from patients undergoing elective Caesarean section at Leeds General Infirmary. Ethical approval (reference CA03/020) was granted by the Leeds NHS Hospitals Local Ethics Committee (UK).

2.2. Methods

2.2.1. Isolation of primary HUVECs

The umbilical vein was cannulated with an 18-gauge blunt needle and flushed twice with 50 ml PBS. The umbilical cord was clamped at one end using a haemostat and the umbilical vein filled with 0.1% (w/v) type IIS collagenase in MCDB131 (Life Technologies, Paisley, UK) for 20 min to detach the endothelial cells. The vein was flushed with 50 ml PBS and the detached cells collected. Cells were pelleted via centrifugation at 140 g for 5 min. The supernatant was aspirated and cells re-suspended in endothelial cell growth medium (ECGM) containing 50 ng/ml amphotericin B. Cells were seeded into a 75 cm^2 vented tissue culture flask (Nunc, Copenhagen, Denmark) pre-coated with 0.1% (w/v) pig skin gelatin (PSG). After 24 h, the cells were washed with PBS 5 times and the medium replaced. Isolated cells were characterised via

Antigen	Species	Concentration (mg/ml)	Dilution factor	Source
Akt	Rabbit	0.5	IB: 1:1000	Cell Signal Technology (Massachusetts, USA)
phospho-Akt (S473)	Rabbit	0.5	IB: 1:1000	Cell Signal Technology (Massachusetts, USA)
CD63	Mouse	0.25	IF: 1:200	AbCam (Cambridge, UK)
EEA1	Mouse	0.25	IF: 1:200	BD Transduction Labs (Oxford, UK)
eNOS	Rabbit	0.5	IB: 1:1000	Cell Signal Technology (Massachusetts, USA)
phospho-eNOS (S117)	Rabbit	0.5	IB: 1:1000	Cell Signal Technology (Massachusetts, USA)
ERK1/2	Rabbit	0.5	IB: 1:1000	Cell Signal Technology (Massachusetts, USA)
phospho-ERK1/2 (T202/Y204)	Mouse	0.5	IB: 1:1000	Cell Signal Technology (Massachusetts, USA)
Goat IgG	Donkey, HRP	0.4	IB: 1:5000	Stratech Scientific (Newmarket, UK)
Goat IgG	Donkey, AlexaFluor 488	2.0	IF: 1:200	Life Technologies (Paisley, UK)
LAMP2	Mouse	0.5	IF: 1:100	Santa Cruz Antibodies (California, USA)
Mouse IgG	Donkey HRP	0.4	IB: 1:5000	Stratech Scientific (Newmarket, UK)
Mouse IgG	Donkey, AlexaFluor 594	2.0	IF: 1:200	Life Technologies (Paisley, UK)
p38 MAPK	Rabbit	0.5	IB: 1:1000	Cell Signal Technology (Massachusetts, USA)
phospho- p38 MAPK (T180/Y182)	Rabbit	0.5	IB: 1:1000	Cell Signal Technology (Massachusetts, USA)
PECAM1 (CD31)	Mouse	0.2	IF: 1:1000	Santa Cruz Antibodies (California, USA)
PLCγ1	Rabbit	0.5	IB: 1:1000	Cell Signal Technology (Massachusetts, USA)
phospho-PLCγ1 (Y783)	Rabbit	0.5	IB: 1:1000	Cell Signal Technology (Massachusetts, USA)
Rabbit IgG	Donkey, HRP	0.4	IB: 1:5000	Stratech Scientific (Newmarket, UK)
Rabbit IgG	Donkey, AlexaFluor 594	2.0	IF: 1:200	Life Technologies (Paisley, UK)
TGN46	Rabbit	1.0	IF: 1:1000	University of Leeds
Transferrin receptor (TfR; CD71)	Mouse	0.2	IB: 1:1000	Santa Cruz Antibodies (California, USA)
α-tubulin	Mouse	2.0	IB: 1:8000	Sigma Aldrich (Poole, UK)
UBA1	Rabbit	0.5	IB: 1:1000	Cell Signal Technology (Massachusetts, USA)
UBE2D1	Rabbit	0.5	IB: 1:1000	AbCam (Cambridge, UK)
UBE2D2	Rabbit	0.5	IB: 1:1000	AbCam (Cambridge, UK)
USP8	Rabbit	0.5	IB: 1:1000	Cell Signal Technology (Massachusetts, USA)
Ubiquitin (FK2)	Mouse	0.5	IB: 1:1000	Caymen Chemicals (Michigan, USA)
K48-linked ubiquitin (Apu2)	Rabbit	0.5	IB: 1:1000	Millipore (Watford, UK)
K63-linked ubiquitin (Apu3)	Rabbit	0.5	IB: 1:1000	Millipore (Watford, UK)
VEGFR1	Goat	0.1	IB: 1:1000 IF: 1:100	R&D Systems (Minnesota, USA)
VEGFR2 extracellular domain	Goat	0.1	IB: 1:1000 IF: 1:100	R&D Systems (Minnesota, USA)
VEGFR2 cytoplasmic domain	Goat	0.1	IB: 1:1000	University of Leeds
phospho-VEGFR2 (Y1175)	Rabbit	0.5	IB: 1:1000	Cell Signal Technology (Massachusetts, USA)

Table 2.1. Primary and secondary antibodies. Details of antibody species, concentration, dilution factor and source. IB; immunoblot, IF; immunofluorescence.

immunofluorescence microscopy of common endothelial cell markers (Fig. 2.1).

2.2.2. Cell passage

HUVECs were cultured in ECGM in a T75 vented tissue culture flask pre-coated with 0.1% (w/v) PSG and incubated at 37°C in a hydrated 5% CO_2 atmosphere until ~70-80% confluent. ECGM was aspirated and the cells washed in PBS prior to incubation in 1 ml TrypLE^{TM} Express (Invitrogen, Amsterdam, Netherlands) at 37°C for 4 min. Trypsinisation was quenched with 5 ml DMEM (+10% foetal calf serum (Life Technologies)). Cells were centrifuged at 140 g for 5 min and the pellet re-suspended in 6 ml ECGM. The ECGM was replaced every 2 days. Cells were split 1:3 and cultured up to passage 5.

2.2.3. VEGF-A stimulation for analysis of intracellular signalling pathways and pharmacological inhibition of protein synthesis or ubiquitination

Endothelial cells were serum-starved in MCDB131 (+0.2% (w/v) BSA) for 2 h prior to treatment with 25 ng/ml VEGF-A$_{165}$ (0-60 min), 20 μg/ml CHX (0-80 min) or 10 μM PYR41 (1 h) and lysed for immunoblotting or immunofluorescence microscopy.

2.2.4. Adhiron treatment of cells

HUVECs were serum-starved in MCDB131 (+0.2% (w/v) BSA) for 2 h, pre-treated with 100 μg/ml Adhiron for 30 min and stimulated with 25 ng/ml VEGF-A.

2.2.5. Preparation of whole cell lysates

Medium was aspirated and cells washed twice with ice-cold PBS. Cells were lysed in 2% (w/v) SDS (+ 1mM PMSF, in PBS) and detached using a sterile cell scraper. Lysates were stored at -20°C. For immunoblot analysis, lysates were incubated at 95°C for 5 min and sonicated for 3 s. Protein concentration was determined using a bicinchoninic acid (BCA) assay.

2.2.6. Lipid-based transfection of siRNA duplexes

Endothelial cells were reverse transfected using lipofectamine RNAiMax (Invitrogen) in
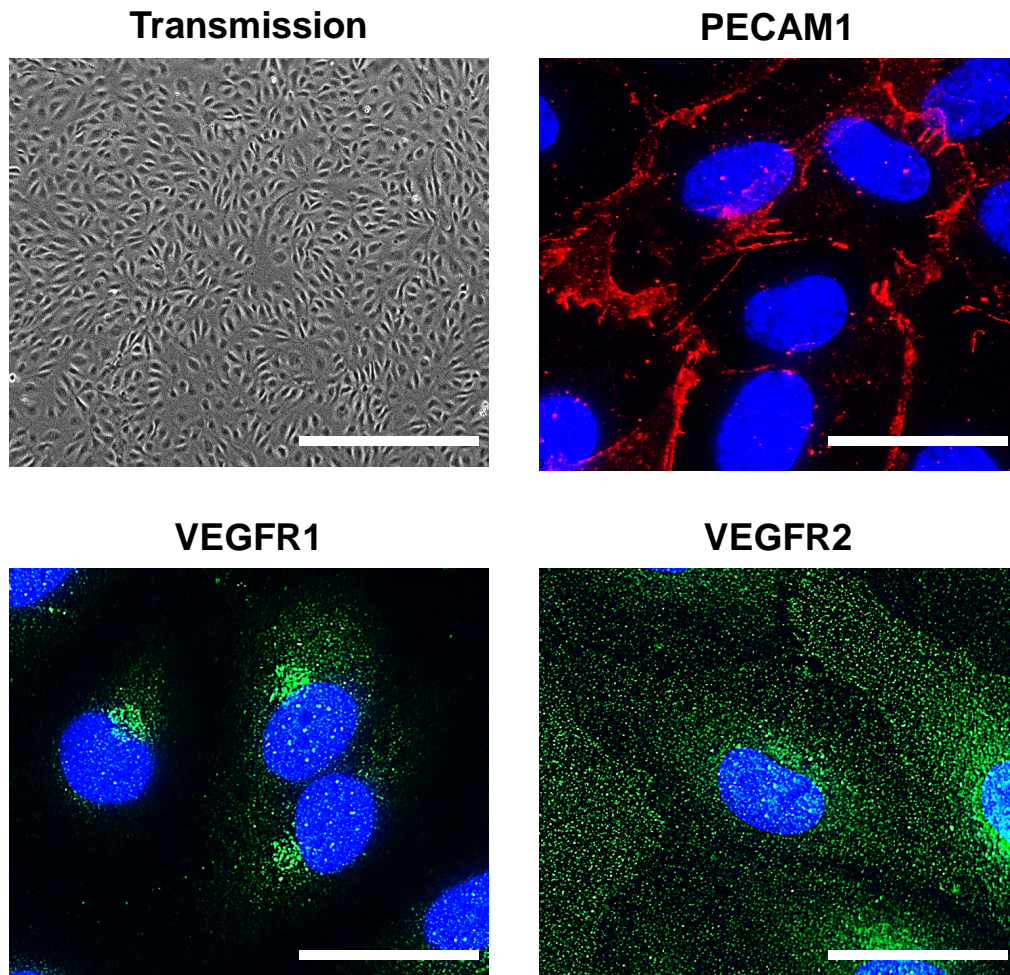
Figure 2.1. Characterisation of HUVECs. (A) A confluent HUVEC monolayer grown on gelatin-coated surfaces and visualised by phase-contrast microscopy at 4x magnification. Scale bar represents 1000 μm. Immunofluorescence microscopy of confluent HUVECs labelled with primary antibodies to (B) PECAM1, (C) VEGFR1 or (D) VEGFR2 followed by species-specific secondary antibodies (green). Nuclei were stained with DNA-binding dye, DAPI (blue). Scale bar represents 70 μm.

6- or 96-well plates with siRNA duplexes as follows.

20 nM non-targeting control siRNA:

5'-UGGUUUACAUGUCGACUAA-3'

5'-UGGUUUACAUGUUGUGUGA-3'

5'-UGGUUUACAUGUUUUCUGA-3'

5'-UGGUUUACAUGUUUUCCUA-3'

20 nM UBA1 siRNA:

5'-GCGUGGAGAUCGCUAAGAA-3'

5'-CCUUAUACCUUUAGCAUCU-3'

5'-CCACAUAUCCGGGUGACAA-3'

5'-GAAGUCAAAUCUGAAUCGA-3'

20 nM USP8 siRNA:

5'-UGAAAUACGUGACUGUUUA-3'

5'-GGACAGGACAGUAUAGAUA-3'

5'-AAAUAAAGCUCAACGAGAA-3'

5'-GGCAAGCCAUUUAAGAUUA-3'

20 nM UBE2D1 siRNA:

5'-CAACAGACAUGCAAGAGAA-3'

5'-GAAAGAAUUGAGUGAUCUA-3'

5'-UACCAGAUAUUGCACAAAU-3'

5'-GCACAAAUCUAUAAAUCAG-3'

20 nM UBE2D2 siRNA:

5'-UCAGAAGUAUGCGAUGUAA-3'

5'-CUAUCAGGGUGGAGUAUUU-3'

5'-GUCCAUCUGUUCUCUGUUG-3'

5'-CCGAAGGAGCUACGUCUUA-3'

All siGENOME SMARTpool siRNA duplexes were used according to the manufacturer's instructions (Dharmacon, GE Healthcare, Little Chalfont, UK). 15 µl of 2 µM siRNA was added to each well of a 6-well plate. 4 µl RNAiMax was incubated

with 301 µl serum/antibiotic-free OptiMEM (Invitrogen) for 5 min at room temperature. The transfection reagent mix was added to the siRNA and incubated for ~20 min at room temperature. Endothelial cells were seeded at ~250,000 cells per well in 1.2 ml serum/antibiotic-free OptiMEM. Cells were incubated for 6 h with siRNA duplexes before replacing the media with ECGM. After 72 h, cells were processed for lysis and immunoblotting or immunofluorescence microscopy.

2.2.7. SDS-PAGE

25 µg of whole cell lysate was re-suspended in an equal volume of 2X SDS sample buffer (1 M Tris-HCl pH 6.8, 20% (v/v) glycerol, 4% (w/v) SDS, 0.1% (w/v) bromophenol blue and 4% (v/v) mercaptoethanol) and incubated at 95°C for 5 min. Lysates were loaded onto a 10% (w/v) SDS-polyacrylamide resolving gel with a 5% (w/v) SDS-polyacrylamide stacking gel and run at 130 V for 90 min in SDS-running buffer (192 mM glycine, 25 mM Tris, 0.1% (w/v) SDS).

2.2.8. Immunoblotting

Proteins subjected to SDS-PAGE were transferred onto nitrocellulose membrane (0.2 µm pore size) (Schleicher & Schuell, Bath, UK) in transfer buffer (106 mM glycine, 25 mM Tris, 0.1% (w/v) SDS, 20% (v/v) methanol) at 300 mA for 3 h at 4°C. Membranes were incubated in 5% (w/v) skimmed milk (in TBS-T (20 mM Tris-HCl pH 7.6, 137 mM NaCl, 0.1% (v/v) Tween-20)) for 30-60 min on a rocker. Membranes were rinsed in TBS-T, incubated in primary antibodies (Table 2.1) overnight at 4°C and washed 3 times for 10 min in TBS-T prior to incubation in HRP-conjugated secondary antibodies (Table 2.1) for 1 h at room temperature, followed by a second round of TBS-T washes and detection using the chemiluminescent solution, EZ-ECL (Geneflow, Nottingham, UK).

2.2.9. Immunoprecipitation

HUVECs were serum-starved for 2 h prior to CHX treatment or VEGF-A stimulation, washed twice in ice-cold PBS and lysed in RIPA buffer (150 mM NaCl, 50 mM Tris-HCl, pH 7.4, 0.1% (w/v) SDS, 0.5% (w/v) sodium deoxycholate, 2 mM EDTA, 1% (v/v) NP-40, 50 mM NaF, 1 mM PMSF, 10 mM iodoacetamide) at 4°C. Lysates were cleared by centrifugation at 16000 g for 15 min at 4°C. Equal concentrations of

supernatant were incubated with 1 µg/ml goat anti-VEGFR2 for 2 h at 4°C and immunoisolated with 25 µl 50:50 protein G-Sepharose slurry (Millipore, Watford, UK) overnight at 4°C. Beads were washed 3 times in RIPA buffer and proteins eluted by heating at 95°C for 5 min in 40 µl 2X SDS sample buffer before SDS-PAGE and immunoblot analysis.

2.2.10. Cell surface biotinylation

HUVECs were serum-starved for 2 h prior to CHX treatment or VEGF-A stimulation, washed twice in ice-cold PBS, cell surface biotinylated by incubation with 0.25 mg/ml biotin (in 2 mM $CaCl_2$, 2 mM $MgCl_2$ in PBS) for 45 min at 4°C, washed in TBS to quench biotinylation and lysed in NP-40 buffer (1% (v/v) NP-40, 50 mM Tris-HCl pH 7.5, 150 mM NaCl, 1 mM PMSF) for 5 min at 4°C. Cell surface proteins were isolated using 35 µl NeutraAvidin agarose beads (ThermoFisher, Massachusetts, USA) overnight at 4°C. Beads were washed 3 times in NP-40 buffer and proteins eluted by heating at 95°C for 5 min in 40 µl 2X SDS sample buffer before SDS-PAGE and immunoblot analysis.

2.2.11. Immunofluorescence microscopy

For immunofluorescence microscopy, serum-starved HUVECs were treated with CHX or VEGF-A in 96-well plates or on coverslips before being fixed in 10% (v/v) formalin (Sigma-Aldrich) for 5 min at 37°C. Cells were washed 3 times in PBS before permeabilisation in 0.1% Triton X-100 (v/v) for 4 min at room temperature. Cells were washed 3 times in PBS and incubated in 5% (w/v) BSA (in PBS) for 60 min at room temperature to block non-specific antibody binding. Cells were washed 3 times in PBS and incubated in primary antibody diluted in 1% (w/v) BSA (in PBS) overnight at room temperature. Cells were washed 3 times in PBS and incubated in species-specific AlexaFluor-conjugated secondary antibodies and 2 µg/ml DNA-binding dye, 4',6-diamidino-2-phenylindole (DAPI) in 1% (w/v) BSA (in PBS) for 2-3 h at room temperature. Cells were washed 3 times in PBS and coverslips mounted onto slides using Fluoromount G (Southern Biotech, Alabama, USA). Images were acquired using an Evos-fI inverted digital microscope (Life Technologies) at 20X magnification or a Delta Vision wide-field deconvolution microscope (Applied Precision Inc., Issaquah,

USA) at 60X magnification. Fluorescence intensity was quantified using NIH ImageJ (http://rsb.info.nih.gov/ij/).

2.2.12. Plasma membrane protein recycling assay

Serum-starved HUVECs were incubated in VEGFR2, transferrin receptor or FGFR1 primary antibody for 30 min at 37°C before VEGF-A stimulation for 15 or 30 min at 37°C. In some experiments cells were pre-treated with 20 μM monensin. Cell surface primary antibody was stripped by washing once in acidic, serum-free MCDB131 (pH 2) at 4°C followed by washing twice in normal medium. Cells were incubated in secondary antibody (anti-sheep AlexaFlour488, Life Technologies) for 15 or 30 min (30 or 60 min total recycling time, respectively) at 37°C before fixation for 5 min at 37°C and staining with 1 μg/ml DNA-binding dye, DAPI. Only cell surface VEGFR2 that had bound primary antibody and undergone internalisation and subsequent recycling would be available to bind secondary antibody after acid-washing. Thus, only VEGFR2 that recycled one or more times was visualised. Images were acquired using an Evos-fI inverted digital microscope at 20X magnification or a Delta Vision wide-field deconvolution microscope at 60X magnification. Fluorescence intensity was quantified using NIH ImageJ (http://rsb.info.nih.gov/ij/).

2.2.13. Cell proliferation assay (BrdU incorporation)

HUVECs were seeded in 96-well plates at 2×10^3 cells per well in ECGM. After 24 h, cells were serum starved in MCDB131 (+0.2% (w/v) BSA) for 2 h prior to stimulation with 25 ng/ml VEGF-A for 24 h. At the 20 h time point 10 μM bromodeoxyuridine (BrdU) was added for 4 h and a cell proliferation ELISA performed according to manufacturer's instructions (Roche Diagnostics, Mannheim, Germany). Colour change was developed using 3,3'5,5'-tetramethylbenzidine solution and the reaction quenched with 1 M H_2SO_4. Absorbance was measured at 450 nm using a variable wavelength 96-well plate reader (Tecan, Mannedorf, Switzerland).

2.2.14. Cell migration assay

HUVECs were seeded in starvation medium (MCDB131 (+0.2% (w/v) BSA)) at 3×10^4 cells per well in an 8 μm pore size transwell filter inserted into a 24-well companion plate (BD Biosciences, Oxford, UK). To set up a chemotactic gradient for cells to

migrate towards, ECGM (control) or MCDB131 (+0.2% (w/v) BSA) containing 25 ng/ml VEGF-A was added to the lower chamber. Cells were incubated for 24 h before being fixed and stained with 0.2% (w/v) crystal violet in 20% (v/v) methanol. Non-migrated cells were removed from the upper chamber using a cotton bud. 3-5 random fields were imaged per transwell filter.

2.2.15. Endothelial cell tubulogenesis assay

Primary human foreskin fibroblasts (Promocell) were cultured to confluency in DMEM containing 10% (v/v) FCS, 1% (v/v) non-essential amino acids and 1% sodium pyruvate in 48-well plates. 6.5×10^3 HUVECs were seeded onto the fibroblast monolayer in a 1:1 mixture of DMEM:ECGM. After 24 h, medium was replaced with ECGM (+ 25 ng/ml VEGF-A) and subsequently replaced every 48 h for 7 days. Tubules were fixed in 10% (v/v) formalin for 20 min at room temperature, blocked in 1% (w/v) BSA for 60 min at room temperature, stained with 1 μg/ml endothelial specific marker PECAM-1 primary antibody overnight at room temperature and incubated in anti-mouse secondary antibody (AlexaFluor 594) and DNA-binding dye, DAPI, for 2 h at room temperature. Tubules were washed three times in PBS between each of the above stages. Images were acquired using an Evos-fI inverted digital microscope. Five random fields were imaged per well at 10X magnification. Both total tubule length and the number of branch points were quantified from each photographic field using the open source software AngioQuant (www.cs.tut.fi/sgn/csb/angioquant).

2.2.16. Statistical analysis

Statistical analysis was performed using a one-way analysis of variance (ANOVA) and Tukey's post-test analysis for multiple comparisons or two-way ANOVA followed by the Bonferroni multiple comparison test using GraphPad Prism software (La Jolla, USA). Significant differences between control and test groups were evaluated with p values less than 0.05 (*), 0.01 (**), 0.001 (***) and 0.0001 (****) indicated on the graphs. Error bars in graphs denote ± standard error of the mean (SEM) from results of at least three independent experiments.

CHAPTER 3

Basal VEGFR2 ubiquitination modulates signal transduction and endothelial function

3.1. Introduction

Cell surface receptors undergo degradation but the biochemical basis for such control remains poorly defined. Endothelial cells express VEGFR2 which binds to circulating VEGF-A, stimulating signal transduction and new blood vessel sprouting i.e. angiogenesis (Olsson et al., 2006, Shibuya, 2010). VEGF-A plays essential roles in both health and disease states (Ferrara, 1999). VEGF-A-stimulated pathological angiogenesis is important in chronic inflammatory diseases, cancer and retinopathy (Coultas et al., 2005, Carmeliet, 2005, Ferrara and Kerbel, 2005) whilst insufficient angiogenesis leads to damaged blood vessels causing tissue ischaemia and heart disease (Ungvari et al., 2010). Multiple controls must exist to enable endothelial cells to integrate RTK activation, trafficking and turnover in regulating functional responses. It is unclear how endothelial cells regulate basal VEGFR2 levels to control the intensity of downstream signal transduction pathways which in turn regulate cellular outcomes.

VEGF-A binding to plasma membrane VEGFR2 causes tyrosine kinase activation and post-translational modifications such as tyrosine trans-autophosphorylation and ubiquitination (Koch and Claesson-Welsh, 2012, Ewan et al., 2006). Ligand-activated VEGFR2 undergoes ubiquitin-linked proteolysis (Bruns et al., 2010, Ewan et al., 2006) but regulation of basal VEGFR2 levels is ill-defined. Ubiquitination is one mechanism to control protein degradation and/or intracellular localisation (Ciechanover et al., 2000), suggesting such post-translational modification(s) could be used to control resting VEGFR2 levels. Protein ubiquitination requires E1 ubiquitin-activating enzyme activity, followed by an E2 ubiquitin-conjugating enzyme working in concert with an E3 ubiquitin ligase (Hershko and Ciechanover, 1992). Eight human E1 enzymes initiate

the activation and conjugation of a number of ubiquitin-like proteins to target proteins, including ubiquitin, SUMO and NEDD8 (Pickart, 2001).

Herein, we provide evidence for a novel pathway requiring the E1 ubiquitin-activating enzyme, UBA1, which programs basal ubiquitin-dependent recycling and proteolysis of resting VEGFR2 to control plasma membrane VEGFR2 levels. This regulatory mechanism controls the initial endothelial response to VEGF-A. VEGFR2 undergoes VEGF-A-independent constitutive degradation via a UBA1-dependent pathway. Depletion of endothelial UBA1 levels caused increased endosome-to-plasma membrane VEGFR2 recycling and reduced proteolysis. UBA1 depletion thus elevated VEGF-A-stimulated signal transduction, exemplified by increased activation of downstream signalling enzymes such as PLCγ1 and ERK1/2. Importantly, UBA1-depleted endothelial cells also displayed increased VEGF-A-stimulated tubulogenesis. Our study reveals the existence of an ubiquitin-linked regulatory pathway that controls VEGFR2 levels by modulating ligand-independent receptor recycling and degradation. Programming basal plasma membrane VEGFR2 levels sets a threshold to influence the intensity and duration of the endothelial response to circulating ligands such as VEGF-A.

3.2. Results

3.2.1. UBA1 regulates basal VEGFR2 levels

Ligand-stimulated ubiquitination of VEGFR2 facilitates trafficking and degradation in the endosome-lysosome system (Bruns et al., 2010). Previous studies have shown that in resting primary endothelial cells, VEGFR2 undergoes proteolysis (Mittar et al., 2009, Ulyatt et al., 2011) but the mechanism underlying this phenomenon was unknown. To characterise such a constitutive, ligand-independent pathway(s) that controls basal VEGFR2 levels, we reasoned that an ubiquitin-linked mechanism targets inactive VEGFR2 for proteolysis. To test this idea, screening of the 8 human E1-like enzymes revealed that UBA1 or UBA2 depletion caused a significant increase in basal VEGFR2 levels in primary human endothelial cells (Fig. 3.1A). Quantification revealed ~2-fold increase in mature VEGFR2 levels in UBA1-depleted cells compared to control cells (Fig. 3.1B). The RNAi screen was repeated in the presence of VEGF-A for 120 min to identify candidate E1s for regulating proteolysis of active VEGFR2. Unexpectedly,
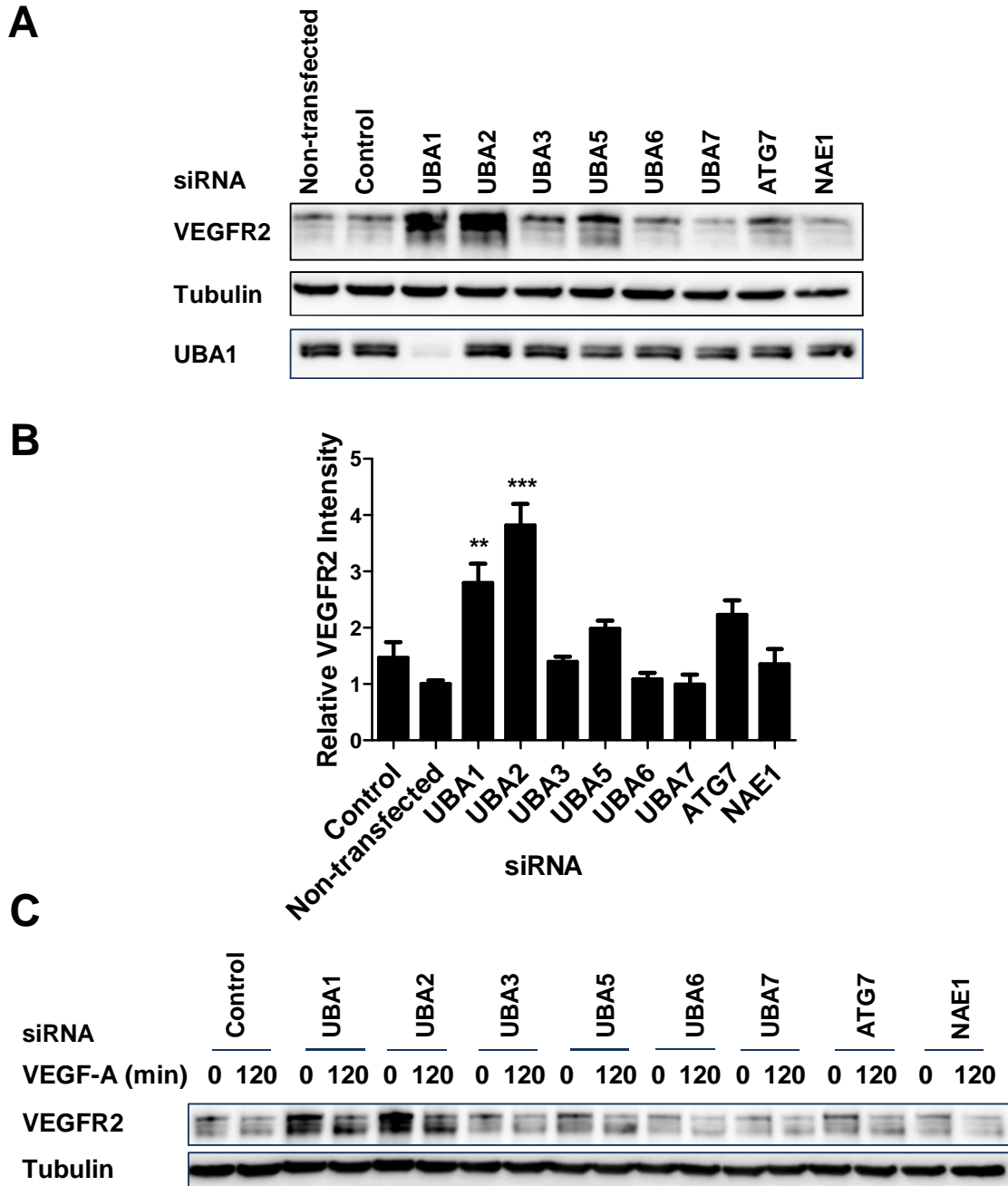
Figure 3.1. An RNAi screen for the E1 enzymes that regulate VEGFR2 turnover. (A) Endothelial cells treated with non-targeting, UBA1, UBA2, UBA3, UBA5, UBA6, UBA7, ATG7 or NAE1 siRNA were lysed and immunoblotted with antibodies to VEGFR2. (B) Quantification of VEGFR2 levels in primary human endothelial cells treated with non-targeting, UBA1, UBA2, UBA3, UBA5, UBA6, UBA7, ATG7 or NAE1 siRNA. (C) Endothelial cells treated with non-targeting, UBA1, UBA2, UBA3, UBA5, UBA6, UBA7, ATG7 or NAE1 siRNA were stimulated with 25 ng/ml VEGF-A for 120 min, lysed and immunoblotted with antibodies to VEGFR2. Error bars denote $\pm$SEM ($n \geq 3$). $p < 0.01$ (**), $p < 0.001$ (***).

immunoblot analysis revealed E1 depletion did not affect VEGFR2 degradation over 120 min VEGF-A stimulation (Fig. 3.1C).

The effect of UBA1 depletion on basal VEGFR2 levels was confirmed by immunofluorescence microscopy of control and UBA1-depleted endothelial cells stained with antibodies to VEGFR1 or VEGFR2 (Fig. 3.2A, B). Whilst UBA2 regulates SUMOylation, UBA1 and UBA6 are the only E1 ubiquitin-activating enzymes known to regulate attachment of ubiquitin to target proteins (Haas et al., 1982, Pelzer et al., 2007). Although VEGFR2 levels increased ~2-fold in UBA1-depleted cells, VEGFR1 levels were unaffected by UBA1 depletion (Fig. 3.2C). Importantly, UBA6 depletion did not affect VEGFR2 levels (Fig 3.2A, B). Thus, UBA1 is an E1 ubiquitin-activating enzyme that regulates constitutive VEGFR2 degradation. To confirm that UBA1 activity is required for basal VEGFR2 degradation, we used the pharmacological inhibitor PYR41 on endothelial cells (Fig. 3.3A). Quantification of control or PYR41-treated cells revealed a statistically significant increase in resting VEGFR2 levels upon treatment with PYR41 (Fig. 3.3B). These findings provide evidence for ubiquitin-dependent control of basal VEGFR2 levels.

3.2.2. UBA1 regulates constitutive ubiquitination and degradation of VEGFR2

Blocking protein synthesis using cycloheximide (CHX) in endothelial cells enables monitoring of mature VEGFR2 degradation in the absence of ligand (Shaik et al., 2012). We combined CHX treatment and UBA1 depletion to assess effects on distal pools of mature VEGFR2 associated with the plasma membrane, endosomes and lysosomes. To test how UBA1 depletion affects basal VEGFR2 turnover, we used RNAi to deplete UBA1 in primary HUVECs, followed by CHX treatment (Fig. 3.4). Immunoblotting confirmed that basal VEGFR2 levels were elevated upon UBA1 depletion although tyrosine phosphorylation was not evident (Fig. 3.4A) suggesting VEGFR2 activation was not required for degradation via this pathway. Importantly, UBA1 depletion did not affect basal levels of other plasma membrane receptors such as FGFR1 or transferrin receptor (TfR) (Fig. 3.4A). Quantification revealed that under control conditions, ~60% of mature VEGFR2 underwent degradation over an 80 min period of CHX treatment (Fig. 3.4B). In contrast, UBA1-depleted endothelial cells exhibited ~40% increase in basal VEGFR2 levels before CHX addition (t=0 min; Fig.

3.4B). Furthermore, ligand-independent VEGFR2 degradation was less pronounced in UBA1-depleted cells after 80 min CHX treatment with only ~30% decrease in VEGFR2 levels (Fig. 3.4B). Depletion of UBA1 thus causes a rise in VEGFR2 levels which undergo reduced degradation upon inhibition of new protein synthesis. Morphological analysis of VEGFR2 distribution using quantitative microscopy further supported a role for UBA1 in basal VEGFR2 degradation (Fig. 3.5A). Comparison of control and UBA1-depleted endothelial cells revealed that basal VEGFR2 (t=0 min) levels were ~40% higher in UBA1-depleted cells (Fig. 3.5B). Upon the addition of CHX, control endothelial cells exhibited ~55% ligand-independent VEGFR2 degradation after 60 min CHX treatment (Fig. 3.5B). However, upon UBA1 depletion basal VEGFR2 levels were reduced by only ~20% in the presence of CHX for 60 min (Fig. 3.5B).

To test the functional requirement for UBA1 in VEGFR2 turnover in other types of blood vessels, we examined this phenomenon in primary human dermal capillary endothelial cells (HDMECs) (Fig. 3.6A). VEGFR2 is abundant in HDMECs and its levels are clearly elevated upon UBA1 depletion (Fig. 3.6A). Quantification showed ~20-30% increase in basal VEGFR2 levels (Fig. 3.6B). In addition, CHX treatment for up to 80 min did not significantly reduce VEGFR2 levels in UBA1-depleted cells (Fig. 3.6B). UBA1 is thus required for ligand-independent VEGFR2 turnover in endothelial cells derived from different types of blood vessels.

The effects of UBA1 depletion on basal VEGFR2 levels suggested that ubiquitination could be one means of programming resting VEGFR2 for degradation. To test this idea, we immunoprecipitated mature VEGFR2 from CHX-treated control or UBA1-depleted endothelial cells and evaluated ubiquitination status using immunoblot analysis (Fig. 3.7A). In control endothelial cells subjected to CHX treatment, ubiquitinated VEGFR2 levels gradually increased by ~50%, peaking after 60 min (Fig. 3.7A, B). In contrast, UBA1-depleted cells displayed no such peak; ligand-independent VEGFR2 ubiquitination remained low and relatively unchanged. Notably, UBA1 depletion reduced peak ubiquitination of VEGFR2 by ~60% in comparison to control cells (Fig. 3.7B). These findings support a requirement for UBA1 in basal VEGFR2 ubiquitination to target this membrane receptor for degradation.
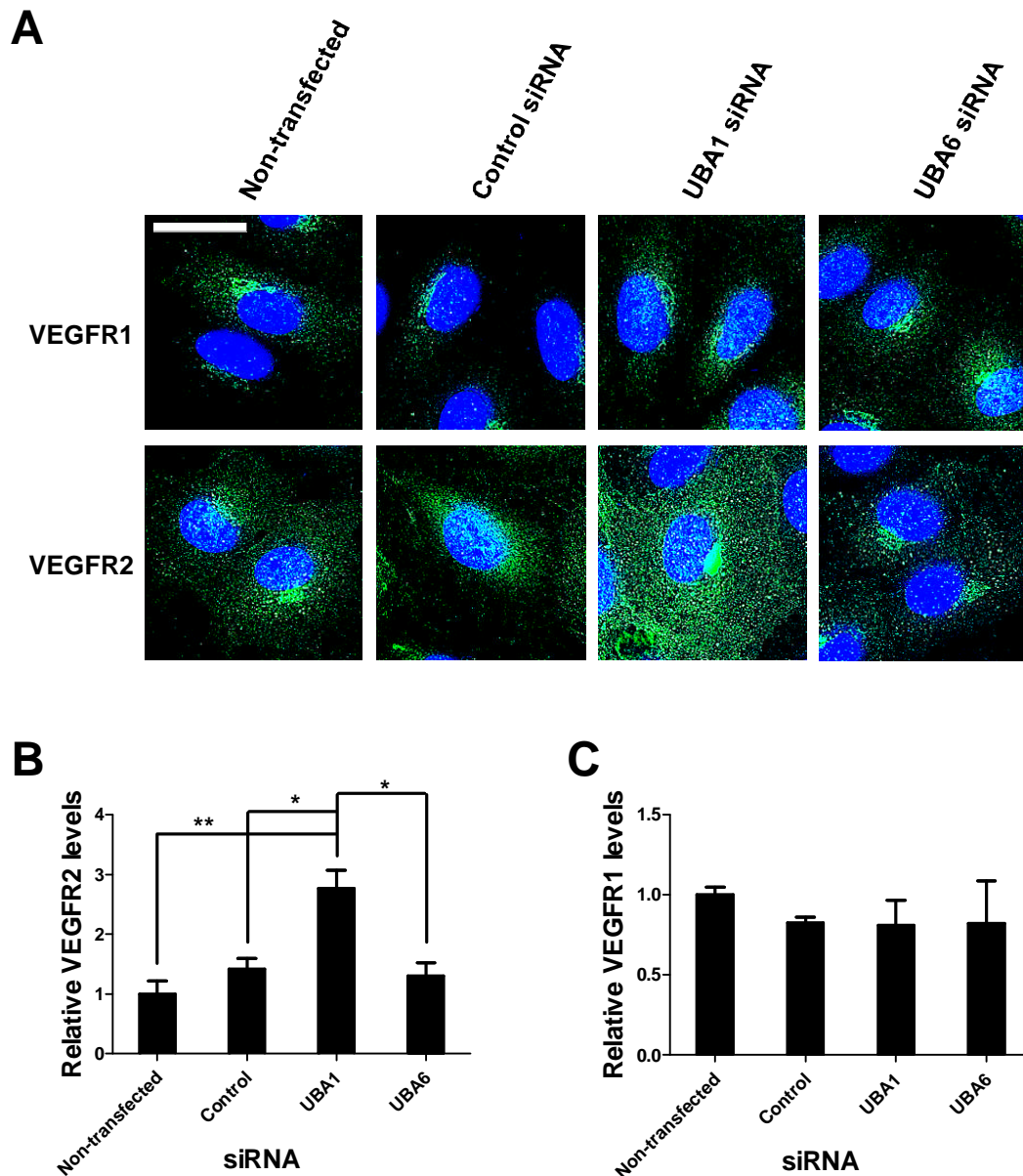
Figure 3.2. UBA1 regulates basal VEGFR2 levels. (A) Immunofluorescence microscopy of endothelial cells transfected with non-targeting, UBA1 or UBA6 siRNA and stained with antibodies to either VEGFR1 or VEGFR2 followed by fluorescent species-specific secondary antibodies (green). Nuclei were stained with DNA-binding dye, DAPI (blue). Scale bar represents 70 μm. VEGFR2 (B) or VEGFR1 (C) levels in endothelial cells treated with non-targeting, UBA1 or UBA6 siRNA determined by quantitative microscopy. Error bars denote ±SEM (n≥3). $p<0.05$ (*), $p<0.01$ (**).
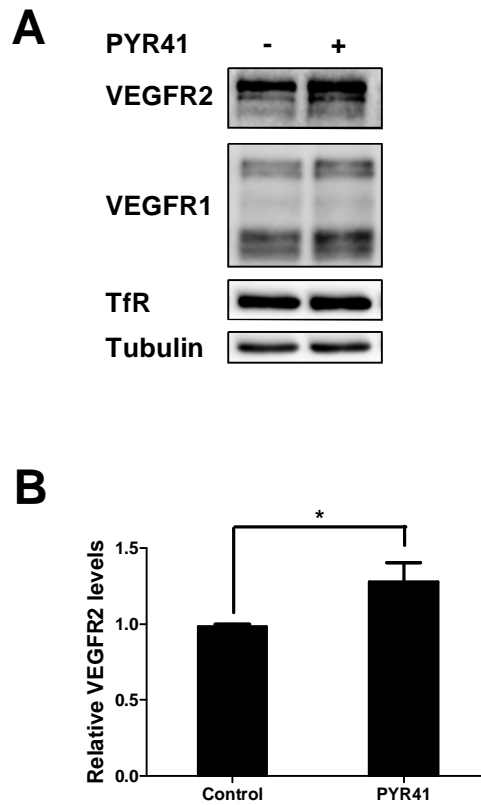
Figure 3.3. Pharmacological inhibition of UBA1 increases basal VEGFR2 levels (A) Endothelial cells treated with the UBA1-specific small molecule inhibitor PYR41 (10 μM) for 1 h were lysed and immunoblotted with antibodies to VEGFR2, VEGFR1 or transferrin receptor (TfR). (B) Quantification of VEGFR2 levels in endothelial cells treated with PYR41. Error bars denote ±SEM (n≥3). $p < 0.05$ (*).

A

B
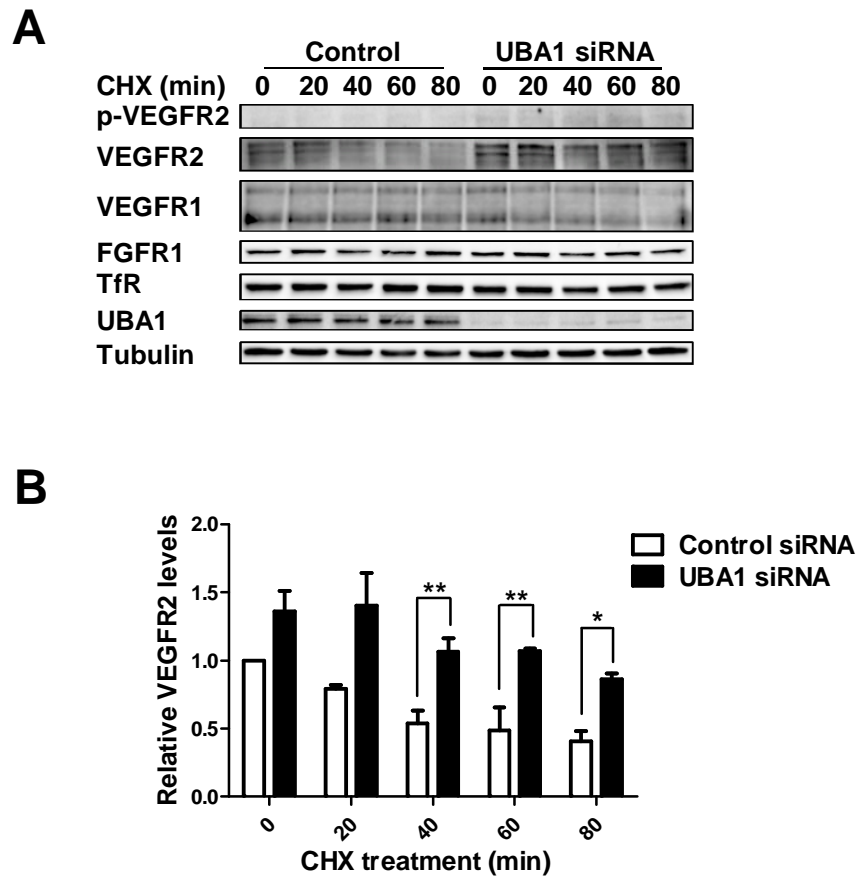
Figure 3.4. UBA1 regulates ligand-independent VEGFR2 degradation. (A) HUVECs transfected with non-targeting or UBA1 siRNA were treated with 20 µg/ml cycloheximide (CHX) over a time course of 80 min and immunoblotted for phospho-VEGFR2, VEGFR2, VEGFR1, FGFR or TfR. (B) Quantification of VEGFR2 levels in HUVECs transfected with non-targeting or UBA1 siRNA and treated with 20 µg/ml CHX for 80 min. Error bars denote ±SEM (n≥3). $p<0.05$ (*), $p<0.01$ (**).
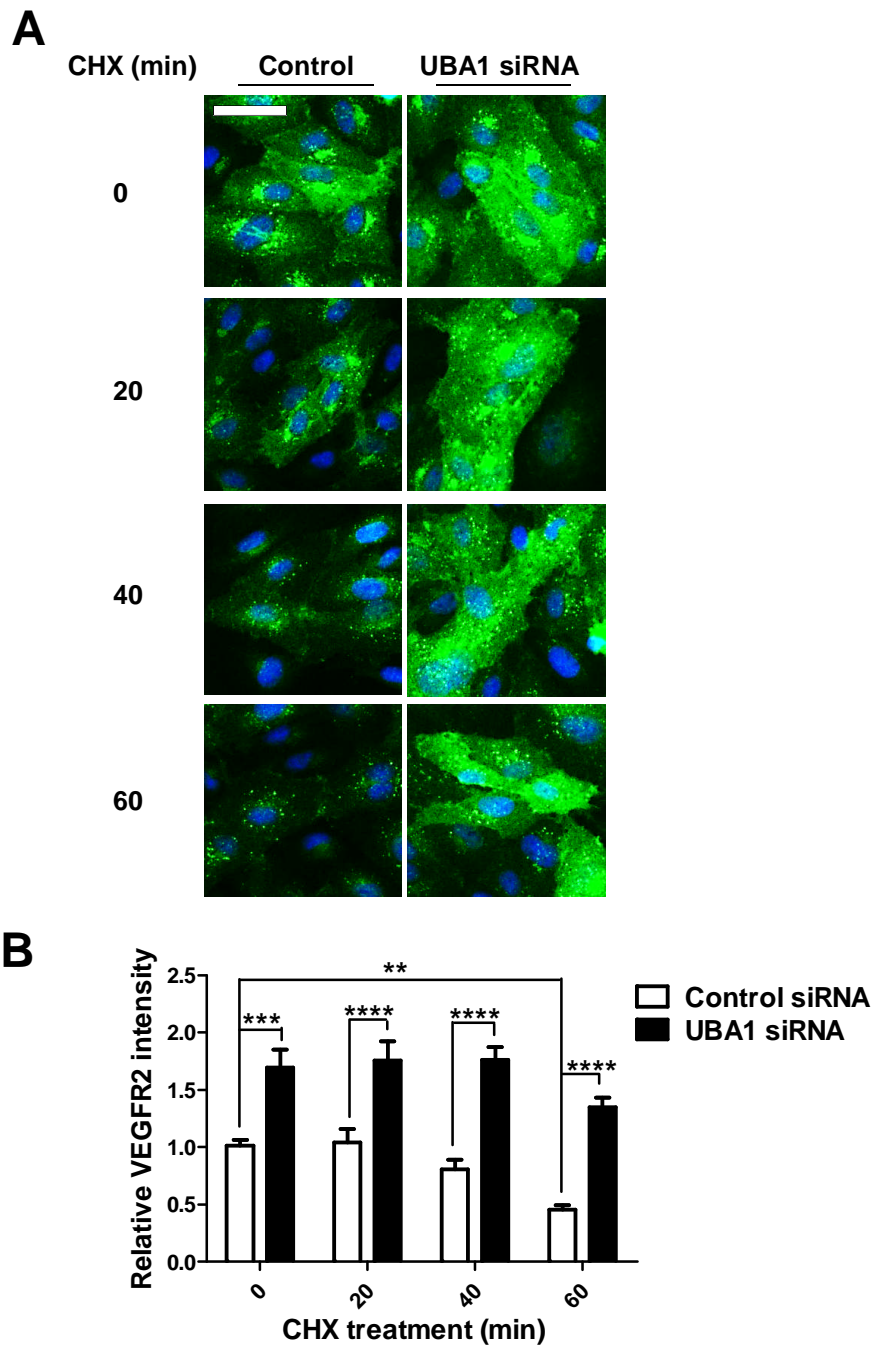
Figure 3.5. Immunofluorescence microscopy reveals UBA1 regulates ligand-independent VEGFR2 degradation. (A) HUVECs transfected with non-targeting or UBA1 siRNA were treated with 20 μg/ml CHX over a time course of 60 min and processed for immunofluorescence microscopy using antibodies to VEGFR2 followed by fluorescent species-specific secondary antibodies (green). Nuclei were stained with DNA-binding dye, DAPI (blue). Scale bar represents 200 μm. (B) VEGFR2 levels in HUVECs treated with 20 μg/ml CHX determined by quantitative microscopy. Error bars denote ±SEM (n≥3). $p < 0.01$ (**), $p < 0.001$ (***), $p < 0.0001$ (****).
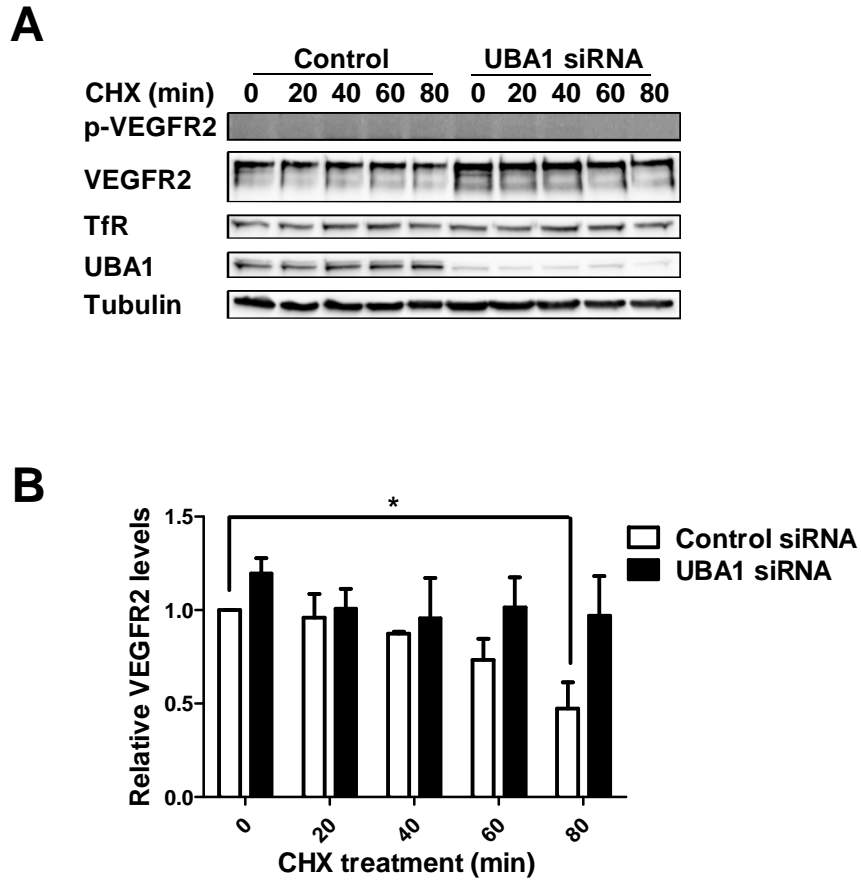
Figure 3.6. UBA1 regulates ligand-independent VEGFR2 degradation in capillary endothelial cells. (A) HDMECs transfected with non-targeting or UBA1 siRNA were treated with 20 μg/ml CHX over a time course of 80 min and immunoblotted for phospho-VEGFR2, VEGFR2 or TfR. (B) Quantification of VEGFR2 levels in HDMECs transfected with non-targeting or UBA1 siRNA and treated with 20 μg/ml CHX for 80 min. Error bars denote ±SEM (n≥3). $p<0.05$ (*).
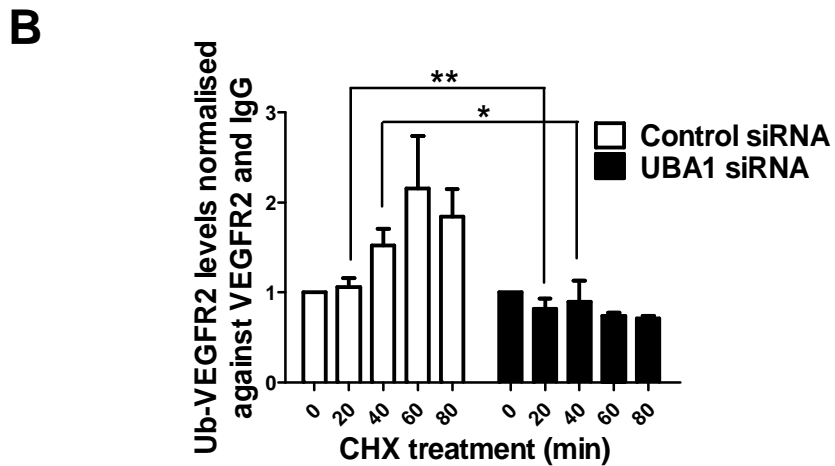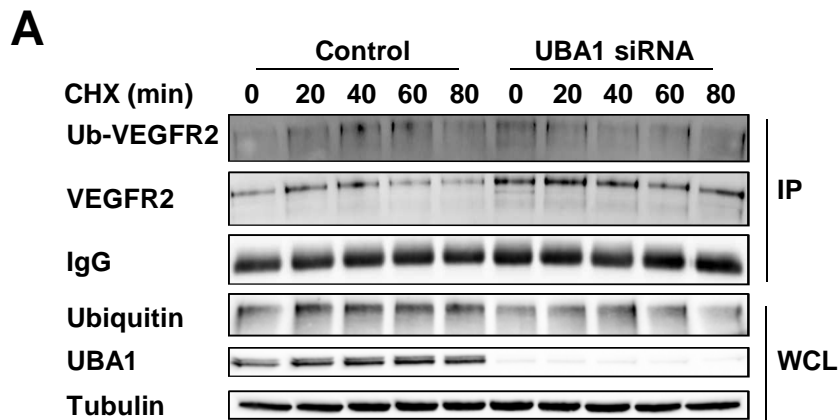
Figure 3.7. UBA1 regulates basal ubiquitination of VEGFR2. (A) Primary human endothelial cells transfected with non-targeting or UBA1 siRNA were treated with 20 μg/ml CHX and lysed. VEGFR2 was immunoprecipitated using antibodies to VEGFR2 and immunoblotted to monitor ubiquitin status using a pan-ubiquitin antibody. (B) Quantification of ubiquitinated VEGFR2 (Ub-VEGFR2) levels in endothelial cells transfected with non-targeting or UBA1 siRNA and treated with 20 μg/ml CHX. Relative Ub-VEGFR2 levels were normalised against both IgG and VEGFR2. Error bars denote ±SEM (n≥3). $p<0.05$ (*), $p<0.01$ (**). IP; immunoprecipitate, WCL; whole cell lysate.

3.2.3. UBA1 regulates basal VEGFR2 recycling

RTK ubiquitination at the plasma membrane precedes internalisation and delivery to early endosomes (Haglund and Dikic, 2012, Ewan et al., 2006, Clague and Urbe, 2001). Ligand-stimulated VEGFR2 ubiquitination promotes trafficking to late endosomes and terminal degradation in lysosomes (Ewan et al., 2006, Bruns et al., 2010). RTK de-ubiquitination in early endosomes is associated with endosome-to-plasma membrane recycling (Clague and Urbe, 2006). Furthermore, it has been previously shown that VEGFR2 undergoes substantial constitutive ligand-independent recycling via endosomes (Jopling et al., 2011). One possibility is that upon UBA1 depletion, VEGFR2 undergoes decreased basal ubiquitination which is a prerequisite for increased endosome-to-plasma membrane recycling. To test this idea, we utilised a microscopy-based VEGFR2 recycling assay (Jopling et al., 2011). Here, control or UBA1-depleted endothelial cells were incubated with extracellular domain-specific antibodies to two different RTKs expressed by endothelial cells i.e. VEGFR2 and FGFR1. Constitutive RTK endocytosis and recycling was monitored using accessibility of either VEGFR2-antibody or FGFR1-antibody complexes to a pulse of labelled secondary antibody. Only VEGFR2-antibody or FGFR1-antibody complexes that had undergone endocytosis followed by endosome-to-plasma membrane recycling were detected (Fig. 3.8A). Quantification revealed that UBA1-depleted endothelial cells displayed ~2-fold increase in basal endosome-to-plasma membrane recycling of VEGFR2 (Fig. 3.8B). In contrast, FGFR1 recycling was unaffected by UBA1 depletion (Fig. 3.8C).

One prediction is that increased basal recycling of VEGFR2 increases overall plasma membrane levels in UBA1-depleted cells. To test this hypothesis, endothelial cells were treated with CHX to block new protein synthesis and then subjected to cell surface biotinylation followed by affinity purification of biotinylated plasma membrane proteins and immunoblot analysis (Fig. 3.9A). VEGFR2 plasma membrane levels were clearly elevated upon UBA1 depletion, whereas another membrane protein and cell surface receptor, transferrin receptor, was not significantly affected (Fig. 3.9A). Quantification revealed that under control conditions, plasma membrane VEGFR2 levels were reduced by ~55% after 80 min CHX treatment (Fig. 3.9B). In contrast, UBA1-depleted cells exhibited ~25% increase in plasma membrane VEGFR2 under steady-state conditions (t=0; Fig. 3.9B). Over an 80 min period of CHX treatment, there was less reduction in
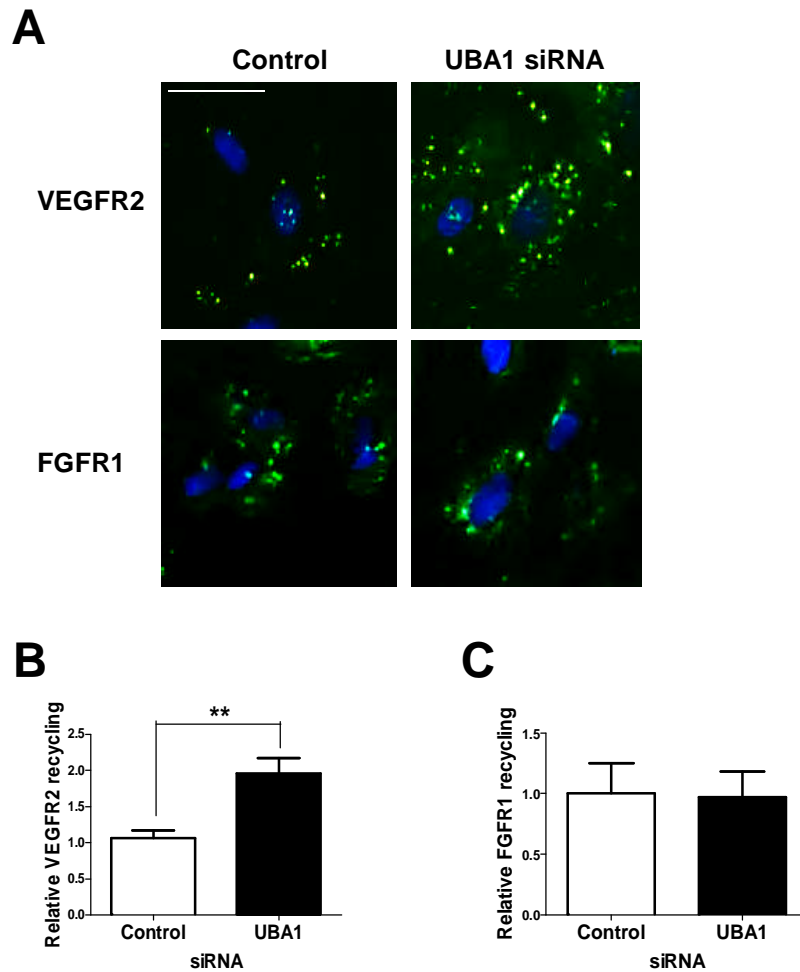
Figure 3.8. UBA1 regulates basal plasma membrane-to-endosome recycling of VEGFR2. (A) Endothelial cells transfected with non-targeting or UBA1 siRNA were incubated with antibodies to VEGFR2 or FGFR1 for 30 min at 37°C before being acid-washed to strip cell surface antibodies and incubated with fluorescent species-specific secondary antibodies for 30 min at 37°C (green). Cells were fixed prior to staining with DNA-binding dye, DAPI (blue). Only VEGFR2 or FGFR1 that underwent plasma membrane-to-endosome-to-plasma membrane recycling is visible. Scale bar represents 200 μm. VEGFR2 (B) or FGFR1 (C) recycling was quantified in cells transfected with non-targeting or UBA1 siRNA . Error bars denote ±SEM (n≥3). $p < 0.01$ (**).
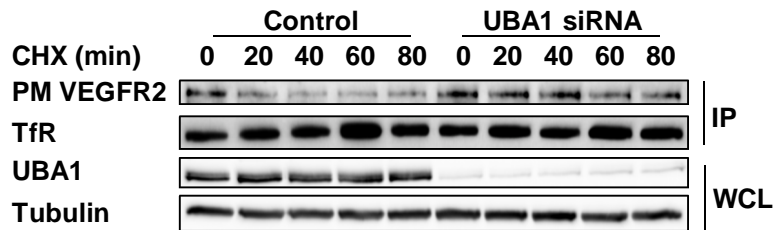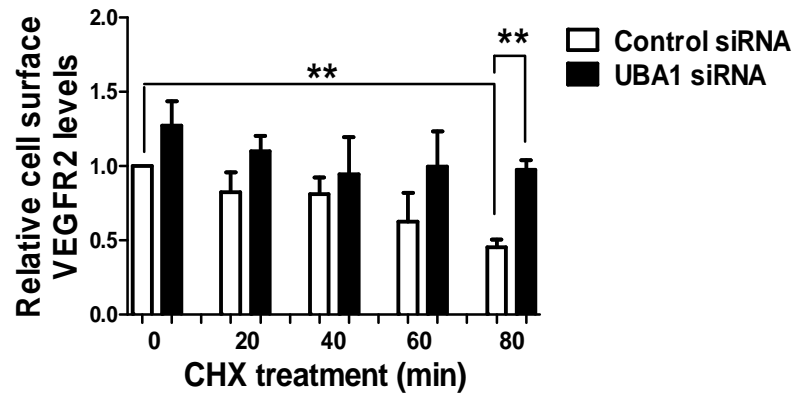
Figure 3.9. UBA1 regulates plasma membrane levels of VEGFR2. (A) Primary human endothelial cells transfected with non-targeting or UBA1 siRNA were treated with 20 μg/ml CHX. Cell surface proteins were biotinylated, isolated and immunoblotted for plasma membrane VEGFR2 (PM VEGFR2) or TfR. (B) Quantification of cell surface VEGFR2 levels in endothelial cells transfected with non-targeting or UBA1 siRNA and treated with 20 μg/ml CHX. Error bars denote ±SEM (n≥3). $p<0.01$ (**). IP; immunoprecipitate, WCL; whole cell lysate.

plasma membrane VEGFR2 levels (Fig. 3.9B). Taken together, these data suggest that UBA1 regulates basal endosome-to-plasma membrane VEGFR2 recycling and VEGFR2 plasma membrane levels in an ubiquitin-dependent manner.

3.2.4. UBA1-mediated control of basal VEGFR2 levels modulates VEGF-A-stimulated signal transduction

VEGF-A binding to plasma membrane VEGFR2 stimulates multiple signal transduction pathways (Koch et al., 2011, Zhang et al., 2008). UBA1 depletion inhibits basal VEGFR2 degradation leading to a net increase in VEGFR2 at the plasma membrane; this could modulate VEGF-A-stimulated signal transduction. To test this idea, control or UBA1-depleted endothelial cells were subjected to VEGF-A stimulation before probing downstream signal transduction events using quantitative immunoblotting (Fig. 3.10A). VEGFR2 trans-autophosphorylation of the cytoplasmic Y1175 epitope is a signature for VEGFR2 activation (Koch et al., 2011). VEGF-A-stimulated appearance of VEGFR2-pY1175 was clearly evident in both control and UBA1-depleted cells (Fig. 3.10A). However, quantification showed ~30% increase in VEGFR2-pY1175 levels upon UBA1 depletion (Fig. 3.10B).

Plasma membrane VEGFR2 activation is linked to recruitment of PLCγ1 followed by tyrosine phosphorylation on residue Y783 and increased phospholipase activity (Koch et al., 2011). UBA1-depleted cells exhibited increased PLCγ1 phosphorylation (Fig. 3.10A) corresponding to ~43% increase in PLCγ1-pY783 levels (Fig. 3.10C). A key feature of VEGF-A-stimulated signal transduction is activation of the MAPK pathway which leads to phosphorylation and activation of ERK1/2, a key event in VEGF-A-stimulated signal transduction (Koch and Claesson-Welsh, 2012). UBA1-depleted endothelial cells displayed ~3-fold increase in VEGF-A-stimulated ERK1/2 phosphorylation in comparison to control cells (Fig. 3.10D). UBA1-mediated regulation of basal VEGFR2 levels thus modulates the VEGF-A-stimulated response through different signal transduction pathways. Interestingly, UBA1 depletion did not affect VEGF-A-stimulated VEGFR2 degradation over a 60 min time course (Fig. 3.10A), suggesting that a UBA1-dependent pathway is not required for ligand-stimulated VEGFR2 degradation.
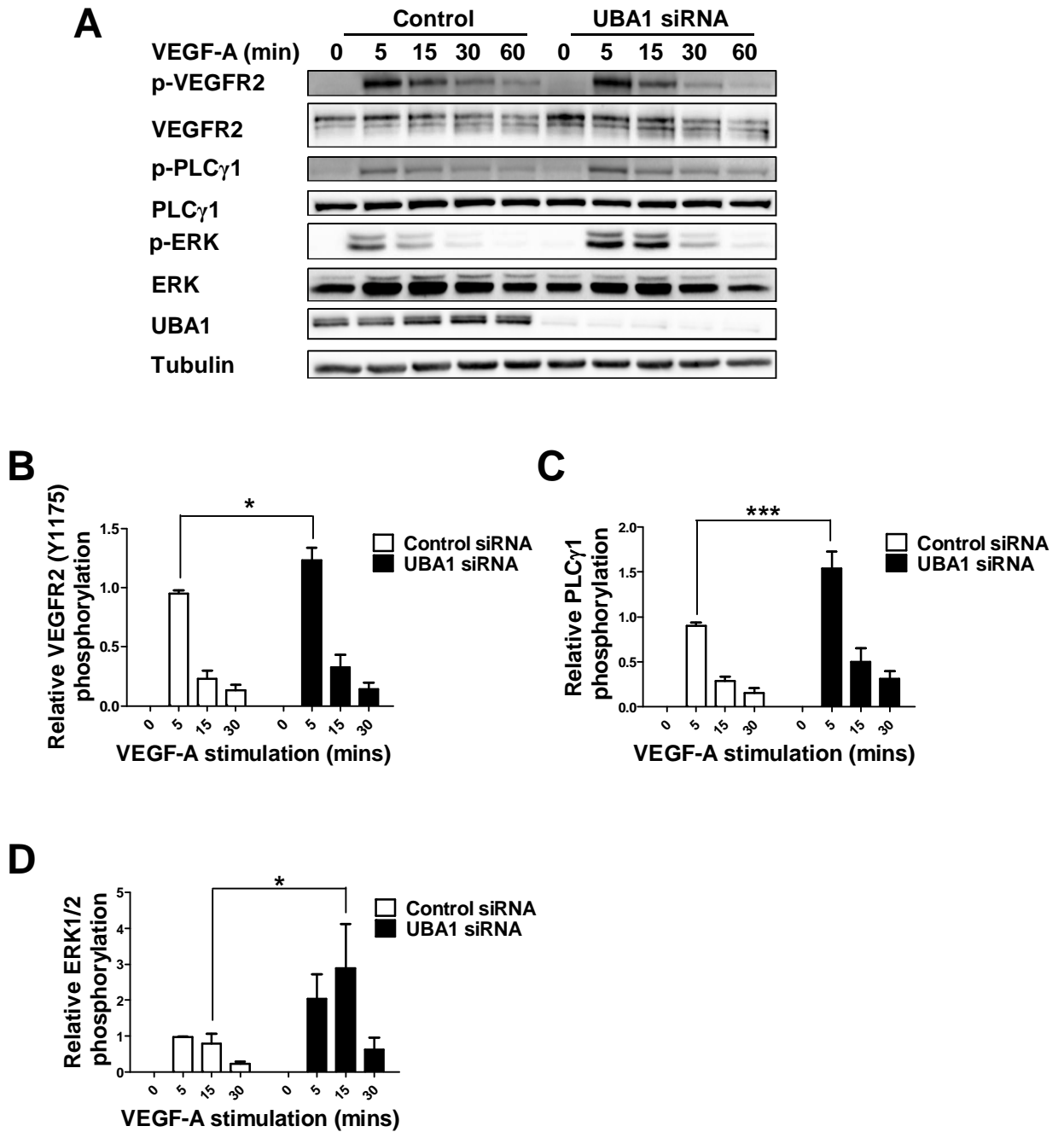
Figure 3.10. UBA1 depletion upregulates VEGF-A-stimulated signal transduction. Endothelial cells transfected with non-targeting or UBA1 siRNA were treated with 25 ng/ml VEGF-A, lysed and immunoblotted for phospho-VEGFR2 (Y1175), phospho-PLCγ1 (Y783) and phospho-ERK1/2 (T202/Y204). Quantification of phospho-VEGFR2 (B), phospho-PLCγ1 (C) and phospho-ERK1/2 (D) levels in endothelial cells transfected with non-targeting or UBA1 siRNA. Errors bars indicated ±SEM (n≥3). $p<0.05$ (*), $p<0.001$ (***).

3.2.5. UBA1 regulates ubiquitination of VEGF-A-stimulated VEGFR2

The identification of UBA1 as a regulator of constitutive VEGFR2 ubiquitination raised the question of whether UBA1 is also involved in ligand-stimulated VEGFR2 ubiquitination. To test this, control or UBA1-depleted endothelial cells were stimulated with VEGF-A followed by immunoblot analysis of VEGFR2 ubiquitination status (Fig. 3.11). Following VEGF-A stimulation, VEGFR2 complexes isolated by immunoprecipitation were subjected to immunoblotting using antibodies specific for K48- and K63-linked forms of ubiquitin or with a pan-ubiquitin (FK2) antibody (Fig. 3.11A). In control cells, VEGFR2 ubiquitination peaked 15 min after VEGF-A stimulation, correlating closely with receptor autophosphorylation (Fig 3.11A). In UBA1-depleted cells, peak VEGF-A-stimulated VEGFR2 ubiquitination was ~60% reduced (Fig. 3.11B). Furthermore, UBA1 depletion decreased the abundance of both K48- and K63-linked polyubiquitin chains associated with the activated VEGFR2 complex (Fig. 3.11A). These findings show that UBA1 is also involved in ubiquitination of ligand-activated VEGFR2. Examination of VEGFR2 degradation revealed an interesting anomaly: although UBA1 depletion reduced ubiquitination of activated VEGFR2, subsequent degradation was relatively unaffected (Fig. 3.11A). Thus, UBA1-mediated ubiquitination of activated VEGFR2 does not regulate downstream degradation. Whilst UBA1 controls basal turnover of resting VEGFR2, additional complexity is introduced by VEGF-A stimulation, with potential participation of other degradative pathways.

3.2.6. Basal VEGFR2 turnover regulates VEGF-A-dependent endothelial cell tubulogenesis

VEGF-A-stimulated activation of VEGFR2 promotes downstream signal transduction leading to new blood vessel sprouting, an essential feature of angiogenesis (Ferrara, 1999). In an organotypic endothelial-fibroblast co-culture assay, VEGF-A stimulated tubulogenesis was revealed by monitoring the endothelial-specific protein PECAM-1 using immunofluorescence microscopy (Fig. 3.12A). Upon comparison of each non-stimulated condition with the corresponding VEGF-A-stimulated condition for non-transfected, control siRNA or UBA1 siRNA-treated cells, VEGF-A-dependent tubulogenesis of UBA1-depleted cells was significantly higher than that of controls (Fig. 3.12B, C). VEGF-A-stimulated endothelial tubule length increased by ~40% in

UBA1-depleted cells (Fig. 3.12B). Furthermore, UBA1-depleted endothelial cells displayed ~5-fold increase in VEGF-A-stimulated branch point number within the endothelial network (Fig. 3.12C). Depletion of endothelial UBA1 thus increases VEGF-A-stimulated tubulogenesis.

3.2.7. VEGF-A-dependent endothelial cell migration and proliferation are increased upon UBA1 depletion

Other functional cellular outputs that are regulated by VEGF-A-stimulated signal transduction include endothelial cell migration and proliferation (Koch and Claesson-Welsh, 2012). In addition to tubulogenesis, it is possible that UBA1 depletion affects these cellular responses. To test this idea, we carried out cell migration assays in which control and UBA1-depleted endothelial cells migrated towards a chemotactic gradient of increasing VEGF-A concentration (Fig. 3.13). Comparison of non-stimulated cells to those treated with VEGF-A revealed that UBA1-depleted endothelial cells displayed a pronounced ~70% increase in VEGF-A-stimulated cell migration (Fig. 3.13A, B). Furthermore, we examined the requirement of UBA1 for VEGF-A-stimulated cell proliferation. UBA1 depletion increased VEGF-A-dependent cell proliferation by ~40% (Fig. 3.13C). Thus UBA1-mediated control of basal VEGFR2 recycling and degradation impacts on endothelial cell responses stimulated by exogenous VEGF-A.

3.3. Discussion

Ubiquitination plays key roles in VEGFR2 trafficking and degradation (Ewan et al., 2006, Bruns et al., 2010). We now provide evidence of a novel pathway requiring the E1 enzyme, UBA1, to program basal VEGFR2 levels for degradation. Our study provides a mechanism to precisely influence net plasma membrane and basal VEGFR2 levels, thus controlling RTK-mediated signal transduction and the cellular response to extracellular ligand (Fig. 3.14). This ligand-independent pathway for surveillance of VEGFR2 levels provides a mechanism for modulating the duration and intensity of VEGF-A-stimulated signal transduction. Perturbation of UBA1 function using RNAi increases plasma membrane VEGFR2 availability and elevates VEGF-A-stimulated signal transduction events. Notably, elevated phosphorylation and activation of VEGFR2, PLCγ1 and ERK1/2 was evident in UBA1-depleted cells. The link between plasma membrane protein ubiquitination and trafficking is highlighted by increased
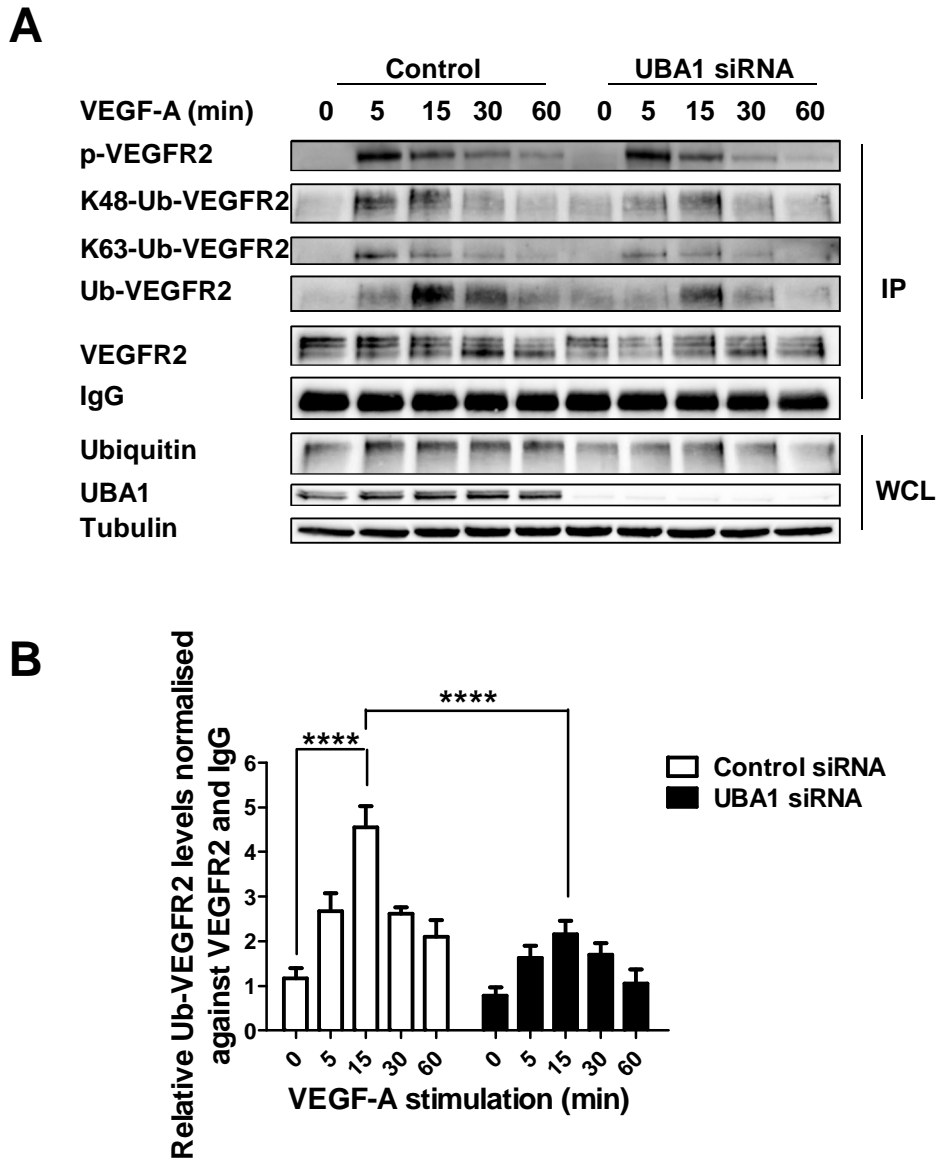
Figure 3.11. UBA1 regulates ubiquitination of VEGF-A-activated VEGFR2.
(A) Endothelial cells transfected with control or UBA1 siRNA, treated with 25 ng/ml VEGF-A and lysed. VEGFR2 was immunoprecipitated and immunoblotted for its ubiquitin status a pan-ubiquitin antibody. (B) Quantification of ubiquitinated VEGFR2 levels in endothelial cells transfected with control or UBA1 siRNA and treated with 25 ng/ml VEGF-A. Error bars denote +SEM (n≥3). $p < 0.001$ (***). IP; immunoprecipitate, WCL; whole cell lysate.
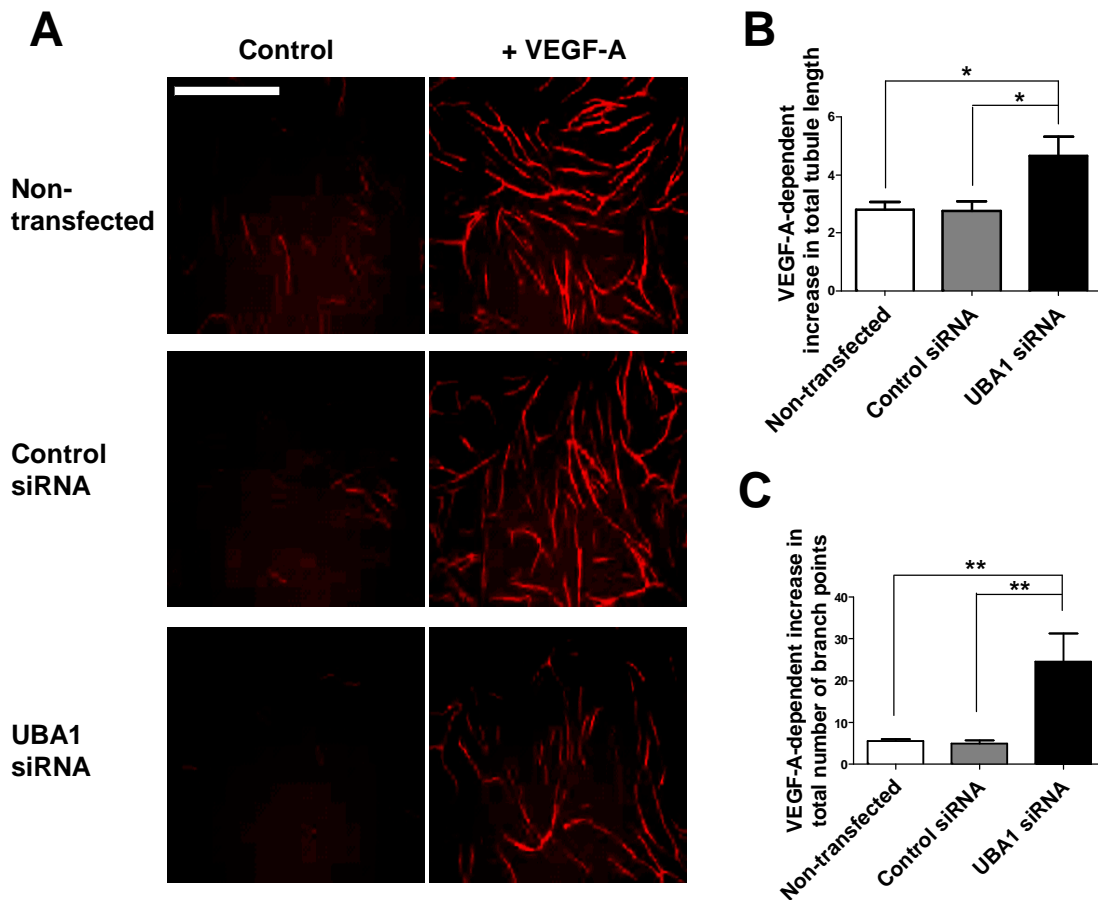
Figure 3.12. Basal VEGFR2 turnover regulates the VEGF-A-dependent endothelial response. (A) Primary human endothelial cells transfected with non-targeting or UBA1 siRNA were co-cultured on a bed of primary human fibroblasts for 7 days, treated with 25 ng/ml VEGF-A, fixed and stained with an antibody to PECAM-1 (red). Scale bar represents 1000 μm. Quantification of VEGF-A-stimulated total tubule length (B) and total number of branch points (C) relative to non-stimulated controls for non-transfected, control siRNA or UBA1 siRNA-treated endothelial cells. Error bars denote ±SEM (n≥3). $p<0.05$ (*), $p<0.01$ (**). Gareth Fearnley (Ponnambalam Laboratory, University of Leeds) contributed to the data shown in this figure.
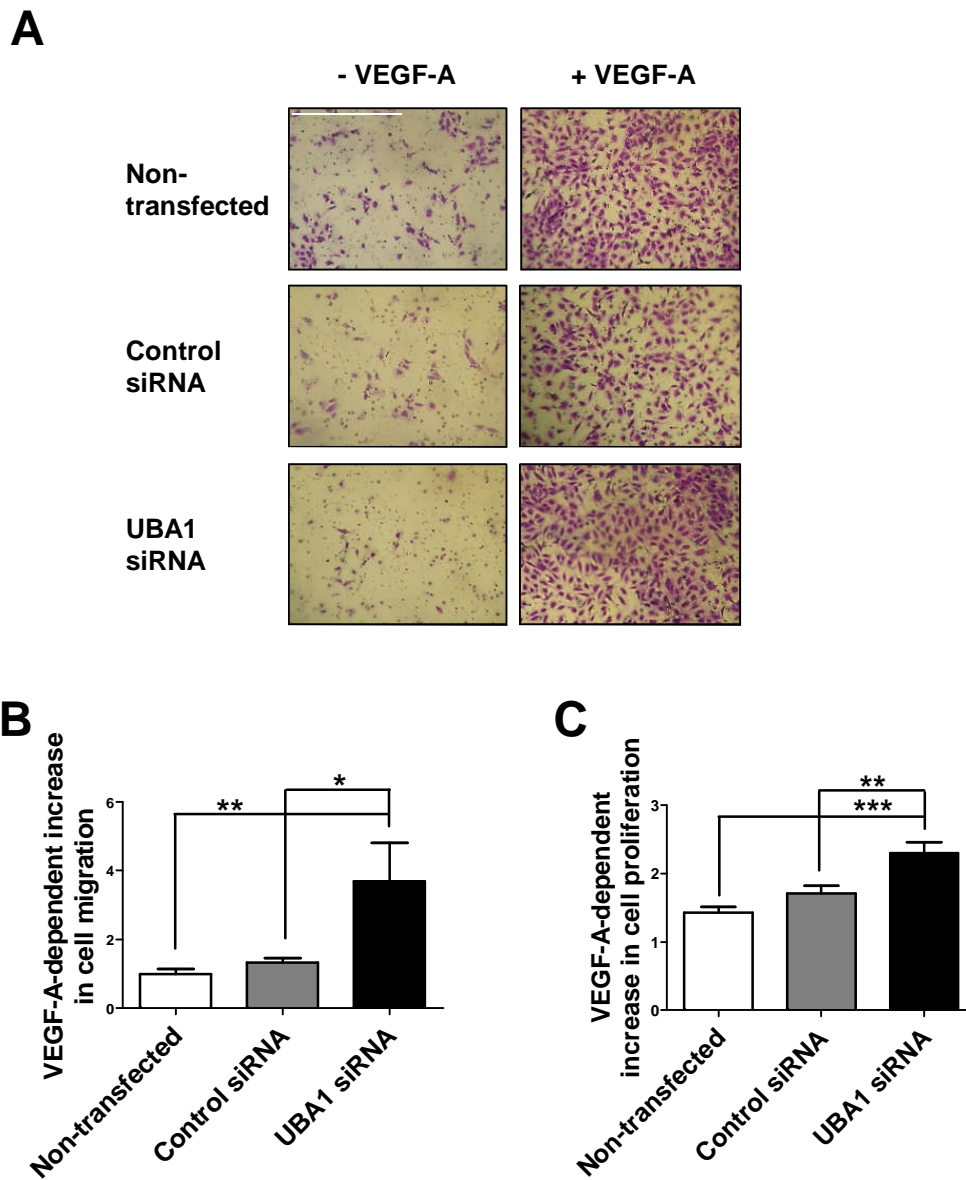
Figure 3.13. Basal VEGFR2 turnover regulates VEGF-A-dependent endothelial cell migration and proliferation. (A) Primary human endothelial cells transfected with non-targeting or UBA1 siRNA were seeded into transwell migration chambers. Cells that migrated towards a chemotactic gradient of VEGF-A over 24 h were fixed and stained with crystal violet. Scale bar represents 1000 μm. (B) Quantification of VEGF-A-dependent migration of endothelial cells transfected with non-targeting or UBA1 siRNA. (C) Proliferation of endothelial cells transfected with control or UBA1 siRNA was monitored by ELISA. Error bars denote ±SEM (n≥3). $p < 0.05$ (*), $p < 0.01$ (**), $p < 0.001$ (***).
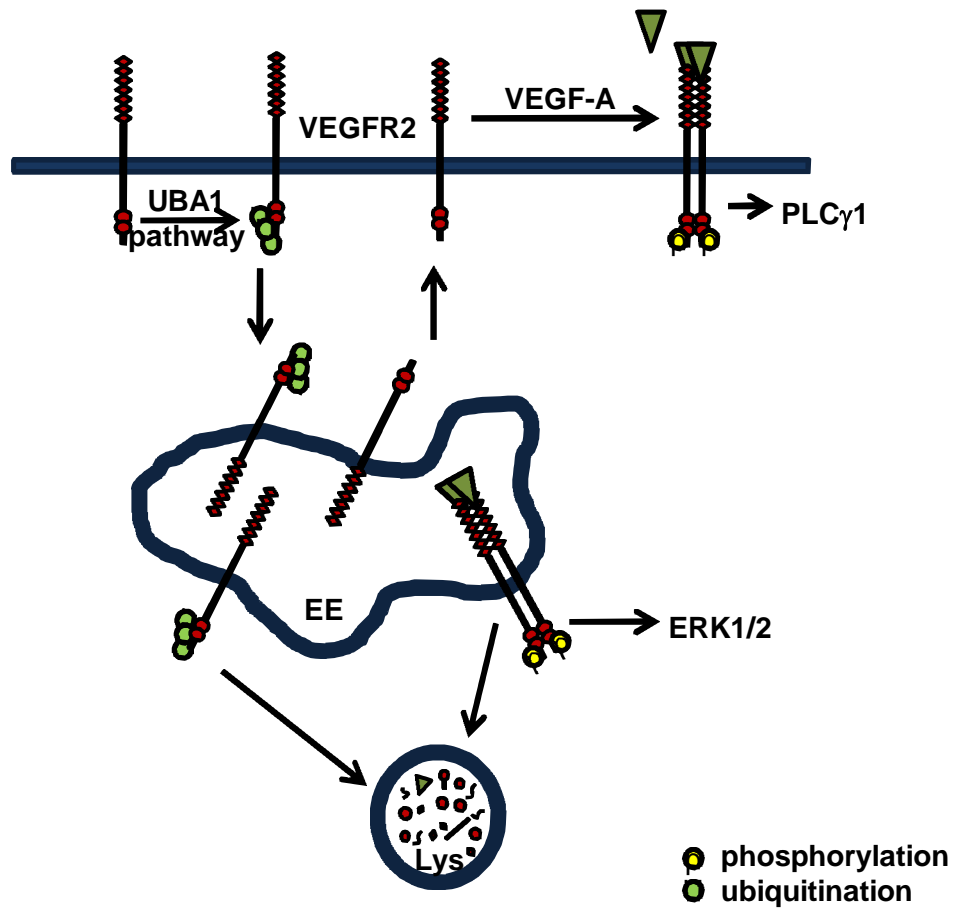
Figure 3.14. Ubiquitin-linked regulation of basal VEGFR2 recycling and plasma membrane levels. UBA1-dependent ubiquitination regulates basal VEGFR2 recycling and degradation. Ubiquitinated VEGFR2 is trafficked to lysosomes (Lys) for degradation, whilst de-ubiquitination in early endosomes (EE) promotes recycling to the plasma membrane. Controlling the balance between basal VEGFR2 recycling and proteolysis regulates plasma membrane VEGFR2 levels to set a threshold for VEGF-A-stimulated signal transduction, thus impacting on downstream cellular responses.

VEGFR2 endosome-to-plasma membrane recycling upon UBA1 depletion. Notably, trafficking of another plasma membrane receptor, FGFR1, was relatively unaffected by UBA1 depletion, suggesting specificity in this pathway for regulating basal VEGFR2 status. Finally, such regulation has significant consequences for VEGF-A-stimulated cellular responses such as endothelial cell tubulogenesis, migration and proliferation: reduction in UBA1 levels elevates the pro-angiogenic response to VEGF-A.

Ligand-stimulated ubiquitination of VEGFR2 programs terminal degradation in lysosomes (Ewan et al., 2006). Conflicting studies implicate E3 ligases c-Cbl and β-TrCP1 in VEGF-A-stimulated proteolysis of VEGFR2 (Duval et al., 2003, Murdaca et al., 2004, Shaik et al., 2012, Bruns et al., 2010, Singh et al., 2007). Furthermore, the differences in proteolytic susceptibility of VEGFR1 and VEGFR2 under both resting (Mittar et al., 2009) and hypoxic (Ulyatt et al., 2011) conditions suggest that endothelial cells exploit VEGFR availability to fine-tune the cellular response to VEGF-A. Interestingly, kinase-independent regulation of RTK function is highlighted by the discovery that constitutive binding of cytosolic adaptors such as Grb2 to basal FGFR2 regulates downstream ligand-independent activation (Lin et al., 2012). Other work has shown that constitutive ubiquitination and endocytosis of EGFR involves endocytic adaptor protein, Hrs (Katz et al., 2002). Furthermore, recent work has highlighted a kinase-independent role for EGFR in autophagy (Tan et al., 2015).

UBA1 regulates VEGF-A-stimulated VEGFR2 ubiquitination. K48-linked polyubiquitin chains are associated with proteasomal degradation whilst K63-linked chains are associated with membrane receptor trafficking in the endosome-lysosome network (Pickart, 2001, Adhikari and Chen, 2009). VEGFR2 exhibited reduced attachment of both K48- and K63-linked polyubiquitin chains upon UBA1 depletion. Reduced VEGFR2 ubiquitination would be predicted to inhibit VEGF-A-stimulated degradation however proteolysis of activated VEGFR2 was unaffected upon UBA1-depletion. This suggested further complexity in the mechanisms underlying programming of activated VEGFR2 for lysosomal degradation. One conclusion is that a UBA1-regulated pathway controls constitutive VEGFR2 recycling and proteolysis as a mechanism to adjust intensity of VEGF-A-stimulated signal transduction. It is likely that multiple degradative pathways exist for regulating ligand-stimulated VEGFR2 turnover.

UBA1 is an essential cellular enzyme expressed by many cells and tissues and is implicated in regulating multiple pathways including DNA replication. Notably, suppression of UBA1 activity in Schwann cells is linked to spinal muscular atrophy (Sugaya et al., 2015, Aghamaleky Sarvestany et al., 2014). Other studies have identified UBA1 as a novel target for the treatment of haematological malignancies (Yang et al., 2007, Xu et al., 2010). It has not escaped our notice that UBA1-mediated surveillance could be utilised for controlling RTK levels and cellular responses in different tissues. The potential for UBA1 to be targeted for disease therapy is highlighted in certain cancers (e.g. prostate cancer) which show reduced UBA1 levels (http://www.proteinatlas.org/). Thus, decreased UBA1 expression could be linked to increased angiogenesis in cancer. UBA1-mediated control of basal VEGFR2 availability for VEGF-A binding provides a dramatic alternative to the canonical view of regulating RTK signal transduction. The existence of a kinase-independent pathway that controls basal VEGFR2 levels to regulate VEGF-A signal transduction provides new routes for therapeutic intervention. Blocking UBA1 activity could upregulate RTK levels and alleviate disease states, such as ischaemic heart disease, to promote angiogenesis, revascularisation and tissue regeneration. Conversely, promoting UBA1 activity could hinder tumour growth in response to circulating growth factors.

CHAPTER 4

E2 ubiquitin-conjugating enzymes UBE2D1 and UBE2D2 regulate basal VEGFR2 turnover and the endothelial response

4.1. Introduction

Ligand-activated VEGFR2 undergoes ubiquitin-linked proteolysis (Bruns et al., 2010, Ewan et al., 2006) but the factors that regulate basal VEGFR2 turnover are unknown. Ubiquitination regulates membrane protein targeting for degradation and/or intracellular localisation (Ciechanover et al., 2000), suggesting a functional role in modulating both resting and activated RTK status. Protein ubiquitination requires initial action of an E1 ubiquitin-activating enzyme, followed by an E2 ubiquitin-conjugating enzyme working in concert with an E3 ubiquitin ligase (Hershko and Ciechanover, 1992). E2 enzymes conjugate ubiquitin by trans-thiolation and act as intermediaries between the E1 and E3 enzymes (Pickart, 2001).

Here, we build on previous work which identified a novel pathway requiring the E1 ubiquitin-activating enzyme, UBA1, to modulate basal plasma membrane VEGFR2 levels. We now show that the E2 ubiquitin-conjugating enzymes, UBE2D1 and UBE2D2, regulate basal VEGFR2 turnover. This regulatory mechanism regulates the initial endothelial response to VEGF-A. VEGFR2 undergoes VEGF-A-independent, constitutive degradation via a UBE2D1/UBE2D2-dependent ubiquitin-linked pathway. Endothelial UBE2D1 or UBE2D2 depletion increased endosome-to-plasma membrane VEGFR2 recycling and reduced proteolysis. UBE2D1 or UBE2D2 depletion thus elevated VEGF-A-stimulated signal transduction, exemplified by increased PLCγ1, p38 MAPK, Akt and ERK1/2 activation. Importantly, UBE2D1 and UBE2D2-depleted endothelial cells displayed increased VEGF-A-stimulated tubulogenesis. Our work reveals the involvement of two E2 enzymes, UBE2D1 and UBE2D2, in programming basal ubiquitin-dependent recycling and proteolysis of resting VEGFR2. Such

regulation is important in controlling the endothelial response to exogenous ligand such as VEGF-A.

4.2. Results

4.2.1. UBE2D1 and UBE2D2 regulate basal VEGFR2 levels

Our previous work identified a novel ligand-independent pathway for regulating VEGFR2 levels in endothelial cells. This work highlighted the role of the E1 enzyme, UBA1, in basal VEGFR2 ubiquitination, recycling and degradation. To identify which of the 39 E2 ubiquitin-conjugating enzymes are involved in this pathway we used RNAi to screen those which interact with UBA1 (http://www.genecards.org/cgi-bin/carddisp.pl?gene=UBA1) (Fig. 4.1A). Of the 20 E2s screened, quantification revealed that siRNAs directed against UBE2D1, UBE2D2, UBE2E3, UBE2I, UBE2C, UBE2H, UBE2K and UBE2N increased basal VEGFR2 levels (Fig. 4.1B).

4.2.2. UBE2D1 and UBE2D2 regulate the VEGF-A-stimulated response

VEGF-A binding to plasma membrane VEGFR2 stimulates multiple signal transduction pathways (Koch et al., 2011, Zhang et al., 2008). UBA1 mediates basal VEGFR2 turnover to regulate plasma membrane VEGFR2 levels, thus controlling the intensity of VEGF-A-stimulated signal transduction. The E2(s) involved in this ligand-independent pathway are unknown. To determine which E2(s) regulates this pathway we screened those identified in Figure 4.1 for effects on VEGF-A-stimulated signal transduction. Endothelial cells treated with control or individual E2 siRNAs were subjected to VEGF-A stimulation before probing downstream signal transduction events using quantitative immunoblotting. Of the 8 E2s screened, UBE2D1 and UBE2D2 depletion showed the most pronounced effect on VEGF-A-stimulated signal transduction, VEGF-A-stimulated VEGFR2 degradation and VEGF-A-induced production of a 160 kDa VEGFR2 proteolytic fragment (Fig. 4.2, 4.3, 4.4, 4.5, 4.6). The cytoplasmic VEGFR2-Y1175 epitope is autophosphorylated upon VEGF-A stimulation (Koch et al., 2011). Quantitative analysis revealed that UBE2D1 and UBE2D2 depletion increased VEGFR2-pY1175 levels by 58% and 50%, respectively (Fig. 4.7A). Plasma membrane VEGFR2 activation is linked to recruitment, tyrosine phosphorylation and activation of PLCγ1 (Koch et al., 2011). PLCγ1 phosphorylation increased by 55% in UBE2D1-
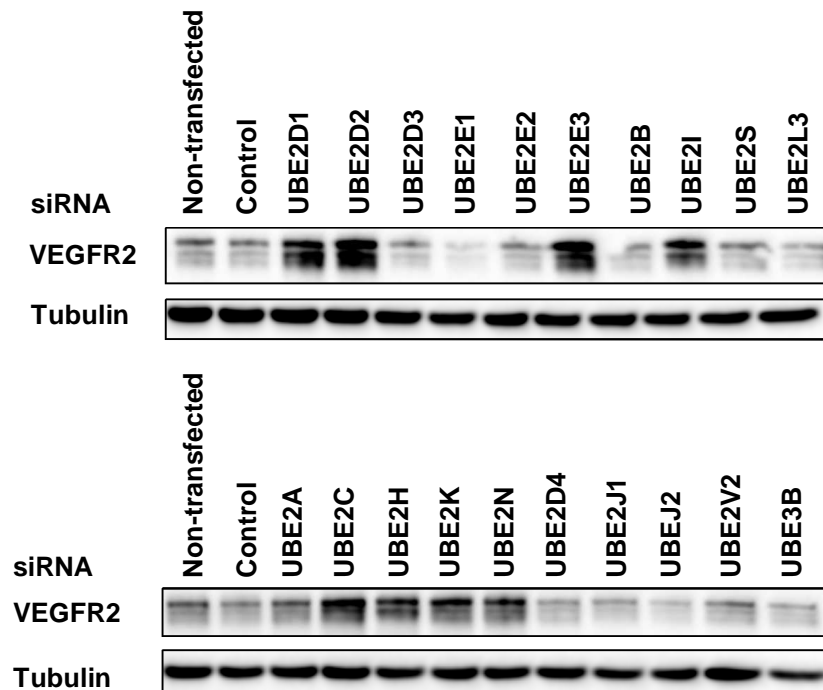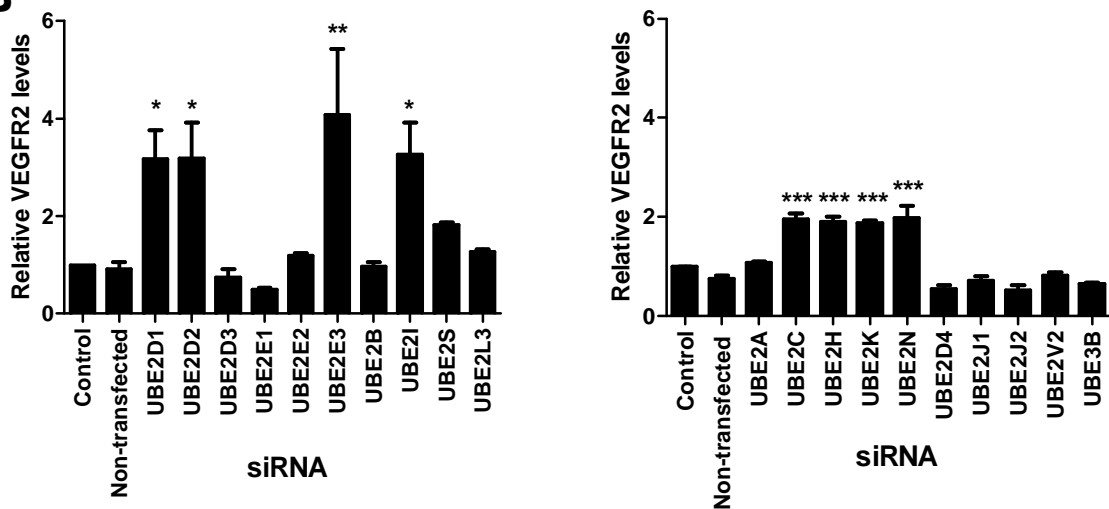
Figure 4.1. An RNAi screen of the E2 ubiquitin-conjugating enzymes for effects on basal VEGFR2 levels. (A) Endothelial cells treated with non-targeting or individual E2-targeting siRNA were lysed and immunoblotted with antibodies for VEGFR2. (B) Quantification of VEGFR2 levels in primary human endothelial cells treated with non-targeting or E2-targeting siRNA. Error bars denote ±SEM (n≥3). $p<0.05$ (*), $p<0.01$ (**), $p<0.001$ (***).
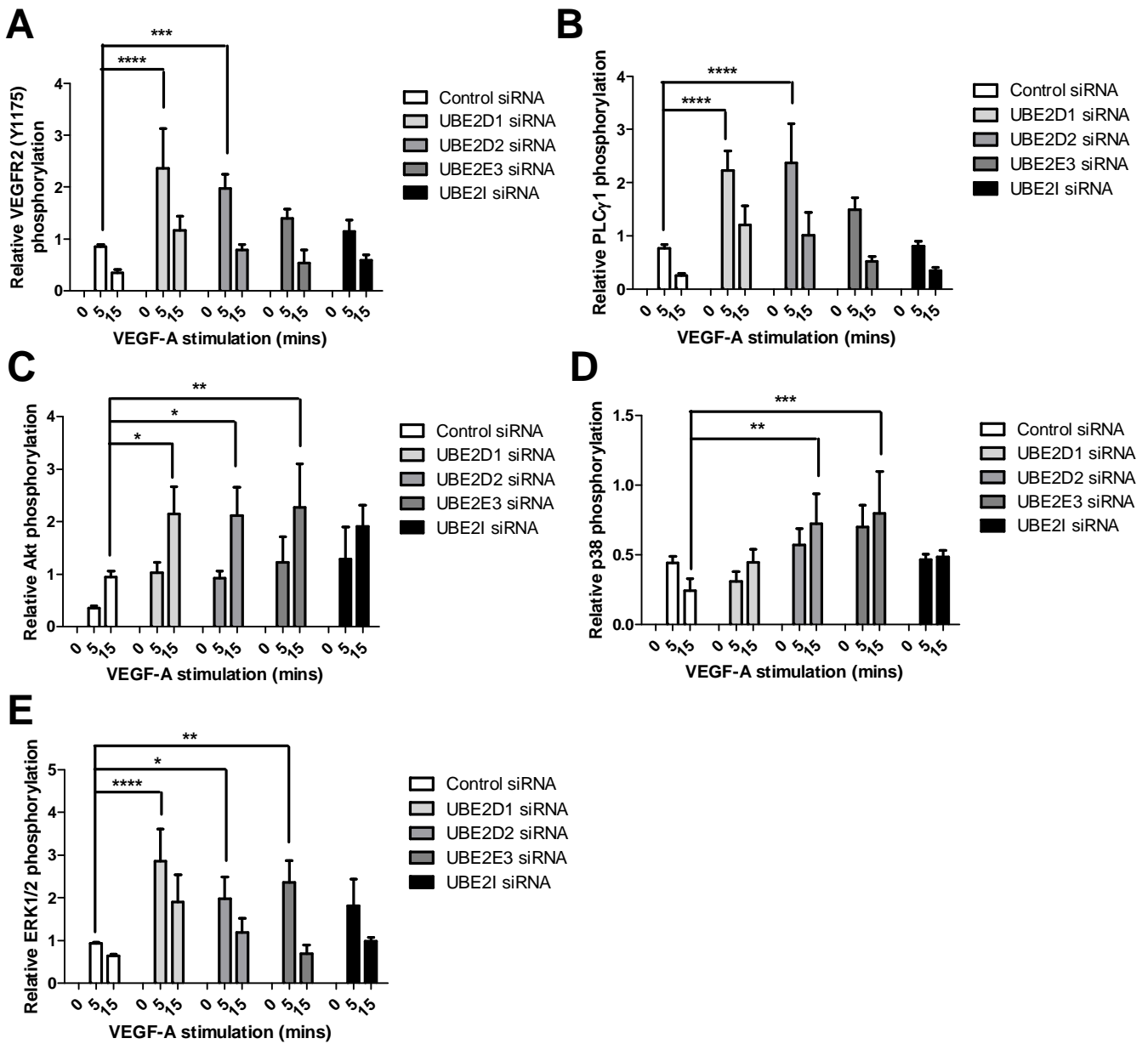
Figure 4.2. A screen of UBE2D1, UBE2D2, UBE2E3 and UBE2I for effects on VEGF-A-stimulated signal transduction. Phospho-VEGFR2 (A), phospho-PLCγ1 (B), phospho-Akt (C), phospho-p38 MAPK (D) and phospho-ERK1/2 (E) levels in endothelial cells transfected with non-targeting, UBE2D1 or UBE2D2, UBE2E3 or UBE2I siRNA and subjected to a VEGF-A (25 ng/ml) time course (0, 5, 15 min) followed by lysis and quantitative immunoblotting. Error bars indicate ±SEM (n≥3). $p<0.05$ (*), $p<0.01$ (**), $p<0.001$ (***), $p<0.0001$ (****).
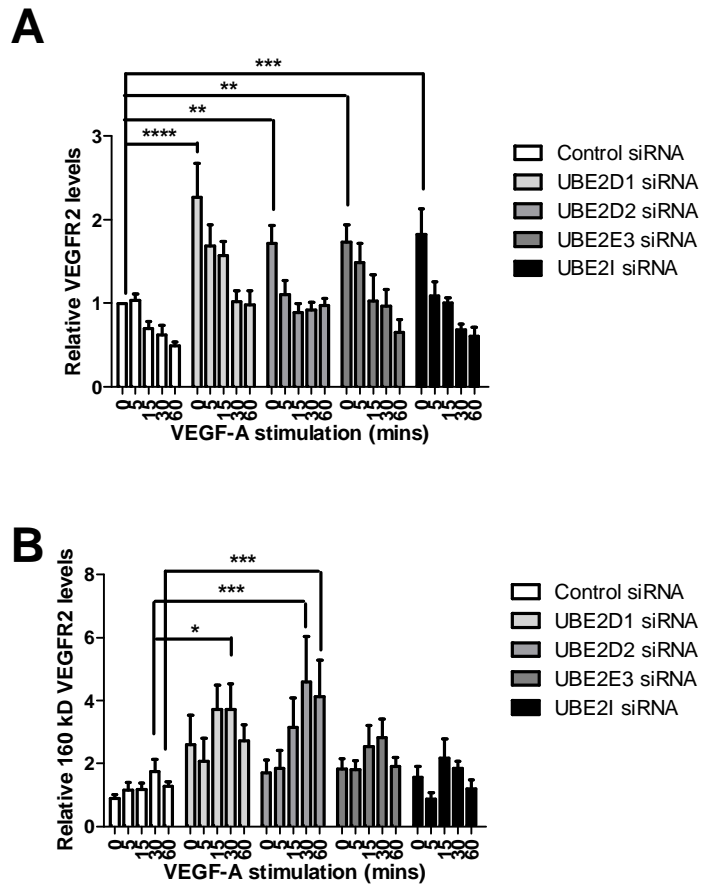
Figure 4.3. A screen of UBE2D1, UBE2D2, UBE2E3 and UBE2I for effects on VEGF-A-stimulated VEGFR2 levels. Quantification of VEGFR2 (A) and VEGFR2-dervied 160 kD fragment (B) levels in endothelial cells transfected with non-targeting, UBE2D1 or UBE2D2, UBE2E3 or UBE2I siRNA subjected to a VEGF-A (25 ng/ml) time course (0, 5, 15, 30, 60 min) followed by lysis and quantitative immunoblotting. Error bars indicate ±SEM (n≥3). $p<0.05$ (*), $p<0.01$ (**), $p<0.001$ (***), $p<0.0001$ (****).
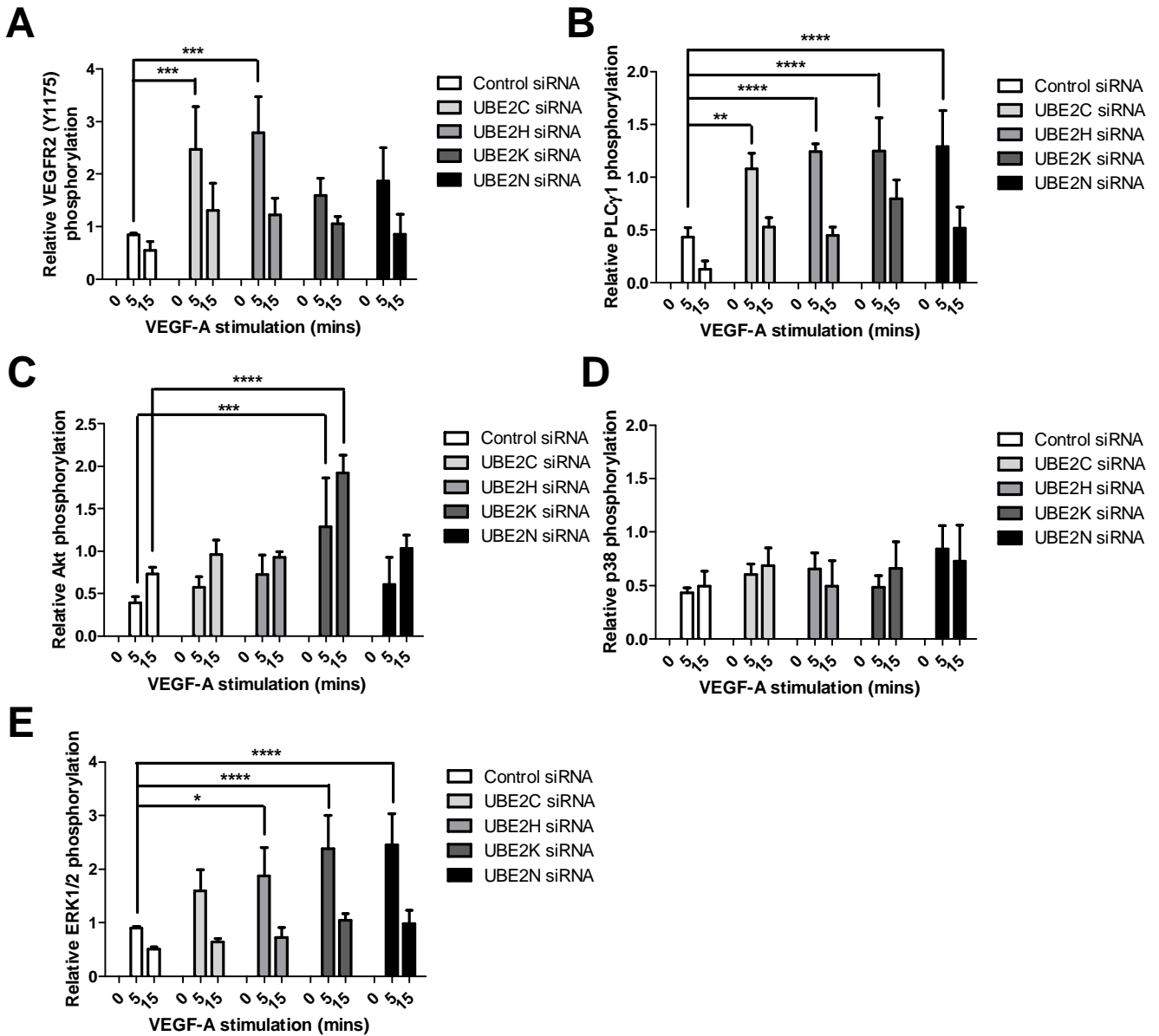
Figure 4.4. A screen of UBE2C, UBE2H, UBE2K and UBE2N for effects on VEGF-A-stimulated signal transduction. Phospho-VEGFR2 (A), phospho-PLCγ1 (B), phospho-Akt (C), phospho-p38 MAPK (D) and phospho-ERK1/2 (E) levels in endothelial cells transfected with non-targeting, UBE2C or UBE2H, UBEK or UBE2N siRNA and subjected to a VEGF-A (25 ng/ml) time course (0, 5, 15 min) followed by lysis and quantitative immunoblotting.. Error bars indicate ±SEM (n≥3). $p<0.05$ (*), $p<0.01$ (**), $p<0.001$ (***), $p<0.0001$ (****).
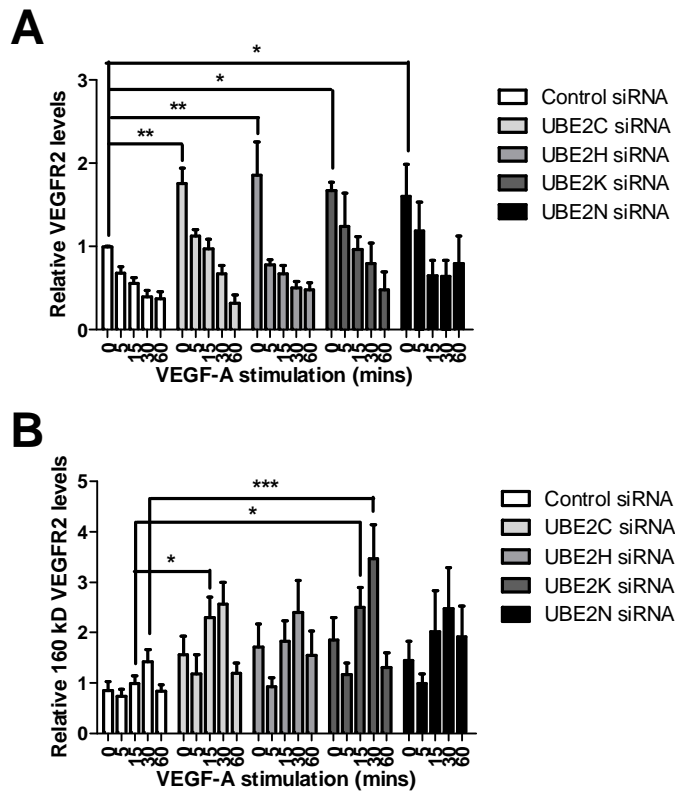
Figure 4.5. A screen of UBE2C, UBE2H, UBE2K and UBE2N for effects on VEGF-A-stimulated VEGFR2 levels. Quantification of VEGFR2 (A) and VEGFR2-dervied 160 kD fragment (B) levels in endothelial cells transfected with non-targeting, UBE2C or UBE2H, UBE2K or UBE2N siRNA and subjected to a VEGF-A (25 ng/ml) time course (0, 5, 15, 30, 60 min) followed by lysis and quantitative immunoblotting. Error bars indicate ±SEM (n≥3). $p<0.05$ (*), $p<0.01$ (**), $p<0.001$ (***).

depleted cells and by 58% in UBE2D2-depleted cells (Fig. 4.7B). VEGF-A-stimulated activation of the master regulator and serine/threonine protein kinase, Akt, was increased by 57% and 56% in UBE2D1 and UBE2D2-depleted endothelial cells, respectively (Fig. 4.7C). Phosphorylation and activation of the p38 MAPK pathway was increased by 56% in UBE2D1-depleted cells and by 67% in UBE2D2-depleted cells (Fig. 4.7D). A key feature of VEGF-A-stimulated signal transduction is activation of the MAPK pathway involving ERK1/2 (Koch and Claesson-Welsh, 2012). ERK1/2 activation displayed a 68% increase in UBE2D1-depleted cells and a 53% increase in UBE2D2-depleted cells (Fig. 4.7E). UBE2D1 and UBE2D2 thus modulate the VEGF-A-stimulated response through a range of signal transduction pathways.

Quantification of basal VEGFR2 levels revealed a 2.3 fold increase in UBE2D1-depleted cells and a 1.7 fold increase in UBE2D2-depleted cells (Fig. 4.7F). In control cells, VEGFR2 underwent 52% VEGF-A-stimulated degradation over 60 min (Fig. 4.7F), whilst VEGFR2 was degraded by 57% and 42% upon VEGF-A stimulation of UBE2D1- and UBE2D2-depleted cells, respectively (Fig. 4.7F). Thus, E2 depletion had limited effect on the degradation rate of activated VEGFR2, however, VEGFR2 levels did remain ~2 fold higher in UBE2D1- and UBE2D2-depleted cells after 60 min VEGF-A stimulation (Fig. 4.7F).

Immunofluorescence microscopy of endothelial cells stained with antibodies to VEGFR2 confirmed that basal VEGFR2 levels were elevated in UBE2D1- and UBE2D2-depleted cells (Fig. 4.8A, B). In control cells depleted of another UBA1-interacting E2, UBE2A, basal VEGFR2 levels were unaffected (Fig. 4.8A, B). UBE2D1 and UBE2D2 are thus E2 ubiquitin-conjugating enzymes that regulate basal VEGFR2 levels.

4.2.3. UBE2D1 and UBE2D2 regulate basal VEGFR2 degradation

Subjecting endothelial cells to a block in protein synthesis allows monitoring of mature VEGFR2 degradation (Shaik et al., 2012). Using CHX to block new protein synthesis thus provides a means of evaluating the effect of UBE2D1 and UBE2D2 depletion on mature plasma membrane VEGFR2 turnover. To test how UBE2D1 or UBE2D2 depletion affects such basal VEGFR2 turnover, we used RNAi to deplete UBE2D1 or
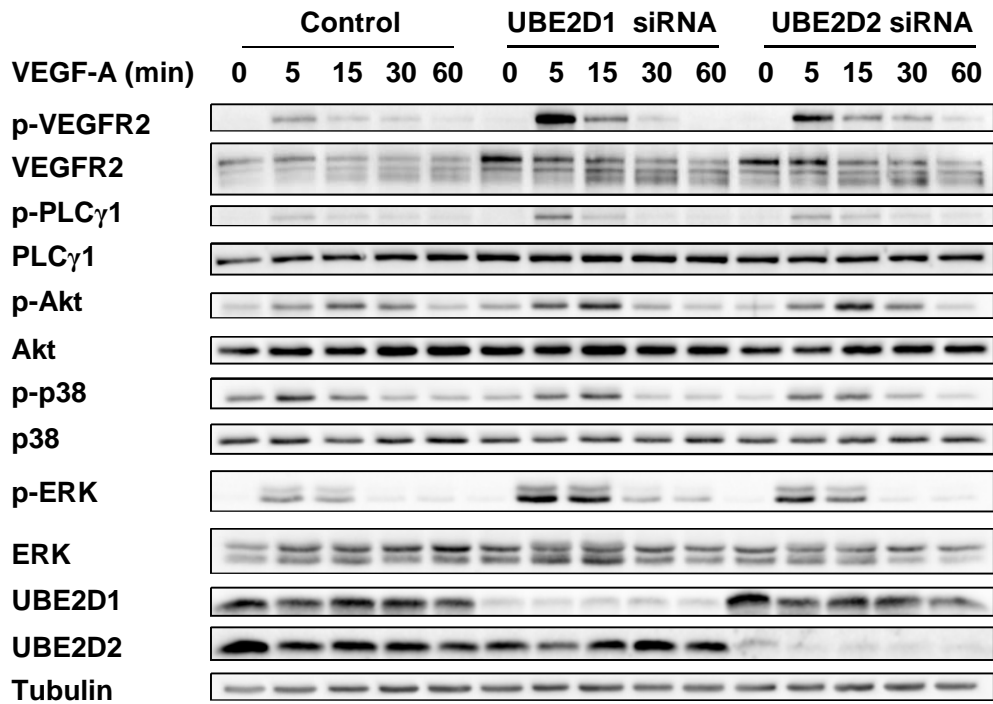
Figure 4.6. UBE2D1 and UBE2D2 depletion upregulates VEGF-A-stimulated signal transduction. Endothelial cells transfected with non-targeting, UBE2D1 or UBE2D2 siRNA were treated with 25 ng/ml VEGF-A, lysed and immunoblotted for phospho-VEGFR2 (Y1175), phospho-PLCγ1 (Y783), phospho-Akt (S473), phospho-p38 MAPK (T180/Y182) and phospho-ERK1/2 (T202/Y204).
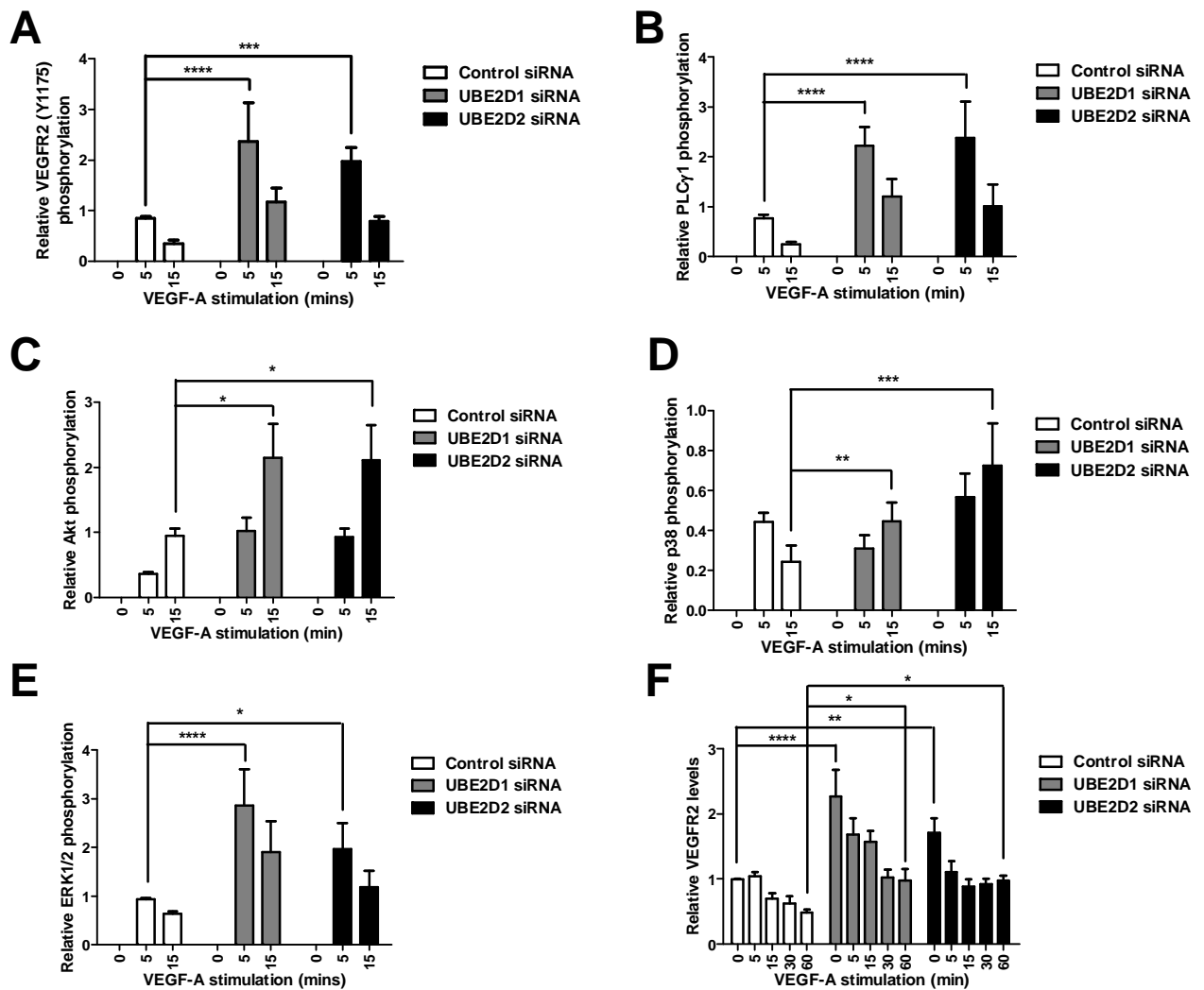
Figure 4.7. UBE2D1 and UBE2D2 depletion upregulates VEGF-A-stimulated signal transduction. Quantification of phospho-VEGFR2 (A), phospho-PLCγ1 (B), phospho-Akt (C), phospho-p38 MAPK (D), phospho-ERK1/2 (E) and VEGFR2 (F) levels in endothelial cells transfected with non-targeting, UBE2D1 or UBE2D2 siRNA and subjected to a VEGF-A (25 ng/ml) time course (0, 5, 15, 30, 60 min) followed by lysis and quantitative immunoblotting. Error bars indicate ±SEM (n≥3). $p<0.05$ (*), $p<0.01$ (**), $p<0.001$ (***), $p<0.0001$ (****).
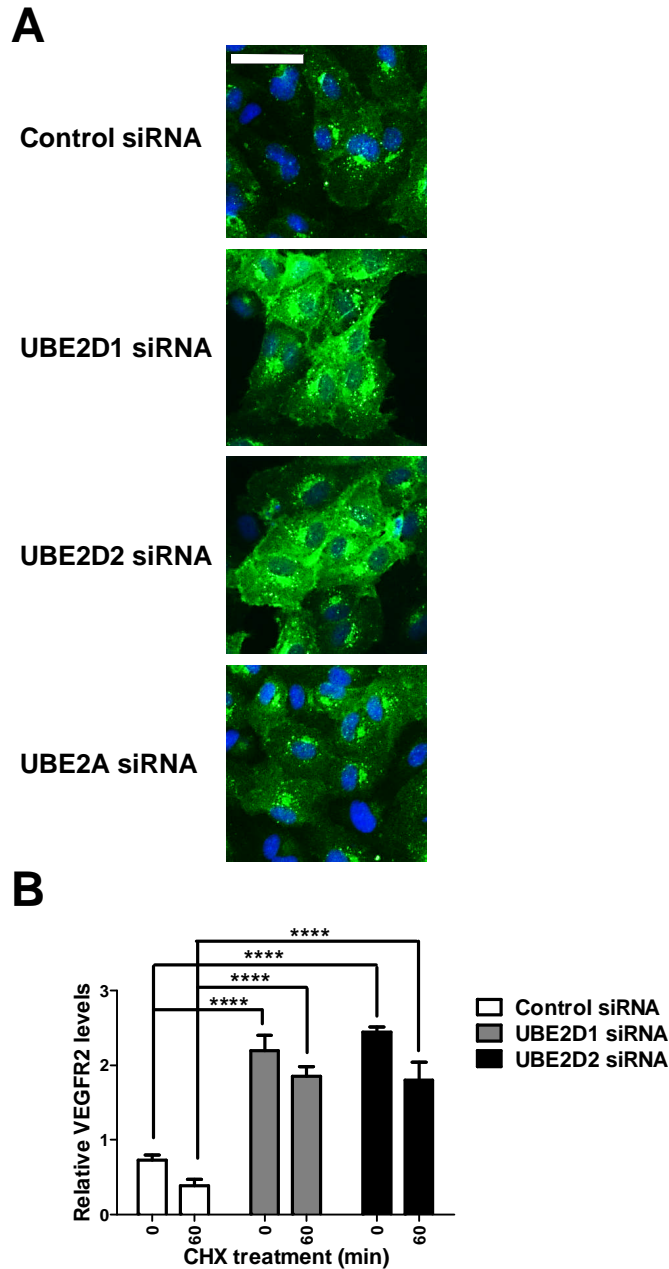
Figure 4.8. UBE2D1 and UBE2D2 regulate basal VEGFR2 levels. (A) Immunofluorescence microscopy of endothelial cells transfected with non-targeting, UBE2D1, UBE2D2 or UBE2A siRNA and stained with antibodies to VEGFR2 followed by fluorescent species-specific secondary antibodies (green). Nuclei were stained with DNA-binding dye, DAPI (blue). Scale bar represents 70 μm. (B) Quantitative microscopy of VEGFR2 levels in endothelial cells treated with non-targeting, UBE2D1, UBE2D2 or UBE2A siRNA. Error bars denote ±SEM (n≥3). $p<0.05$ (*), $p<0.01$ (**).

UBE2D2 in endothelial cells, followed by CHX treatment to block protein synthesis (Fig. 4.9A). Immunoblotting confirmed that basal (0 min) VEGFR2 levels were elevated in UBE2D1- or UBE2D2-depleted endothelial cells in which RTK phosphorylation/activation was not evident (Fig. 4.9A). Importantly, UBA1 depletion did not affect levels of other plasma membrane receptors such TfR (Fig. 4.9A). Quantification revealed that under control conditions, 59% of mature VEGFR2 underwent degradation over an 80 min period of CHX treatment (Fig. 4.9B). Upon UBE2D1 depletion, VEGFR2 exhibited 49% basal degradation. In UBE2D2-depleted endothelial cells, VEGFR2 was degraded by 31% after 80 min CHX treatment (Fig. 4.9B). Thus, E2 depletion substantially reduced the rate of constitutive VEGFR2 degradation (Fig. 4.9C). Endothelial cells depleted of both UBE2D1 and UBE2D2 exhibited a response in between that produced when UBE2D1 or UBE2D2 were depleted individually (Fig. 4.9A).

Morphological analysis of VEGFR2 distribution using quantitative microscopy further supported a role for UBE2D1 and UBE2D2 in basal VEGFR2 degradation and turnover (Fig. 4.10). Comparison of control and UBE2D1- or UBE2D2-depleted endothelial cells revealed that basal (0 min) VEGFR2 levels were 67% and 71% higher in UBE2D1- and UBE2D2-depleted cells, respectively (Fig. 4.10B). Furthermore, in the presence of CHX, control cells exhibited 47% degradation after 60 min (Fig. 4.10B). However, basal VEGFR2 levels were reduced by only 15% upon UBE2D1 depletion and 25% in UBE2D2-depleted cells (Fig. 4.10B). These findings confirm that UBE2D1 and UBE2D2 regulate basal VEGFR2 turnover in a ligand-independent manner.

4.2.4. UBE2D1 and UBE2D2 regulate basal VEGFR2 ubiquitination

Direct ubiquitination could be one means through which UBE2D1 and UBE2D2 regulate basal VEGFR2 turnover. To test this idea, we immunoprecipitated mature VEGFR2 from CHX-treated control, UBE2D1- or UBE2D2-depleted endothelial cells and evaluated ubiquitination status by immunoblot analysis (Fig 4.11A). Although levels of ubiquitinated receptor appear higher than in control cells, particularly upon UBE2D2 depletion (Fig. 4.11A), this is counteracted by higher levels of VEGFR2 to begin with in UBE2D1 or UBE2D2-depleted cells (Fig. 4.11A). In control cells subjected to a CHX time course, basal VEGFR2 ubiquitination peaked after 40 min
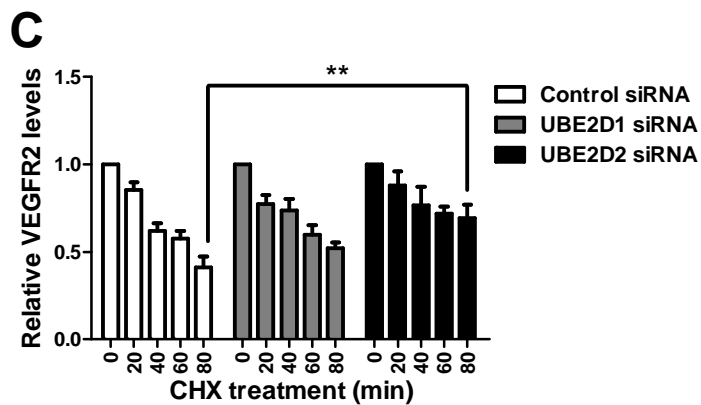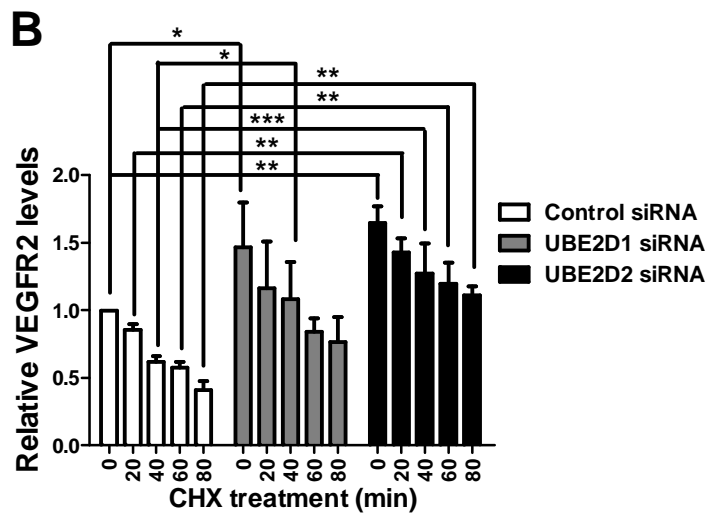
Figure 4.9. UBE2D1 and UBE2D2 regulate ligand-independent VEGFR2 degradation. (A) Endothelial cells transfected with non-targeting, UBE2D1 or UBE2D2 siRNA were treated with 20 μg/ml CHX over a time course of 80 min and immunoblotted for phospho-VEGFR2, VEGFR2, transferrin receptor (TfR), UBE2D1, UBE2D2 or tubulin. (B) VEGFR2 levels in endothelial cells transfected with non-targeting, UBE2D1 or UBE2D2 siRNA, treated with 20 μg/ml CHX (80 min) and analysed by quantitative immunoblotting. (C) VEGFR2 degradation rate quantified by comparison of the 0 min time point with corresponding CHX-treated time points. Error bars denote ±SEM (n≥3). $p<0.05$ (*), $p<0.01$ (**), $p<0.001$ (***).
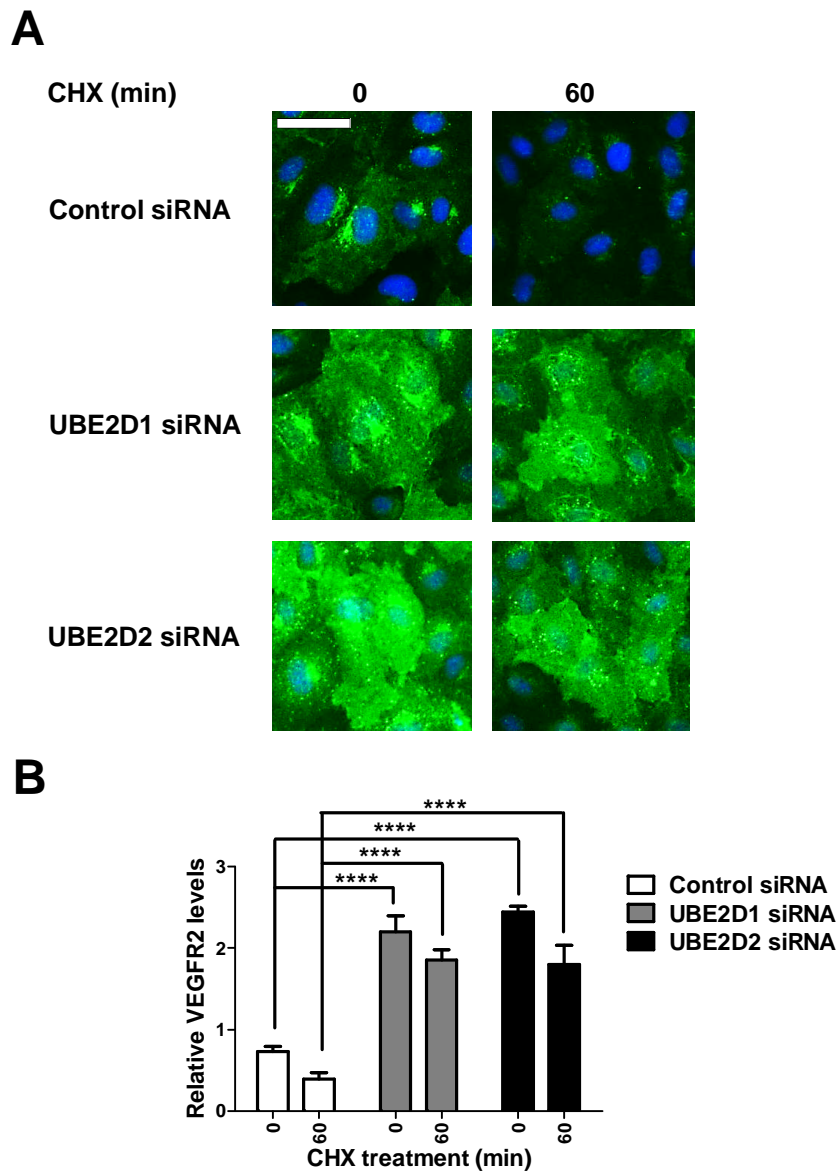
Figure 4.10. Confirmation that UBE2D1 and UBE2D2 regulate ligand-independent VEGFR2 degradation by quantitative microscopy. (A) Endothelial cells transfected with non-targeting, UBE2D1 or UBE2D2 siRNA were treated with 20 μg/ml CHX over a time course of 60 min and processed for immunofluorescence microscopy using antibodies to VEGFR2 followed by fluorescent species-specific secondary antibodies (green). Nuclei were stained with DNA-binding dye, DAPI (blue). Scale bar represents 200 μm. (E) VEGFR2 levels in endothelial cells treated with 20 μg/ml CHX quantified using microscopy datasets. Error bars denote ±SEM (n≥3). $p<0.05$ (*), $p<0.01$ (**), $p<0.001$ (***), $p<0.0001$ (****).

103

(Fig. 4.11B). In contrast, VEGFR2 ubiquitination did not peak until 80 min in UBE2D1- or UBE2D2-depleted endothelial cells (Fig. 4.11B). These findings support a role for UBE2D1 and UBE2D2 in regulating basal VEGFR2 ubiquitination to promote ligand-independent degradation.

4.2.5. UBE2D1 and UBE2D2 regulate basal VEGFR2 recycling

RTK ubiquitination at the plasma membrane precedes internalisation and delivery to early endosomes (Haglund and Dikic, 2012, Ewan et al., 2006, Clague and Urbe, 2001). Ligand-stimulated VEGFR2 ubiquitination promotes trafficking to late endosomes and terminal degradation in lysosomes (Ewan et al., 2006, Bruns et al., 2010). RTK de-ubiquitination in early endosomes is associated with endosome-to-plasma membrane recycling (Clague and Urbe, 2006). Furthermore, VEGFR2 undergoes substantial constitutive, ligand-independent recycling via endosomes (Jopling et al., 2011). One possibility is that upon UBE2D1 or UBE2D2 depletion, VEGFR2 undergoes decreased basal ubiquitination which is a prerequisite for increased endosome-to-plasma membrane recycling. To test this idea, we utilised a microscopy-based VEGFR2 recycling assay (Jopling et al., 2011). Here, control, UBE2D1- or UBE2D2-depleted endothelial cells were incubated with extracellular domain-specific antibodies to VEGFR2. Constitutive VEGFR2 endocytosis and recycling was monitored using accessibility of VEGFR2-antibody complexes to a subsequent pulse of labelled secondary antibody. Only VEGFR2-antibody complexes that had undergone endocytosis followed by endosome-to-plasma membrane recycling were detected (Fig. 4.12A). Quantification revealed that UBE2D1- or UBE2D2-depleted endothelial cells displayed 50% or 57% increase in basal VEGFR2 recycling, respectively (Fig. 4.12B). VEGF-A-stimulated recycling was also increased in UBE2D1- or UBE2D2-depleted cells, however, this increase was not VEGF-A-dependent and likely resulted from elevated levels of resting VEGFR2 (Fig. 4.12B).

One prediction is that increased basal recycling of VEGFR2 increases overall plasma membrane levels in UBE2D1- or UBE2D2-depleted cells. To test this hypothesis, endothelial cells were treated with CHX to block new protein synthesis and subjected to cell surface biotinylation followed by purification of biotinylated plasma membrane proteins and immunoblot anaylsis (Fig. 4.13A). VEGFR2 plasma membrane levels were clearly elevated upon UBE2D1 or UBE2D2 depletion, whereas another integral plasma

A

B
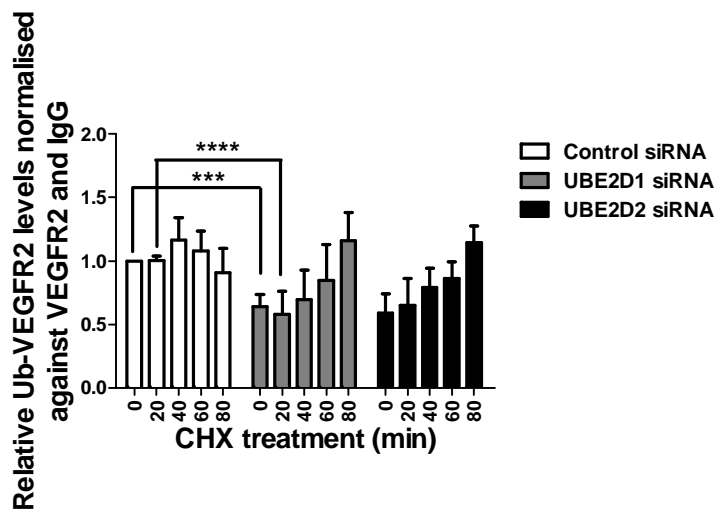
Figure 4.11. UBE2D1 and UBE2D2 regulate basal ubiquitination of VEGFR2. (A) Primary human endothelial cells transfected with non-targeting, UBE2D1 or UBE2D2 siRNA were treated with 20 μg/ml CHX and lysed. VEGFR2 was immunoprecipitated and immunoblotted for ubiquitin status using a pan-ubiquitin antibody. (B) Quantification of ubiquitinated VEGFR2 (Ub-VEGFR2) levels in endothelial cells transfected with non-targeting, UBE2D1 or UBE2D2 siRNA and treated with 20 μg/ml CHX. Relative Ub-VEGFR2 levels were normalised against IgG and VEGFR2. Error bars denote ±SEM (n≥3). $p<0.001$ (***), $p<0.0001$ (****). IP; immunoprecipitate, WCL, whole cell lysate.
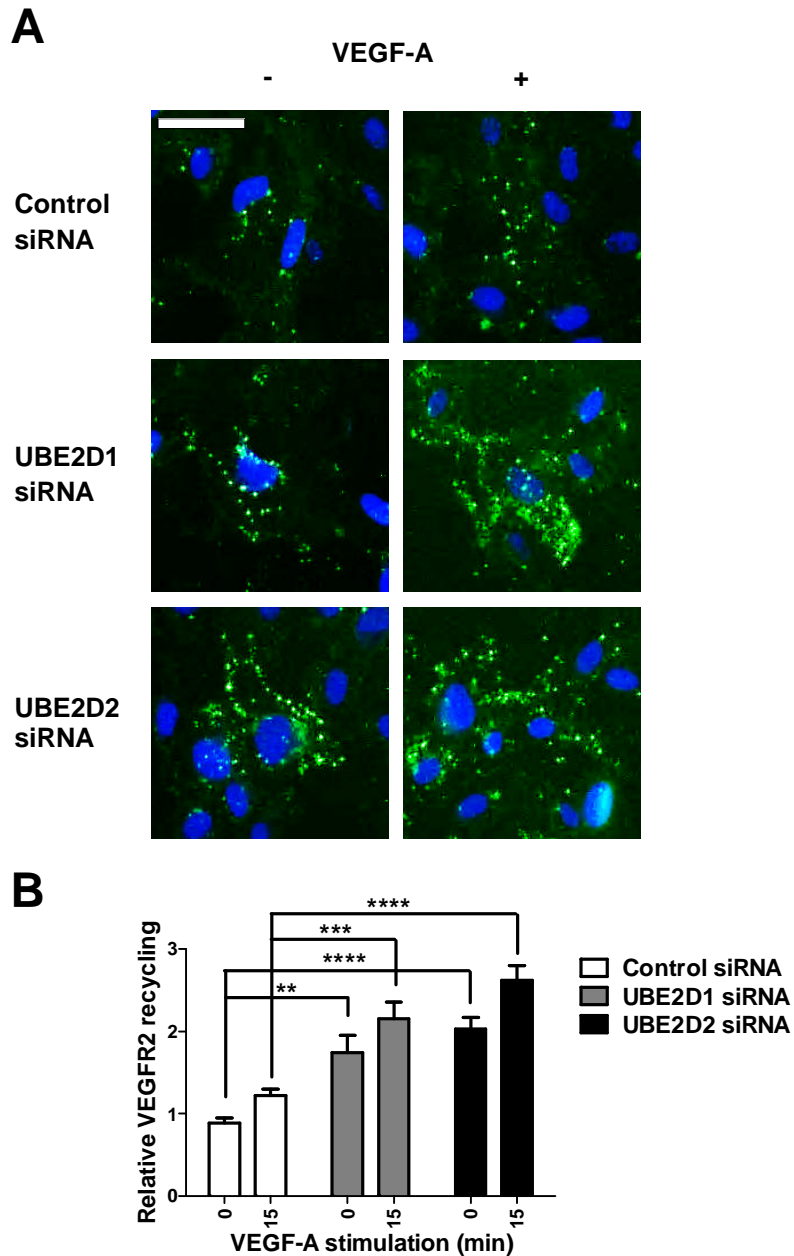
Figure 4.12. UBE2D1 and UBE2D2 regulate basal recycling of VEGFR2. (A) Endothelial cells transfected with non-targeting, UBE2D1 or UBE2D2 siRNA were incubated with antibodies to VEGFR2 for 30 min at 37°C before being treated with 25 ng/ml VEGF-A, acid-washed to strip cell surface antibodies and incubated with fluorescent species-specific secondary antibodies for 30 min at 37°C (green). Cells were fixed prior to staining with DNA-binding dye, DAPI (blue). Only VEGFR2 that underwent plasma membrane-to-endosome-to-plasma membrane recycling is visible. Scale bar represents 200 μm. (B) Basal and VEGF-A-stimulated VEGFR2 recycling quantified in cells transfected with non-targeting, UBE2D1 or UBE2D2 siRNA. Error bars denote ±SEM (n≥3). $p<0.01$ (**), $p<0.001$ (***), $p<0.0001$ (****).

membrane protein, TfR, was unaffected (Fig. 4.13A). Quantification revealed that under control conditions, plasma membrane VEGFR2 levels were gradually reduced by 68% over an 80 min period of CHX treatment (Fig. 4.13B). In UBE2D1-depleted cells plasma membrane VEGFR2 levels remained relatively stable until 80 min after CHX treatment when levels dropped by 35% (Fig. 4.13B). In contrast to control cells, UBE2D2-depleted cells exhibited 31% increase in cell surface (0 min) VEGFR2 levels which decreased by 45% after CHX treatment for 80 min (Fig. 4.13B). Taken together, these data suggest that UBE2D1 and UBE2D2 regulate basal endosome-to-plasma membrane recycling and plasma membrane VEGFR2 levels in an ubiquitin-dependent manner. Biotinylation of plasma membrane proteins also revealed that whilst basal (0 min) plasma membrane VEGFR2 levels were higher in UBE2D1- and UBE2D2-depleted cells (Fig. 4.14A), VEGF-A-stimulated internalisation was unaffected (Fig. 4.14B).

4.2.6. Basal VEGFR2 turnover by UBE2D1 and UBE2D2 regulates VEGF-A-dependent endothelial cell tubulogenesis

VEGF-A-stimulated activation of VEGFR2 promotes downstream signal transduction leading to new blood vessel sprouting, an essential feature of angiogenesis (Ferrara, 1999). In an endothelial-fibroblast co-culture assay, VEGF-A stimulated tubulogenesis was revealed by staining for the endothelial-specific protein, PECAM-1 (Fig. 4.15A). In the absence of VEGF-A, tubule growth of UBE2D1- or UBE2D2-depleted endothelial cells was unaffected (Fig. 4.15B, C). Upon comparison of each non-stimulated condition with the corresponding VEGF-A-stimulated condition for non-transfected, control, UBE2D1, or UBE2D2 siRNA-treated cells VEGF-A-dependent tubulogenesis of UBE2D1- and UBE2D2-depleted cells was significantly higher than that of control cells (Fig. 4.15B, C). VEGF-A-stimulated endothelial tubule length increased by 55% and 54% in UBE2D1- and UBE2D2-depleted cells, respectively (Fig. 4.15B). Furthermore, UBE2D1- and UBE2D2-depleted endothelial cells displayed 3.5-fold and 2-fold increase in branch point number, respectively (Fig. 4.15C). Depletion of UBE2D1 or UBE2D2 thus increases VEGF-A-stimulated tubulogenesis.
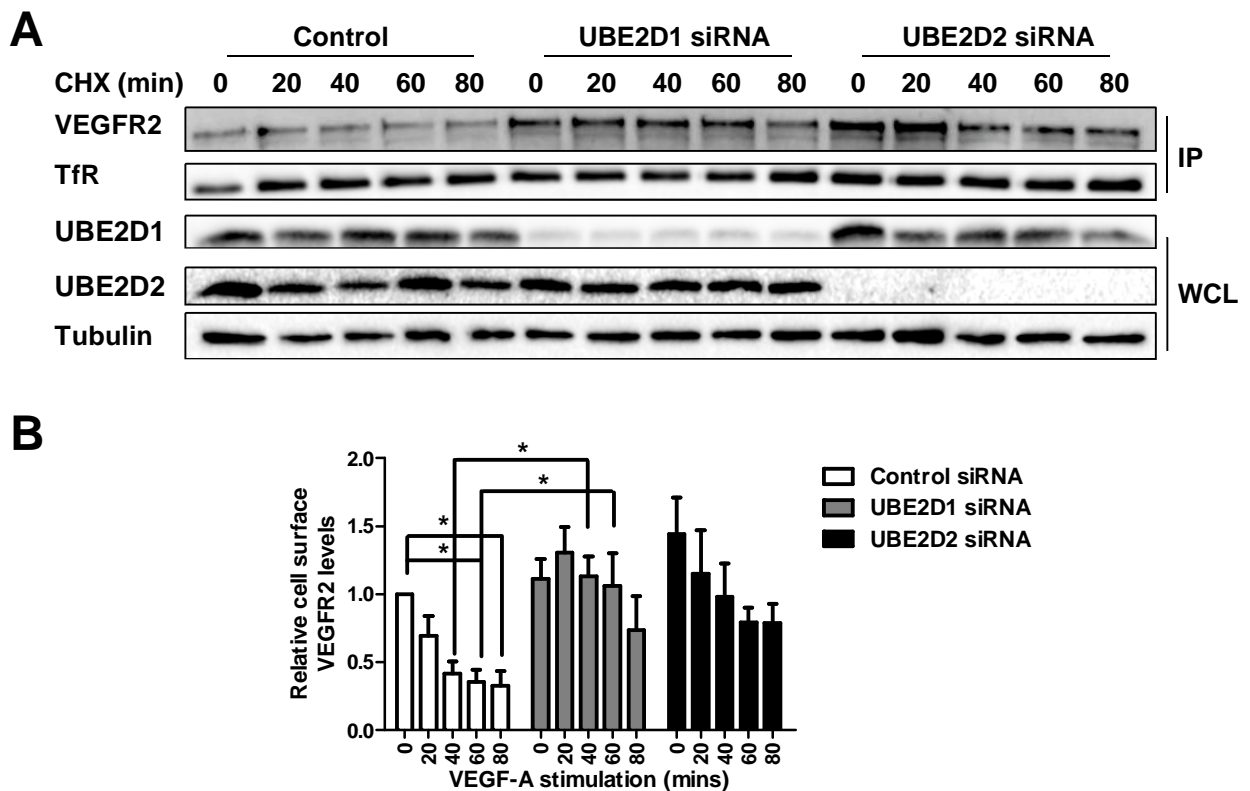
Figure 4.13. UBE2D1 and UBE2D2 regulate plasma membrane VEGFR2 levels. (A) Primary human endothelial cells transfected with non-targeting, UBE2D1 or UBE2D2 siRNA were treated with 20 μg/ml CHX. Cell surface proteins were biotinylated, isolated and immunoblotted for plasma membrane VEGFR2 (PM VEGFR2) or transferrin receptor (TfR). (B) Cell surface VEGFR2 levels in endothelial cells transfected with non-targeting, UBE2D1 or UBE2D2 siRNA and treated with 20 μg/ml CHX determined using quantitative immunoblotting. Error bars denote ±SEM (n≥3). $p<0.05$ (*). IP; immunoprecipitate, WCL; whole cell lysate.
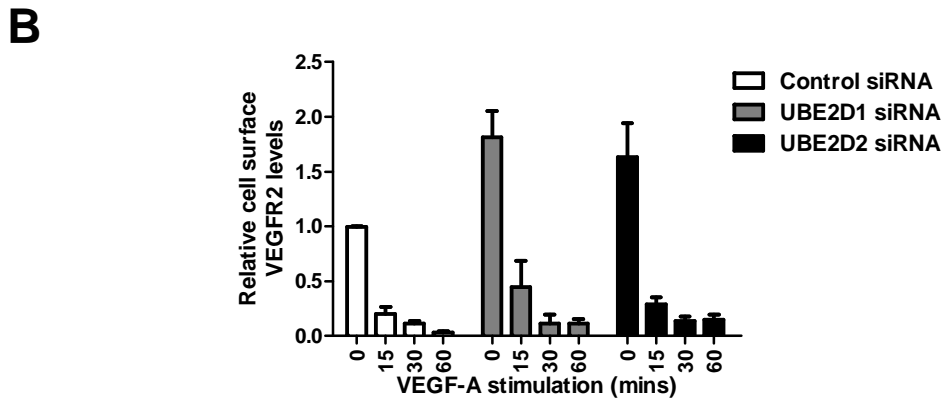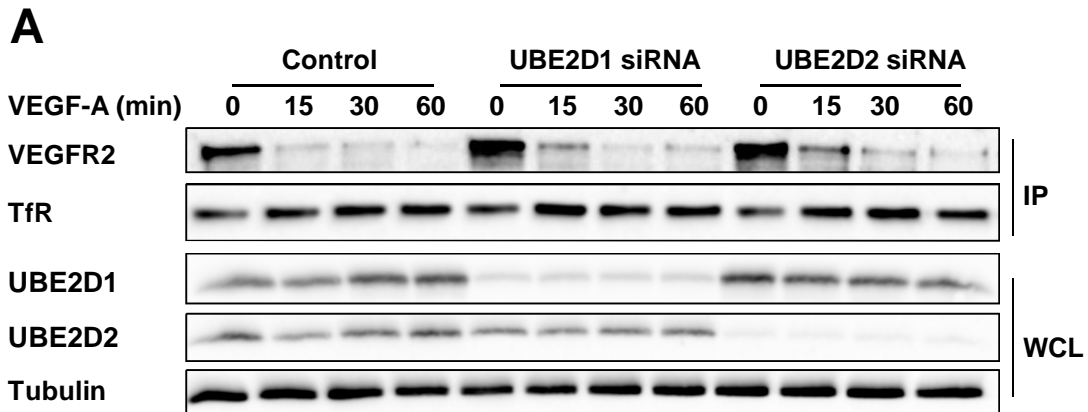
Figure 4.14. UBE2D1 and UBE2D2 regulate basal plasma membrane VEGFR2 levels. (A) Endothelial cells transfected with non-targeting, UBE2D1 or UBE2D2 siRNA were treated with 25 ng/ml VEGF-A, cell surface biotinylated and lysed. Biotinylated proteins were isolated and immunoblotted using antibodies against VEGFR2. (B) Cell surface VEGFR2 levels over a time course of 25 ng/ml VEGF-A stimulation in endothelial cells transfected with non-targeting, UBE2D1 or UBE2D2 siRNA determined using quantitative immunoblotting. Error bars denote ±SEM (n≥3). IP; immunoprecipitate, WCL; whole cell lysate.
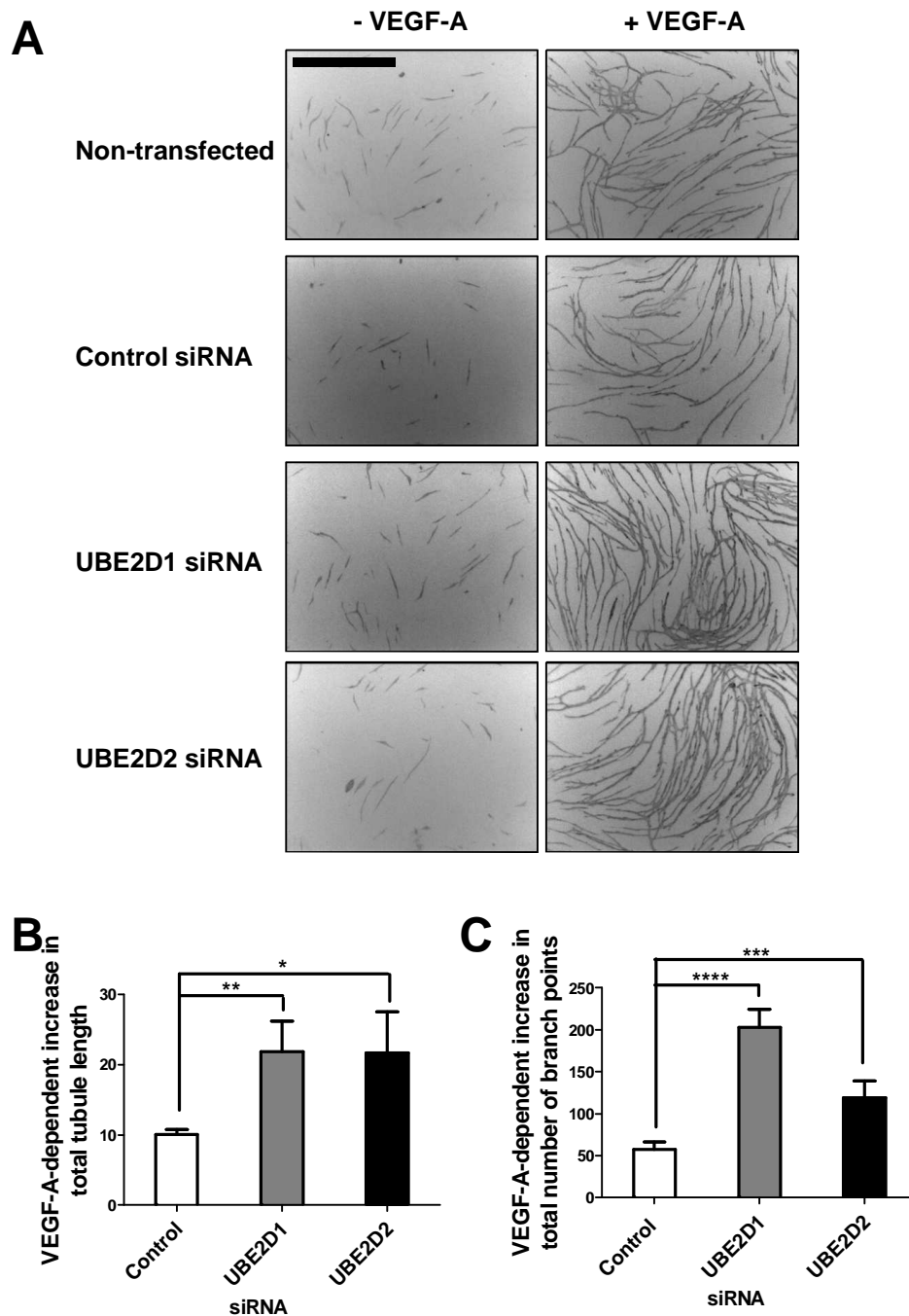
Figure 4.15. Basal VEGFR2 turnover by UBE2D1 or UBE2D2 regulates the VEGF-A-dependent endothelial response. (A) Primary human endothelial cells transfected with non-targeting, UBE2D1 or UBE2D2 siRNA were co-cultured on a bed of primary human fibroblasts for 7 days, treated with 25 ng/ml VEGF-A, fixed and stained with an antibody to PECAM-1. Scale bar represents 1000 μm. Quantification of total tubule length (B) and total number of branch points (C) from non-transfected or non-targeting, UBE2D1 or UBE2D2 siRNA-treated endothelial cells. Error bars denote ±SEM (n≥3). $p<0.05$ (*), $p<0.01$ (**), $p<0.001$ (***), $p<0.0001$ (****).

110

4.2.7. UBE2D1 and UBE2D2 regulate VEGF-A-stimulated ubiquitination of VEGFR2

The identification of UBE2D1 and UBE2D2 as regulators of constitutive VEGFR2 ubiquitination raised the question of whether they also play a role in ligand-stimulated VEGFR2 ubiquitination. To test this, control, UBE2D1- or UBE2D2-depleted endothelial cells were stimulated with VEGF-A followed by analysis of VEGFR2 ubiquitination status (Fig. 4.16). Following VEGF-A stimulation, immunoisolated VEGFR2 complexes were subjected to immunoblotting using antibodies specific for K48- and K63-linked forms of polyubiquitin or a pan-ubiquitin (FK2) antibody (Fig. 4.16). In control cells, VEGFR2 ubiquitination peaked 5-15 min after VEGF-A stimulation (Fig 4.16B). Although levels of ubiquitinated receptor appear higher than in control cells (Fig. 4.16A), this is counteracted by higher levels of VEGFR2 to begin with in UBE2D1 or UBE2D2-depleted cells (Fig. 4.16A). These results provide evidence for UBE2D1- and UBE2D2-mediated ubiquitination of ligand-activated VEGFR2. In UBE2D1-depleted cells, VEGF-A-stimulated VEGFR2 ubiquitination was 31% reduced (Fig. 4.16B), whilst UBE2D2 caused a 45% reduction in ubiquitination of activated VEGFR2 (Fig. 4.16B). This 45% reduction could be significant enough to explain the 10% decrease in VEGF-A-stimulated VEGFR2 degradation upon UBE2D2 depletion (Fig. 4.7F). Nonetheless, the effect of UBE2D2 depletion on ligand-activated VEGFR2 degradation is minimal suggesting that further ubiquitin-linked degradative pathways exist to control VEGF-A-stimulated VEGFR2 proteolysis.

4.3. Discussion

Ubiquitination is involved in VEGFR2 trafficking and degradation (Ewan et al., 2006, Bruns et al., 2010). Previously we identified a novel pathway in which the E1 ubiquitin-activating enzyme, UBA1, programs VEGFR2 for basal degradation. This ligand-independent mechanism precisely influences net plasma membrane VEGFR2 levels, thus controlling RTK-mediated signal transduction and the cellular response to extracellular ligand (Fig. 4.17). This pathway for surveillance of basal VEGFR2 levels provides a mechanism for modulating the duration and intensity of VEGF-A-stimulated signal transduction. We provide evidence that the E2 ubiquitin-conjugating enzymes, UBE2D1 and UBE2D2, work downstream of UBA1 to regulate basal VEGFR2 degradation. The UBE2D family of E2s consists of three highly homologous proteins,
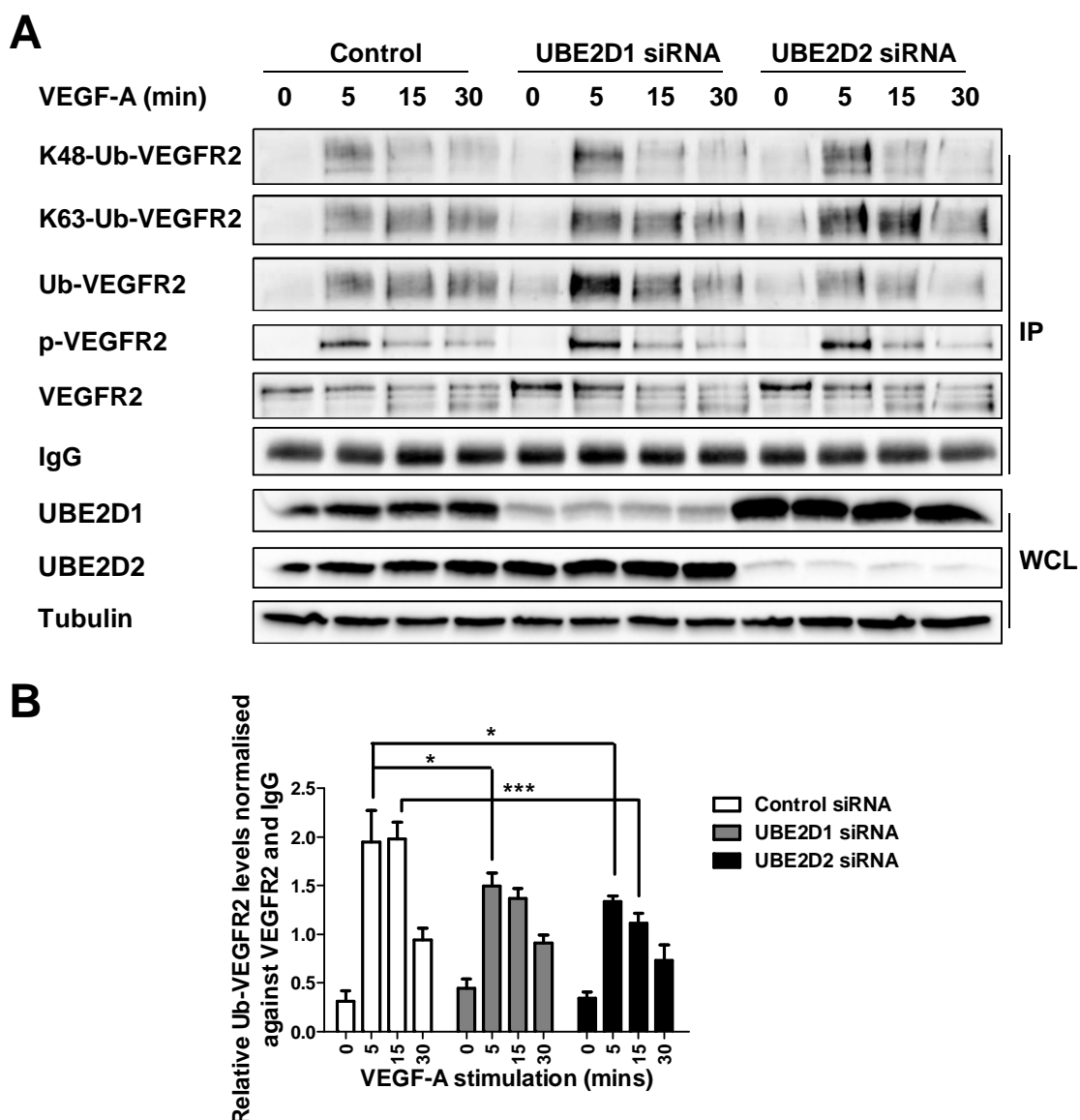
Figure 4.16. UBE2D1 and UBE2D2 regulate ubiquitination of VEGF-A-activated VEGFR2. (A) Endothelial cells transfected with non-targeting, UBE2D1 or UBE2D2 siRNA were treated with 25 ng/ml VEGF-A and lysed. VEGFR2 was immunoprecipitated and immunoblotted for its ubiquitin status using antibodies against K48-linked polyubiquitin, K63-linked polyubiquitin and pan-ubiquitin. (B) Quantification of ubiquitinated VEGFR2 levels in endothelial cells transfected with non-targeting, UBE2D1 or UBE2D2 siRNA and treated with 25 ng/ml VEGF-A. Relative Ub-VEGFR2 levels were normalised against IgG and VEGFR2. Error bars denote ±SEM (n≥3). $p<0.05$ (*), $p<0.001$ (***). IP; immunoprecipitate, WCL; whole cell lysate.

UBE2D1, UBE2D2 and UBE2D3. Perturbation of UBE2D1 or UBE2D2 function using RNAi increases plasma membrane VEGFR2 availability and elevates VEGF-A-stimulated signal transduction. Notably, elevated phosphorylation and activation of VEGFR2, PLCγ1, p38 MAPK, Akt and ERK1/2 was evident in UBE2D1- and UBE2D2-depleted cells. The link between plasma membrane protein ubiquitination and trafficking is highlighted by increased VEGFR2 endosome-to-plasma membrane recycling upon UBE2D1 or UBE2D2 depletion. Finally, such regulation has significant consequences for VEGF-A-stimulated cellular responses such as endothelial tubulogenesis: reduction in UBE2D1 or UBE2D2 levels elevates the pro-angiogenic response to VEGF-A.

Ligand-stimulated ubiquitination of VEGFR2 programs terminal degradation in lysosomes (Ewan et al., 2006). Other studies implicate E3 ubiquitin ligases, c-Cbl and β-TrCP1, in VEGF-A-stimulated VEGFR2 proteolysis (Duval et al., 2003, Murdaca et al., 2004, Shaik et al., 2012, Bruns et al., 2010, Singh et al., 2007). Interestingly, UBE2D2 shows specific binding to the RING domain of c-Cbl and is required for c-Cbl-linked ubiquitin transfer to downstream targets (Huang et al., 2009). For example, UBE2D2 is the E2 ubiquitin-conjugating enzyme upstream of c-Cbl in mediating EGF-stimulated polyubiquitination of EGFR, both at the plasma membrane and after internalisation (Umebayashi 2008). UBE2D2 is also involved in polyubiquitination of dopamine transporter (DAT) in cooperation with the E3 ligase, Nedd4 (Vina-Vilaseca and Sorkin, 2010). Thus, UBE2D enzymes can be coupled to both HECT and RING domain (c-Cbl) E3 ligases to promote polyubiquitination. Another study described polyubiquitination of IκBα by β-TrCP2. In this model, polyubiquitination is initiated by UBE2D1-mediated transfer of a single ubiquitin to IκBα. Monoubiquitin acts as a receptor to direct cdc34 (UBE2R1)-mediated elongation of the ubiquitin chain to initiate β-TrCP2-dependent polyubiquitination (Wu et al., 2010). Thus, UBE2D1 and UBE2D2 are capable of initiating chain elongation independently of an E3 ligase. It is possible that other E2s and their interacting E3s are involved in chain elongation to generate polyubiquitin as a signal for VEGFR2 degradation. It is also interesting to note that UBE2D1/UBE2D2 are E2s for c-Cbl and β-TrCP isoforms, both of which are implicated in VEGF-A-stimulated ubiquitination of VEGFR2 (Duval et al., 2003, Murdaca et al., 2004, Shaik et al., 2012, Bruns et al., 2010, Singh et al., 2007).
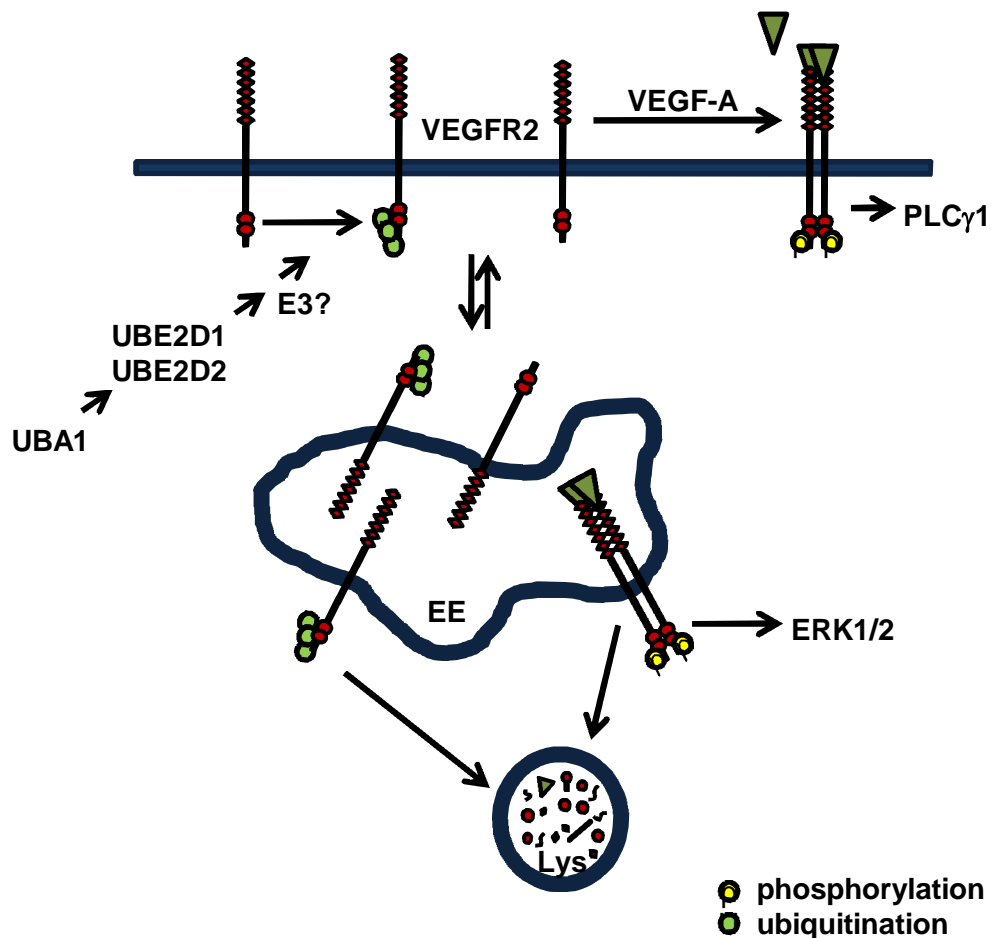
Figure 4.17. Regulation of basal VEGFR2 ubiquitination by UBA1, UBE2D1 and UBE2D2. The E1 ubiquitin-activating enzyme, UBA1, and the E2 ubiquitin-conjugating enzymes, UBE2D1 and UBE2D2, ubiquitinate VEGFR2 in a ligand-independent manner to regulate basal VEGFR2 recycling and degradation. Ubiquitinated VEGFR2 is trafficked to lysosomes (Lys) for degradation, whilst de-ubiquitination in early endosomes (EE) promotes recycling to the plasma membrane. Controlling the balance between basal VEGFR2 recycling and degradation regulates plasma membrane VEGFR2 levels to set a threshold for VEGF-A-stimulated signal transduction, thus impacting on downstream cellular responses.

UBE2D1 has been associated with hypoxia-linked angiogenesis and capillarisation in skeletal muscle (Basic et al., 2014). TNF stimulation increases protein expression of anti-angiogenic VHL, PHD2 and UBE2D1 in skeletal muscle myocytes, disturbing angiogenesis-linked signal transduction under hypoxic conditions (Basic et al., 2014). This association between systemic inflammation and impaired angiogenesis is linked to muscle wasting and cachexia in chronic inflammatory diseases such as chronic obstructive pulmonary disease (COPD) (Basic et al., 2014).

UBA1-mediated control of basal VEGFR2 turnover to regulate availability for VEGF-A binding provides a dramatic alternative to the canonical view of regulating RTK signal transduction. The existence of a kinase-independent pathway that controls basal VEGFR2 levels to regulate VEGF-A-stimulated signal transduction provides new routes for therapeutic intervention. This work reveals the role of UBA1-interacting, E2 ubiquitin-conjugating enzymes, UBE2D1 and UBE2D2, in regulating basal VEGFR2 turnover. Blocking activity of the regulatory components of this pathway could upregulate RTK levels to alleviate disease states such as ischaemic heart disease by promoting angiogenesis, revascularisation and tissue regeneration. Conversely, promoting UBA1, UBE2D1 or UBE2D2 activity could hinder tumour growth in response to circulating growth factors.

CHAPTER 5

VEGFR2 signalling, trafficking and proteolysis is regulated by the ubiquitin isopeptidase USP8

5.1. Introduction

VEGFR2 is the principal receptor through which VEGF-A transmits its pro-angiogenic signals in vascular endothelial cells (Olsson et al., 2006, Shibuya, 2010). VEGF-A binding to VEGFR2 promotes dimerisation and transautophosphorylation of several key tyrosine residues present within its cytoplasmic kinase domain (Koch and Claesson-Welsh, 2012). Upon activation, VEGFR2 enters the endosome-lysosome system through incorporation into clathrin-coated vesicles and trafficking to early endosomal vesicular compartments (Ewan et al., 2006).

Ubiquitination of activated VEGFR2 acts as an endosomal sorting signal that binds to the UIM of ESCRT-0 components, Hrs and STAM (de Melker et al., 2001, Ewan et al., 2006, Bruns et al., 2010). Internalised VEGFR2 recycles back to the plasma membrane or is committed for lysosomal degradation (Bruns et al., 2010, Jopling et al., 2014). Ubiquitination is a dynamic protein modification that co-ordinates receptor trafficking, recycling and degradation (Clague et al., 2012). The reversibility of ubiquitination is credited to the action of DUBs (Clague et al., 2012). These enzymes thus play a distinct but crucial role in RTK trafficking and turnover (Clague et al., 2012).

DUBs are a superfamily of 91 enzymes that can be subdivided into five distinct subfamilies with differing specificities for the isopeptide bond that links ubiquitin chains (Gao et al., 2013). De-ubiquitination of plasma membrane receptors promotes recycling and is essential for maintaining the free ubiquitin pool upon which receptor trafficking is dependent. Similar to the co-ordinated but opposing effects of kinase and phosphatase activity, ubiquitination is kept in balance by the activity of DUBs (Wing, 2003).

Although it is known that VEGFR2 is recycled from endosomes back to the plasma membrane, it is unknown which DUBs prevent its lysosomal degradation. USP8 is a DUB known to be involved in EGFR trafficking (Row et al., 2006, Mizuno et al., 2006, MacDonald et al., 2014). USP8 is a cysteine protease and member of the ubiquitin-specific protease (UBP) family of DUB enzymes capable of catalysing complete breakdown of both K48- and K63-linked polyubiquitin into its component monomers (McCullough et al., 2004, Mizuno et al., 2005, Row et al., 2006). USP8 has diverse roles in membrane trafficking ranging from endosomal regulation to retrograde transport (Row et al., 2006, MacDonald et al., 2014). The early endosome ESCRT-0 subunit, STAM, is a USP8-binding partner (Tanaka, 1999, Kato et al., 2000). This interaction occurs via the SH3 domain of STAM and the proline-rich STAM-binding motif in USP8 (Kato et al., 2000). USP8 depletion inhibits EGFR degradation and causes accumulation of ubiquitinated proteins on enlarged endosomes which co-localise with early endosomal markers (Row et al., 2006, Mizuno et al., 2006).

Once internalised cargo is committed for degradation, conjugated ubiquitin must be recycled and removed by endosomal DUBs such as USP8, which can also associate with the ESCRT-III complex on late endosomes (Hurley and Yang, 2008, Clague et al., 2012). A model was proposed in which USP8 acts further downstream of early endosomes to recycle ubiquitin after endosomal sorting and prior to lysosomal sequestration suggesting a role in facilitating membrane receptor degradation (McCullough et al., 2004). USP8 thus functions at two stages of plasma membrane receptor trafficking: in early endosomes via ESCRT-0 interaction or in late endosomes via ESCRT-III interaction.

Activated VEGFR2 undergoes ubiquitination but the enzymes that regulate this post-translational modification are unclear. In this chapter, the de-ubiquitinating enzyme, USP8, is shown to regulate VEGFR2 trafficking, de-ubiquitination, signal transduction and proteolysis. Depletion of USP8 caused VEGFR2 accumulation in early endosomes and impaired signal transduction. Furthermore, USP8-depleted endothelial cells displayed altered VEGFR2 ubiquitination and production of a unique VEGFR2 extracellular domain proteolytic fragment caused by perturbed trafficking in the endosome-lysosome system. Thus, regulation of VEGFR2 ubiquitination and de-

ubiquitination has important consequences for the endothelial cell response and vascular physiology.

5.2. Results

5.2.1. USP8 regulates VEGFR2 trafficking

Previous studies report that USP8 depletion causes EGFR accumulation in early endosomes and inhibits downstream degradation due to general defects in endosomal sorting (Row et al., 2006). USP8 thus seemed a likely candidate for regulating VEGFR2 trafficking. To test this idea, we used siRNA duplexes to deplete USP8 in primary human endothelial cells prior to VEGF-A stimulation and immunofluorescence microscopy (Fig. 5.1A). In control cells treated with non-targeting siRNA, internalised VEGFR2 was detected in punctate structures at early (0-15 min) stages of VEGF-A stimulation (Fig. 5.1A). After VEGF-A stimulation for 60 min, VEGFR2 staining was substantially reduced consistent with significant degradation (Fig. 5.1A).

However, in USP8-depleted endothelial cells resting VEGFR2 was already accumulated in enlarged punctate structures (Fig. 5.1A). This pattern of VEGFR2 distribution persisted following VEGF-A stimulation suggesting accumulation of VEGFR2 within the endosome-lysosome system. Persistence of these enlarged, VEGFR2-enriched punctate structures over a 60 min time course of VEGF-A stimulation indicated perturbed VEGFR2 trafficking and degradation (Fig. 5.1A). VEGFR2 accumulation also occurred when cells were treated with individual USP8 siRNAs to limit off-target effects (Fig. 5.2). To quantify distribution of mature VEGFR2 in the endosomal pathway, USP8-depleted endothelial cells were pre-treated with CHX to block protein synthesis followed by VEGF-A stimulation (Fig. 5.1A). Although the biosynthetic pool of Golgi-localised VEGFR2 was absent after CHX treatment, mature VEGFR2 still accumulated in USP8-depleted cells (Fig.5.1A). Quantification of VEGFR2 residing in the endosome-lysosome system upon CHX treatment revealed VEGFR2 levels were 30% higher in non-stimulated, USP8-depleted cells (Fig. 5.1B). In addition, VEGFR2 underwent 20% VEGF-A-stimulated degradation in control cells. Contrastingly, high levels of accumulated VEGFR2 persisted in USP8-depleted cells, undergoing only 5% VEGF-A-stimulated degradation (Fig. 5.1B).
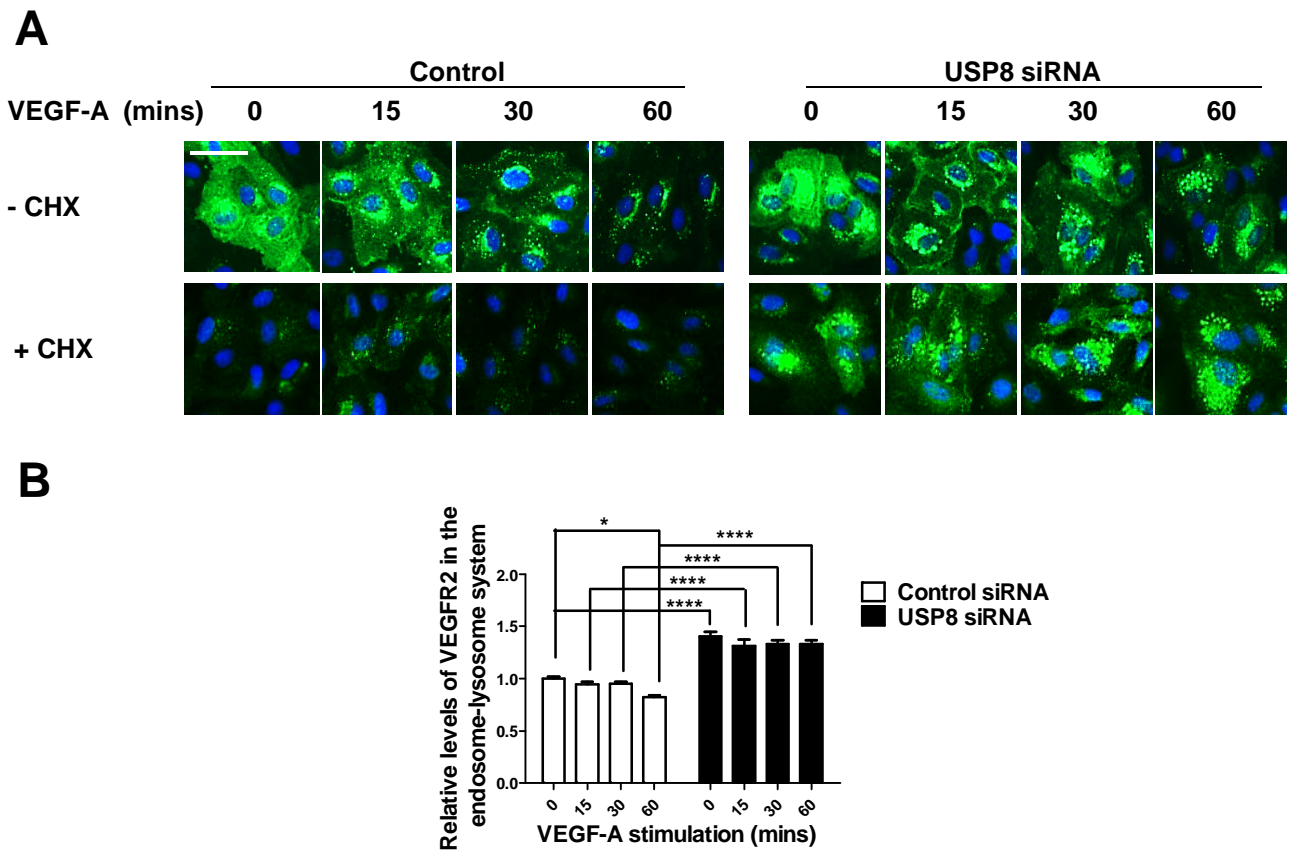
Figure 5.1. USP8 is essential for VEGFR2 trafficking. (A) Endothelial cells transfected with non-targeting or USP8 siRNA, pre-treated with CHX and stimulated with 25 ng/ml VEGF-A were fixed and processed for immunofluorescence microscopy using antibodies to VEGFR2 followed by fluorescent species-specific secondary antibodies (green). Nuclei were stained with DNA-binding dye, DAPI (blue). Scale bar represents 200 μm. (B) VEGFR2 levels residing in the endosome-lysosome system in endothelial cells pre-treated with CHX and stimulated with VEGF-A determined using quantitative microscopy. Errors bars indicate ±SEM (n≥3). $p<0.05$ (*), $p<0.0001$ (****).
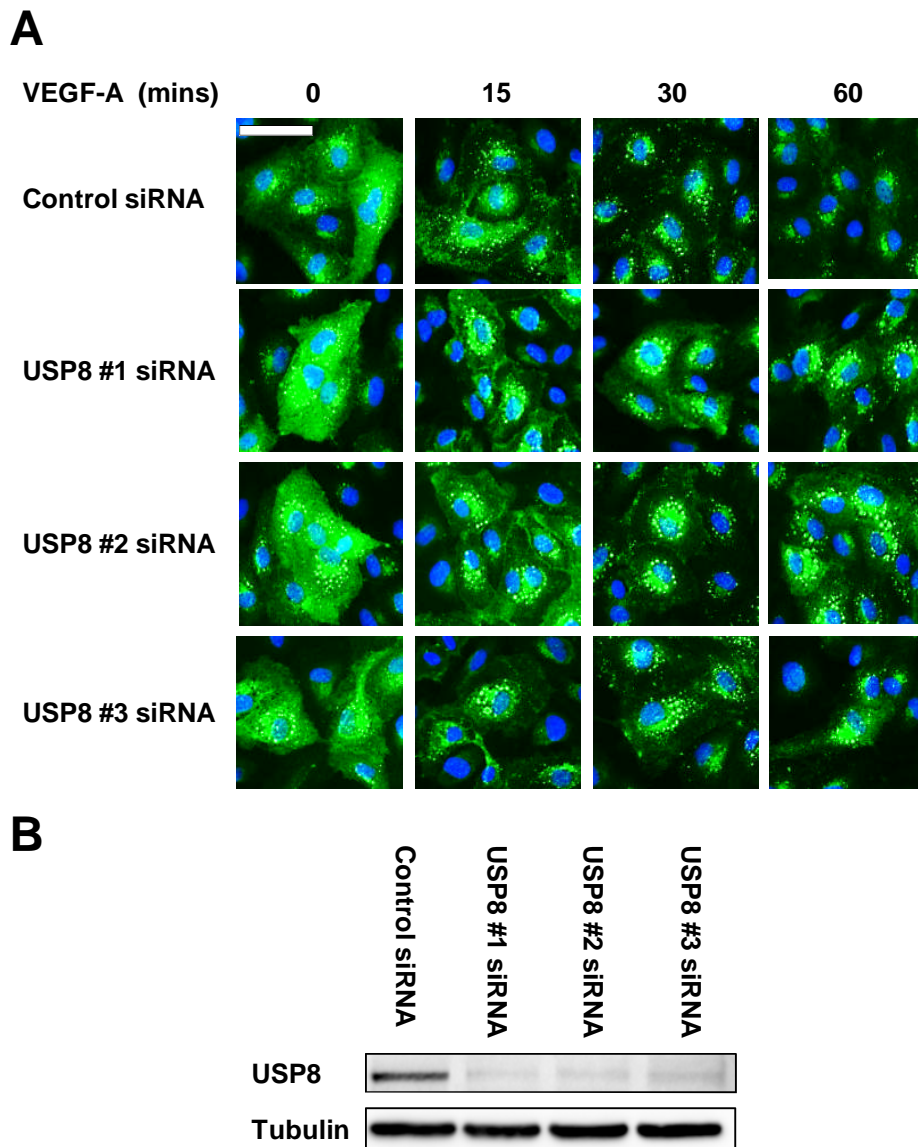
Figure 5.2. Individual USP8 siRNAs perturb VEGFR2 trafficking. (A) Endothelial cells transfected with non-targeting or individual USP8 siRNAs and stimulated with 25 ng/ml VEGF-A were fixed and processed for immunofluorescence microscopy using antibodies to VEGFR2 followed by fluorescent species-specific secondary antibodies (green). Nuclei were stained with DNA-binding dye, DAPI (blue). Scale bar represents 200 μm. (B) To confirm USP8 depletion, endothelial cells transfected with non-targeting or individual USP8 siRNAs were lysed and immunoblotted with antibodies against USP8.

To ascertain the nature of these VEGFR2-enriched structures, USP8-depleted endothelial cells were stained for VEGFR2 and an early endosome marker, early endosome antigen-1 (EEA-1) (Fig. 5.3A). Quantification revealed increased co-distribution between VEGFR2 and EEA1 before and after VEGF-A stimulation in USP8-depleted cells (Fig. 5.3B). To determine localisation of the remaining VEGFR2, USP8-depleted cells were co-stained with markers for the plasma membrane (PECAM1), Golgi (TGN46), early endosomes (EEA1), late endosomes (CD63) and lysosomes (LAMP2) (Fig. 5.4A). Quantification revealed that VEGFR2 distribution across other organelles was minimally affected by USP8 depletion whilst accumulation took place in EEA1-positive early endosomes (Fig. 5.4B).

VEGFR2 also accumulated in EEA1-positive early endosomes when cells were treated with individual USP8 siRNAs to limit off-target effects (Fig. 5.5). In addition, the enlarged VEGFR2-positive endosomes did not co-distribute with late endosome marker, CD63 (Fig. 5.6). These findings confirm that VEGFR2 accumulates in early endosomes of USP8-depleted cells. Thus, USP8 is essential for VEGFR2 trafficking through the endosome-lysosome system.

5.2.2. USP8 regulates VEGFR2 proteolysis

VEGFR2 proteolysis is regulated by ubiquitination (Bruns et al., 2010, Bruns et al., 2012). A characteristic feature of VEGFR2 activation is trafficking through the endosome-lysosome system and generation of a transient ~160 kDa N-terminal lumenal fragment in endosomes (Bruns et al., 2010). Immunoblotting revealed that the 160 kDa VEGFR2 proteolytic fragment was generated in both control and USP8-depleted endothelial cells (Fig. 5.7). However, a novel ~120 kDa VEGFR2-derived proteolytic fragment was also produced in USP8-depleted cells (Fig. 5.7). Notably, this VEGFR2-related fragment was also immunoprecipitated from USP8-depleted cells (Fig. 5.9A, B and 5.10A).

The novel 120 kDa VEGFR2-derived proteolytic fragment was present at very low levels in control cells (Fig. 5.7, 5.8A). However, levels increased >3-fold upon USP8 depletion (Fig. 5.8B). Treatment with CHX to block new protein synthesis did not prevent appearance of the 120 kDa fragment, confirming that it is derived from proteolytic cleavage of mature VEGFR2 (Fig. 5.8A, B). USP8-depleted cells also
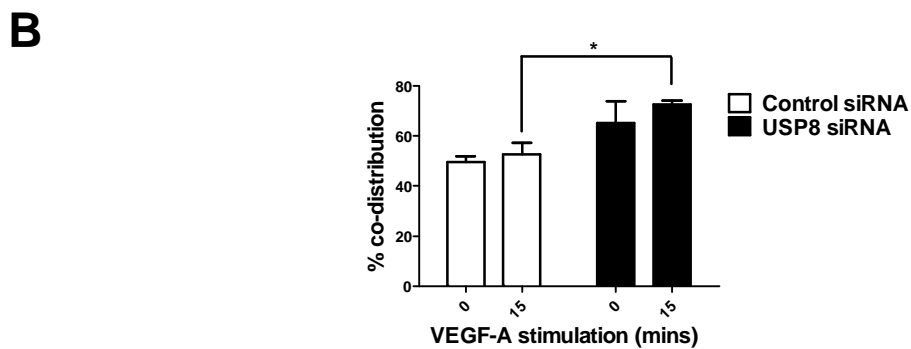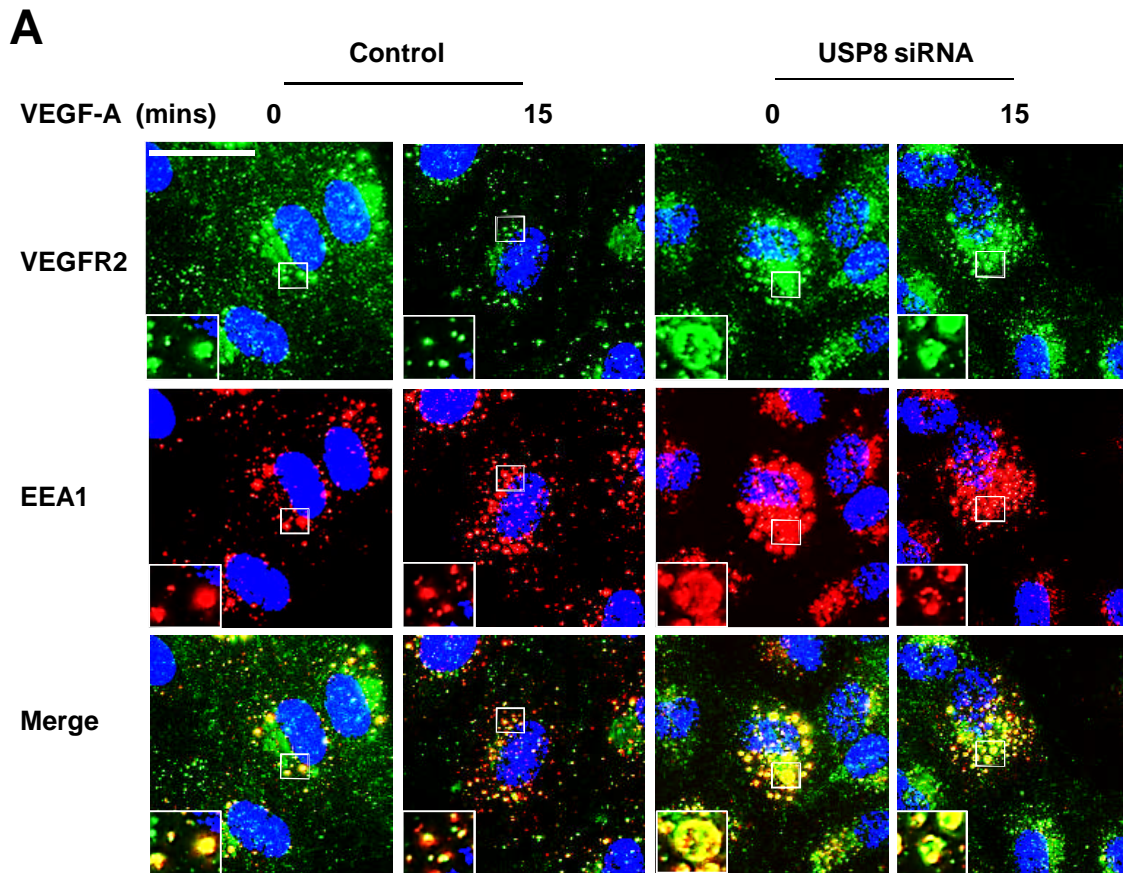
Figure 5.3. USP8 depletion causes VEGFR2 accumulation in early endosomes. (A) Endothelial cells transfected with control or USP8 siRNA and stimulated with 25 ng/ml VEGF-A for 15 min were fixed and processed for immunofluorescence microscopy using antibodies to VEGFR2 (green) and EEA1 (red) followed by fluorescent species-specific secondary antibodies. Nuclei were stained with DNA-binding dye, DAPI (blue). Scale bar represents 70 μm. (B) Co-distribution between VEGFR2 and EEA1 in endothelial cells treated with non-targeting or USP8 siRNA and stimulated with VEGF-A prior to quantitative microscopy. Errors bars indicate ±SEM (n≥3). $p<0.05$ (*), $p<0.0001$ (****).

122
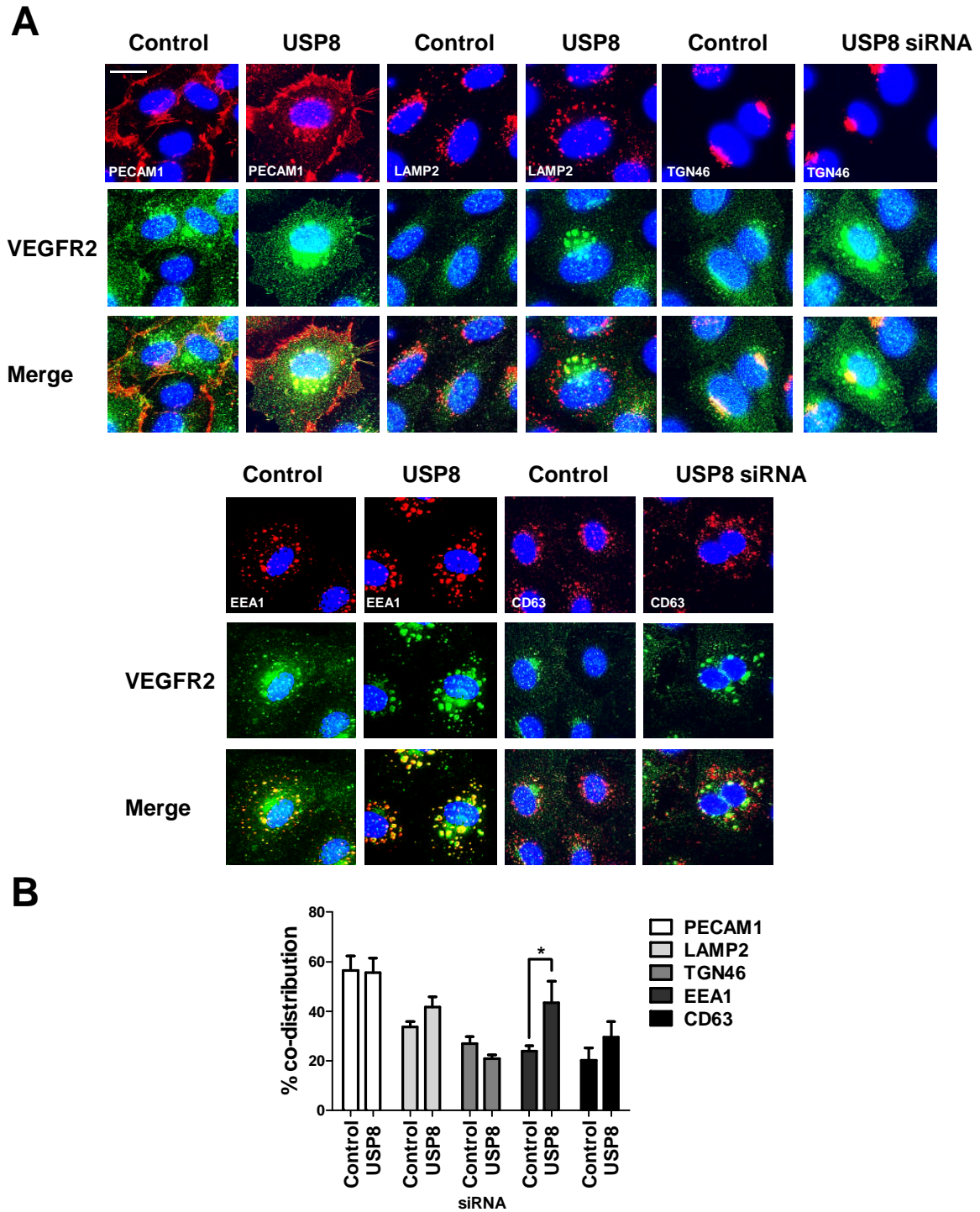
Figure 5.4. Cellular distribution of VEGFR2 in USP8-depleted cells. (A) Endothelial cells transfected with non-targeting or USP8 siRNA were fixed and processed for immunofluorescence microscopy using antibodies to VEGFR2 (green) and PECAM1, LAMP2, TGN46, EEA1 or CD63 (red) followed by species-specific secondary antibodies. Nuclei were stained with DNA-binding dye, DAPI (blue). Scale bar represents 70 μm. (B) Co-distribution between VEGFR2 and cellular markers in endothelial cells treated with control or USP8 siRNA determined using quantitative microscopy. Error bars denote ±SEM (n≥3). $p<0.05$ (*).
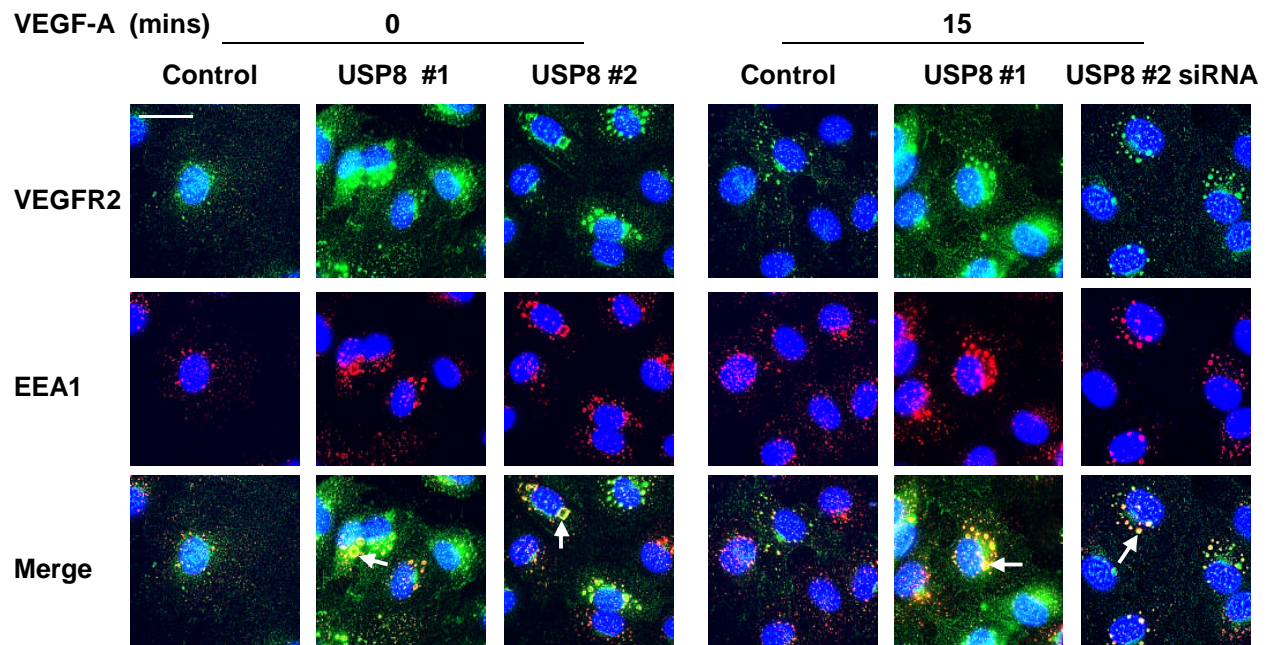
Figure 5.5. Individual USP8 siRNAs cause VEGFR2 accumulation in early endosomes. Endothelial cells transfected with individual USP8 siRNAs and stimulated with 25 ng/ml VEGF-A for 15 min were fixed and processed for immunofluorescence microscopy using antibodies to VEGFR2 (green) and EEA1 (red) followed by fluorescent species-specific secondary antibodies. Nuclei were stained with DNA-binding dye, DAPI (blue). Arrows indicate enlarged VEGFR2-positive early endosomes. Scale bar represents 70 μm. Izma Abdul Zani (Ponnambalam Laboratory, University of Leeds) contributed to the data shown in this figure.

VEGF-A (mins)	0			15		
	Control	**USP8 #1**	**USP8 #2**	**Control**	**USP8 #1**	**USP8 #2 siRNA**
VEGFR2						
CD63						
Merge						
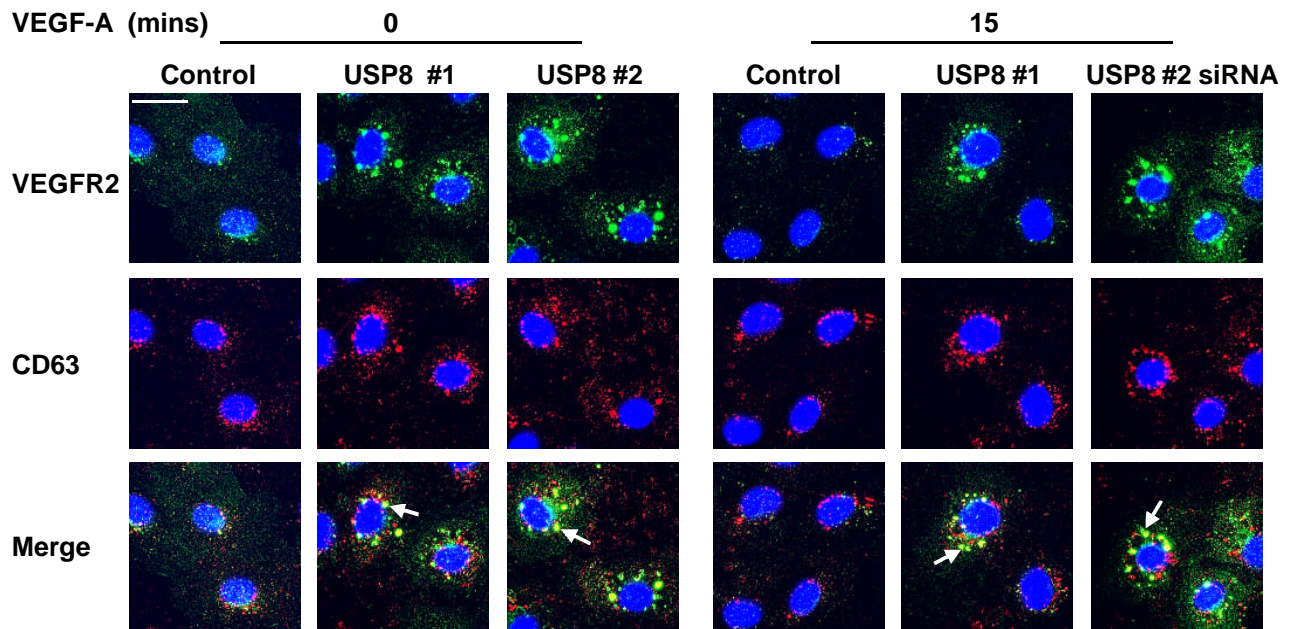
Figure 5.6. Individual USP8 siRNAs do not cause VEGFR2 accumulation in late endosomes. Endothelial cells transfected with individual USP8 siRNAs and stimulated with 25 ng/ml VEGF-A for 15 min were fixed and processed for immunofluorescence microscopy using antibodies to VEGFR2 (green) and CD63 (red) followed by fluorescent species-specific secondary antibodies. Nuclei were stained with DNA-binding dye, DAPI (blue). Arrows indicate enlarged VEGFR2-positive early endosomes. Scale bar represents 70 μm. Izma Abdul Zani (Ponnambalam Laboratory, University of Leeds) contributed to the data shown in this figure.
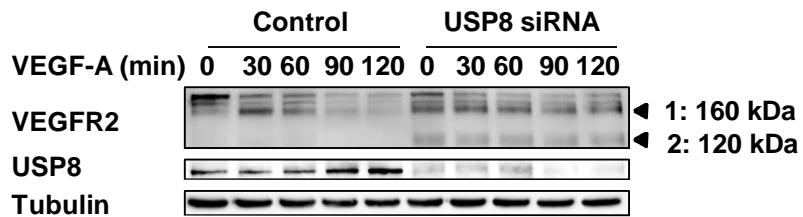
Figure 5.7. USP8 depletion promotes accumulation of a novel 120 kDa VEGFR2 proteolytic cleavage fragment. Endothelial cells transfected with non-targeting or USP8 siRNA were treated with 25 ng/ml VEGF-A, lysed and immunoblotted with antibodies against VEGFR2. Numbered arrowheads denote the 160 kDa VEGFR2 fragment (1) and the novel 120 kDa VEGFR2 fragment (2).
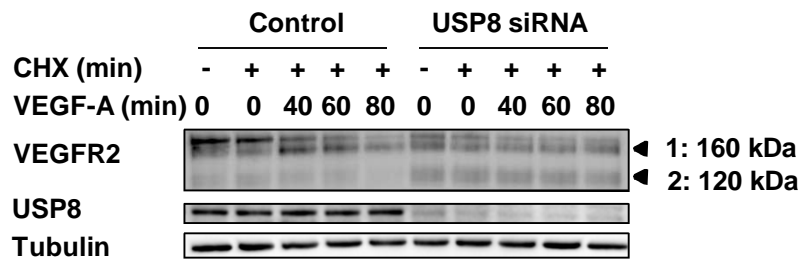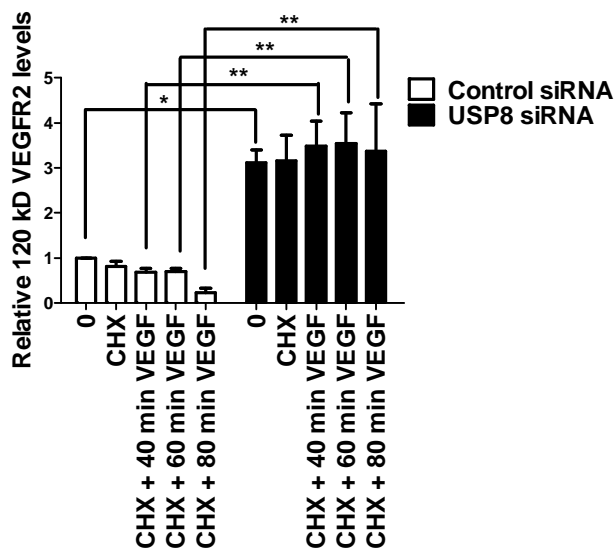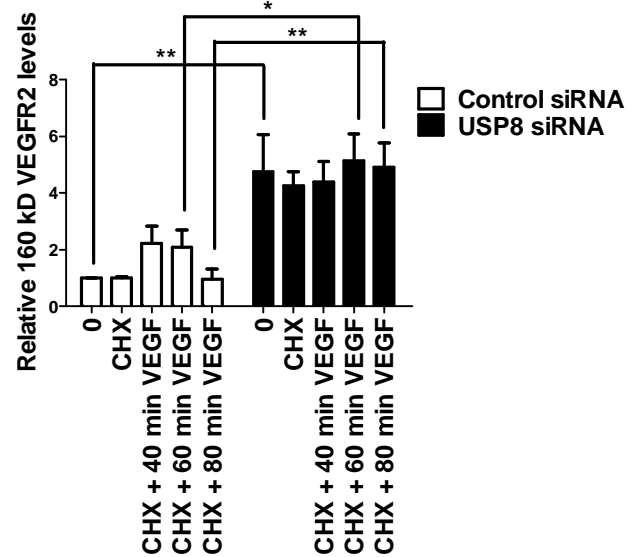
Figure 5.8. USP8 depletion promotes accumulation of a novel 120 kDa VEGFR2 proteolytic cleavage fragment. (A) Endothelial cells transfected with non-targeting or USP8 siRNA were treated with 20 μg/ml CHX and 25 ng/ml VEGF-A, lysed and immunoblotted with antibodies against VEGFR2. Quantification of 120 kDa (B) or 160 kDa (C) VEGFR2 fragment levels in endothelial cells transfected with non-targeting or USP8 siRNA and treated with 20 μg/ml CHX and 25 ng/ml VEGF-A. Error bars denote ±SEM (n≥3). $p<0.05$ (*), $p<0.01$ (**). Numbered arrowheads denote the 160 kDa VEGFR2 fragment (1) and the novel 120 kDa VEGFR2 fragment (2).

displayed increased production of the 160 kDa proteolytic fragment (Fig. 5.8C). Thus, the 160 kDa VEGFR2 fragment could be a precursor of the smaller 120 kDa fragment. Alternatively, the 120 kDa fragment may be a unique proteolytic cleavage product that is not cleared efficiently due to a block in forward transport towards the lysosome in USP8-depleted cells. To resolve the identity of the 120 kDa VEGFR2 fragment, VEGFR1 and VEGFR2 were immunoprecipitated from USP8-depleted cells followed by immunoblot analysis with antibodies to the extracellular and cytoplasmic domains of VEGFR2 (Fig. 5.9A). The VEGFR2 extracellular domain antibody detected all species of VEGFR2 in USP8-depleted cells. In contrast, the cytoplasmic domain antibody only detected full length immature and mature VEGFR2 (Fig. 5.9A). Thus, similarly to the 160 kDa fragment, the 120 kDa VEGFR2 cleavage product is N-terminal. These findings suggest that USP8 is vital for efficient clearance of VEGFR2 proteolytic cleavage products.

5.2.3. USP8 regulates VEGFR2 de-ubiquitination

VEGF-A binding programs VEGFR2 ubiquitination, endocytosis and proteolysis (Ewan et al., 2006, Bruns et al., 2010, Bruns et al., 2012). De-ubiquitination is required to divert internalised VEGFR2 away from lysosomal degradation and towards recycling (Clague et al., 2012). Based on the above findings, one possibility is that perturbed VEGFR2 endosome-lysosome trafficking is linked to altered VEGFR2 ubiquitination status in USP8-depleted cells. To assess VEGFR2 ubiquitination in control and USP8-depleted cells, VEGFR2 immunoprecipitates were probed by immunoblotting using K48- and K63-linked polyubiquitin-specific antibodies or a pan-ubiquitin antibody (Fig. 5.10A). In control cells, VEGFR2 ubiquitination peaked 15 min after VEGF-A stimulation (Fig. 5.10A). Accumulation of proteolytic cleavage products in USP8-depleted cells reduced levels of mature VEGFR2 and resulted in lower levels of ubiquitinated full-length receptor (Fig. 5.10A). However, a lower molecular weight species of ubiquitinated VEGFR2 that corresponds to the 160 kDa proteolytic fragment and represents increased and persistent ubiquitination of this cleavage product was evident in USP8-depleted cells (Fig. 5.10A, arrowhead). USP8 depletion increased levels of this K48- and K63-linked polyubiquitinated species of VEGFR2. Unlike in control cells, this species of ubiquitinated VEGFR2 was present in non-stimulated cells and persisted over a time course of VEGF-A stimulation (Fig. 5.10A). Quantification of immunoblot data showed that whereas ligand-stimulated VEGFR2 ubiquitination
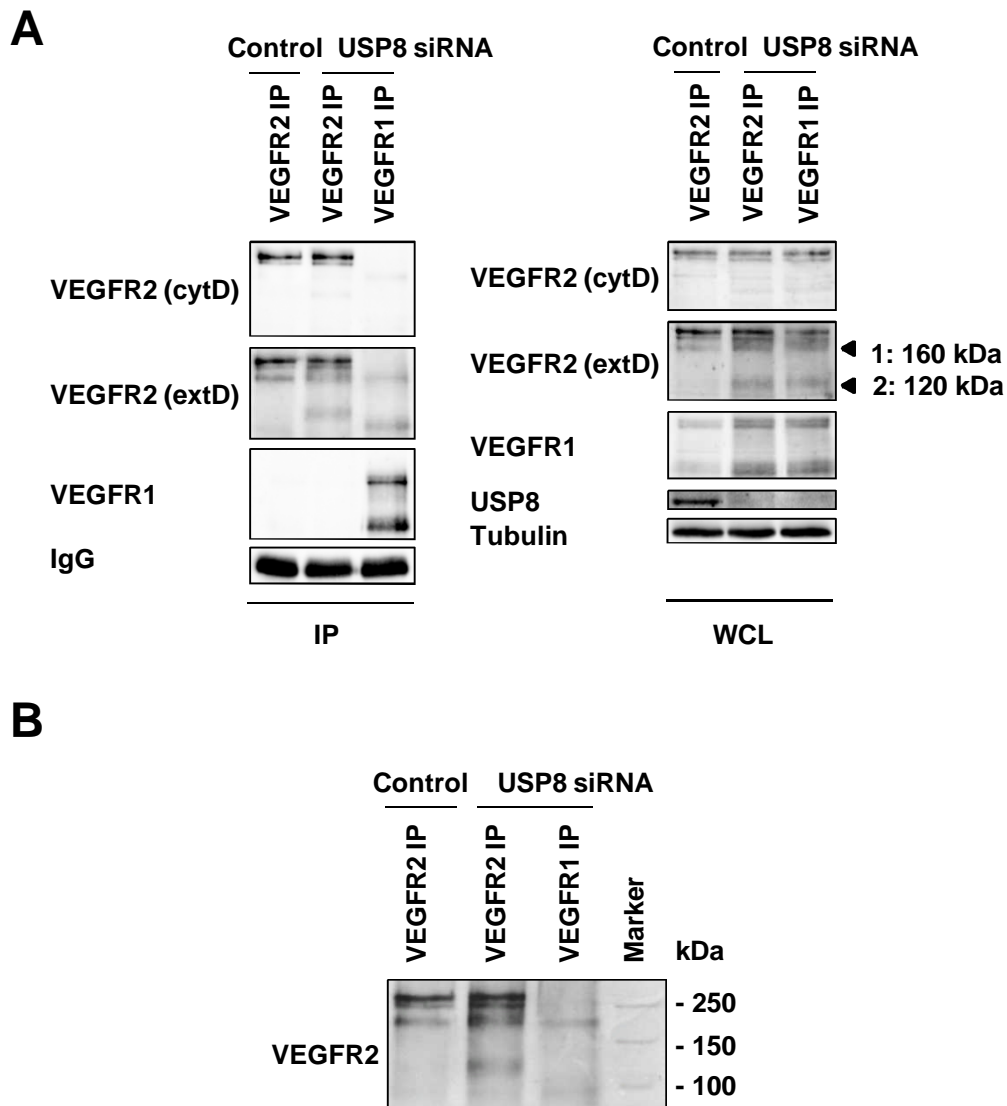
Figure 5.9. USP8 depletion promotes generation of a novel 120 kDa VEGFR2 proteolytic cleavage fragment. (A) VEGFR1 or VEGFR2 were immunoprecipitated from endothelial cells transfected with non-targeting or USP8 siRNA and immunoblotted with antibodies to the extracellular and cytoplasmic domains of VEGFR2 (B) and run alongside marker ladders to confirm band size. Numbered arrowheads denote the 160 kDa VEGFR2 fragment (1) and the novel 120 kDa VEGFR2 fragment (2). cytD; cytoplasmic domain, extD; extracellular domain.
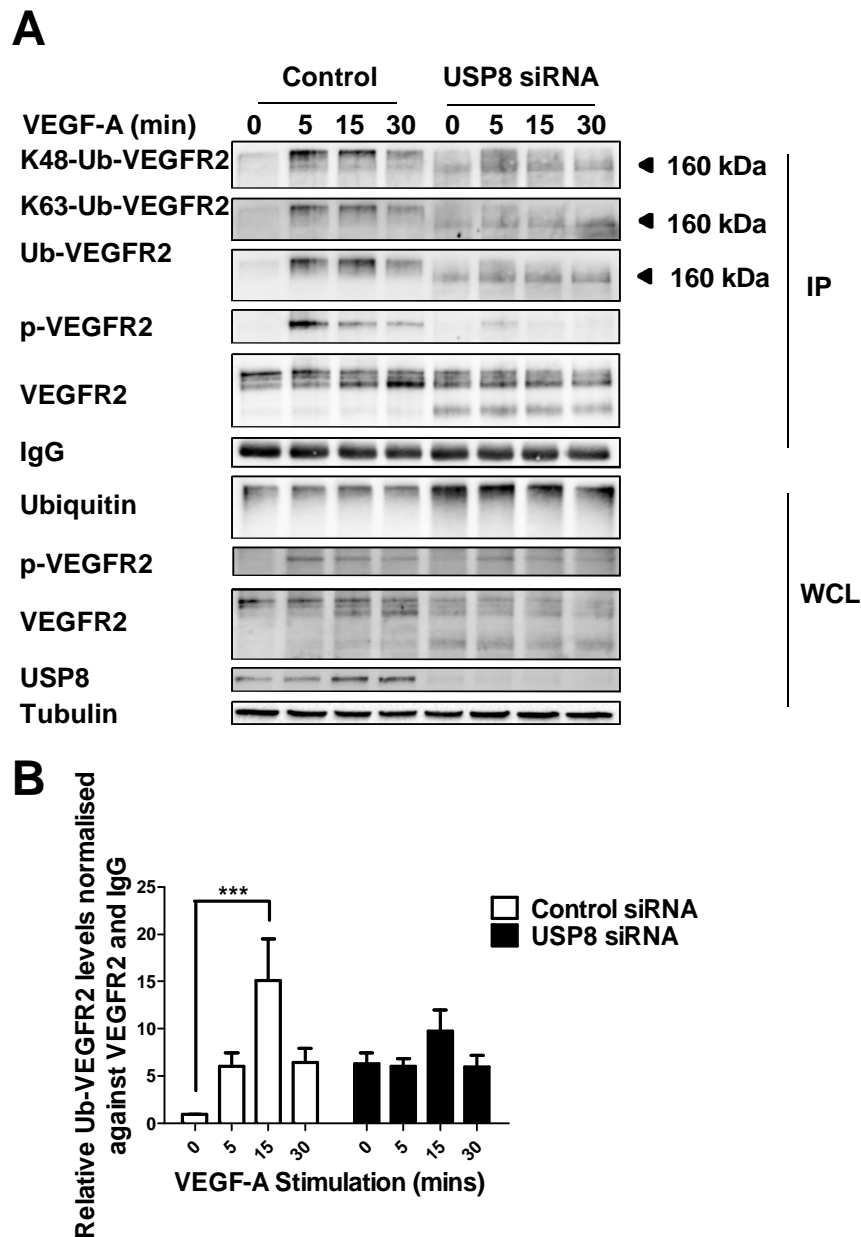
Figure 5.10. USP8 regulates VEGFR2 de-ubiquitination. (A) Endothelial cells transfected with non-targeting or USP8 siRNA were treated with 25 ng/ml VEGF-A and lysed. VEGFR2 was immunoprecipitated and immunoblotted for its ubiquitination status using antibodies against K48-linked polyubiquitin, K63-linked polyubiquitin and pan-ubiquitin. Arrowheads denote the ubiquitinated VEGFR2 species present at higher levels in USP8-depleted cells. (B) Quantification of ubiquitinated VEGFR2 levels in endothelial cells transfected with non-targeting or USP8 siRNA and treated with 25 ng/ml VEGF-A. Error bars denote ±SEM (n≥3). $p<0.001$ (***). IP; immunoprecipitate, WCL; whole cell lysate.

displayed a characteristic peak and decline, under conditions of USP8 depletion VEGFR2 ubiquitination persisted (Fig. 5.10B). One possibility is that reduced de-ubiquitination of accumulated, mature VEGFR2 in USP8-depleted cells increases susceptibility to proteolysis. Thus, proteolytic cleavage products remain ubiquitinated and accumulate in early endosomes. These data suggest that USP8 is a key regulator of VEGFR2 de-ubiquitination.

5.2.4. VEGF-A-stimulated VEGFR2 signal transduction is perturbed by USP8 depletion

VEGF-A stimulates multiple signal transduction pathways in endothelial cells (Koch et al., 2011) that regulate many cellular responses (Zhang et al., 2008). Furthermore, VEGF-A-stimulated signal transduction is dependent on positional location of VEGFR2 at the plasma membrane or within endosome-related compartments (Bruns et al., 2010, Koch et al., 2011, Horowitz and Seerapu, 2012). However, the role of the ubiquitination/de-ubiquitination cycle in RTK signal transduction is unclear. Perturbed VEGFR2 endosomal trafficking caused by USP8 depletion could modulate endosome-linked signal transduction. Control or USP8-depleted endothelial cells were subjected to a time course of VEGF-A stimulation followed by immunoblot analysis to assess VEGFR2 activation and downstream signal transduction (Fig. 5.11A). VEGF-A binding causes autophosphorylation of VEGFR2 cytoplasmic residue Y1175, creating a key binding site for downstream effectors (Koch et al., 2011). Quantification of immunoblot analysis revealed VEGFR2-pY1175 levels were ~60% reduced in USP8-depleted endothelial cells (Fig. 5.11B). VEGF-A-stimulated activation of the master regulator and serine/threonine protein kinase, Akt, was ~90% reduced in USP8-depleted cells (Fig. 5.11C). In addition, VEGF-A-stimulated activation of the MAPK pathway involving ERK1/2 was ~60% reduced in USP8-depleted cells (Fig. 5.11D). Interestingly, USP8 depletion did not significantly affect plasma membrane-associated phosphorylation and activation of p38 MAPK or PLCγ1 (Fig. 5.11E, F). USP8 activity thus modulates VEGF-A-stimulated Akt and ERK1/2 activation but does not affect other VEGFR2-associated signal transduction pathways.

Levels of mature, full-length VEGFR2 appear reduced in USP8-depleted cells (Fig. 5.11A) yet VEGFR2 is accumulated in early endosomes (Fig. 5.1A). VEGFR2 proteolysis in early endosomes generates 120 kDa and 160 kDa N-terminal fragments.
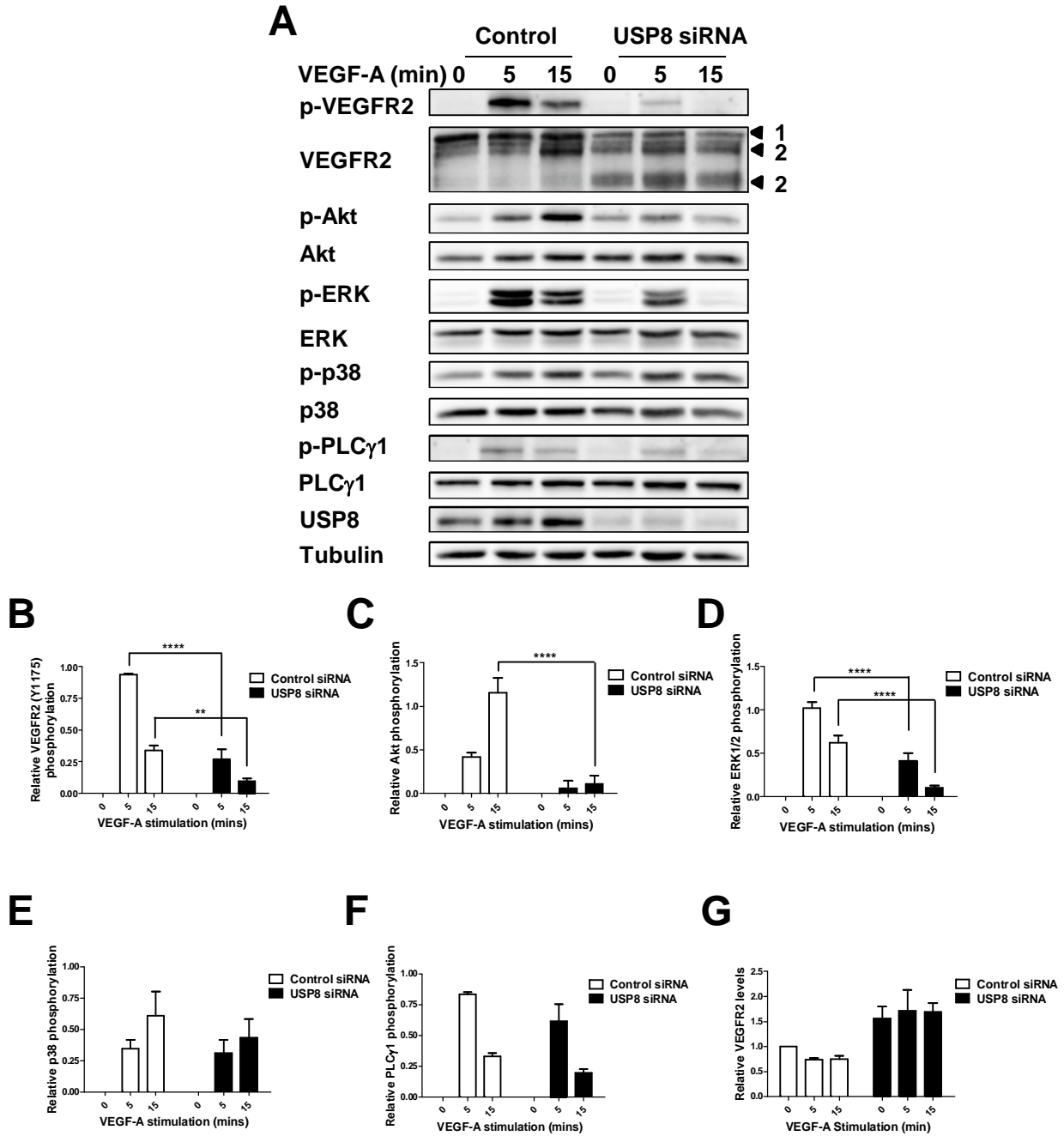
Figure 5.11. USP8 depletion inhibits VEGF-A-stimulated VEGFR2 signal transduction. Endothelial cells transfected with non-targeting or USP8 siRNA were treated with 25 ng/ml VEGF-A, lysed and immunoblotted for phospho-VEGFR2 (Y1175), phospho-Akt (S473), phospho-ERK1/2 (T202/Y204) phospho-p38 MAPK (T180/Y182), and phospho-PLCγ1 (Y783). Levels of phospho-VEGFR2 (B), phospho-Akt (C), phospho-ERK1/2 (D), phospho-p38 MAPK (E), phopho-PLCγ1 (F) and VEGFR2 (G) in endothelial cells transfected with non-targeting or USP8 siRNA determined using quantitative immunoblotting. Numbered arrowheads denote mature VEGFR2 (1) and proteolytic VEGFR2 fragments (2). Errors bars indicate ±SEM (n≥3). $p<0.01$ (**), $p<0.0001$ (****).

132

Proteolytic cleavage products of mature VEGFR2 accumulate in early endosomes of USP8-depleted cells after failure to reach a degradative compartment thus causing an overall increase in total VEGFR2 levels (Fig. 5.11G).

5.2.5. VEGFR2 plasma membrane dynamics

In USP8-depleted endothelial cells non-stimulated VEGFR2 displayed accumulation in early endosomes (Fig. 5.12A). Reduced VEGFR2 availability at the plasma membrane could thus diminish response to exogenously added VEGF-A. To investigate this possibility, we used cell surface biotinylation to compare plasma membrane VEGFR2 pools in control and USP8-depleted cells (Fig. 5.12A). Quantification revealed little difference in non-stimulated, plasma membrane VEGFR2 levels between control and USP8-depleted cells (Fig. 5.12B). Furthermore, USP8 depletion had little effect on relative VEGFR2 levels at the plasma membrane over a 60 min time course of VEGF-A stimulation. Thus reduced plasma membrane VEGFR2 availability did not account for diminished VEGF-A-dependent Akt and ERK1/2 activation (Fig 5.11C, D and 5.12B). Monitoring peak VEGFR2-Y1175 phosphorylation at the plasma membrane also revealed little difference between control and USP8-depleted cells (Fig. 5.12C). Thus, inhibition of VEGFR2 phosphorylation (Fig. 5.11B) in USP8-depleted cells likely represents an effect on the total VEGFR2 pool which continues to be phosphorylated after internalisation. These findings suggest that USP8 does not regulate VEGFR2 levels and subsequent activation at the plasma membrane.

5.2.6. USP8 regulates VEGFR2 endosome-to-plasma membrane recycling

Previous studies showed VEGFR2 undergoes ligand-independent endosome-to-plasma membrane recycling (Jopling et al., 2014, Gampel et al., 2006). Ubiquitination of plasma membrane-associated VEGFR2 precedes endocytosis and delivery via the endosome-lysosome system for terminal degradation (Ewan et al., 2006). Contrastingly, RTK de-ubiquitination in early endosomes is associated with recycling back to the plasma membrane (Clague and Urbe, 2006). To test a role for USP8 in endosome-to-plasma membrane recycling of VEGFR2, we used a previously described microscopy-based recycling assay (Jopling et al., 2011) (Fig. 5.13C). Control or USP8-depleted endothelial cells were incubated with extracellular domain-specific VEGFR2 antibodies to label plasma membrane VEGFR2. Endocytosis and recycling over a time course of
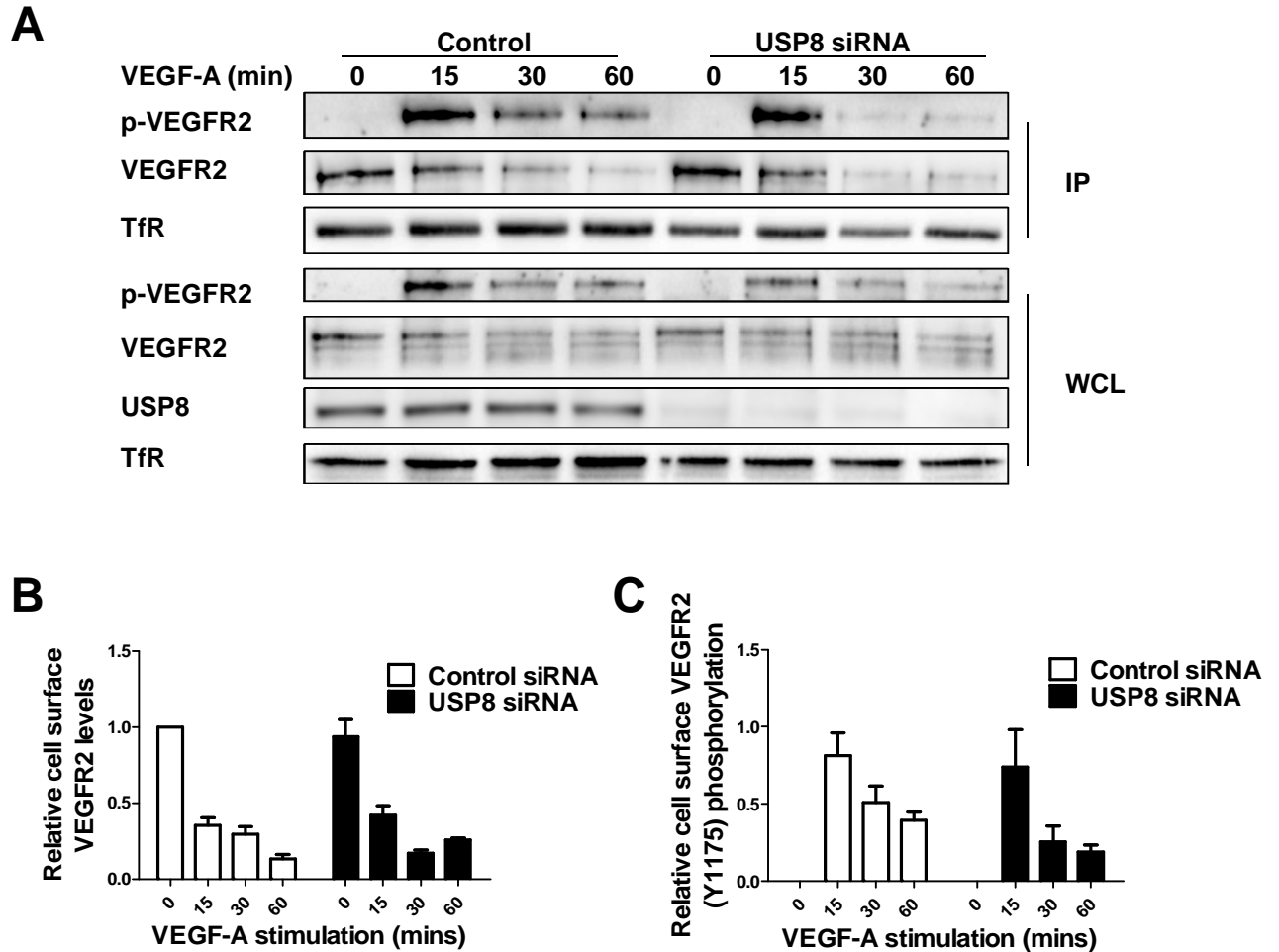
Figure 5.12. USP8 depletion does not affect VEGFR2 levels or activation at the plasma membrane. (A) Endothelial cells transfected with non-targeting or USP8 siRNA were treated with 25 ng/ml VEGF-A, cell surface biotinylated and lysed. Biotinylated proteins were isolated using neutravidin-agarose and immunoblotted using antibodies against phospho-VEGFR2 (Y1175) and VEGFR2. Quantification of cell surface VEGFR2 (B) or phospho-VEGFR2 (C) levels over a time course of VEGF-A stimulation in endothelial cells transfected with non-targeting or USP8 siRNA. Error bars denote ±SEM (n≥3). IP; immunoprecipitate, WCL; whole cell lysate.
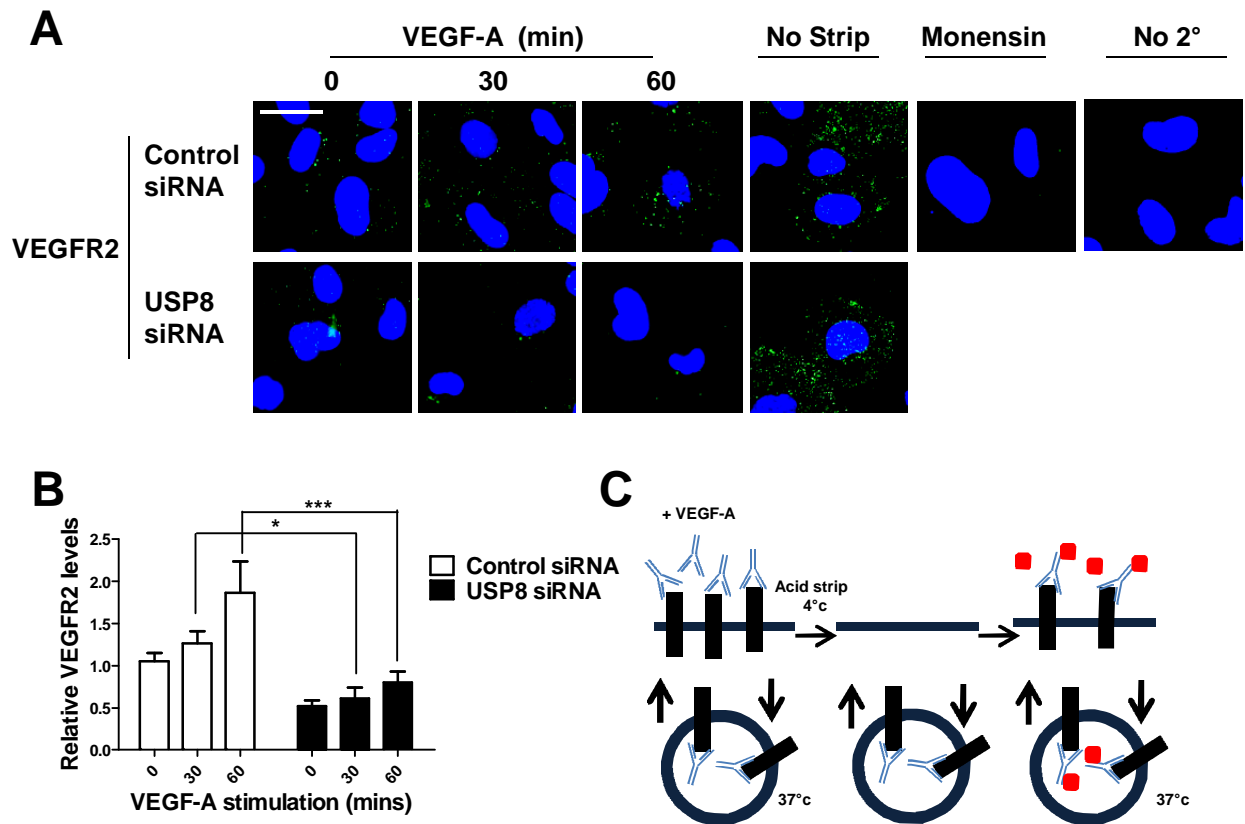
Figure 5.13. Endosome-to-plasma membrane VEGFR2 recycling is inhibited in USP8-depleted cells. (A) Endothelial cells transfected with non-targeting or USP8 siRNA were incubated with primary antibodies to VEGFR2 for 30 min at 37°C and treated with 20 μM monensin (endosome-to-plasma membrane recycling inhibitor) or stimulated with VEGF-A for 15 or 30 min before stripping of cell surface primary antibodies and incubation with fluorescent species-specific secondary antibodies for 15 or 30 min (30 or 60 min total recycling time respectively) at 37°C (green). No strip controls represent both cell surface and recycled VEGFR2. Cells were fixed prior to staining with DNA-binding dye, DAPI (blue). Only VEGFR2 that underwent plasma membrane-endosome-plasma membrane recycling is visible. Scale bar represents 200 μm. (B) Quantification of VEGFR2 recycling in cells transfected with non-targeting or USP8 siRNA and treated with 25 ng/ml VEGF-A. Error bars denote ±SEM ($n \geq 3$). $p < 0.05$ (*), $p < 0.001$ (***). (C) Schematic outline of the antibody-based assay to monitor VEGFR2 recycling between the plasma membrane and internal compartments.

135

VEGF-A stimulation were assessed using accessibility of the VEGFR2-antibody complex to exogenous, labelled secondary antibody (Fig. 5.13A). Monensin is an ionophore that inhibits endosome-to-plasma membrane recycling. Pre-treatment with monensin inhibited VEGFR2 recycling (Fig 5.13A). In controls with no secondary antibody incubation, VEGFR2 was not detected (Fig. 5.13A). Only VEGFR2 that had undergone endocytosis followed by endosome-to-plasma membrane recycling was detected in this assay (Fig 5.13A). Quantification revealed that addition of VEGF-A caused ~2-fold increase in VEGFR2 recycling in control cells (Fig. 5.13B). However, USP8-depleted cells underwent ~60% reduction in re-appearance of plasma membrane VEGFR2 under both non-stimulated and VEGF-A stimulated conditions (Fig. 5.13C). USP8 is thus required for constitutive and ligand-stimulated endosome-to-plasma membrane recycling of VEGFR2.

VEGFR2 accumulates in early endosomes and recycling is profoundly affected in USP8-depleted cells yet plasma membrane levels are unaffected (Fig. 5.1A, 5.12B, 5.13B). One possibility is that plasma membrane VEGFR2 is replenished by newly synthesised receptor. To test this we used biotinylation to compare plasma membrane and internal VEGFR2 pools in control and USP8-depleted cells treated with CHX. Biotinylated plasma membrane proteins were isolated and internal VEGFR2 was immunoprecipitated followed by immunoblot analysis (Fig 5.14A). Quantification revealed that levels of internal VEGFR2 were significantly higher in USP8-depleted cells after accumulation in early endosomes, whilst plasma membrane VEGFR2 was unaffected. Upon CHX treatment, cell surface VEGFR2 levels were significantly reduced in USP8-depleted cells. Thus, plasma membrane VEGFR2 that accumulates in early endosomes following cleavage into proteolytic fragments is replenished by the biosynthetic pool of receptor.

5.2.7. USP8 depletion inhibits VEGF-A-stimulated tubulogenesis

A key functional aspect of VEGF-A-stimulated signal transduction in endothelial cells is the capacity to stimulate the formation of tubes which resemble hollow blood vessels (Fearnley et al., 2014). Control or USP8-depleted cells were monitored for the formation of endothelial tubes i.e. tubulogenesis, using an endothelial-fibroblast co-
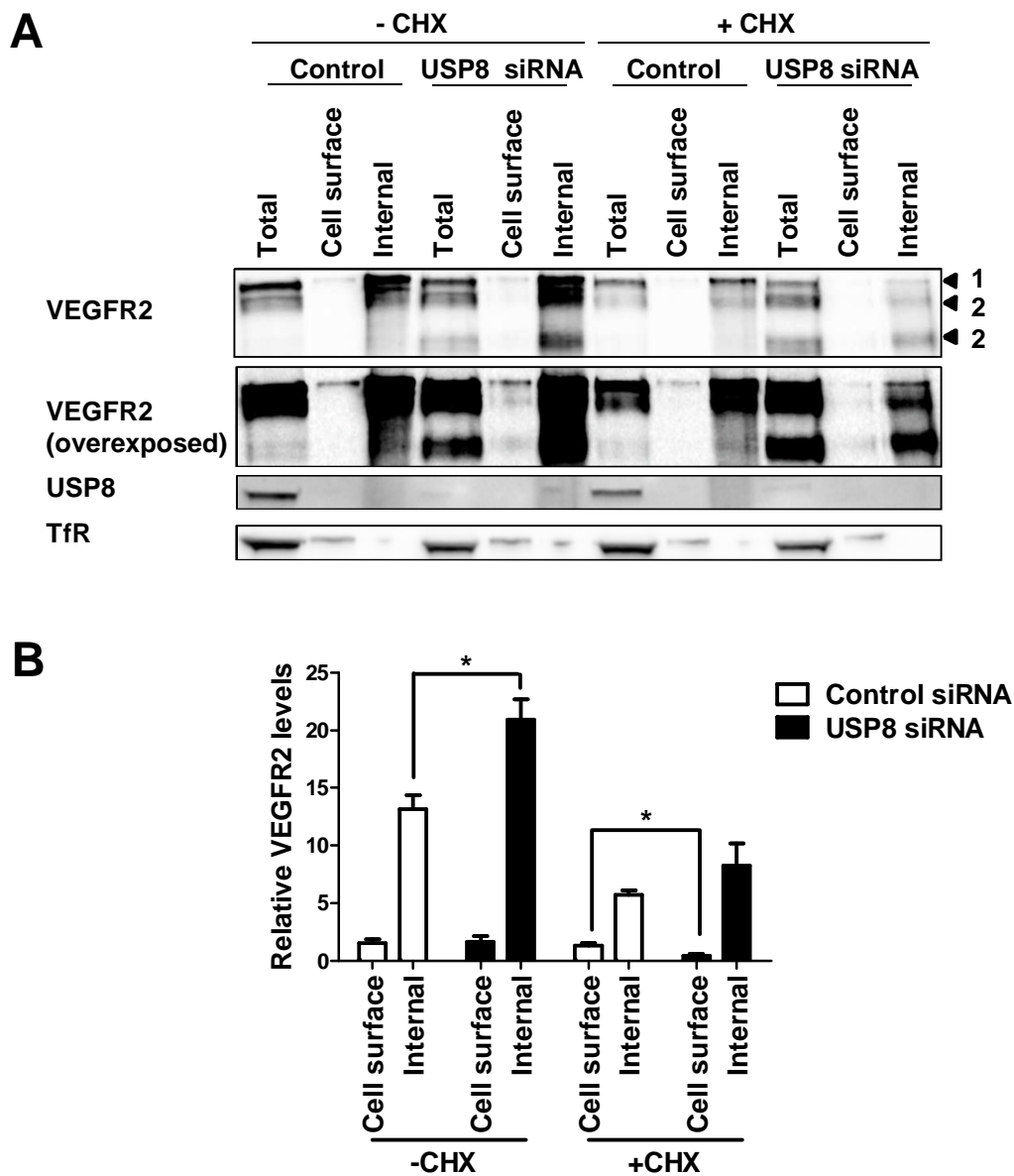
Figure 5.14. Plasma membrane VEGFR2 is replenished by newly synthesised receptor in USP8-depleted cells. (A) Endothelial cells transfected with non-targeting or USP8 siRNA were treated with 10 µg/ml CHX, cell surface biotinylated and lysed. Biotinylated proteins were isolated using neutravidin-agarose and internal VEGFR2 immunoprecipitated (from the supernatant) followed by immunoblot analysis using antibodies to VEGFR2. (B) VEGFR2 levels in cells transfected with non-targeting or USP8 siRNA and treated with 10 µg/ml CHX determined using quantitative immunoblotting. Numbered arrowheads denote mature VEGFR2 (1) and proteolytic VEGFR2 fragments (2). Error bars denote ±SEM (n≥3). $p<0.05$ (*).

137
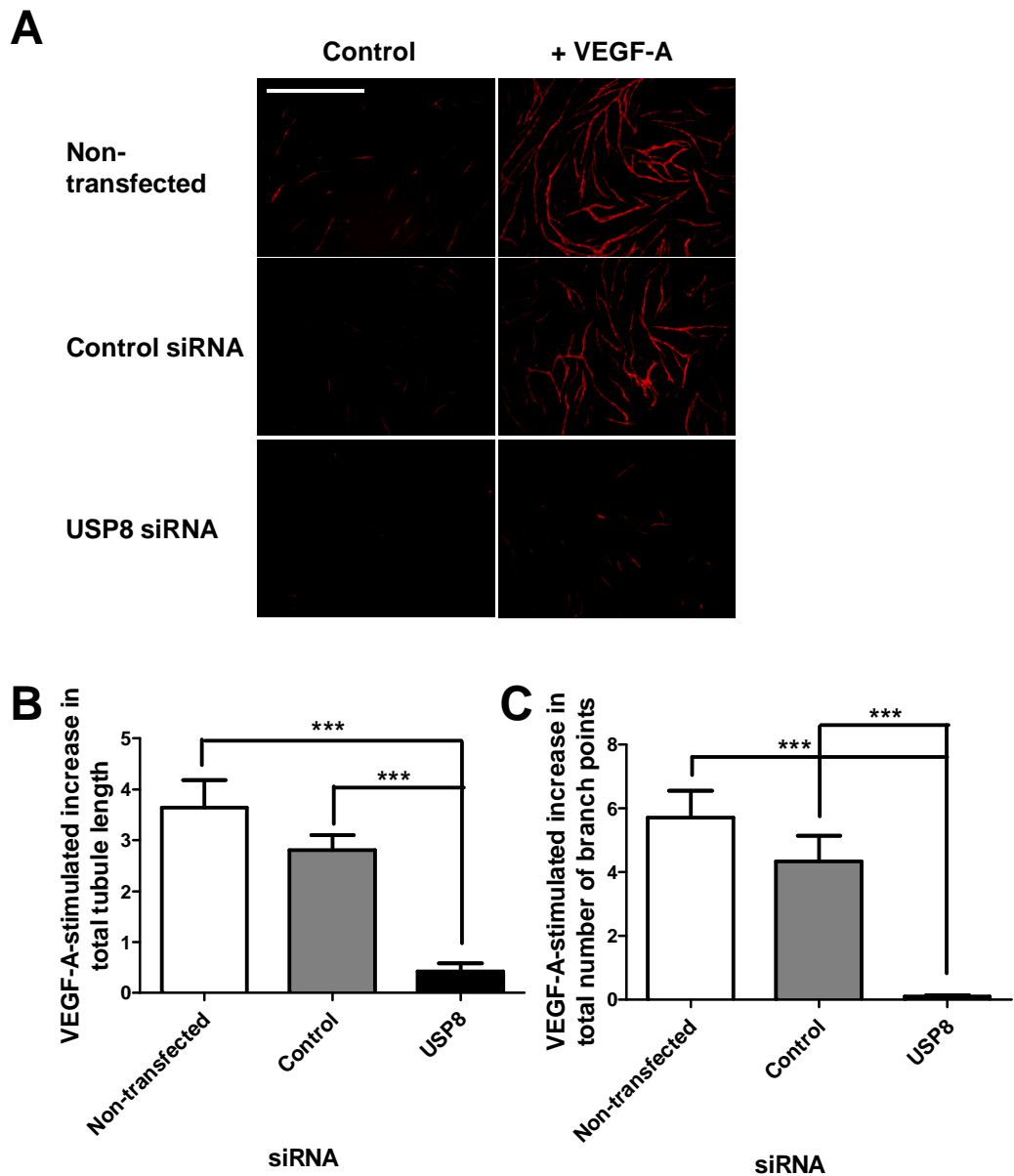
Figure 5.15. USP8 depletion inhibits VEGF-A-stimulated tubulogenesis. (A) Primary human endothelial cells transfected with non-targeting or USP8 siRNA were co-cultured on a bed of primary human fibroblasts for 7 days, treated with 25 ng/ml VEGF-A, fixed and stained with an antibody to PECAM-1 (red). Quantification of total endothelial tubule length (B) and total number of endothelial branch points (C) relative to controls treated with non-targeting siRNA. Error bars denote ±SEM (n≥3). $p<0.001$ (***). Scale bar represents 1000 µm. Gareth Fearnley (Ponnambalam Laboratory, University of Leeds) contributed to the data shown in this figure.

culture assay (Fig. 5.15). Endothelial tubules were stained with the endothelial-specific marker PECAM-1 to reveal complex tubular networks in response to VEGF-A stimulation (Fig. 5.15A). Quantification of both tubule length and number of branch points revealed >90% inhibition of endothelial-specific tubulogenesis in USP8-depleted cells relative to controls (Fig. 5.15B, C).

5.3. Discussion

In this study we show that USP8 plays a key role in VEGFR2 trafficking and proteolysis in the endosome-lysosome system. In this model, sustained VEGFR2 ubiquitination in the absence of USP8 promotes generation of a novel 120 kDa VEGFR2 proteolytic fragment (Fig. 5.16). In addition, USP8-mediated de-ubiquitination and trafficking of VEGFR2 is linked to spatio-temporal control of VEGF-A-stimulated signal transduction (Fig. 5.16).

Our conclusions are based on four lines of evidence. First, USP8 depletion leads to VEGFR2 accumulation within an endosome-like compartment that also contains the early endosome marker, EEA-1. Secondly, the appearance of a novel ~120 kDa VEGFR2-derived proteolytic fragment indicates the existence of a sequence of compartmental-specific machinery that regulates VEGFR2 proteolysis. Depletion of USP8 is marked by aberrant VEGFR2 ubiquitination, recycling and turnover, hallmarks of perturbed ubiquitination and sorting in the endosome-lysosome system. Whereas ERK1/2 and Akt signalling is inhibited by USP8 depletion, other signal transduction pathways are unaffected. The temporal sequence of events in this pathway suggests that ubiquitination and de-ubiquitination are closely associated with endosomes and have major implications for cellular decision making processes e.g. tubulogenesis.

Endosomal DUBs are postulated to remove ubiquitin chains on membrane 'cargo' to prevent terminal degradation in lysosomes. Previous work reported that USP8 depletion severely inhibits EGFR degradation (Row et al., 2006). Ubiquitinated EGFR accumulated in EEA1-positive endosomes caused by failure to reach a terminal degradative compartment (Row et al., 2006). Other work also supported the view that EGFR down-regulation is USP8-dependent (Mizuno et al., 2006). Our study now shows that a different RTK, VEGFR2, accumulates in early endosomes of USP8-depleted
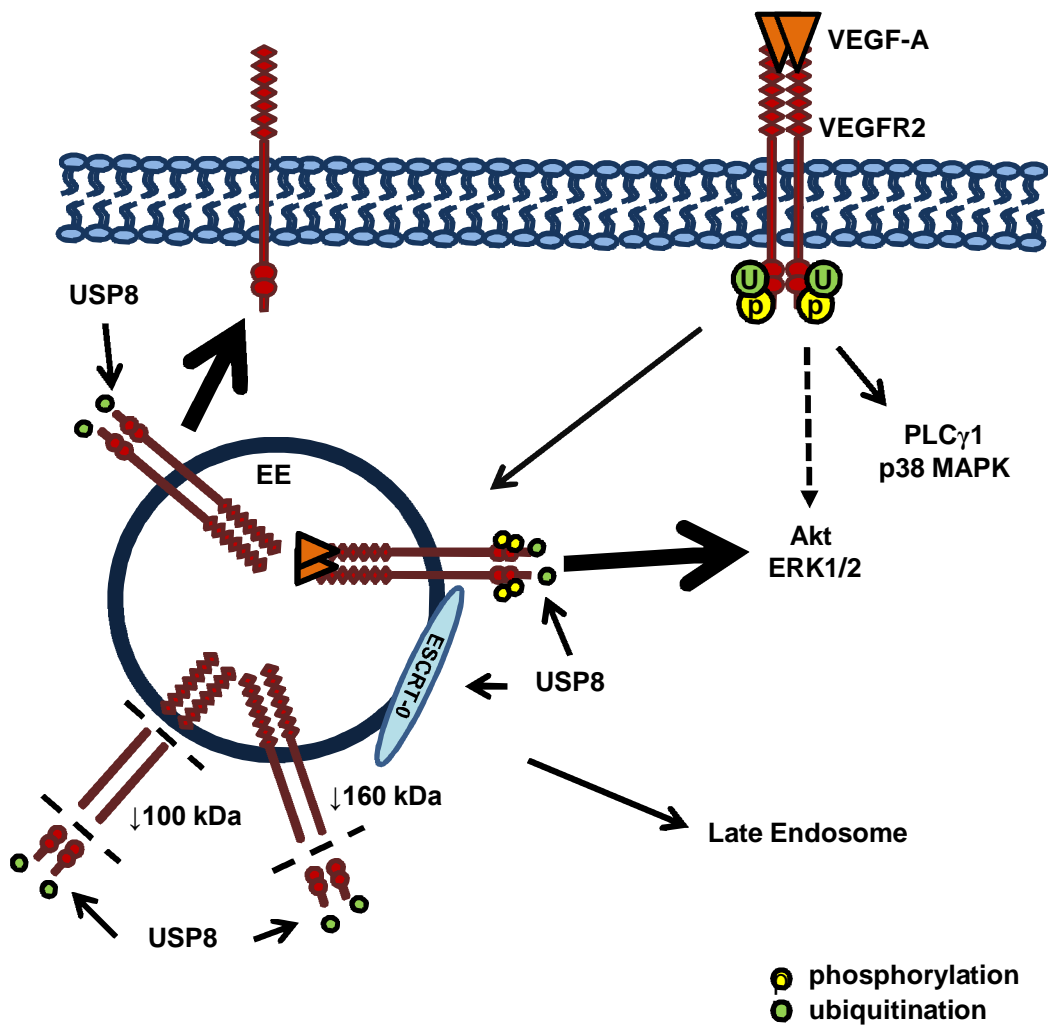
Figure 5.15. Regulation of VEGFR2 trafficking, signalling and proteolysis by USP8. Sustained VEGFR2 residence and ubiquitination in early endosomes leads to proteolysis that generates 160 kDa and 120 kDa VEGFR2-derived fragments in USP8-depleted cells. The 160 kDa fragment remains ubiquitinated and both VEGFR2 cleavage products accumulate in early endosomes due to an indirect effect of USP8 depletion on the ESCRT-0 trafficking machinery. Both reduced de-ubiquitination and enhanced proteolysis of accumulated VEGFR2 down-regulate endosome-linked signal transduction.

cells. It is likely that both full-length and partially proteolysed VEGFR2 accumulates in these endosomes upon USP8 depletion.

Ubiquitin-linked enzyme activity of DUBs plays vital roles in RTK trafficking (Clague and Urbe, 2010). USP8 modulates EGFR trafficking by regulating STAM de-ubiquitination on early endosomes (Row et al., 2006). STAM protection from proteasomal degradation facilitates forward movement of ubiquitinated receptors through the endosome-lysosome system. USP8 depletion causes almost complete STAM degradation and hinders further trafficking of cargo proteins (McCullough et al., 2004). Our studies also lead to the conclusion that USP8 regulates endosomal machinery (e.g. ESCRT-0) that is essential for onward trafficking of activated VEGFR2 through the endosome-lysosome system.

VEGFR2 localisation in early endosomes is linked to subsequent 26S proteasome-dependent proteolysis and production of a 160 kDa proteolytic fragment (Bruns et al., 2010). Furthermore, production of the 160 kDa fragment has been linked to down-regulation of VEGFR2 endosomal signal transduction (Bruns et al., 2010). This study shows that USP8 depletion is linked to generation of a novel 120 kDa proteolytic fragment derived from mature, plasma membrane VEGFR2. We postulate that the 230 kDa mature VEGFR2 protein undergoes sequential proteolysis in the endosomal network into 160 kDa and 120 kDa extracellular domain fragments. However, these VEGFR2 fragments could also be individual cleavage products that remain trapped in early endosomes and inaccessible to lysosomal degradation due to disruption of ESCRT-0 components and endosome-lysosome delivery in USP8-depleted cells. Another possibility is that an imbalance in the levels of hydrolases as a result of USP8 depletion promotes increased VEGFR2 processing and release of the extracellular domain within early endosomes.

USP8 regulates de-ubiquitination of EGFR/ErbB1 and ErbB2 (Mizuno et al., 2005, Row et al., 2006, Meijer and van Leeuwen, 2011). We now provide evidence that USP8 de-ubiquitinates VEGFR2. Whereas VEGFR2 ubiquitination showed a ligand-dependent peak and decline in control cells, ubiquitination of the 160 kDa VEGFR2 proteolytic fragment persisted over a time course of VEGF-A stimulation in USP8-depleted cells. Reduced VEGFR2 de-ubiquitination upon USP8 depletion did not

promote increased lysosomal degradation due to the indirect effect of USP8 depletion on the trafficking machinery, causing accumulation of ubiquitinated VEGFR2 in early endosomes. This ubiquitinated VEGFR2 was susceptible to proteolysis which reduced levels of full length receptor but caused accumulation of cleavage products in the endosome-lysosome system. VEGFR2 proteolytic fragments of 160 and 120 kDa thus accumulated in early endosomes causing an overall increase in total VEGFR2 levels.

K48-linked polyubiquitin chains are associated with proteasomal degradation whilst K63-linked chains are associated with membrane receptor trafficking and targeting in the endosome-lysosome system (Pickart, 2001, Adhikari and Chen, 2009). Our finding that increased levels of both K48- and K63-linked polyubiquitin are present on VEGFR2 upon USP8 depletion agrees with other studies that USP8 removes both such polyubiquitin chains from protein substrates (McCullough et al., 2004).

VEGFR2 signal transduction is postulated to be location-dependent with different outcomes at the plasma membrane vs. endosomes (Horowitz and Seerapu, 2012). A requirement for USP8 was evident in VEGF-A-stimulated ERK1/2 and Akt activation but not in p38 MAPK and PLCγ1 activation. This outcome could be linked to perturbed VEGFR2 localisation in endosomes whilst plasma membrane dynamics are unaffected due to replenishment from the biosynthetic pool in USP8-depleted cells. Other studies have also linked activated VEGFR2 residence in endosomes to ERK1/2 (Lanahan et al., 2010, Bruns et al., 2010, Jopling et al., 2009, Horowitz and Seerapu, 2012, Koch et al., 2011) and Akt (Lanahan et al., 2010, Sawamiphak et al., 2010, Horowitz and Seerapu, 2012, Koch et al., 2011) activation. One possible explanation is that activated VEGFR2 must undergo USP8-mediated de-ubiquitination on early endosomes as a pre-requisite for engagement with ERK1/2 and Akt-linked signal transduction machinery.

A key conclusion is that USP8 regulates VEGFR2 recycling. De-ubiquitination of activated VEGFR2 on early endosomes by a USP8-regulated mechanism could precede recycling back to the plasma membrane. However, reduced VEGFR2 recycling in USP8-depleted cells could be an indirect effect caused by perturbation of the ESCRT-0 complex. The pathway for VEGFR2 endosome-to-plasma membrane recycling has been shown to require Rab4a (Jopling et al., 2014) and c-Src (Gampel et al., 2006). An

alternate Rab11a endosome-to-plasma membrane pathway specifically regulates recycling of activated VEGFR2-NRP1 complexes (Ballmer-Hofer et al., 2011).

Our model proposes that sustained VEGFR2 residence and ubiquitination in early endosomes leads to proteolysis that generates 160 kDa and 120 kDa VEGFR2 fragments in USP8-depleted cells. (Fig. 5.16). Although the 160 kDa fragment remains ubiquitinated, both VEGFR2 cleavage products accumulate in early endosomes due to the indirect effect of USP8 depletion on trafficking machinery. Both reduced de-ubiquitination and enhanced proteolysis of accumulated VEGFR2 down-regulate endosome-linked signal transduction (Fig. 5.16).

USP8 is required for efficient VEGFR2 trafficking, de-ubiquitination, signal transduction, recycling and proteolysis. This study emphasises the idea that plasma membrane receptor ubiquitination and de-ubiquitination is more complex than a simple system for targeting receptor degradation in lysosomes. The modulation of VEGFR2 ubiquitination status could provide a new and alternative therapeutic strategy to target disease states that display aberrant angiogenesis.

CHAPTER 6

Novel artificial binding proteins modulate VEGFR signal transduction and endothelial function

6.1. Introduction

VEGF-A is a potent pro-angiogenic growth factor involved in regulating angiogenesis (Koch and Claesson-Welsh, 2012). Pathological conditions associated with VEGF-A-stimulated angiogenesis include cancer and age-related macular degeneration whilst insufficient angiogenesis leads to tissue ischaemia and heart disease. VEGFR2 is the principal RTK through which VEGF-A transmits its pro-angiogenic signals in vascular endothelial cells (Olsson et al., 2006, Shibuya, 2010). VEGF-A binding to VEGFR2 promotes dimerisation and transautophosphorylation of several key cytoplasmic domain tyrosine residues, leading to activation of signalling proteins including PLCγ1, ERK1/2 and Akt (Koch and Claesson-Welsh, 2012). Functional cellular responses of the VEGFR2-VEGF-A axis include endothelial cell proliferation, migration, survival and ultimately formation of endothelial tubules (Koch and Claesson-Welsh, 2012). In contrast, VEGFR1 is considered a 'decoy' receptor in endothelial cells due to its low tyrosine kinase activity and existence of a soluble VEGFR1 isoform which restrict the VEGF-A-stimulated response (Robinson and Stringer, 2001). Thus, inhibiting VEGFR1-VEGF-A binding could promote VEGF-A-induced VEGFR2 signal transduction and stimulate angiogenesis in ischaemic tissues.

Antibodies are the most commonly used binding proteins with several clinically approved to inhibit VEGFR2 activity in cancer and >240 candidates in clinical development (Reichert, 2010, Tugues et al, 2011). Nonetheless, limitations of antibodies include their large size as multimeric proteins that require glycosylation and disulphide bonds for stability. Antibody production is expensive and relies upon the use of animals whilst clinical application requires humanised versions. Improved non-antibody-based artificial binding proteins (Adhirons) have been developed to mimic the molecular recognition properties of antibodies but with improved properties i.e they are

monomeric, soluble, stable and have no cysteine or glycosylation sites (Tiede et al., 2014, Gebauer and Skerra, 2009). Adhirons contain a cystatin-like fold based on a phytocystatin consensus sequence. Two variable peptide regions containing 9 amino acids facilitate generation of a phage display library with approximately 1.3×10^{10} clones (Tiede et al, 2014). Interestingly, other non-antibody binding proteins called DARPins have been shown to inhibit VEGFR2 activity (Hyde et al, 2012). In this chapter, we used Adhirons screened by ELISA to specifically bind the extracellular domains of VEGFR1 or VEGFR2. Here we show that VEGFR1 Adhirons promote VEGFR2 activation and VEGF-A-stimulated signal transduction and enhance VEGF-A-stimulated endothelial tube formation. Contrastingly, VEGFR2 Adhirons inhibit VEGF-A-stimulated signal transduction and endothelial tube formation. These highly specific binding proteins have potential *in vivo* clinical applications including vascular imaging. In addition, Adhirons could be used as therapeutic agents in tissue ischaemia, retinopathies or the tumour microenvironment through pro- or anti-angiogenic targeting of VEGFR1 or VEGFR2, respectively.

6.2. Results

6.2.1. VEGFR2-specific Adhirons inhibit VEGF-A-stimulated signal transduction

Phage display was used to select Adhirons that bind to recombinant soluble VEGFR1 or VEGFR2 proteins. In these studies, 4 VEGFR1-binding Adhirons and 3 VEGFR2-binding Adhirons were selected for further analysis. Two VEGFR2 Adhirons that demonstrated inhibitory potential were chosen for detailed functional analysis. Of the 4 VEGFR1 Adhirons screened for their potential to regulate endothelial cell tubulogenesis, 1 promoted VEGF-A-stimulated tubule formation and was chosen for detailed analysis. An analysis of Adhiron-specific binding to VEGFR1 or VEGFR2 proteins was carried out by the Tomlinson laboratory (University of Leeds, UK) using biophysical techniques (data not shown). It was reported that these Adhirons displayed dissociation constants for VEGFRs in the nanomolar range (C. Tiede and D. Tomlinson, University of Leeds, personal communication).

VEGFR2 is activated upon VEGF-A-induced structural changes in the receptor extracellular domain which initiate transautophosphorylation and downstream signal

transduction (Koch et al., 2011). VEGFR2-Adhiron binding could prevent VEGFR2-VEGF-A interaction or inhibit the structural changes required to initiate receptor activation. To test this idea, endothelial cells were subjected to pre-treatment with varying concentrations of VEGFR2-specific Adhirons 30 min prior to stimulation with 25 ng/ml VEGF-A. Downstream signal transduction events were analysed by quantitative immunoblotting (Fig. 6.1A, 6.3A, 6.5A, 6.7A). VEGF-A binding causes VEGFR2 autophosphorylation of cytoplasmic residue Y1175, creating a key binding site for downstream effectors (Koch et al., 2011). Quantification of immunoblot analysis revealed VEGFR2-pY1175 levels were 72% reduced in endothelial cells treated with 150 µg B8 Adhiron (Fig. 6.2A). Plasma membrane VEGFR2 activation is associated with recruitment, tyrosine phosphorylation and activation of PLCγ1 (Koch et al., 2011). Cells treated with B8 Adhiron exhibited 92% reduction in PLCγ1 phosphorylation (Fig. 6.2B). VEGF-A-stimulated activation of the serine/threonine protein kinase, Akt, was 46% reduced in B8 Adhiron-treated cells (Fig. 6.2C). In addition, VEGF-A-stimulated activation of the MAPK pathway involving ERK1/2 was 67% inhibited in cells treated with B8 Adhiron (Fig. 6.2D). Phosphorylation of eNOS and p38 MAPK was inhibited by 93% in B8 Adhiron-treated endothelial cells (Fig. 6.2E, F). Adhiron-induced inhibition of VEGF-A-stimulated VEGFR2 signal transduction showed a dose-dependent decline.

In cells treated with A9 Adhiron VEGF-A-stimulated VEGFR2 (Y1175) and PLCγ1 phosphorylation was inhibited by 75% (Fig. 6.4A, B). Activation of Akt and ERK1/2 was inhibited by 94% and 89%, respectively (Fig. 6.4C, D). In contrast, eNOS phosphorylation was not significantly inhibited. Although p38 MAPK phosphorylation was up to 90% reduced in cells treated with A9 Adhiron this was not significant (Fig. 6.4E, F). In cells treated with a control Adhiron that does not bind VEGFR2, VEGF-A-stimulated VEGFR2 phosphorylation and activation of downstream signalling proteins was not significantly inhibited (Fig. 6.6). Another VEGFR2-specific Adhiron, H5, did not inhibit VEGF-A-stimulated signal transduction (Fig.6.8). These results showed that only VEGFR2-specific Adhirons, A9 and B8, inhibit VEGF-A-stimulated signal transduction.

6.2.2. Functional characterisation of VEGFR2-specific Adhirons

VEGF-A-stimulated activation of VEGFR2 promotes downstream signal transduction and leads to new blood vessel sprouting, an essential feature of angiogenesis (Ferrara, 1999). In an endothelial-fibroblast co-culture assay, VEGF-A stimulated tubulogenesis was revealed by staining for the endothelial-specific protein PECAM-1. Co-cultures were pre-treated with Adhiron 30 min before VEGF-A stimulation every 2 days for a 7 day period to screen VEGFR2 Adhirons for effects on the VEGF-A-stimulated endothelial response (Fig. 6.9A). Quantification of tubule length and number of branch points revealed that B8 Adhiron significantly inhibited VEGF-A-stimulated endothelial tubulogenesis (Fig. 6.9A). Tubule length was reduced by 80% whilst number of branch points was reduced by 98% (Fig. 6.9B, C). Treatment with A9 Adhiron had a less pronounced effect on VEGF-A-stimulated tubulogenesis (Fig. 6.9). In addition, there was no reduction in tubule length or number of branch points following treatment with a control Adhiron that does not bind VEGFR2 (Fig. 6.9). These results highlight that the VEGFR2-specific Adhiron, B8, inhibits VEGF-A-stimulated endothelial tubulogenesis.

6.2.3. Functional characterisation of VEGFR1-specific Adhirons

VEGFR1 is considered a negative regulator of VEGFR2 activity by preferentially binding VEGF-A (Devries et al., 1992). Adhirons to VEGFR1 could prevent VEGFR1-VEGF-A interaction, thus promoting increased VEGFR2-VEGF-A binding and increasing the endothelial response to VEGF-A. VEGFR1 Adhirons were screened for effects on VEGF-A-stimulated tubulogenesis (Fig. 6.10A). Of the 4 Adhirons screened, treatment with 35c Adhiron produced a significant increase in both basal and VEGF-A-stimulated tubulogenesis (Fig. 6.10A). Quantification revealed a 51% increase in tubule length and 84% increase in branch point number under basal conditions (Fig. 6.10B, C). Under VEGF-A-stimulated conditions, tubule length increased by 15% and branch point number increased by 26% (Fig. 6.10B, C). Thus, VEGFR1 Adhirons promote endothelial tubulogenesis.
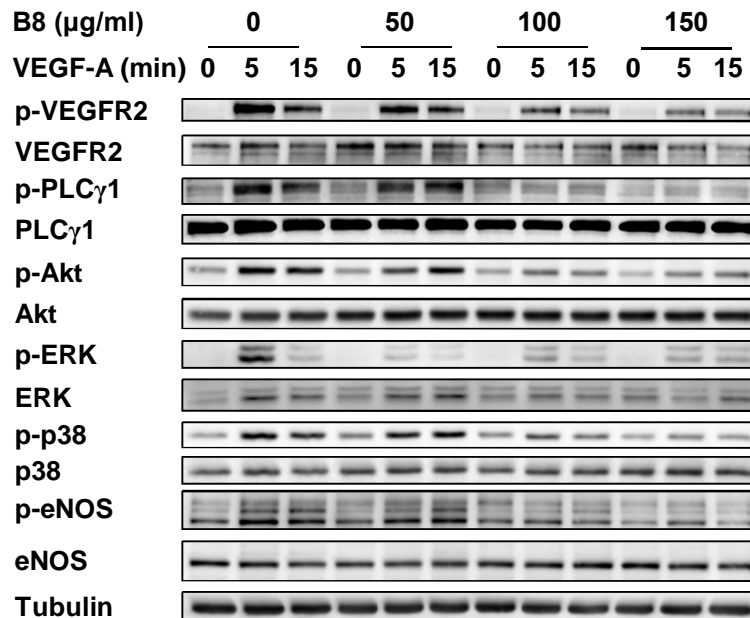
Figure 6.1. VEGFR2-specific Adhiron B8 inhibits VEGF-A-stimulated signal transduction. Endothelial cells were pre-treated with 0, 50, 100 or 150 μg/ml B8 (30 min) prior to 25 ng/ml VEGF-A stimulation, lysed and immunoblotted for phospho-VEGFR2 (Y1175), phospho-PLCγ1, phospho-Akt (S473), phospho-ERK1/2 (T202/Y204), phospho-p38 MAPK (T180/Y182) and phospho-eNOS (S117).
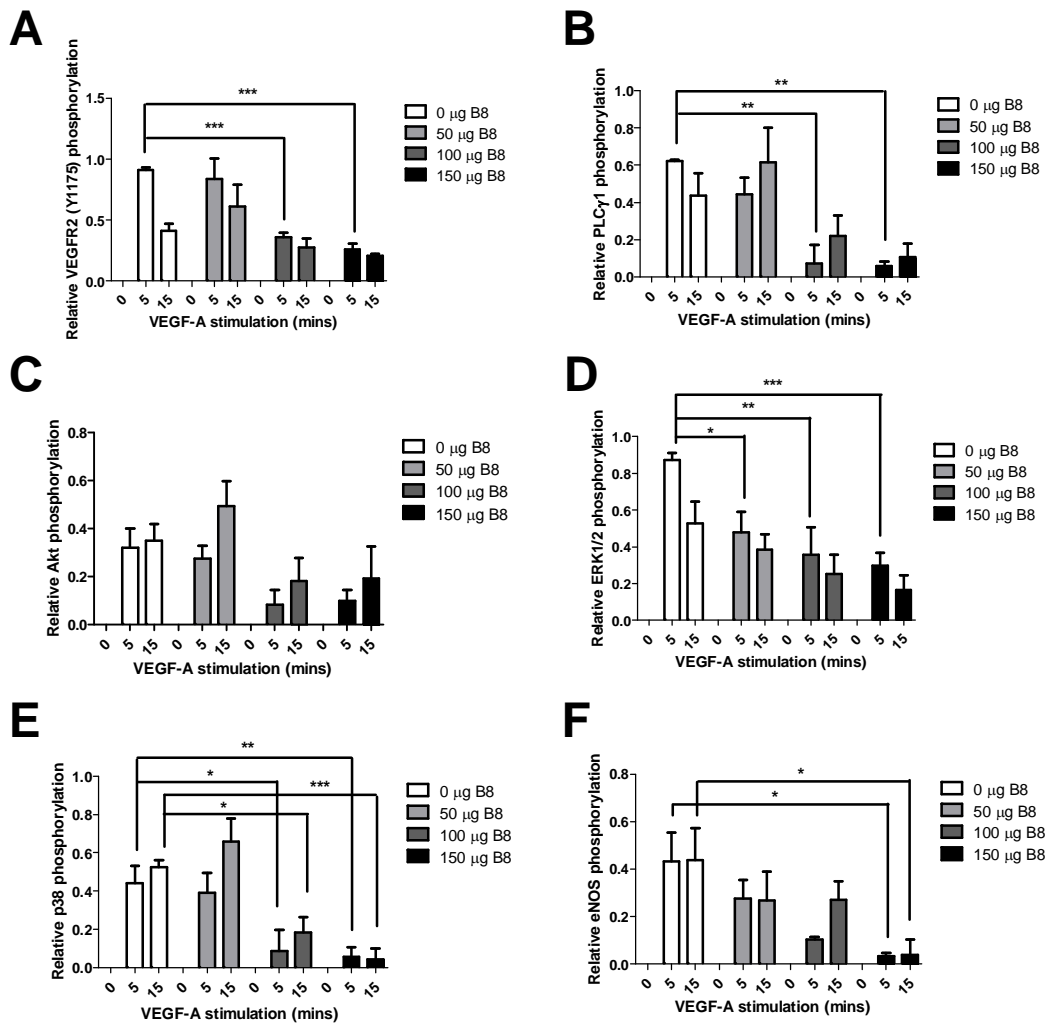
Figure 6.2. Quantification of VEGFR2-specific Adhiron B8 inhibition of VEGF-A-stimulated signal transduction. Phospho-VEGFR2 (A), phospho-PLCγ1 (B), phospho-Akt (C), phospho-ERK1/2 (D), phospho-p38 MAPK (E) and phospho-eNOS (F) levels in endothelial cells pre-treated with 0, 50, 100 or 150 μg/ml B8 (30 min) prior to 25 ng/ml VEGF-A stimulation and quantitative immunoblot analyses. Errors bars indicate +SEM (n≥3). $p<0.05$ (*), $p<0.01$ (**), $p<0.001$ (***).
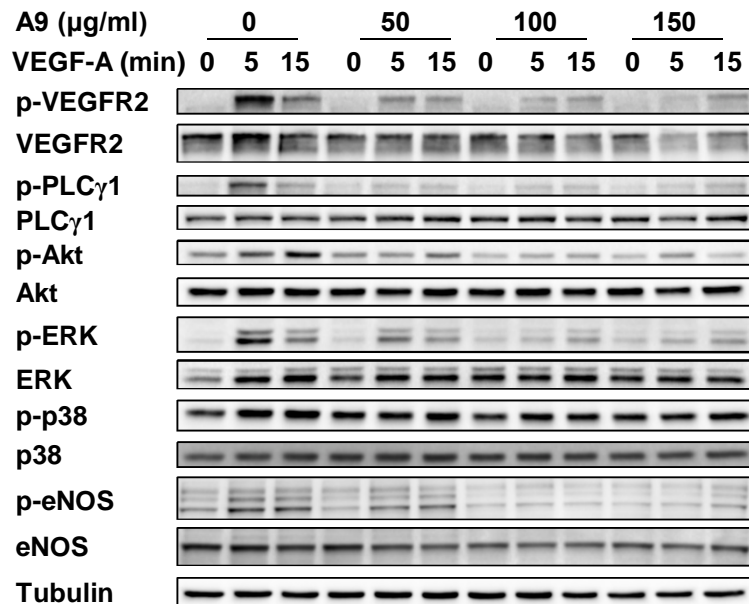
Figure 6.3. VEGFR2-specific Adhiron A9 inhibits VEGF-A-stimulated signal transduction. Endothelial cells were pre-treated with 0, 50, 100 or 150 μg/ml A9 (30 min) prior to 25 ng/ml VEGF-A stimulation, lysed and immunoblotted for phospho-VEGFR2 (Y1175), phospho-PLCγ1, phospho-Akt (S473), phospho-ERK1/2 (T202/Y204), phospho-p38 MAPK (T180/Y182) and phospho-eNOS (S117).
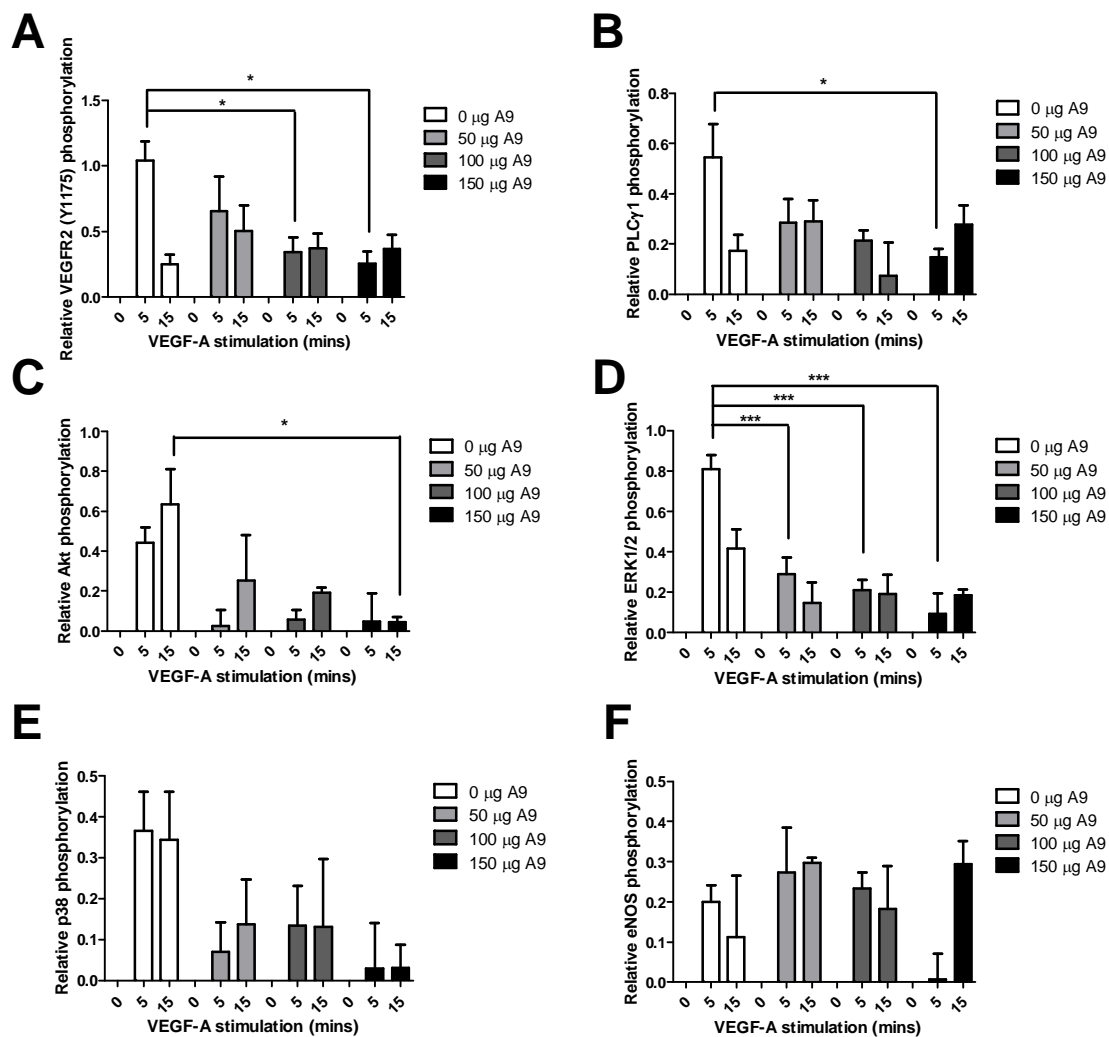
Figure 6.4. Quantification of VEGFR2-specific Adhiron A9 inhibition of VEGF-A-stimulated VEGFR2 signal transduction. Levels of phospho-VEGFR2 (A), phospho-PLCγ1 (B), phospho-Akt (C), phospho-ERK1/2 (D), phospho-p38 MAPK (E) and phospho-eNOS (F) in endothelial cells pre-treated with 0, 50, 100 or 150 μg/ml A9 (30 min) prior to 25 ng/ml VEGF-A stimulation and quantitative immunoblot analyses. Errors bars indicate +SEM (n≥3). $p<0.05$ (*), $p<0.01$ (**), $p<0.001$ (***).
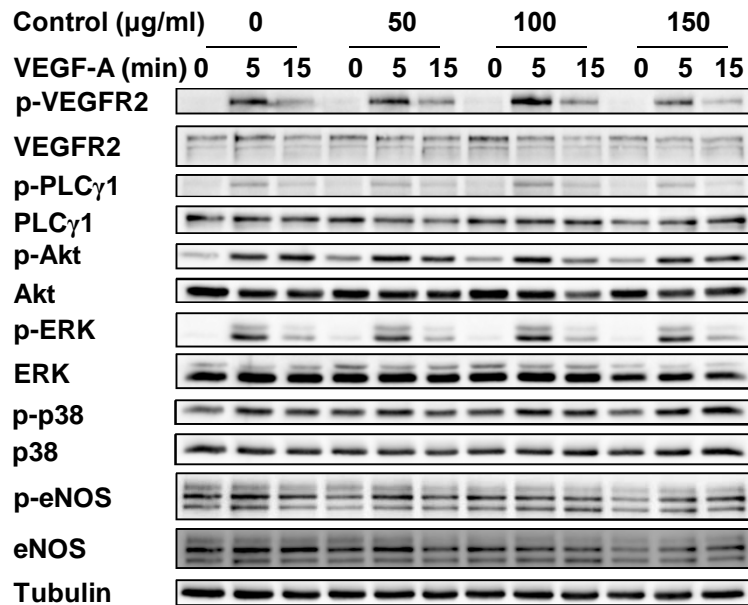
Figure 6.5. Control Adhiron does not inhibit VEGF-A-stimulated signal transduction. Endothelial cells were pre-treated with 0, 50, 100 or 150 μg/ml control Adhiron (30 min) prior to 25 ng/ml VEGF-A stimulation, lysed and immunoblotted for phospho-VEGFR2 (Y1175), phospho-PLCγ1, phospho-Akt (S473), phospho-ERK1/2 (T202/Y204), phospho-p38 MAPK (T180/Y182) and phospho-eNOS (S117).
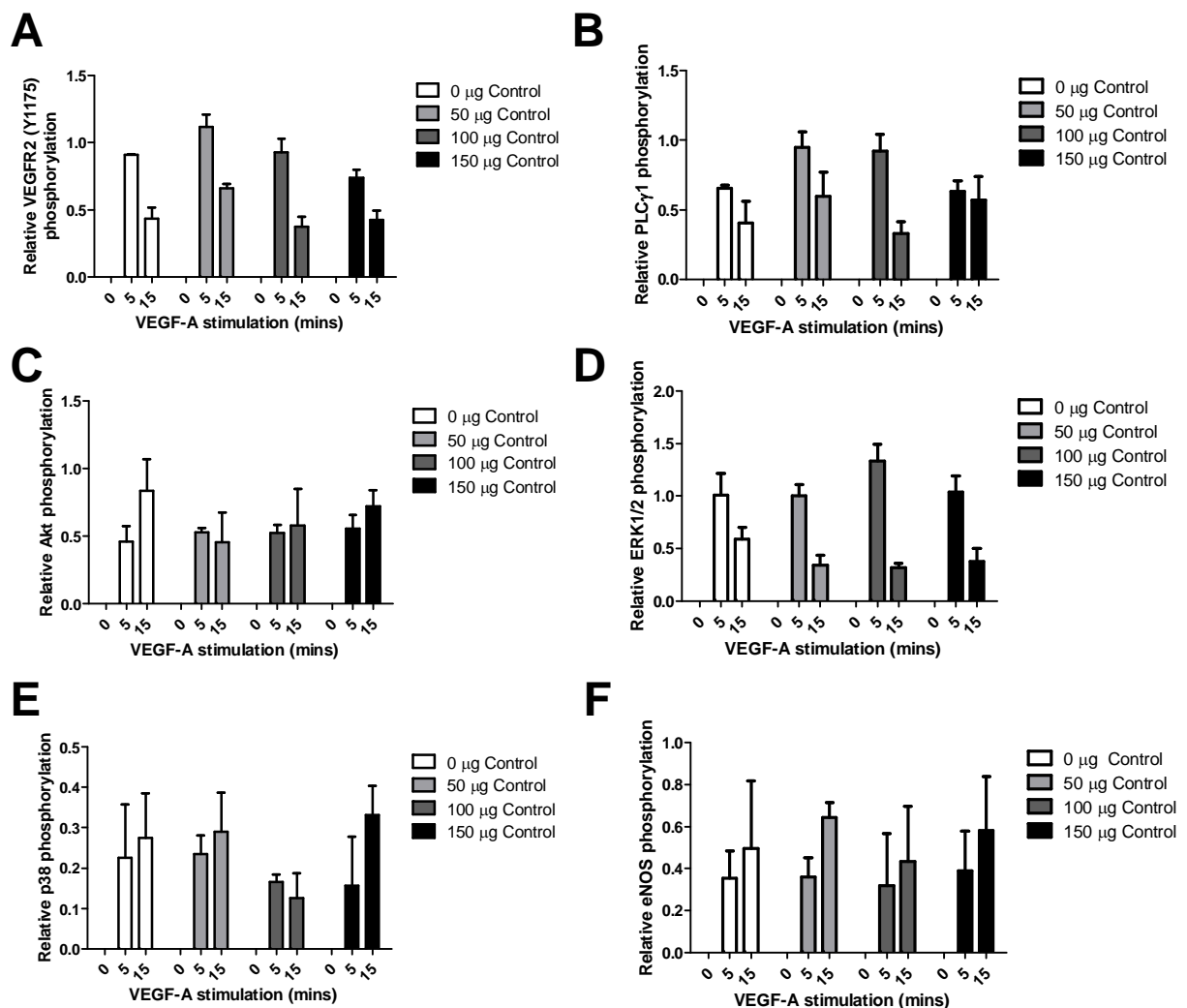
Figure 6.6. Control Adhiron does not inhibit VEGF-A-stimulated signal transduction. Quantification of phospho-VEGFR2 (A), phospho-PLCγ1 (B), phospho-Akt (C), phospho-ERK1/2 (D), phospho-p38 MAPK (E) and phospho-eNOS (F) levels in endothelial cells pre-treated with 0, 50, 100 or 150 μg/ml control (30 min) prior to 25 ng/ml VEGF-A stimulation and quantitative immunoblot analyses. Errors bars indicate +SEM (n≥3).
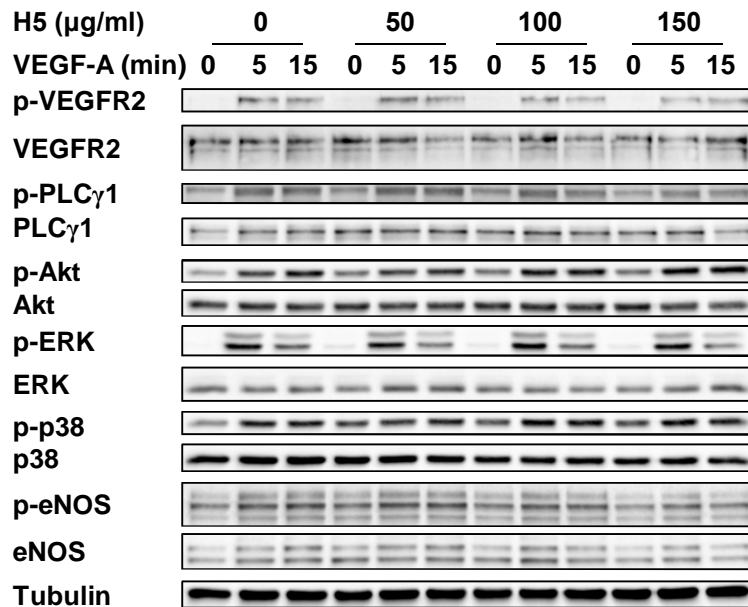
Figure 6.7. VEGFR2-specific Adhiron H5 does not inhibit VEGF-A-stimulated signal transduction. Endothelial cells were pre-treated with 0, 50, 100 or 150 μg/ml H5 Adhiron (30 min) prior to 25 ng/ml VEGF-A stimulation, lysed and immunoblotted for phospho-VEGFR2 (Y1175), phospho-PLCγ1, phospho-Akt (S473), phospho-ERK1/2 (T202/Y204), phospho-p38 MAPK (T180/Y182) and phospho-eNOS (S117).

154
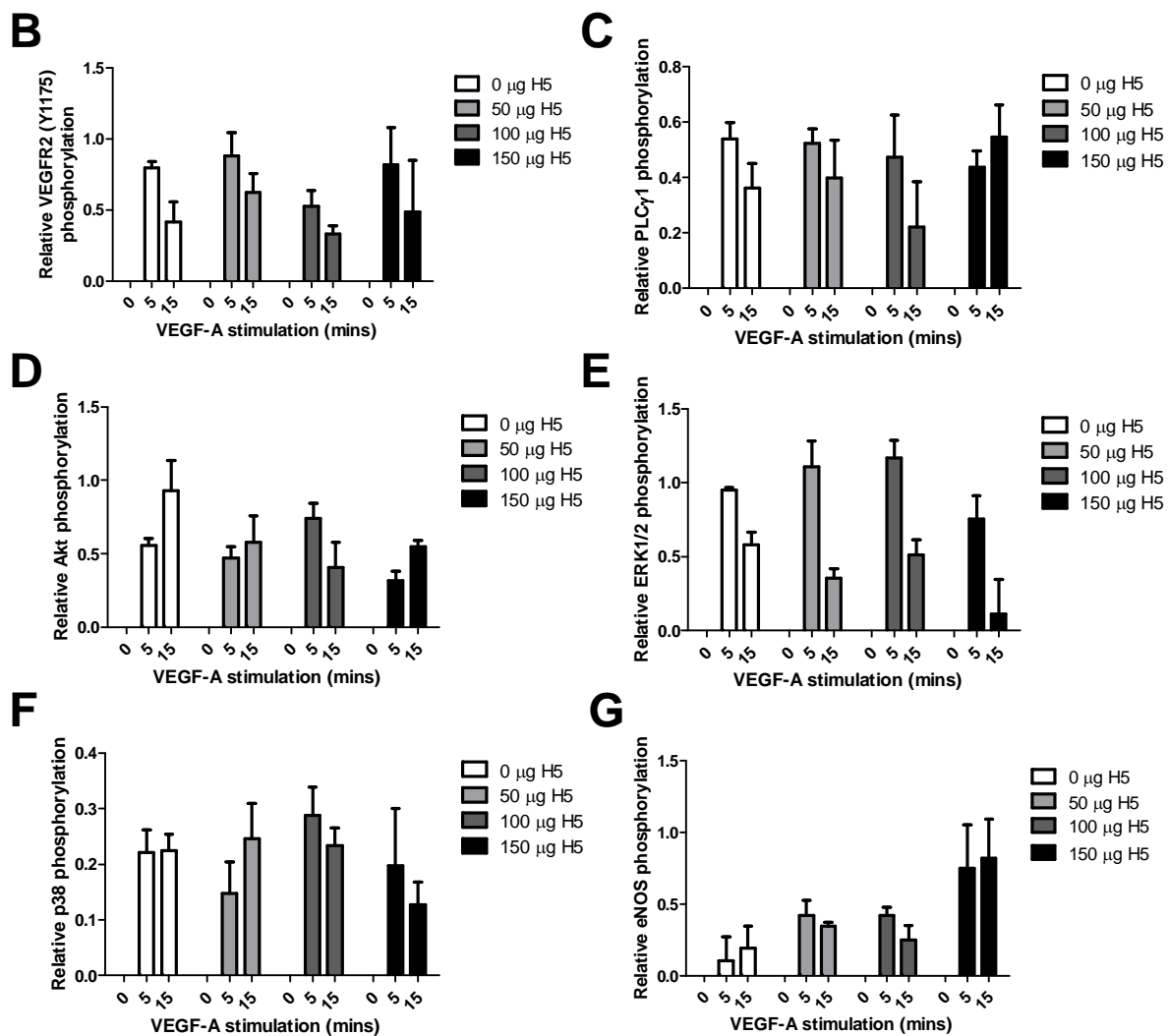
Figure 6.8. VEGFR2-specific Adhiron H5 does not inhibit VEGF-A-stimulated signal transduction. Quantification of phospho-VEGFR2 (A), phospho-PLCγ1 (B), phospho-Akt (C), phospho-ERK1/2 (D), phospho-p38 MAPK (E) and phospho-eNOS (F) levels in endothelial cells pre-treated with 0, 50, 100 or 150 µg/ml H5 (30 min) prior to 25 ng/ml VEGF-A stimulation and quantitative immunoblot analyses. Errors bars indicate +SEM (n≥3).
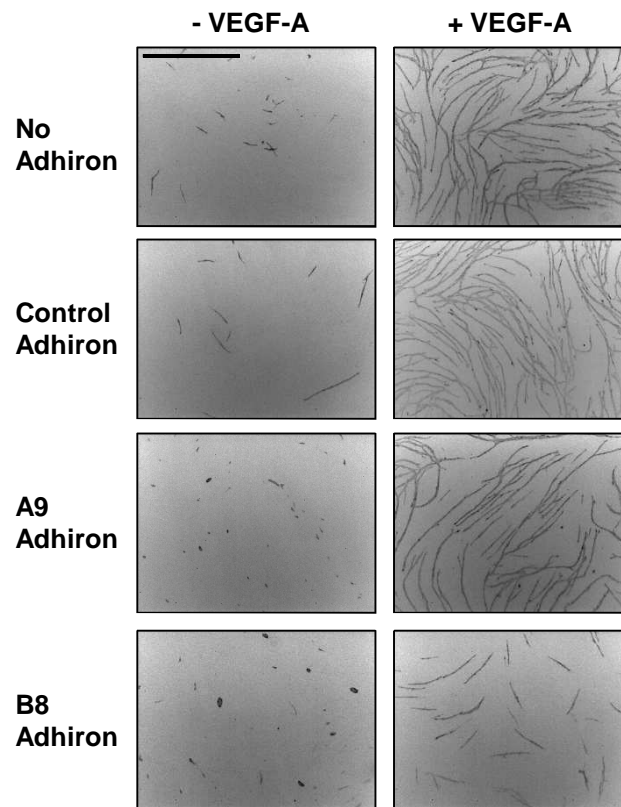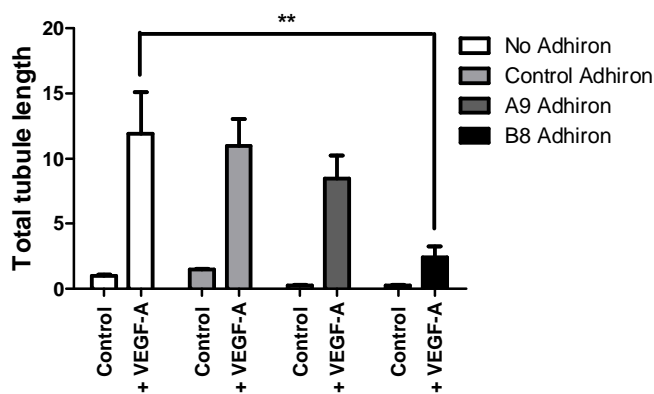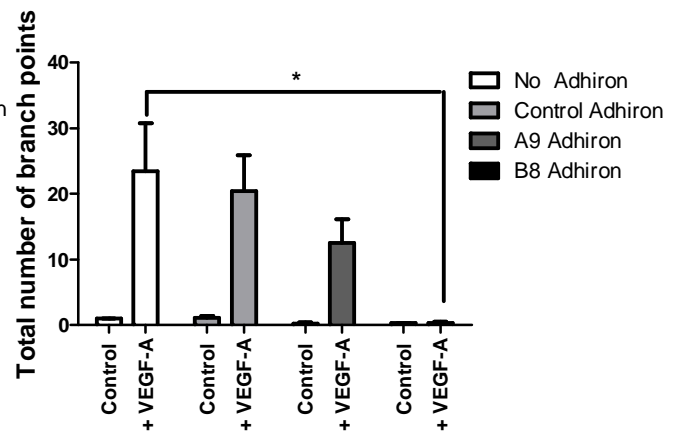
Figure 6.9. VEGFR2-specific Adhirons inhibit VEGF-A-stimulated endothelial cell tubulogenesis. (A) Primary human endothelial cells were co-cultured on a bed of primary human fibroblasts for 7 days, treated with 100 μg/ml control, A9, or B8 VEGFR2 Adhiron 30 min prior to stimulation with 25 ng/ml VEGF-A, fixed and stained with an antibody to PECAM-1. Scale bar represents 1000 μm. Quantification of VEGF-A-stimulated total endothelial tubule length (B) and total number of endothelial branch points (C) following treatment with control, A9 or B8 Adhirons. Error bars denote ±SEM (n≥3). $p<0.05$ (*), $p<0.01$ (**).

6.2.4. VEGFR1-specific Adhirons promote VEGF-A-stimulated VEGFR2 activation

VEGFR1 forms a non-productive signalling complex upon VEGF-A binding and thus sequesters VEGF-A to limit the VEGF-A-stimulated VEGFR2 signal transduction response (Robinson and Stringer, 2001). Adhirons specific for VEGFR1 could prevent VEGFR1-VEGF-A interaction; increasing availability of VEGF-A to bind VEGFR2 and upregulating VEGF-A-stimulated signal transduction. To test this idea, endothelial cells were pre-treated with VEGFR1-specific Adhirons 30 min before stimulation with 25 ng/ml VEGF-A. Downstream signal transduction events were analysed by quantitative immunoblotting (Fig. 6.11). VEGFR2 (Y1175) phosphorylation increased by 24% in cells treated with 35c Adhiron (Fig. 6.12A). In addition, activation of PLCγ1, Akt and eNOS increased by 64%, 52% and 75%, respectively (Fig. 6.12B, C, F). Whilst ERK1/2 activation was not effected by treatment with 35c Adhiron, p38 MAPK activation was 45% increased, although this was not significant (Fig. 6.12D, E). Thus, VEGFR1-specific Adhirons have the capacity to promote VEGFR2 phosphorylation and activation of downstream signal transduction cascades.

Treatment of endothelial cells with 37c Adhiron, which did not significantly increase endothelial tubule formation, had limited effects on VEGF-A-stimulated VEGFR2 phosphorylation and activation of downstream signal transduction (Fig. 6.12).

6.2.5. Adhirons to VEGFR1 or VEGFR2 have opposing effects on endothelial cell migration and proliferation

To test the effect of Adhirons on additional cellular outcomes we performed cell migration and proliferation assays (Fig. 6.13). Pre-treatment of endothelial cells with VEGFR2-specific Adhiron, B8, reduced cell migration by 63% and cell proliferation by 22% (Fig. 6.13, 6.14A, B). Contrastingly, pre-treatment of endothelial cells with VEGFR1-specific Adhiron, 35c, increased cell migration by 36% and cell proliferation by 25% (Fig. 6.13, 6.14A, B). To exclude the possibility that toxic side effects were responsible for inhibition of endothelial cell responses, we performed cell viability assays. All of the Adhirons were non-toxic at the concentration used in tubulogenesis, migration and proliferation experiments, with a cell viability of >90% (Fig. 6.14C).
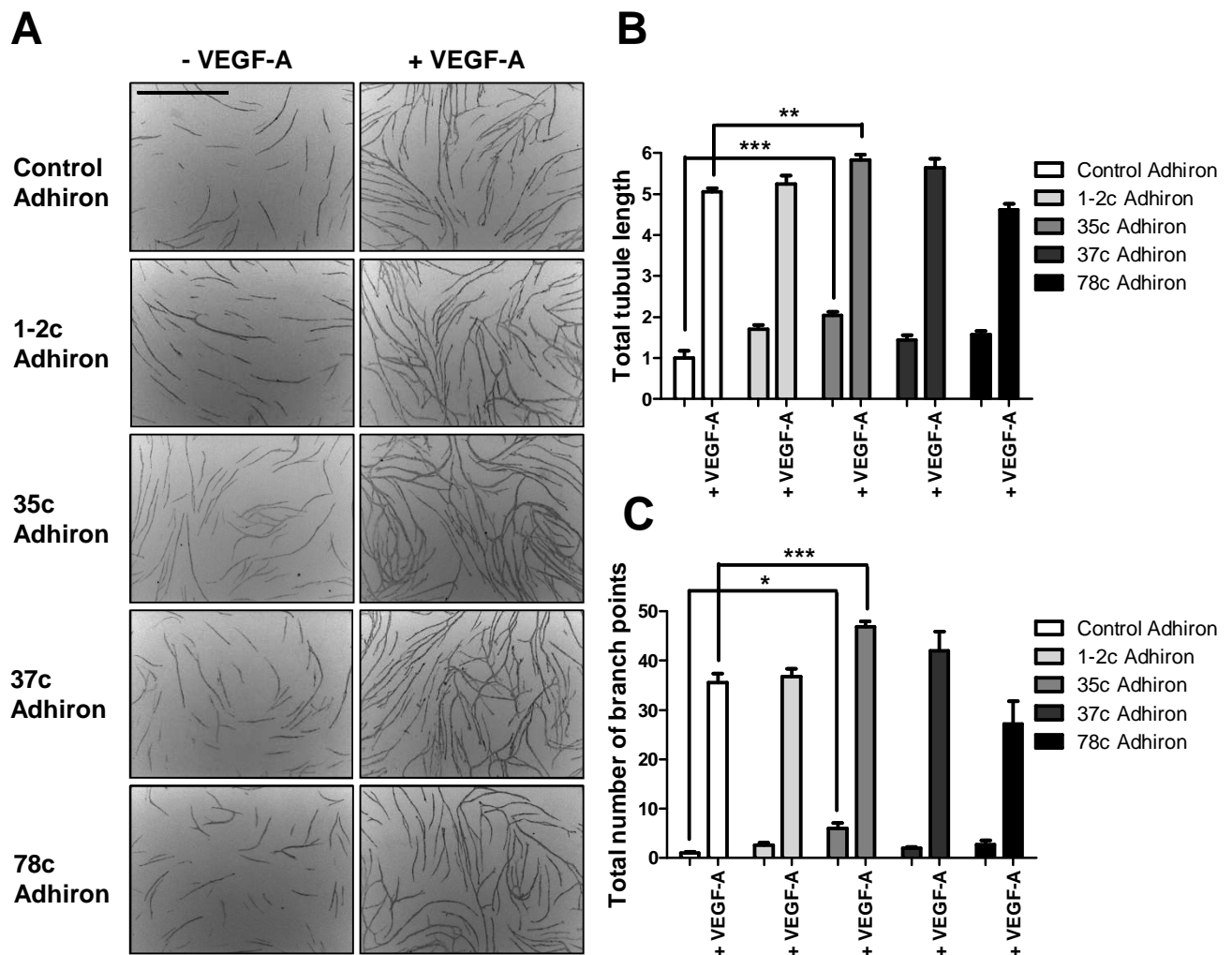
Figure 6.10. VEGFR1-specific Adhirons promote VEGF-A-stimulated endothelial cell tubulogenesis. (A) Primary human endothelial cells were co-cultured on a bed of primary human fibroblasts for 7 days, treated with 100 µg/ml control or VEGFR1 Adhirons 30 min prior to 25 ng/ml VEGF-A stimulation, fixed and stained with an antibody to PECAM-1. Scale bar represents 1000 µm. Quantification of VEGF-A-stimulated total endothelial tubule length (B) and total number of endothelial branch points (C) following treatment with control and 1-2c, 35c, 37c or 78c VEGFR1 Adhirons. Error bars denote ±SEM (n≥3). $p<0.05$ (*), $p<0.01$ (**), $p<0.001$ (***).
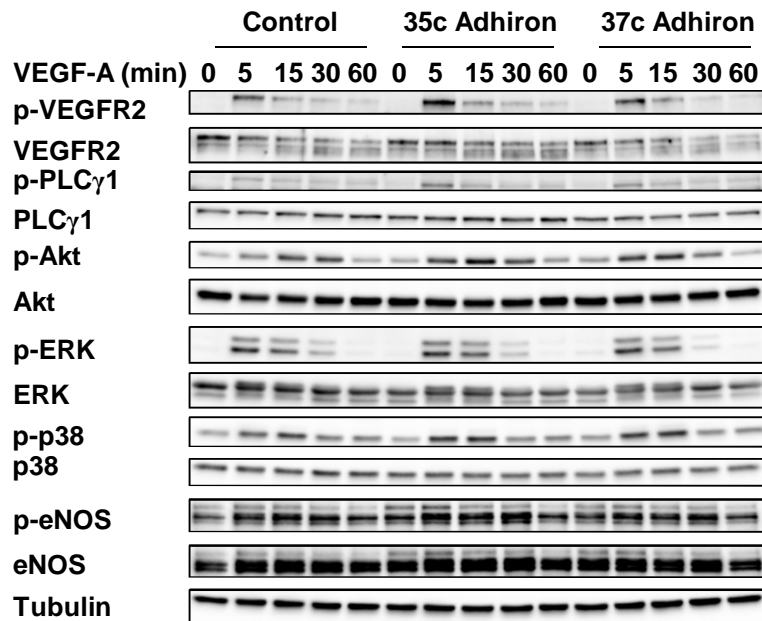
Figure 6.11. VEGFR1-specific Adhiron 35c promotes VEGF-A-stimulated VEGFR2 phosphorylation and downstream signal transduction. Endothelial cells were pre-treated with 100 μg/ml control, 35c or 37c VEGFR1 Adhirons (30 min) prior to stimulation with 25 ng/ml VEGF-A, lysed and immunoblotted for phospho-VEGFR2 (Y1175), phospho-PLCγ1, phospho-Akt (S473), phospho-ERK1/2 (T202/Y204), phospho-p38 MAPK (T180/Y182) and phospho-eNOS (S117).
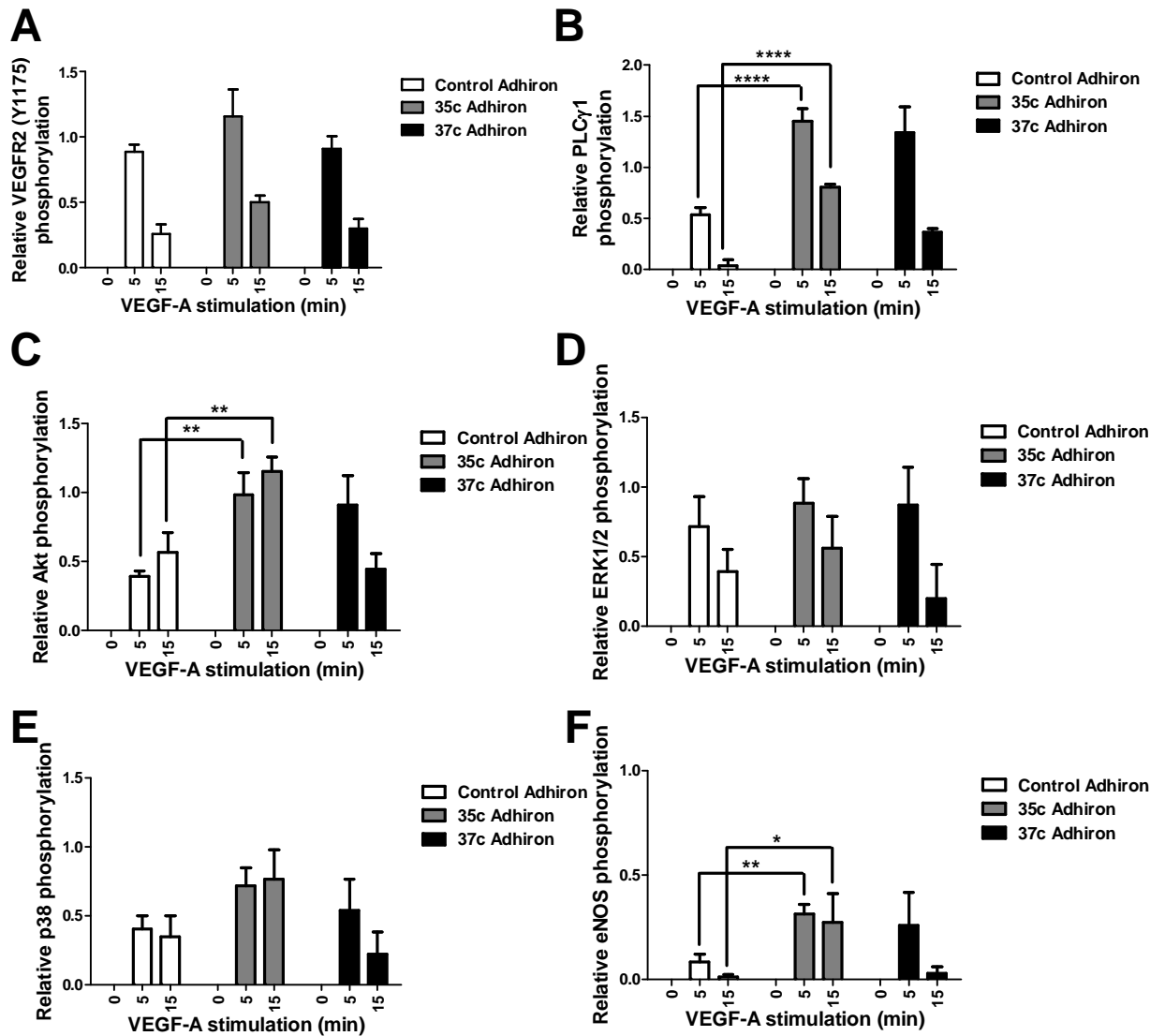
Figure 6.12. VEGFR1-specific Adhiron 35c promotes VEGF-A-stimulated VEGFR2 phosphorylation and downstream signal transduction. Phospho-VEGFR2 (A), phospho-PLCγ1 (B), phospho-Akt (C), phospho-ERK1/2 (D), phospho-p38 MAPK (E) and phospho-eNOS (F) levels in endothelial cells pre-treated with 100 μg/ml VEGFR1-specific 35c or 37c Adhirons (30 min) prior to 25 ng/ml VEGF-A stimulation and quantitative immunoblot analyses. Errors bars indicate +SEM (n≥3). $p < 0.05$ (*), $p < 0.01$ (**), $p < 0.0001$ (****).

160
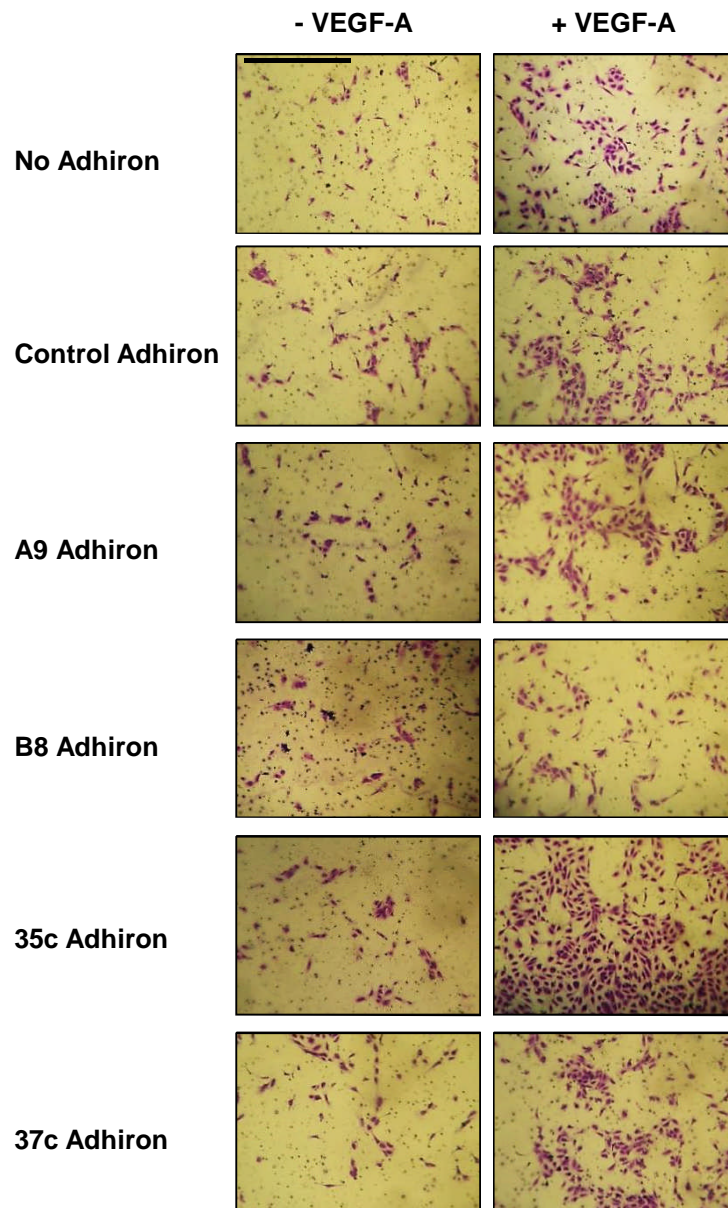
Figure 6.13. Adhirons specific for either VEGFR1 or VEGFR2 have opposing effects on endothelial cell migration. Primary human endothelial cells were seeded into transwell migration chambers and pre-treated with 100 µg/ml control, VEGFR1 (35c and 37c) or VEGFR2 (A9 and B8) Adhirons for 30 min prior to stimulation with 25 ng/ml VEGF-A. Cells that had migrated towards a chemotactic gradient of VEGF-A over 24 h were fixed and stained with crystal violet. Scale bar represents 1000 µm.
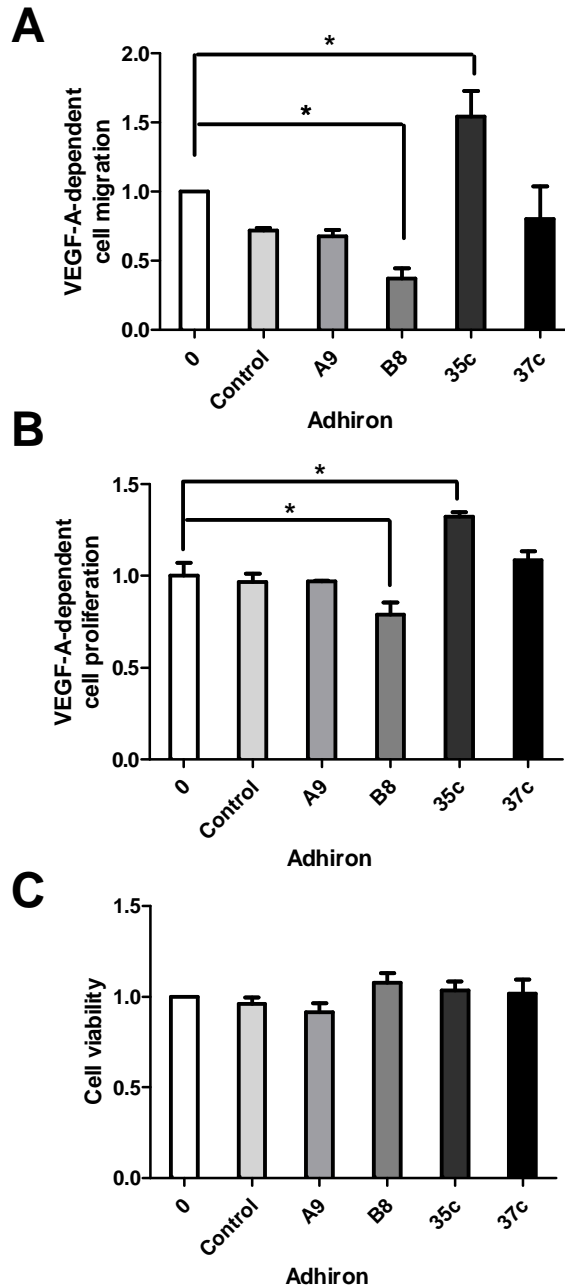
Figure 6.14. Adhirons to VEGFR1 or VEGFR2 have opposing effects on endothelial cell migration and proliferation. (A) Levels of VEGF-A-dependent endothelial cell migration upon treatment with 100 µg/ml control, VEGFR1 (35c and 37c) or VEGFR2 (A9 and B8) Adhirons. (B) Levels of VEGF-A-dependent endothelial cell proliferation upon treatment with 100 µg/ml control, VEGFR1 (35c and 37c) or VEGFR2 (A9 and B8) Adhirons for 30 min prior to 25 ng/ml VEGF-A stimulation were monitored by ELISA. (C) Endothelial cell viability upon pre-treatment with 100 µg/ml control, VEGFR1 (35c and 37c) or VEGFR2 (A9 and B8) Adhirons for 30 min prior to 25 ng/ml VEGF-A stimulation was monitored by an MTS assay. Error bars denote ±SEM (n≥3). $p<0.05$ (*).

6.3. Discussion

We have developed VEGFR-specific synthetic protein scaffolds called Adhirons which inhibit VEGFR1 or VEGFR2 activity to promote or restrict VEGF-A-stimulated signal transduction, respectively (Fig. 6.15). Incubating endothelial cells with VEGFR2-specific Adhirons prior to VEGF-A stimulation can significantly decrease receptor phosphorylation and inhibit downstream activation of signalling targets including PLCγ1, Akt, ERK1/2, p38 MAPK and eNOS in a dose-dependent manner (Fig. 6.15). Tubulogenesis is an *in vitro* assay that mimics angiogenic sprouting. The VEGFR2 Adhiron, B8, effectively blocked VEGF-A-induced endothelial tubule formation.

Incubating endothelial cells with the VEGFR1-specific Adhiron, 35c, prior to VEGF-A stimulation increased VEGFR2 phosphorylation and downstream activation of PLCγ1, Akt and eNOS (Fig. 6.15). In addition, 35c Adhiron promoted VEGF-A-stimulated tubulogenesis. Thus, VEGFR1-Adhiron binding could prevent sequestration of VEGF-A, facilitating increased VEGFR2-VEGF-A interaction and promoting enhanced VEGF-A-stimulated signal transduction and tubulogenesis (Fig. 6.15). Endothelial cells were treated with Adhiron and stimulated with VEGF-A every 2 days for a 7 day period. Endothelial cell growth media contains low levels of VEGF-A so a more pronounced effect on basal tubule growth was not unexpected if treatment with VEGFR1 Adhirons acted over a period of prolonged, continuous exposure to low levels of ligand. Furthermore, the opposing effects of VEGFR1 and VEGFR2 Adhirons on VEGF-A-dependent tubulogenesis highlighted their specificity for individual RTKs.

The molecular mechanism for VEGFR inhibition could involve preventing VEGF-A-VEGFR binding or obstruction of the correct three dimensional organisation of receptor monomers in ligand-bound dimers. Previous work has shown that artificial ankyrin repeat proteins (DARPins) screened to specifically interact with VEGFR2 extracellular Ig domains inhibit VEGFR2 signal transduction (Hyde et al., 2012). DARPins that interact with Ig domain, D23, block VEGF-A binding, receptor dimerisation and activation, whilst those that interact with D4 or D7 inhibit receptor activity without blocking dimerisation (Hyde et al., 2012). Differential inhibition of PLCγ1, Akt and ERK1/2 but not p38 MAPK or eNOS implies that VEGFR2-specific Adhiron, A9, does not prevent ligand binding but interferes with VEGF-A-induced receptor dimerisation.
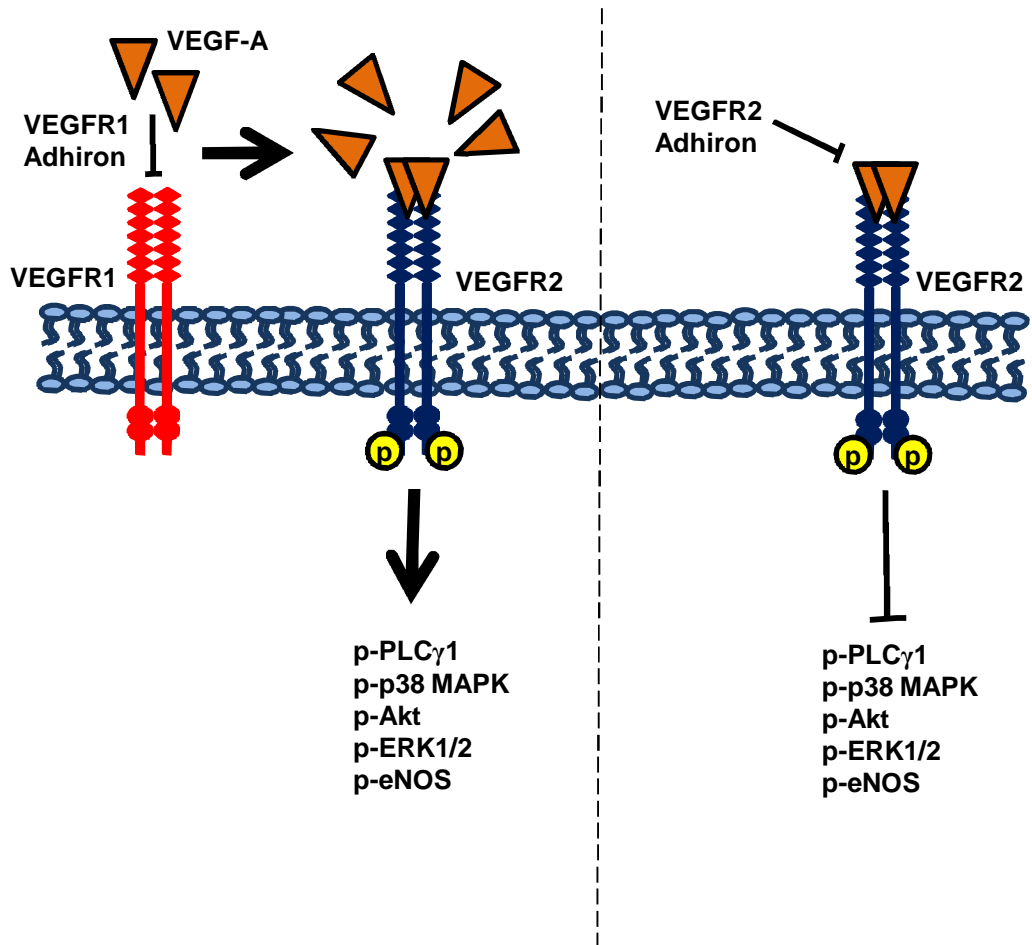
Figure 6.15. Adhirons specific for either VEGFR1 or VEGFR2 show opposing modulatory effects on VEGF-A-stimulated signal transduction. VEGFR2-specific Adhirons inhibit VEGF-A-stimulated activation and downstream signal transduction. In contrast, VEGFR1-specific Adhirons prevent VEGF-A binding to VEGFR1, increasing VEGF-A availability for VEGFR2 binding and stimulating downstream intracellular signalling events in endothelial cells.

In this study, we have identified novel inhibitory proteins of VEGFR1 or VEGFR2 which can be used to manipulate VEGF-A-stimulated signal transduction and endothelial cell tubulogenesis. Furthermore, we demonstrate that VEGFR1- and VEGFR2-specific Adhirons show high receptor specificity and modulate multiple cellular outputs associated with specific disease states. These reagents represent novel VEGFR regulators that could have *in vivo* applications including anti- or pro-angiogenic therapies or medical diagnostics.

CHAPTER 7
GENERAL DISCUSSION

The studies presented in this PhD thesis provide new insights into the mechanisms underlying VEGFR2 ubiquitination, trafficking and proteolysis in primary human endothelial cells. This chapter provides a broad overview of the role of ubiquitination in VEGFR2 trafficking, signal transduction, proteolysis and endothelial responses, and potential therapeutic implications for cancer and other vascular diseases.

7.1. VEGFR2 ubiquitination

VEGF-A-stimulated VEGFR2 tyrosine phosphorylation is linked to internalisation and endocytic trafficking towards lysosomal degradation (Koch and Claesson-Welsh, 2012). Work on other RTKs, such as EGFR, revealed that receptor ubiquitination at the plasma membrane is a prerequisite for recognition by ESCRT-0 trafficking machinery to initiate transport through the endosome-lysosome system and limit responsiveness to growth factor (McCullough et al., 2004, de Melker et al., 2001).

Although the E3 ubiquitin ligases, c-Cbl and β-TrCP, have been implicated in ligand-stimulated ubiquitination and degradation of EGFR and VEGFR2, the existence of multiple pathways to control activated RTK degradation complicate these studies (Duval et al., 2003, Murdaca et al., 2004, Shaik et al., 2012, Bruns et al., 2010, Singh et al., 2007). Depletion of the 8 E1s or the UBA1-associated E2s did not inhibit VEGF-A-stimulated VEGFR2 degradation suggesting that contrary to other reports, ubiquitination of activated VEGFR2 is not essential for its ligand-stimulated down-regulation. A reason for this discrepancy could be incomplete siRNA knockdown, especially since UBE2D2 depletion did result in a small inhibitory effect on VEGFR2 degradation following exposure to VEGF-A. Alternatively, a principle role for VEGFR2 ubiquitination could be to regulate ligand-independent turnover and/or endosome-lysosome trafficking. A drawback of this study is the absence of UBA1/UBE2D1/UBE2D2 overexpression studies, mutational analysis or RNAi rescue experiments to validate the results produced exclusively by siRNA depletion.

Although many studies have attempted to identify pathways for ligand-activated RTK degradation, work presented in this thesis describes for the first time an ubiquitin-dependent pathway for controlling ligand-independent VEGFR2 turnover. This pathway is important for regulating plasma membrane levels of VEGFR2 and the endothelial response to VEGF-A. Kinase-independent regulation of RTK function has previously been highlighted by studies on FGFR2 and EGFR. FGFR2 can undergo ligand-independent activation whilst EGFR undergoes ligand-independent ubiquitination and endocytosis (Katz et al., 2002, Lin et al., 2012). In addition, previous studies from our laboratory provided evidence for constitutive endocytosis and recycling of VEGFR2 (Jopling et al., 2011). Work presented in this thesis reveals that upon depletion of the DUB, USP8, disruption to endosomal trafficking causes ubiquitinated and proteolysed VEGFR2 to accumulate in early endosomes of resting cells. These findings confirm that VEGFR2 undergoes basal internalisation and recycling (Fig. 7.1).

Whilst the E1 and E2 components of the ubiquitin cascade for ligand-independent VEGFR2 turnover have been identified in this work, future experiments should include screening E3 ubiquitin ligases that interact with UBE2D1 and UBE2D2. Whilst UBA1 is the predominant E1 enzyme in humans and thus has wide ranging roles across multiple cell types, the downstream E3 ligase involved in basal VEGFR2 ubiquitination and turnover could present a more direct therapeutic target. There is also evidence that the E2 enzymes, UBE2D1 and UBE2D2, can attach ubiquitin to lysine residues on target substrates in the absence of a downstream E3 ligase (Wu et al., 2010).

Work in this thesis suggests that ubiquitination is important for regulating VEGFR2 recycling (Fig. 7.1). Ubiquitination down-regulates ligand-independent recycling and de-ubiquitination of either the endosomal sorting machinery or VEGFR2 itself is essential for endosome-to-plasma membrane recycling. Previous work reported that ligand-stimulated recycling prolongs the cellular response to ligand, whilst in non-stimulated cells recycling RTKs may be directed to specific membrane domains (Jones et al., 2006).

Work on EGFR and VEGFR2 has highlighted the co-ordinated role of ubiquitin and ESCRT-0 components, Hrs and STAM, in endosomal trafficking of internalised RTK (Ewan et al., 2006, Bruns et al., 2010, Row et al., 2006). Importantly, the DUB, USP8,

regulates the stability of both Hrs and STAM. This is supported by evidence in this thesis that USP8 is essential for VEGFR2 trafficking from early endosomes. In addition, correct endosomal trafficking of VEGFR2 is essential for VEGF-A-stimulated signal transduction through the Akt and ERK1/2 pathways. These findings support other work that suggested VEGFR2 signal transduction is location-dependent (Horowitz and Seerapu, 2012). Other studies have also linked activated VEGFR2 residence in endosomes to ERK1/2 (Lanahan et al., 2010, Bruns et al., 2010, Jopling et al., 2009, Horowitz and Seerapu, 2012, Koch et al., 2011) and Akt (Lanahan et al., 2010, Sawamiphak et al., 2010, Horowitz and Seerapu, 2012, Koch et al., 2011) activation. Furthermore, links between endocytosis and signal transduction have been identified for other RTKs and ERK1/2 does localise to endosomes (Sorkin and Von Zastrow, 2002). USP8 activity is essential for VEGFR2 trafficking by mediating de-ubiquitination of both the endosomal trafficking machinery (ESCRT-0) and VEGFR2. Work in this thesis focused on USP8 due to its role in EGFR trafficking however it would be interesting to determine whether any of the remaining 90 DUBs are also involved in VEGFR2 de-ubiquitination and endosome-lysosome transport.

Previous work linked VEGFR2 proteolysis to early endosomes (Bruns et al., 2010). Work in this thesis identifies a novel VEGFR2 cleavage fragment that is generated upon accumulation of ubiquitinated VEGFR2 in early endosomes of USP8-depleted endothelial cells. Thus, VEGFR2 proteolysis is a staggered process that takes place gradually during transport from the plasma membrane to lysosomes for terminal degradation (Fig. 7.1), possibly as a mechanism to restrict endosome-linked signal transduction. The 120 kDa VEGFR2 fragment is also produced in non-transfected cells at low levels suggesting a potential functional role. One possibility is that the VEGFR2 fragment recycles to the cell surface where it binds VEGF-A but is unable to signal due to the absence of a kinase domain. The role of this negative feedback cycle could be to sequester VEGF-A, limiting the temporal response to ligand and preventing excess pro-angiogenic signalling. Previous work has identified soluble VEGFR2 as a ~75 kDa N-terminal splice variant (Albuquerque et al., 2009). Perhaps the 120 kDa fragment is a precursor of soluble VEGFR2 which could also be produced by proteolytic cleavage in response to VEGF-A.
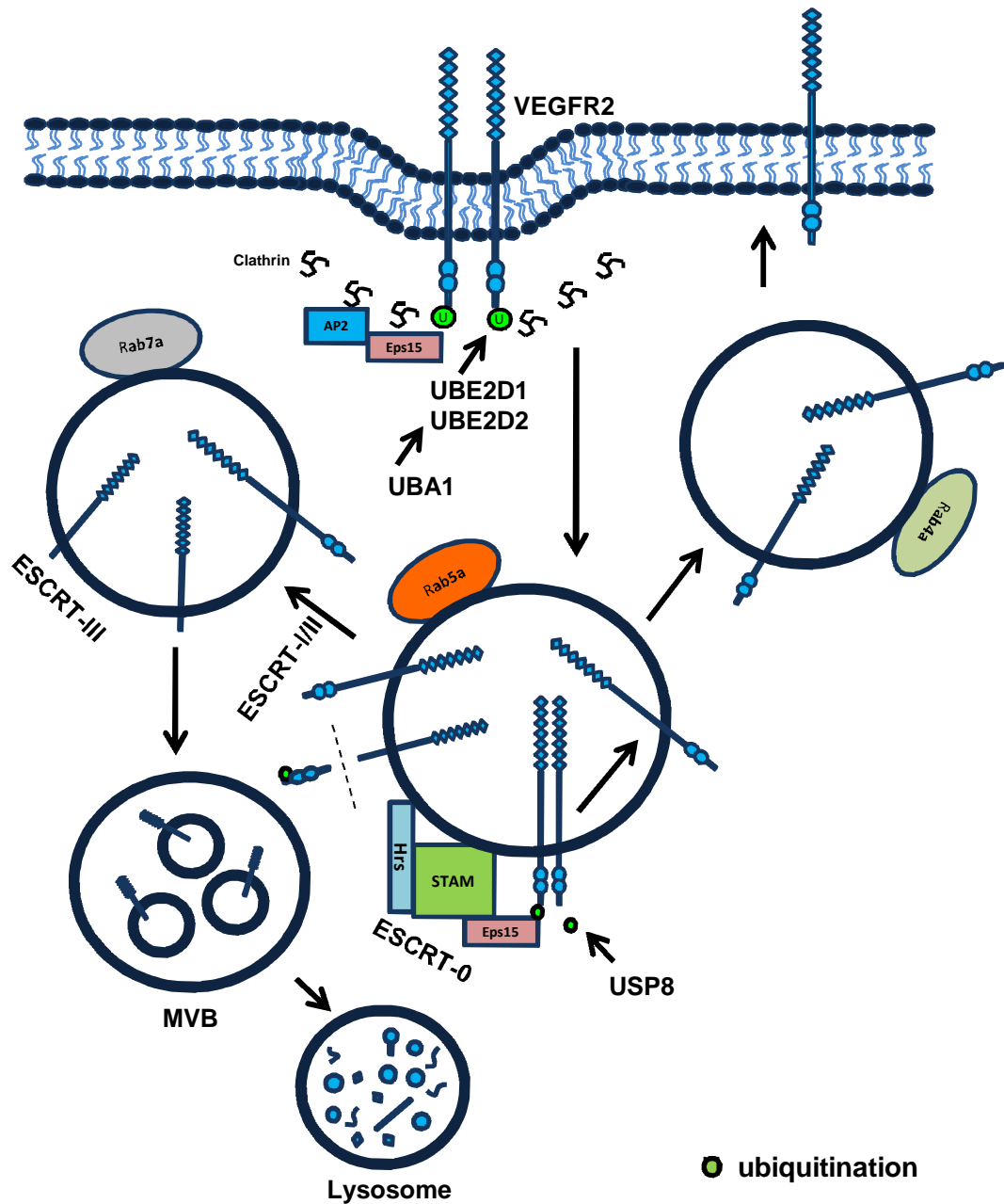
Figure 7.1. Ubiquitin-dependent VEGFR2 trafficking through the endosome-lysosome system. Ligand-independent ubiquitination of VEGFR2 promotes internalisation and downstream proteolysis and reduces recycling. The opposing effect of USP8-mediated de-ubiquitination promotes VEGFR2 recycling and reduces proteolytic cleavage.

7.2. Targeting ubiquitin homeostasis in disease

Collateral arteries provide an alternative blood supply to preserve myocardial tissue perfusion in the event of obstructive coronary artery disease (CAD). Recent studies have revealed genetic heterogeneity between CAD patients with sufficient or insufficient collateral vessels. CAD patients that exhibit a well-developed collateral network are less vulnerable to adverse cardiac events and demonstrate better preservation of myocardial function and slower lesion progression (Hakimzadeh et al., 2014). Insufficient collateral vessel growth is associated with rapid plaque progression, resulting in severe ischaemia, hypoxia, necrosis and scar tissue formation. Progress is been made to re-evaluate molecular and cellular targets in CAD. Patients with poor collateral vessel development are genetically predisposed to overexpression of signalling pathways that inhibit arteriogenesis. Thus a new focus in pro-angiogenic research includes blocking such inhibitory pathways to promote arteriogenesis (Hakimzadeh et al., 2014). Ubiquitin-dependent, ligand-independent degradation of VEGFR2 could be one such inhibitory pathway of the VEGF-A-stimulated pro-angiogenic response in diseases such as CAD. The ubiquitination enzymes involved in this pathway ultimately impact on the ligand-stimulated response and could be cellular targets for future therapeutics. Further work into ligand-independent VEGFR2 turnover could involve identification of suitable clinical endpoints to enable appropriate assessment of therapeutic outcomes. In addition, CAD patients could be screened for perturbed UBA1 gene expression to identify a canonical role for UBA1 and ubiquitin homeostasis in cardiovascular disease. Alternatively, the more substrate-specific E2 enzymes, UBE2D1 or UBE2D2, could be considered viable therapeutic targets. Interestingly, VEGF-A is a trophic factor for nerve cells, cardiac muscle fibres and lung epithelial cells, with insufficient VEGF-A levels linked to neurodegeneration, cardiac failure and respiratory diseases. Thus, VEGF-A and its cognate receptors are important therapeutic targets for a range of diseases.

UBA1 is an essential cellular enzyme expressed by many cells and tissues. Notably, suppression of UBA1 activity in Schwann cells disrupts ubiquitin homeostasis, causing aberrant accumulation of target proteins and neuromuscular degeneration in spinal muscular atrophy (Sugaya et al., 2015, Aghamaleky Sarvestany et al., 2014). In Huntington's disease, a gradual decrease in UBA1 expression leads to selective

accumulation of toxic forms of huntingtin protein in the brain (Groen and Gillingwater, 2015). UBA1-mediated surveillance could be utilised for controlling RTK levels and cellular responses in different tissues. Other studies used chemical inhibitors as novel anti-cancer agents to identify UBA1 as a target for the treatment of haematological malignancies (Yang et al., 2007, Xu et al., 2010). The therapeutic potential and biological effects of inhibiting ubiquitination/UBA1 are poorly understood. However, UBA1 inhibition causes an unfolded protein response that induces cell death in malignant cells over normal cells (Xu et al., 2013). Paradoxically, certain cancers (e.g. prostate cancer) show reduced UBA1 levels (http://www.proteinatlas.org/). From this standpoint, decreased UBA1 expression could be linked to increased angiogenesis in cancer.

7.3. Therapies using anti-angiogenic or pro-angiogenic agents

Work in this thesis identified VEGFR2-specific Adhirons as inhibitors of *in vitro* angiogenesis. Advancement in anti-angiogenic therapies is required since current TKIs prolong survival of responsive patients by months rather than providing long-term progression-free survival and are often only effective in combination with chemotherapy. Inhibition of a single RTK does not provide long term benefits due to a reduction in tumour dependency on VEGF-A (Sennino and McDonald, 2012). Combination therapy or design of multi-targeted TKIs is considered a more attractive proposition to overcome resistance mechanisms (Caglevic et al., 2015). It would be interesting to test whether VEGFR2-specific Adhirons have inhibitory effects on other RTK signalling pathways in endothelial cells, such as those of FGFR1.

Although currently used drugs such as Sutent and Avastin provide some benefit in terms of short-term progression-free survival in RCC, they are relatively uneffective in metastatic disease or more aggressive cancers. Thus, improving anti-angiogenic therapies requires overcoming significant challenges (Sennino and McDonald, 2012). Identification of predictive biomarkers to indicate responsive patients and discovery of resistance mechanisms which drive tumour progression in patients for which VEGFR2 inhibition has limited benefit would provide steps forward. In addition, the duration and frequency of combination therapies should be optimised on an individual basis with the assistance of known genetic predisposition. For example, a single nucleotide

polymorphism in the tyrosine kinase domain of *VEGFR1* in genomic DNA correlates with overall survival in bevacizumab-treated patients with metastatic pancreatic cancer (Sennino and McDonald, 2012).

In this thesis, novel non-antibody based artificial binding proteins screened to bind VEGFR1 or VEGFR2 were tested for effects on VEGF-A-stimulated signal transduction and the downstream endothelial response. It would be interesting to identify which extracellular VEGFR2 domain the Adhirons bind to and whether this prevents ligand binding or receptor dimerisation. Further research could test VEGFR2-specific Adhirons as novel anti-cancer agents to inhibit tumour angiogenesis in mouse models.

Other research aims to discover pro-angiogenic drugs to treat patients with cardiovascular disease. Atherosclerosis is the principle pathological disorder responsible for cardiovascular disease which accounts for 30% of deaths worldwide. Peripheral arterial disease (PAD) is a manifestation of atherosclerosis that is evident by blockages in the major arteries and limbs. In these patients, there is a clinical need to promote vascular regeneration after angioplasty, stenting or bypass surgery due to the progressive nature of atherosclerosis and limited longevity of the aforementioned techniques (Mughal et al., 2012). Frequently, patients re-present with worsening critical limb ischaemia which in the absence of a pharmacological solution often leads to amputation.

Current pro-angiogenic therapies focus on using gene therapy to express a range of pro-angiogenic factors including VEGF, FGF and hepatocyte growth factor (HGF) (Mughal et al., 2012). As the most extensively studied pro-angiogenic growth factor, VEGF-A has been subjected to multiple clinical trials aimed at promoting new blood vessel formation in PAD patients. VEGF-A gene therapy promotes angiogenesis in ischaemic tissues (Makinen et al., 2002, Isner, 1998). However, the latest clinical trials on therapeutic angiogenesis provide few satisfactory results. Although the efficacy of VEGF gene therapy appears promising in preclinical and Phase I trials, this has not transcribed into meaningful benefits in Phase II trials (Mughal et al., 2012). Thus, it is important to identify new agents for disease therapy.

VEGFR1-specific Adhirons inhibit VEGF-A binding to VEGFR1, promoting increased VEGFR2-VEGF-A interaction to increase VEGF-A-stimulated signal transduction and the endothelial response. Using Adhirons as pro-angiogenic agents could be beneficial to cardiovascular disease patients. Alternative growth factors, delivery methods and dose regimens need to be explored to enhance the clinical benefit of therapeutic angiogenesis (Ribatti and Baiguera, 2013). An alternative approach could be to use Adhirons to inhibit negative regulators of angiogenesis, such as VEGFR1. This could be used to increase pro-angiogenic ligand availability following VEGF-A gene therapy.

7.4. Conclusion

The work in this thesis has demonstrated the importance of ubiquitination in regulating VEGFR2 trafficking, signal transduction and proteolysis. A novel ubiquitin-dependent pathway regulates basal plasma membrane VEGFR2 levels to control the intensity of the VEGF-A-stimulated response. This pathway is mediated by the E1 ubiquitin-activating enzyme, UBA1, and the E2 ubiquitin-conjugating enzymes, UBE2D1 and UBE2D2. In addition, USP8-mediated de-ubiquitination is essential for normal VEGFR2 trafficking through the endosome-lysosome system and endosome-linked signal transduction, whilst preventing excess VEGFR2 proteolysis in early endosomes.

Novel non-antibody-based artificial binding proteins (Adhirons) can be used to promote or inhibit VEGF-A-stimulated signal transduction. Unlike studies based on transformed cell lines and overexpressed RTKs, the primary cell system used in these studies provides a better model for relating endogenous RTK function to human physiology. Thus, this cell system and the mechanisms uncovered for VEGFR2 ubiquitination, trafficking, signalling and proteolysis may be useful for development of improved pro- and anti-angiogenic therapeutics.

REFERENCES

ACHEN, M. G., JELTSCH, M., KUKK, E., MAKINEN, T., VITALI, A., WILKS, A. F., ALITALO, K. & STACKER, S. A. 1998. Vascular endothelial growth factor D (VEGF-D) is a ligand for the tyrosine kinases VEGF receptor 2 (Flk1) and VEGF receptor 3 (Flt4). *Proc Natl Acad Sci U S A,* 95**,** 548-53.

ADAM, A. P., SHARENKO, A. L., PUMIGLIA, K. & VINCENT, P. A. 2010. Src-induced tyrosine phosphorylation of VE-cadherin is not sufficient to decrease barrier function of endothelial monolayers. *J Biol Chem,* 285**,** 7045-7055.

ADHIKARI, A. & CHEN, Z. J. 2009. Diversity of Polyubiquitin Chains. *Dev Cell,* 16**,** 485-486.

AGHAMALEKY SARVESTANY, A., HUNTER, G., TAVENDALE, A., LAMONT, D. J., LLAVERO HURTADO, M., GRAHAM, L. C., WISHART, T. M. & GILLINGWATER, T. H. 2014. Label-free quantitative proteomic profiling identifies disruption of ubiquitin homeostasis as a key driver of schwann cell defects in spinal muscular atrophy. *J Proteome Res,* 13**,** 4546-57.

AGUAYO, A., GILES, F. & ALBITAR, M. 2003. Vascularity, angiogenesis and angiogenic factors in leukemias and myelodysplastic syndromes. *Leuk Lymphoma,* 44**,** 213-22.

AIRD, W. C. 2011. Discovery of the cardiovascular system: from Galen to William Harvey. *J Thromb Haemost,* 9 Suppl 1**,** 118-29.

ALBUQUERQUE, R. J., HAYASHI, T., CHO, W. G., KLEINMAN, M. E., DRIDI, S., TAKEDA, A., BAFFI, J. Z., YAMADA, K., KANEKO, H., GREEN, M. G., CHAPPELL, J., WILTING, J., WEICH, H. A., YAMAGAMI, S., AMANO, S., MIZUKI, N., ALEXANDER, J. S., PETERSON, M. L., BREKKEN, R. A., HIRASHIMA, M., CAPOOR, S., USUI, T., AMBATI, B. K. & AMBATI, J. 2009. Alternatively spliced vascular endothelial growth factor receptor-2 is an essential endogenous inhibitor of lymphatic vessel growth. *Nat Med,* 15**,** 1023-30.

ANCELIN, M., BUTEAU-LOZANO, H., MEDURI, G., OSBORNE-PELLEGRIN, M., SORDELLO, S., PLOUET, J. & PERROT-APPLANAT, M. 2002. A dynamic shift of VEGF isoforms with a transient and selective progesterone-induced expression of VEGF189 regulates angiogenesis and vascular permeability in human uterus. *Proc Natl Acad Sci U S A,* 99**,** 6023-8.

ARANY, Z., FOO, S. Y., MA, Y., RUAS, J. L., BOMMI-REDDY, A., GIRNUN, G., COOPER, M., LAZNIK, D., CHINSOMBOON, J., RANGWALA, S. M., BAEK, K. H., ROSENZWEIG, A. & SPIEGELMAN, B. M. 2008. HIF-independent regulation of VEGF and angiogenesis by the transcriptional coactivator PGC-1alpha. *Nature,* 451**,** 1008-12.

AUTIERO, M., WALTENBERGER, J., COMMUNI, D., KRANZ, A., MOONS, L., LAMBRECHTS, D., KROLL, J., PLAISANCE, S., DE MOL, M., BONO, F., KLICHE, S., FELLBRICH, G., BALLMER-HOFER, K., MAGLIONE, D., MAYR-BEYRLE, U., DEWERCHIN, M., DOMBROWSKI, S., STANIMIROVIC, D., VAN HUMMELEN, P., DEHIO, C., HICKLIN, D. J., PERSICO, G., HERBERT, J. M., COMMUNI, D., SHIBUYA, M., COLLEN, D., CONWAY, E. M. & CARMELIET, P. 2003. Role of PlGF in the intra- and intermolecular cross talk between the VEGF receptors Flt1 and Flk1. *Nat Med,* 9**,** 936-43.

AVRAHAM-DAVIDI, I., ELY, Y., PHAM, V. N., CASTRANOVA, D., GRUNSPAN, M., MALKINSON, G., GIBBS-BAR, L., MAYSELESS, O., ALLMOG, G., LO, B., WARREN, C. M., CHEN, T. T., UNGOS, J., KIDD, K., SHAW, K., ROGACHEV, I., WAN, W., MURPHY, P. M., FARBER, S. A., CARMEL, L., SHELNESS, G. S., IRUELA-ARISPE, M. L., WEINSTEIN, B. M. & YANIV, K. 2012. ApoB-containing lipoproteins regulate angiogenesis by modulating expression of VEGF receptor 1. *Nat Med,* 18**,** 967-73.

BAILLY, M., WYCKOFF, J., BOUZAHZAH, B., HAMMERMAN, R., SYLVESTRE, V., CAMMER, M., PESTELL, R. & SEGALL, J. E. 2000. Epidermal growth factor receptor distribution during chemotactic responses. *Mol Biol Cell,* 11**,** 3873-3883.

BALDWIN, M. E., ROUFAIL, S., HALFORD, M. M., ALITALO, K., STACKER, S. A. & ACHEN, M. G. 2001. Multiple forms of mouse vascular endothelial growth factor-D are generated by RNA splicing and proteolysis. *J Biol Chem,* 276**,** 44307-14.

BALLMER-HOFER, K., ANDERSSON, A. E., RATCLIFFE, L. E. & BERGER, P. 2011. Neuropilin-1 promotes VEGFR-2 trafficking through Rab11 vesicles thereby specifying signal output. *Blood,* 118**,** 816-826.

BASIC, V. T., JACOBSEN, A., SIRSJO, A. & ABDEL-HALIM, S. M. 2014. TNF stimulation induces VHL overexpression and impairs angiogenic potential in skeletal muscle myocytes. *Int J Mol Med,* 34**,** 228-36.

BENEDITO, R., ROCA, C., SORENSEN, I., ADAMS, S., GOSSLER, A., FRUTTIGER, M. & ADAMS, R. H. 2009. The notch ligands Dll4 and Jagged1 have opposing effects on angiogenesis. *Cell,* 137**,** 1124-35.

BHATTACHARYA, R., KANG-DECKER, N., HUGHES, D. A., MUKHERJEE, P., SHAH, V., MCNIVEN, M. A. & MUKHOPADHYAY, D. 2005. Regulatory role of dynamin-2 in VEGFR-2/KDR-mediated endothelial signaling. *FASEB J,* 19**,** 1692-4.

BIKFALVI, A. & BICKNELL, R. 2002. Recent advances in angiogenesis, anti-angiogenesis and vascular targeting. *Trends Pharmacol Sci,* 23**,** 576-82.

BILODEAU, P. S., URBANOWSKI, J. L., WINISTORFER, S. C. & PIPER, R. C. 2002. The Vps27p-Hse1p complex binds ubiquitin and mediates endosomal protein sorting. *Nat Cell Biol,* 4**,** 534-539.

BRUNS, A. F., BAO, L., WALKER, J. H. & PONNAMBALAM, S. 2009. VEGF-A-stimulated signalling in endothelial cells via a dual receptor tyrosine kinase system is dependent on co-ordinated trafficking and proteolysis. *Biochem Soc Trans,* 37**,** 1193-1197.

BRUNS, A. F., HERBERT, S. P., ODELL, A. F., JOPLING, H. M., HOOPER, N. M., ZACHARY, I. C., WALKER, J. H. & PONNAMBALAM, S. 2010. Ligand-stimulated VEGFR2 signaling is regulated by co-crdinated trafficking and proteolysis. *Traffic,* 11**,** 161-174.

BRUNS, A. F., YULDASHEVA, N., LATHAM, A. M., BAO, L., PELLET-MANY, C., FRANKEL, P., STEPHEN, S. L., HOWELL, G. J., WHEATCROFT, S. B., KEARNEY, M. T., ZACHARY, I. C. & PONNAMBALAM, S. 2012. A heat-shock protein axis regulates VEGFR2 proteolysis, blood vessel development and repair. *PLoS One,* 7**,** e48539.

CAGLEVIC, C., GRASSI, M., RAEZ, L., LISTI, A., GIALLOMBARDO, M., BUSTAMANTE, E., GIL-BAZO, I. & ROLFO, C. 2015. Nintedanib in non-small cell lung cancer: from preclinical to approval. *Ther Adv Respir Dis*.

CAI, H. B. & REED, R. R. 1999. Cloning and characterization of neuropilin-1-interacting protein: A PSD-95/Dlg/ZO-1 domain-containing protein that interacts with the cytoplasmic domain of neuropilin-1. *J Neurosci,* 19**,** 6519-6527.

CAI, J., AHMAD, S., JIANG, W. G., HUANG, J., KONTOS, C. D., BOULTON, M. & AHMED, A. 2003. Activation of vascular endothelial growth factor receptor-1 sustains angiogenesis and Bcl-2 expression via the phosphatidylinositol 3-kinase pathway in endothelial cells. *Diabetes,* 52**,** 2959-68.

CAI, J., CHEN, Z., RUAN, Q., HAN, S., LIU, L., QI, X., BOYE, S. L., HAUSWIRTH, W. W., GRANT, M. B. & BOULTON, M. E. 2011. gamma-Secretase and presenilin mediate cleavage and phosphorylation of vascular endothelial growth factor receptor-1. *J Biol Chem,* 286**,** 42514-23.

CAIRNS, R. A., HARRIS, I. S. & MAK, T. W. 2011. Regulation of cancer cell metabolism. *Nat Rev Cancer,* 11**,** 85-95.

CARMELIET, P. 2005. Angiogenesis in life, disease and medicine. *Nature,* 438**,** 932-936.

CARMELIET, P., DE SMET, F., LOGES, S. & MAZZONE, M. 2009. Branching morphogenesis and antiangiogenesis candidates: tip cells lead the way. *Nat Rev Clin Oncol,* 6**,** 315-26.

CARMELIET, P., FERREIRA, V., BREIER, G., POLLEFEYT, S., KIECKENS, L., GERTSENSTEIN, M., FAHRIG, M., VANDENHOECK, A., HARPAL, K.,

EBERHARDT, C., DECLERCQ, C., PAWLING, J., MOONS, L., COLLEN, D., RISAU, W. & NAGY, A. 1996. Abnormal blood vessel development and lethality in embryos lacking a single VEGF allele. *Nature,* 380**,** 435-9.

CARMELIET, P. & JAIN, R. K. 2011. Molecular mechanisms and clinical applications of angiogenesis. *Nature,* 473**,** 298-307.

CARMELIET, P., MOONS, L., LUTTUN, A., VINCENTI, V., COMPERNOLLE, V., DE MOL, M., WU, Y., BONO, F., DEVY, L., BECK, H., SCHOLZ, D., ACKER, T., DIPALMA, T., DEWERCHIN, M., NOEL, A., STALMANS, I., BARRA, A., BLACHER, S., VANDENDRIESSCHE, T., PONTEN, A., ERIKSSON, U., PLATE, K. H., FOIDART, J. M., SCHAPER, W., CHARNOCK-JONES, D. S., HICKLIN, D. J., HERBERT, J. M., COLLEN, D. & PERSICO, M. G. 2001. Synergism between vascular endothelial growth factor and placental growth factor contributes to angiogenesis and plasma extravasation in pathological conditions. *Nat Med,* 7**,** 575-83.

CARMELIET, P., WONG, B. W. & DE BOCK, K. 2012. Treating diabetes by blocking a vascular growth factor. *Cell Metab,* 16**,** 553-5.

CARTER, S., URBE, S. & CLAGUE, M. J. 2004. The met receptor degradation pathway: requirement for Lys48-linked polyubiquitin independent of proteasome activity. *J Biol Chem,* 279**,** 52835-9.

CHEN, T. T., LUQUE, A., LEE, S., ANDERSON, S. M., SEGURA, T. & IRUELA-ARISPE, M. L. 2010. Anchorage of VEGF to the extracellular matrix conveys differential signaling responses to endothelial cells. *J Cell Biol,* 188**,** 595-609.

CHIARELLI, F., GASPARI, S. & MARCOVECCHIO, M. L. 2009. Role of growth factors in diabetic kidney disease. *Horm Metab Res,* 41**,** 585-93.

CHITTENDEN, T. W., CLAES, F., LANAHAN, A. A., AUTIERO, M., PALAC, R. T., TKACHENKO, E. V., ELFENBEIN, A., DE ALMODOVAR, C. R., DEDKOV, E., TOMANEK, R., LI, W., WESTMORE, M., SINGH, J., HOROWITZ, A., MULLIGAN-KEHOE, M. J., MOODIE, K. L., ZHUANG, Z. W., CARMELIET, P. & SIMONS, M. 2006. Selective regulation of arterial branching morphogenesis by synectin. *Dev Cell,* 10**,** 783-795.

CIECHANOVER, A. 2006. Intracellular protein degradation: From a vague idea thru the lysosome and the ubiquitin-proteasome system and onto human diseases and drug targeting. *Exp Biol Med,* 231**,** 1197-1211.

CIECHANOVER, A., FINLEY, D. & VARSHAVSKY, A. 1984. Ubiquitin dependence of selective protein degradation demonstrated in the mammalian cell cycle mutant ts85. *Cell,* 37**,** 57-66.

CIECHANOVER, A., ORIAN, A. & SCHWARTZ, A. L. 2000. The ubiquitin-mediated proteolytic pathway: mode of action and clinical implications. *J Cell Biochem Suppl,* 34**,** 40-51.

CIOMBOR, K. K., BERLIN, J. & CHAN, E. 2013. Aflibercept. *Clin Cancer Res,* 19**,** 1920-5.

CLAGUE, M. J., COULSON, J. M. & URBE, S. 2012. Cellular functions of the DUBs. *J Cell Sci,* 125**,** 277-286.

CLAGUE, M. J., HERIDE, C. & URBE, S. 2015. The demographics of the ubiquitin system. *Trends Cell Biol,* 25**,** 417-26.

CLAGUE, M. J. & URBE, S. 2001. The interface of receptor trafficking and signalling. *J Cell Sci,* 114**,** 3075-3081.

CLAGUE, M. J. & URBE, S. 2006. Endocytosis: the DUB version. *Trends Cell Biol,* 16**,** 551-559.

CLAGUE, M. J. & URBE, S. 2010. Ubiquitin: same molecule, different degradation pathways. *Cell,* 143**,** 682-685.

COULTAS, L., CHAWENGSAKSOPHAK, K. & ROSSANT, J. 2005. Endothelial cells and VEGF in vascular development. *Nature,* 438**,** 937-945.

CUNNINGHAM, S. A., ARRATE, M. P., BROCK, T. A. & WAXHAM, M. N. 1997. Interactions of FLT-1 and KDR with phospholipase C gamma: identification of the phosphotyrosine binding sites. *Biochem Biophys Res Commun,* 240**,** 635-9.

DAAKA, Y., LUTTRELL, L. M., AHN, S., DELLA ROCCA, G. J., FERGUSON, S. S., CARON, M. G. & LEFKOWITZ, R. J. 1998. Essential role for G protein-coupled receptor endocytosis in the activation of mitogen-activated protein kinase. *J Biol Chem,* 273**,** 685-8.

DAGHER, Z., RUDERMAN, N., TORNHEIM, K. & IDO, Y. 2001. Acute regulation of fatty acid oxidation and amp-activated protein kinase in human umbilical vein endothelial cells. *Circ Res,* 88**,** 1276-82.

DATTA, S. R., BRUNET, A. & GREENBERG, M. E. 1999. Cellular survival: a play in three Akts. *Genes Dev,* 13**,** 2905-27.

DE BOCK, K., GEORGIADOU, M. & CARMELIET, P. 2013a. Role of endothelial cell metabolism in vessel sprouting. *Cell Metab,* 18**,** 634-47.

DE BOCK, K., GEORGIADOU, M., SCHOORS, S., KUCHNIO, A., WONG, B. W., CANTELMO, A. R., QUAEGEBEUR, A., GHESQUIERE, B., CAUWENBERGHS, S., EELEN, G., PHNG, L. K., BETZ, I., TEMBUYSER, B., BREPOELS, K., WELTI, J., GEUDENS, I., SEGURA, I., CRUYS, B., BIFARI, F., DECIMO, I., BLANCO, R., WYNS, S., VANGINDERTAEL, J., ROCHA, S., COLLINS, R. T., MUNCK, S., DAELEMANS, D., IMAMURA, H., DEVLIEGER, R., RIDER, M., VAN VELDHOVEN, P. P., SCHUIT, F., BARTRONS, R., HOFKENS, J., FRAISL, P.,

TELANG, S., DEBERARDINIS, R. J., SCHOONJANS, L., VINCKIER, S., CHESNEY, J., GERHARDT, H., DEWERCHIN, M. & CARMELIET, P. 2013b. Role of PFKFB3-driven glycolysis in vessel sprouting. *Cell,* 154**,** 651-63.

DE MELKER, A. A., VAN DER HORST, G., CALAFAT, J., JANSEN, H. & BORST, J. 2001. c-Cbl ubiquitinates the EGF receptor at the plasma membrane and remains receptor associated throughout the endocytic route. *J Cell Sci,* 114**,** 2167-2178.

DE RENZIS, S., SONNICHSEN, B. & ZERIAL, M. 2002. Divalent Rab effectors regulate the sub-compartmental organization and sorting of early endosomes. *Nat Cell Biol,* 4**,** 124-33.

DE SAEDELEER, C. J., COPETTI, T., PORPORATO, P. E., VERRAX, J., FERON, O. & SONVEAUX, P. 2012. Lactate activates HIF-1 in oxidative but not in Warburg-phenotype human tumor cells. *PLoS One,* 7**,** e46571.

DEJANA, E., ORSENIGO, F. & LAMPUGNANI, M. G. 2008. The role of adherens junctions and VE-cadherin in the control of vascular permeability. *J Cell Sci,* 121**,** 2115-22.

DEVRIES, C., ESCOBEDO, J. A., UENO, H., HOUCK, K., FERRARA, N. & WILLIAMS, L. T. 1992. THE FMS-LIKE TYROSINE KINASE, A RECEPTOR FOR VASCULAR ENDOTHELIAL GROWTH-FACTOR. *Science,* 255**,** 989-991.

DI GUGLIELMO, G. M., BAASS, P. C., OU, W. J., POSNER, B. I. & BERGERON, J. J. 1994. Compartmentalization of SHC, GRB2 and mSOS, and hyperphosphorylation of Raf-1 by EGF but not insulin in liver parenchyma. *EMBO J,* 13**,** 4269-77.

DIKIC, I. & GIORDANO, S. 2003. Negative receptor signalling. *Curr Opin Cell Biol,* 15**,** 128-135.

DISALVO, J., BAYNE, M. L., CONN, G., KWOK, P. W., TRIVEDI, P. G., SODERMAN, D. D., PALISI, T. M., SULLIVAN, K. A. & THOMAS, K. A. 1995. Purification and characterization of a naturally occurring vascular endothelial growth factor.placenta growth factor heterodimer. *J Biol Chem,* 270**,** 7717-23.

DIXELIUS, J., MAKINEN, T., WIRZENIUS, M., KARKKAINEN, M. J., WERNSTEDT, C., ALITALO, K. & CLAESSON-WELSH, L. 2003. Ligand-induced vascular endothelial growth factor receptor-3 (VEGFR-3) heterodimerization with VEGFR-2 in primary lymphatic endothelial cells regulates tyrosine phosphorylation sites. *J Biol Chem,* 278**,** 40973-9.

DOHMEN, R. J., STAPPEN, R., MCGRATH, J. P., FORROVA, H., KOLAROV, J., GOFFEAU, A. & VARSHAVSKY, A. 1995. An essential yeast gene encoding a homolog of ubiquitin-activating enzyme. *J Biol Chem,* 270**,** 18099-109.

DOUGHER, M. & TERMAN, B. I. 1999. Autophosphorylation of KDR in the kinase domain is required for maximal VEGF-stimulated kinase activity and receptor internalization. *Oncogene,* 18**,** 1619-27.

DUDA, D. M., WALDEN, H., SFONDOURIS, J. & SCHULMAN, B. A. 2005. Structural analysis of Escherichia coli ThiF. *J Mol Biol,* 349**,** 774-86.

DUMONT, D. J., JUSSILA, L., TAIPALE, J., LYMBOUSSAKI, A., MUSTONEN, T., PAJUSOLA, K., BREITMAN, M. & ALITALO, K. 1998. Cardiovascular failure in mouse embryos deficient in VEGF receptor-3. *Science,* 282**,** 946-9.

DUVAL, M., BEDARD-GOULET, S., DELISLE, C. & GRATTON, J. P. 2003. Vascular endothelial growth factor-dependent down-regulation of Flk-1/KDR involves Cbl-mediated ubiquitination - Consequences on nitric oxide production from endothelial cells. *J Biol Chem,* 278**,** 20091-20097.

EELEN, G., CRUYS, B., WELTI, J., DE BOCK, K. & CARMELIET, P. 2013. Control of vessel sprouting by genetic and metabolic determinants. *Trends Endocrinol Metab,* 24**,** 589-96.

EICHMANN, A., CORBEL, C., NATAF, V., VAIGOT, P., BREANT, C. & LE DOUARIN, N. M. 1997. Ligand-dependent development of the endothelial and hemopoietic lineages from embryonic mesodermal cells expressing vascular endothelial growth factor receptor 2. *Proc Natl Acad Sci U S A,* 94**,** 5141-6.

EICHMANN, A. & SIMONS, M. 2012. VEGF signaling inside vascular endothelial cells and beyond. *Curr Opin Cell Biol,* 24**,** 188-93.

ELMASRI, H., KARAASLAN, C., TEPER, Y., GHELFI, E., WENG, M., INCE, T. A., KOZAKEWICH, H., BISCHOFF, J. & CATALTEPE, S. 2009. Fatty acid binding protein 4 is a target of VEGF and a regulator of cell proliferation in endothelial cells. *FASEB J,* 23**,** 3865-73.

ERRICO, M., RICCIONI, T., IYER, S., PISANO, C., ACHARYA, K. R., PERSICO, M. G. & DE FALCO, S. 2004. Identification of placenta growth factor determinants for binding and activation of Flt-1 receptor. *J Biol Chem,* 279**,** 43929-39.

ESWARAPPA, S. M., POTDAR, A. A., KOCH, W. J., FAN, Y., VASU, K., LINDNER, D., WILLARD, B., GRAHAM, L. M., DICORLETO, P. E. & FOX, P. L. 2014. Programmed translational readthrough generates antiangiogenic VEGF-Ax. *Cell,* 157**,** 1605-18.

EWAN, L. C., JOPLING, H. M., JIA, H., MITTAR, S., BAGHERZADEH, A., HOWELL, G. J., WALKER, J. H., ZACHARY, I. C. & PONNAMBALAM, S. 2006. Intrinsic tyrosine kinase activity is required for vascular endothelial growth factor receptor 2 ubiquitination, sorting and degradation in endothelial cells. *Traffic,* 7**,** 1270-1282.

FANG, L., CHOI, S. H., BAEK, J. S., LIU, C., ALMAZAN, F., ULRICH, F., WIESNER, P., TALEB, A., DEER, E., PATTISON, J., TORRES-VAZQUEZ, J., LI, A. C. & MILLER, Y. I. 2013. Control of angiogenesis by AIBP-mediated cholesterol efflux. *Nature,* 498**,** 118-22.

FEARNLEY, G. W., ODELL, A. F., LATHAM, A. M., MUGHAL, N. A., BRUNS, A. F., BURGOYNE, N. J., HOMER-VANNIASINKAM, S., ZACHARY, I. C., HOLLSTEIN, M. C., WHEATCROFT, S. B. & PONNAMBALAM, S. 2014. VEGF-A isoforms differentially regulate ATF-2-dependent VCAM-1 gene expression and endothelial-leukocyte interactions. *Mol Biol Cell.*

FEENER, E. P. & KING, G. L. 1997. Vascular dysfunction in diabetes mellitus. *Lancet,* 350 Suppl 1**,** SI9-13.

FENG, D., NAGY, J. A., BREKKEN, R. A., PETTERSSON, A., MANSEAU, E. J., PYNE, K., MULLIGAN, R., THORPE, P. E., DVORAK, H. F. & DVORAK, A. M. 2000. Ultrastructural localization of the vascular permeability factor/vascular endothelial growth factor (VPF/VEGF) receptor-2 (FLK-1, KDR) in normal mouse kidney and in the hyperpermeable vessels induced by VPF/VEGF-expressing tumors and adenoviral vectors. *J Histochem Cytochem,* 48**,** 545-555.

FERRARA, N. 1999. Role of vascular endothelial growth factor in the regulation of angiogenesis. *Kidney Int,* 56**,** 794-814.

FERRARA, N. 2010. Binding to the extracellular matrix and proteolytic processing: two key mechanisms regulating vascular endothelial growth factor action. *Mol Biol Cell,* 21**,** 687-90.

FERRARA, N., CARVER-MOORE, K., CHEN, H., DOWD, M., LU, L., O'SHEA, K. S., POWELL-BRAXTON, L., HILLAN, K. J. & MOORE, M. W. 1996. Heterozygous embryonic lethality induced by targeted inactivation of the VEGF gene. *Nature,* 380**,** 439-42.

FERRARA, N. & KERBEL, R. S. 2005. Angiogenesis as a therapeutic target. *Nature,* 438**,** 967-974.

FIJALKOWSKA, I., XU, W., COMHAIR, S. A., JANOCHA, A. J., MAVRAKIS, L. A., KRISHNAMACHARY, B., ZHEN, L., MAO, T., RICHTER, A., ERZURUM, S. C. & TUDER, R. M. 2010. Hypoxia inducible-factor1alpha regulates the metabolic shift of pulmonary hypertensive endothelial cells. *Am J Pathol,* 176**,** 1130-8.

FLYVBJERG, A., DAGNAES-HANSEN, F., DE VRIESE, A. S., SCHRIJVERS, B. F., TILTON, R. G. & RASCH, R. 2002. Amelioration of long-term renal changes in obese type 2 diabetic mice by a neutralizing vascular endothelial growth factor antibody. *Diabetes,* 51**,** 3090-4.

FOLKMAN, J. 1971. Tumor angiogenesis: therapeutic implications. *N Engl J Med,* 285**,** 1182-6.

FOLKMAN, J. 2007. Angiogenesis: an organizing principle for drug discovery? *Nat Rev Drug Discov,* 6**,** 273-86.

FONG, G. H., ROSSANT, J., GERTSENSTEIN, M. & BREITMAN, M. L. 1995. Role of the Flt-1 receptor tyrosine kinase in regulating the assembly of vascular endothelium. *Nature,* 376**,** 66-70.

FONTANELLA, C., ONGARO, E., BOLZONELLO, S., GUARDASCIONE, M., FASOLA, G. & APRILE, G. 2014. Clinical advances in the development of novel VEGFR2 inhibitors. *Ann Transl Med,* 2**,** 123.

FRAISL, P., MAZZONE, M., SCHMIDT, T. & CARMELIET, P. 2009. Regulation of angiogenesis by oxygen and metabolism. *Dev Cell,* 16**,** 167-79.

GALLAND, F., KARAMYSHEVA, A., PEBUSQUE, M. J., BORG, J. P., ROTTAPEL, R., DUBREUIL, P., ROSNET, O. & BIRNBAUM, D. 1993. The FLT4 gene encodes a transmembrane tyrosine kinase related to the vascular endothelial growth factor receptor. *Oncogene,* 8**,** 1233-40.

GAMPEL, A., MOSS, L., JONES, M. C., BRUNTON, V., NORMAN, J. C. & MELLOR, H. 2006. VEGF regulates the mobilization of VEGFR2/KDR from an intracellular endothelial storage compartment. *Blood,* 108**,** 2624-2631.

GAO, T., LIU, Z., WANG, Y., CHENG, H., YANG, Q., GUO, A., REN, J. & XUE, Y. 2013. UUCD: a family-based database of ubiquitin and ubiquitin-like conjugation. *Nucleic Acids Res,* 41**,** D445-51.

GEBAUER, M. & SKERRA, A. 2009. Engineered protein scaffolds as next-generation antibody therapeutics. *Curr Opin Chem Biol,* 13**,** 245-55.

GERHARDT, H., GOLDING, M., FRUTTIGER, M., RUHRBERG, C., LUNDKVIST, A., ABRAMSSON, A., JELTSCH, M., MITCHELL, C., ALITALO, K., SHIMA, D. & BETSHOLTZ, C. 2003. VEGF guides angiogenic sprouting utilizing endothelial tip cell filopodia. *J Cell Biol,* 161**,** 1163-1177.

GILLE, H., KOWALSKI, J., YU, L., CHEN, H., PISABARRO, M. T., DAVIS-SMYTH, T. & FERRARA, N. 2000. A repressor sequence in the juxtamembrane domain of Flt-1 (VEGFR-1) constitutively inhibits vascular endothelial growth factor-dependent phosphatidylinositol 3'-kinase activation and endothelial cell migration. *EMBO J,* 19**,** 4064-73.

GRABBE, C., HUSNJAK, K. & DIKIC, I. 2011. The spatial and temporal organization of ubiquitin networks. *Nat Rev Mol Cell Biol,* 12**,** 295-307.

GRIMMOND, S., LAGERCRANTZ, J., DRINKWATER, C., SILINS, G., TOWNSON, S., POLLOCK, P., GOTLEY, D., CARSON, E., RAKAR, S., NORDENSKJOLD, M., WARD, L., HAYWARD, N. & WEBER, G. 1996. Cloning and characterization of a novel human gene related to vascular endothelial growth factor. *Genome Res,* 6**,** 124-31.

GROEN, E. J. & GILLINGWATER, T. H. 2015. UBA1: At the Crossroads of Ubiquitin Homeostasis and Neurodegeneration. *Trends Mol Med,* 21**,** 622-32.

GROSSHANS, B. L., ORTIZ, D. & NOVICK, P. 2006. Rabs and their effectors: achieving specificity in membrane traffic. *Proc Natl Acad Sci U S A,* 103**,** 11821-7.

GRUNEWALD, F. S., PROTA, A. E., GIESE, A. & BALLMER-HOFER, K. 2010. Structure-function analysis of VEGF receptor activation and the role of coreceptors in angiogenic signaling. *Biochim Biophys Acta,* 1804**,** 567-80.

HAAS, A. L. & ROSE, I. A. 1982. The mechanism of ubiquitin activating enzyme. A kinetic and equilibrium analysis. *J Biol Chem,* 257**,** 10329-37.

HAAS, A. L., WARMS, J. V., HERSHKO, A. & ROSE, I. A. 1982. Ubiquitin-activating enzyme. Mechanism and role in protein-ubiquitin conjugation. *J Biol Chem,* 257**,** 2543-8.

HAGBERG, C. E., FALKEVALL, A., WANG, X., LARSSON, E., HUUSKO, J., NILSSON, I., VAN MEETEREN, L. A., SAMEN, E., LU, L., VANWILDEMEERSCH, M., KLAR, J., GENOVE, G., PIETRAS, K., STONE-ELANDER, S., CLAESSON-WELSH, L., YLA-HERTTUALA, S., LINDAHL, P. & ERIKSSON, U. 2010. Vascular endothelial growth factor B controls endothelial fatty acid uptake. *Nature,* 464**,** 917-21.

HAGLUND, K., DI FIORE, P. P. & DIKIC, I. 2003a. Distinct monoubiquitin signals in receptor endocytosis. *Trends Biochem Sci,* 28**,** 598-603.

HAGLUND, K. & DIKIC, I. 2012. The role of ubiquitylation in receptor endocytosis and endosomal sorting. *J Cell Sci,* 125**,** 265-75.

HAGLUND, K., SCHMIDT, M. H. H., WONG, E. S. M., GUY, G. R. & DIKIC, I. 2005. Sprouty2 acts at the Cbl/CIN85 interface to inhibit epidermal growth factor receptor downregulation. *EMBO Rep,* 6**,** 635-641.

HAGLUND, K., SIGISMUND, S., POLO, S., SZYMKIEWICZ, I., DI FIORE, P. P. & DIKIC, I. 2003b. Multiple monoubiquitination of RTKs is sufficient for their endocytosis and degradation. *Nat Cell Biol,* 5**,** 461-466.

HAKIMZADEH, N., VERBERNE, H. J., SIEBES, M. & PIEK, J. J. 2014. The future of collateral artery research. *Curr Cardiol Rev,* 10**,** 73-86.

HARPER, S. J. & BATES, D. O. 2008. VEGF-A splicing: the key to anti-angiogenic therapeutics? *Nat Rev Cancer,* 8**,** 880-887.

HARTSOUGH, E. J., MEYER, R. D., CHITALIA, V., JIANG, Y., MARQUEZ, V. E., ZHDANOVA, I. V., WEINBERG, J., COSTELLO, C. E. & RAHIMI, N. 2013. Lysine methylation promotes VEGFR-2 activation and angiogenesis. *Sci Signal,* 6**,** ra104.

HASINOFF, B. B. & PATEL, D. 2010. The lack of target specificity of small molecule anticancer kinase inhibitors is correlated with their ability to damage myocytes in vitro. *Toxicol Appl Pharmacol,* 249**,** 132-9.

HEILIG, C. W., DEB, D. K., ABDUL, A., RIAZ, H., JAMES, L. R., SALAMEH, J. & NAHMAN, N. S., JR. 2013. GLUT1 regulation of the pro-sclerotic mediators of diabetic nephropathy. *Am J Nephrol,* 38**,** 39-49.

HEILKER, R., SPIESS, M. & CROTTET, P. 1999. Recognition of sorting signals by clathrin adaptors. *Bioessays,* 21**,** 558-67.

HEITZER, T., SCHLINZIG, T., KROHN, K., MEINERTZ, T. & MUNZEL, T. 2001. Endothelial dysfunction, oxidative stress, and risk of cardiovascular events in patients with coronary artery disease. *Circulation,* 104**,** 2673-8.

HERBST, J. J., OPRESKO, L. K., WALSH, B. J., LAUFFENBURGER, D. A. & WILEY, H. S. 1994. Regulation of postendocytic trafficking of the epidermal growth factor receptor through endosomal retention. *J Biol Chem,* 269**,** 12865-73.

HERRMANN, J., LERMAN, L. O. & LERMAN, A. 2007. Ubiquitin and ubiquitin-like proteins in protein regulation. *Circ Res,* 100**,** 1276-1291.

HERSHKO, A. & CIECHANOVER, A. 1992. The ubiquitin system for protein degradation. *Annu Rev Biochem,* 61**,** 761-807.

HIRATSUKA, S., MARU, Y., OKADA, A., SEIKI, M., NODA, T. & SHIBUYA, M. 2001. Involvement of Flt-1 tyrosine kinase (vascular endothelial growth factor receptor-1) in pathological angiogenesis. *Cancer Res,* 61**,** 1207-13.

HOCHSTRASSER, M. 2002. Molecular biology. New proteases in a ubiquitin stew. *Science,* 298**,** 549-52.

HOCHSTRASSER, M. 2006. Lingering mysteries of ubiquitin-chain assembly. *Cell,* 124**,** 27-34.

HOELLER, D., CROSETTO, N., BLAGOEV, B., RAIBORG, C., TIKKANEN, R., WAGNER, S., KOWANETZ, K., BREITLING, R., MANN, M., STENMARK, H. & DIKIC, I. 2006. Regulation of ubiquitin-binding proteins by monoubiquitination. *Nat Cell Biol,* 8**,** 163-9.

HOFMANN, K. & BUCHER, P. 1996. The UBA domain: a sequence motif present in multiple enzyme classes of the ubiquitination pathway. *Trends Biochem Sci,* 21**,** 172-173.

HOLMES, D. I. & ZACHARY, I. 2005. The vascular endothelial growth factor (VEGF) family: angiogenic factors in health and disease. *Genome Biol,* 6**,** 209.

HOLMQVIST, K., CROSS, M., RILEY, D. & WELSH, M. 2003. The Shb adaptor protein causes Src-dependent cell spreading and activation of focal adhesion kinase in murine brain endothelial cells. *Cell Signal,* 15**,** 171-9.

HORNIG, B., ARAKAWA, N., KOHLER, C. & DREXLER, H. 1998. Vitamin C improves endothelial function of conduit arteries in patients with chronic heart failure. *Circulation,* 97**,** 363-8.

HOROWITZ, A. & SEERAPU, H. R. 2012. Regulation of VEGF signaling by membrane traffic. *Cell Signal,* 24**,** 1810-20.

HUANG, A., DE JONG, R. N., WIENK, H., WINKLER, G. S., TIMMERS, H. T. & BOELENS, R. 2009. E2-c-Cbl recognition is necessary but not sufficient for ubiquitination activity. *J Mol Biol,* 385**,** 507-19.

HUANG, F., GOH, L. K. & SORKIN, A. 2007. EGF receptor ubiquitination is not necessary for its internalization. *Proc Natl Acad Sci U S A,* 104**,** 16904-9.

HUANG, F., JIANG, X. & SORKIN, A. 2003. Tyrosine phosphorylation of the beta2 subunit of clathrin adaptor complex AP-2 reveals the role of a di-leucine motif in the epidermal growth factor receptor trafficking. *J Biol Chem,* 278**,** 43411-7.

HUANG, F. T. & SORKIN, A. 2005. Growth factor receptor binding protein 2-mediated recruitment of the RING domain of Cbl to the epidermal growth factor receptor is essential and sufficient to support receptor endocytosis. *Mol Biol Cell,* 16**,** 1268-1281.

HUANG, Y. & CARBONE, D. P. 2015. Mechanisms of and strategies for overcoming resistance to anti-vascular endothelial growth factor therapy in non-small cell lung cancer. *Biochim Biophys Acta,* 1855**,** 193-201.

HUGHES, D. C. 2001. Alternative splicing of the human VEGFGR-3/FLT4 gene as a consequence of an integrated human endogenous retrovirus. *J Mol Evol,* 53**,** 77-9.

HURLEY, J. H. & YANG, D. 2008. MIT domainia. *Dev Cell,* 14**,** 6-8.

HYDE, C. A., GIESE, A., STUTTFELD, E., ABRAM SALIBA, J., VILLEMAGNE, D., SCHLEIER, T., BINZ, H. K. & BALLMER-HOFER, K. 2012. Targeting extracellular domains D4 and D7 of vascular endothelial growth factor receptor 2 reveals allosteric receptor regulatory sites. *Mol Cell Biol,* 32**,** 3802-13.

IKEDA, F., CROSETTO, N. & DIKIC, I. 2010. What determines the specificity and outcomes of ubiquitin signaling? *Cell,* 143**,** 677-681.

IRRTHUM, A., KARKKAINEN, M. J., DEVRIENDT, K., ALITALO, K. & VIKKULA, M. 2000. Congenital hereditary lymphedema caused by a mutation that inactivates VEGFR3 tyrosine kinase. *Am J Hum Genet,* 67**,** 295-301.

ISNER, J. M. 1998. Arterial gene transfer of naked DNA for therapeutic angiogenesis: early clinical results. *Adv Drug Deliv Rev,* 30**,** 185-197.

ISNER, J. M., PIECZEK, A., SCHAINFELD, R., BLAIR, R., HALEY, L., ASAHARA, T., ROSENFIELD, K., RAZVI, S., WALSH, K. & SYMES, J. F. 1996. Clinical evidence of angiogenesis after arterial gene transfer of phVEGF165 in patient with ischaemic limb. *Lancet,* 348**,** 370-4.

ITO, N., WERNSTEDT, C., ENGSTROM, U. & CLAESSON-WELSH, L. 1998. Identification of vascular endothelial growth factor receptor-1 tyrosine phosphorylation sites and binding of SH2 domain-containing molecules. *J Biol Chem,* 273**,** 23410-8.

JAIN, R. K., DUDA, D. G., CLARK, J. W. & LOEFFLER, J. S. 2006. Lessons from phase III clinical trials on anti-VEGF therapy for cancer. *Nat Clin Pract Oncol,* 3**,** 24-40.

JAKOBSSON, L., FRANCO, C. A., BENTLEY, K., COLLINS, R. T., PONSIOEN, B., ASPALTER, I. M., ROSEWELL, I., BUSSE, M., THURSTON, G., MEDVINSKY, A., SCHULTE-MERKER, S. & GERHARDT, H. 2010. Endothelial cells dynamically compete for the tip cell position during angiogenic sprouting. *Nat Cell Biol,* 12**,** 943-53.

JANG, C. & ARANY, Z. 2013. Metabolism: Sweet enticements to move. *Nature,* 500**,** 409-11.

JIA, H., JEZEQUEL, S., LOHR, M., SHAIKH, S., DAVIS, D., SOKER, S., SELWOOD, D. & ZACHARY, I. 2001. Peptides encoded by exon 6 of VEGF inhibit endothelial cell biological responses and angiogenesis induced by VEGF. *Biochem Biophys Res Commun,* 283**,** 164-73.

JIANG, B. H. & LIU, L. Z. 2009. PI3K/PTEN signaling in angiogenesis and tumorigenesis. *Adv Cancer Res,* 102**,** 19-65.

JIANG, X., HUANG, F., MARUSYK, A. & SORKIN, A. 2003. Grb2 regulates internalization of EGF receptors through clathrin-coated pits. *Mol Biol Cell,* 14**,** 858-70.

JIN, F., HAGEMANN, N., BROCKMEIER, U., SCHAFER, S. T., ZECHARIAH, A. & HERMANN, D. M. 2013. LDL attenuates VEGF-induced angiogenesis via mechanisms involving VEGFR2 internalization and degradation following endosome-trans-Golgi network trafficking. *Angiogenesis,* 16**,** 625-37.

JONES, M. C., CASWELL, P. T. & NORMAN, J. C. 2006. Endocytic recycling pathways: emerging regulators of cell migration. *Curr Opin Cell Biol,* 18**,** 549-57.

JOPLING, H. M., HOWELL, G. J., GAMPER, N. & PONNAMBALAM, S. 2011. The VEGFR2 receptor tyrosine kinase undergoes constitutive endosome-to-plasma membrane recycling. *Biochem Biophys Res Commun,* 410**,** 170-176.

JOPLING, H. M., ODELL, A. F., HOOPER, N. M., ZACHARY, I. C., WALKER, J. H. & PONNAMBALAM, S. 2009. Rab GTPase Regulation of VEGFR2 Trafficking and Signaling in Endothelial Cells. *Arterioscl Thromb Vasc Biol,* 29**,** 1119-U206.

JOPLING, H. M., ODELL, A. F., PELLET-MANY, C., LATHAM, A. M., FRANKEL, P., SIVAPRASADARAO, A., WALKER, J. H., ZACHARY, I. C. & PONNAMBALAM, S. 2014. Endosome-to-plasma membrane recycling of VEGFR2 receptor tyrosine kinase regulates endothelial function and blood vessel formation. *Cells,* 3**,** 363-85.

JORDENS, I., MARSMAN, M., KUIJL, C. & NEEFJES, J. 2005. Rab proteins, connecting transport and vesicle fusion. *Traffic,* 6**,** 1070-7.

JOUKOV, V., SORSA, T., KUMAR, V., JELTSCH, M., CLAESSON-WELSH, L., CAO, Y., SAKSELA, O., KALKKINEN, N. & ALITALO, K. 1997. Proteolytic processing regulates receptor specificity and activity of VEGF-C. *EMBO J,* 16**,** 3898-911.

KANNO, S., ODA, N., ABE, M., TERAI, Y., ITO, M., SHITARA, K., TABAYASHI, K., SHIBUYA, M. & SATO, Y. 2000. Roles of two VEGF receptors, Flt-1 and KDR, in the signal transduction of VEGF effects in human vascular endothelial cells. *Oncogene,* 19**,** 2138-46.

KAPPERT, K., PETERS, K. G., BOHMER, F. D. & OSTMAN, A. 2005. Tyrosine phosphatases in vessel wall signaling. *Cardiovasc Res,* 65**,** 587-98.

KATO, M., MIYAZAWA, K. & KITAMURA, N. 2000. A deubiquitinating enzyme UBPY interacts with the Src homology 3 domain of Hrs-binding protein via a novel binding motif PX(V/I)(D/N)RXXKP. *J Biol Chem,* 275**,** 37481-7.

KATZ, M., SHTIEGMAN, K., TAL-OR, P., YAKIR, L., MOSESSON, Y., HARARI, D., MACHLUF, Y., ASAO, H., JOVIN, T., SUGAMURA, K. & YARDEN, Y. 2002. Ligand-independent degradation of epidermal growth factor receptor involves receptor ubiquitylation and hgs, an adaptor whose ubiquitin-interacting motif targets ubiquitylation by Nedd4. *Traffic,* 3**,** 740-751.

KAWAMURA, H., LI, X., GOISHI, K., VAN MEETEREN, L. A., JAKOBSSON, L., CEBE-SUAREZ, S., SHIMIZU, A., EDHOLM, D., BALLMER-HOFER, K., KJELLEN, L., KLAGSBRUN, M. & CLAESSON-WELSH, L. 2008. Neuropilin-1 in regulation of VEGF-induced activation of p38MAPK and endothelial cell organization. *Blood,* 112**,** 3638-3649.

KENDALL, R. L. & THOMAS, K. A. 1993. Inhibition of vascular endothelial cell growth factor activity by an endogenously encoded soluble receptor. *Proc Natl Acad Sci U S A,* 90**,** 10705-9.

KENDALL, R. L., WANG, G., DISALVO, J. & THOMAS, K. A. 1994. Specificity of vascular endothelial cell growth factor receptor ligand binding domains. *Biochem Biophys Res Commun,* 201**,** 326-30.

KEYT, B. A., BERLEAU, L. T., NGUYEN, H. V., CHEN, H., HEINSOHN, H., VANDLEN, R. & FERRARA, N. 1996. The carboxyl-terminal domain (111-165) of vascular endothelial growth factor is critical for its mitogenic potency. *J Biol Chem,* 271**,** 7788-95.

KOBAYASHI, S., SAWANO, A., NOJIMA, Y., SHIBUYA, M. & MARU, Y. 2004. The c-Cbl/CD2AP complex regulates VEGF-induced endocytosis and degradation of Flt-1 (VEGFR-1). *FASEB J,* 18**,** 929-31.

KOCH, S. & CLAESSON-WELSH, L. 2012. Signal transduction by vascular endothelial growth factor receptors. *Cold Spring Harb Perspect Med,* 2**,** a006502.

KOCH, S., TUGUES, S., LI, X., GUALANDI, L. & CLAESSON-WELSH, L. 2011. Signal transduction by vascular endothelial growth factor receptors. *Biochem J,* 437**,** 169-183.

KOOMAGI, R., ZINTL, F., SAUERBREY, A. & VOLM, M. 2001. Vascular endothelial growth factor in newly diagnosed and recurrent childhood acute lymphoblastic leukemia as measured by real-time quantitative polymerase chain reaction. *Clin Cancer Res,* 7**,** 3381-4.

KOWANETZ, K., SZYMKIEWICZ, I., HAGLUND, K., KOWANETZ, M., HUSNJAK, K., TAYLOR, J. D., SOUBEYRAN, P., ENGSTROM, U., LADBURY, J. E. & DIKIC, I. 2003a. Identification of a novel proline-arginine motif involved in CIN85-dependent clustering of Cbl and down-regulation of epidermal growth factor receptors. *J Biol Chemistry,* 278**,** 39735-39746.

KOWANETZ, K., TERZIC, J. & DIKIC, I. 2003b. Dab2 links CIN85 with clathrin-mediated receptor internalization. *FEBS Letters,* 554**,** 81-87.

LABRECQUE, L., ROYAL, I., SURPRENANT, D. S., PATTERSON, C., GINGRAS, D. & BELIVEAU, R. 2003. Regulation of vascular endothelial growth factor receptor-2 activity by caveolin-1 and plasma membrane cholesterol. *Mol Biol Cell,* 14**,** 334-347.

LAMALICE, L., HOULE, F. & HUOT, J. 2006. Phosphorylation of Tyr1214 within VEGFR-2 triggers the recruitment of Nck and activation of Fyn leading to SAPK2/p38 activation and endothelial cell migration in response to VEGF. *J Biol Chem,* 281**,** 34009-20.

LAMPUGNANI, M. G. & DEJANA, E. 2007. Adherens junctions in endothelial cells regulate vessel maintenance and angiogenesis. *Thromb Res,* 120 Suppl 2**,** S1-6.

LAMPUGNANI, M. G., ORSENIGO, F., GAGLIANI, M. C., TACCHETTI, C. & DEJANA, E. 2006. Vascular endothelial cadherin controls VEGFR-2 internalization and signaling from intracellular compartments. *J Cell Biol,* 174**,** 593-604.

LANAHAN, A. A., HERMANS, K., CLAES, F., KERLEY-HAMILTON, J. S., ZHUANG, Z. W., GIORDANO, F. J., CARMELIET, P. & SIMONS, M. 2010. VEGF receptor 2 endocytic trafficking regulates arterial morphogenesis. *Dev Cell,* 18**,** 713-24.

LATHAM, A. M., BRUNS, A. F., KANKANALA, J., JOHNSON, A. P., FISHWICK, C. W., HOMER-VANNIASINKAM, S. & PONNAMBALAM, S. 2012. Indolinones and anilinophthalazines differentially target VEGF-A- and basic fibroblast growth factor-mediated responses in primary human endothelial cells. *Br J Pharmacol,* 165**,** 245-59.

LATHAM, A. M., KANKANALA, J., FEARNLEY, G. W., GAGE, M. C., KEARNEY, M. T., HOMER-VANNIASINKAM, S., WHEATCROFT, S. B., FISHWICK, C. W. & PONNAMBALAM, S. 2014. In silico design and biological evaluation of a dual specificity kinase inhibitor targeting cell cycle progression and angiogenesis. *PLoS One,* 9**,** e110997.

LE ROY, C. & WRANA, J. L. 2005. Clathrin- and non-clathrin-mediated endocytic regulation of cell signalling. *Nat Rev Mol Cell Biol,* 6**,** 112-126.

LEE, S., CHEN, T. T., BARBER, C. L., JORDAN, M. C., MURDOCK, J., DESAI, S., FERRARA, N., NAGY, A., ROOS, K. P. & IRUELA-ARISPE, M. L. 2007. Autocrine VEGF signaling is required for vascular homeostasis. *Cell,* 130**,** 691-703.

LEE, T. Y., FOLKMAN, J. & JAVAHERIAN, K. 2010. HSPG-binding peptide corresponding to the exon 6a-encoded domain of VEGF inhibits tumor growth by blocking angiogenesis in murine model. *PLoS One,* 5**,** e9945.

LEOPOLD, J. A., WALKER, J., SCRIBNER, A. W., VOETSCH, B., ZHANG, Y. Y., LOSCALZO, A. J., STANTON, R. C. & LOSCALZO, J. 2003. Glucose-6-phosphate dehydrogenase modulates vascular endothelial growth factor-mediated angiogenesis. *J Biol Chem,* 278**,** 32100-6.

LETERRIER, C., BONNARD, D., CARREL, D., ROSSIER, J. & LENKEI, Z. 2004. Constitutive endocytic cycle of the CB1 cannabinoid receptor. *J Biol Chem,* 279**,** 36013-21.

LEUNG, D. W., CACHIANES, G., KUANG, W. J., GOEDDEL, D. V. & FERRARA, N. 1989. Vascular endothelial growth factor is a secreted angiogenic mitogen. *Science,* 246**,** 1306-9.

LI, H. X. & SETH, A. 2004. An RNF11: Smurf2 complex mediates ubiquitination of the AMSH protein. *Oncogene,* 23**,** 1801-1808.

LI, W., BENGTSON, M. H., ULBRICH, A., MATSUDA, A., REDDY, V. A., ORTH, A., CHANDA, S. K., BATALOV, S. & JOAZEIRO, C. A. P. 2008a. Genome-Wide and Functional Annotation of Human E3 Ubiquitin Ligases Identifies MULAN, a Mitochondrial E3 that Regulates the Organelle's Dynamics and Signaling. *PLoS One,* 3.

LI, X., TJWA, M., VAN HOVE, I., ENHOLM, B., NEVEN, E., PAAVONEN, K., JELTSCH, M., JUAN, T. D., SIEVERS, R. E., CHORIANOPOULOS, E., WADA, H., VANWILDEMEERSCH, M., NOEL, A., FOIDART, J. M., SPRINGER, M. L., VON DEGENFELD, G., DEWERCHIN, M., BLAU, H. M., ALITALO, K., ERIKSSON, U., CARMELIET, P. & MOONS, L. 2008b. Reevaluation of the role of VEGF-B suggests a restricted role in the revascularization of the ischemic myocardium. *Arterioscler Thromb Vasc Biol,* 28**,** 1614-20.

LIN, C. C., MELO, F. A., GHOSH, R., SUEN, K. M., STAGG, L. J., KIRKPATRICK, J., AROLD, S. T., AHMED, Z. & LADBURY, J. E. 2012. Inhibition of basal FGF receptor signaling by dimeric Grb2. *Cell,* 149**,** 1514-24.

LOCASALE, J. W. & CANTLEY, L. C. 2011. Metabolic flux and the regulation of mammalian cell growth. *Cell Metab,* 14**,** 443-51.

LOUKAS, M., CLARKE, P., TUBBS, R. S., KAPOS, T. & TROTZ, M. 2008. The His family and their contributions to cardiology. *Int J Cardiol,* 123**,** 75-8.

LU, Z. & HUNTER, T. 2009. Degradation of Activated Protein Kinases by Ubiquitination. *Annu Rev Biochem.*

LUND, K. A., LAZAR, C. S., CHEN, W. S., WALSH, B. J., WELSH, J. B., HERBST, J. J., WALTON, G. M., ROSENFELD, M. G., GILL, G. N. & WILEY, H. S. 1990. Phosphorylation of the epidermal growth factor receptor at threonine 654 inhibits ligand-induced internalization and down-regulation. *J Biol Chem,* 265**,** 20517-20523.

MAC GABHANN, F. & POPEL, A. S. 2007. Dimerization of VEGF receptors and implications for signal transduction: a computational study. *Biophys Chem,* 128**,** 125-39.

MACDONALD, E., URBE, S. & CLAGUE, M. J. 2014. USP8 controls the trafficking and sorting of lysosomal enzymes. *Traffic,* 15**,** 879-88.

MAGLIONE, D., GUERRIERO, V., VIGLIETTO, G., DELLI-BOVI, P. & PERSICO, M. G. 1991. Isolation of a human placenta cDNA coding for a protein related to the vascular permeability factor. *Proc Natl Acad Sci U S A,* 88**,** 9267-71.

MAGLIONE, D., GUERRIERO, V., VIGLIETTO, G., FERRARO, M. G., APRELIKOVA, O., ALITALO, K., DEL VECCHIO, S., LEI, K. J., CHOU, J. Y. & PERSICO, M. G. 1993. Two alternative mRNAs coding for the angiogenic factor, placenta growth factor (PlGF), are transcribed from a single gene of chromosome 14. *Oncogene,* 8**,** 925-31.

MAGNIFICO, A., ETTENBERG, S., YANG, C. H., MARIANO, J., TIWARI, S., FANG, S. Y., LIPKOWITZ, S. & WEISSMAN, A. M. 2003. WW domain HECT E3s target Cbl RING finger E3s for proteasomal degradation. *J Biol Chem,* 278**,** 43169-43177.

MAHER, E. R., NEUMANN, H. P. & RICHARD, S. 2011. von Hippel-Lindau disease: a clinical and scientific review. *Eur J Hum Genet,* 19**,** 617-23.

MAJMUNDAR, A. J., WONG, W. J. & SIMON, M. C. 2010. Hypoxia-inducible factors and the response to hypoxic stress. *Mol Cell,* 40**,** 294-309.

MAKINEN, K., MANNINEN, H., HEDMAN, M., MATSI, P., MUSSALO, H., ALHAVA, E. & YLA-HERTTUALA, S. 2002. Increased vascularity detected by digital subtraction angiography after VEGF gene transfer to human lower limb artery: a randomized, placebo-controlled, double-blinded phase II study. *Mol Ther,* 6**,** 127-33.

MAKINEN, T., OLOFSSON, B., KARPANEN, T., HELLMAN, U., SOKER, S., KLAGSBRUN, M., ERIKSSON, U. & ALITALO, K. 1999. Differential binding of vascular endothelial growth factor B splice and proteolytic isoforms to neuropilin-1. *J Biol Chem,* 274**,** 21217-22.

MANETTI, M., GUIDUCCI, S., IBBA-MANNESCHI, L. & MATUCCI-CERINIC, M. 2010. Mechanisms in the loss of capillaries in systemic sclerosis: angiogenesis versus vasculogenesis. *J Cell Mol Med,* 14**,** 1241-54.

MANICKAM, V., TIWARI, A., JUNG, J.-J., BHATTACHARYA, R., GOEL, A., MUKHOPADHYAY, D. & CHOUDHURY, A. 2011. Regulation of vascular

endothelial growth factor receptor 2 trafficking and angiogenesis by Golgi localized t-SNARE syntaxin 6. *Blood,* 117**,** 1425-1435.

MARKOWSKA, A. I., JEFFERIES, K. C. & PANJWANI, N. 2011. Galectin-3 protein modulates cell surface expression and activation of vascular endothelial growth factor receptor 2 in human endothelial cells. *J Biol Chem,* 286**,** 29913-21.

MARMOR, M. D. & YARDEN, Y. 2004. Role of protein ubiquitylation in regulating endocytosis of receptor tyrosine kinases. *Oncogene,* 23**,** 2057-2070.

MASTRANDREA, L. D., YOU, J., NILES, E. G. & PICKART, C. M. 1999. E2/E3-mediated assembly of lysine 29-linked polyubiquitin chains. *J Biol Chem,* 274**,** 27299-306.

MATSUMOTO, T., BOHMAN, S., DIXELIUS, J., BERGE, T., DIMBERG, A., MAGNUSSON, P., WANG, L., WIKNER, C., QI, J. H., WERNSTEDT, C., WU, J., BRUHEIM, S., MUGISHIMA, H., MUKHOPADHYAY, D., SPURKLAND, A. & CLAESSON-WELSH, L. 2005. VEGF receptor-2 Y951 signaling and a role for the adapter molecule TSAd in tumor angiogenesis. *EMBO J,* 24**,** 2342-53.

MCCULLOUGH, J., CLAGUE, M. J. & URBE, S. 2004. AMSH is an endosome-associated ubiquitin isopeptidase. *J Cell Biol,* 166**,** 487-492.

MEIJER, I. M. & VAN LEEUWEN, J. E. 2011. ERBB2 is a target for USP8-mediated deubiquitination. *Cell Signal,* 23**,** 458-67.

MENDEL, D. B., LAIRD, A. D., XIN, X., LOUIE, S. G., CHRISTENSEN, J. G., LI, G., SCHRECK, R. E., ABRAMS, T. J., NGAI, T. J., LEE, L. B., MURRAY, L. J., CARVER, J., CHAN, E., MOSS, K. G., HAZNEDAR, J. O., SUKBUNTHERNG, J., BLAKE, R. A., SUN, L., TANG, C., MILLER, T., SHIRAZIAN, S., MCMAHON, G. & CHERRINGTON, J. M. 2003. In vivo antitumor activity of SU11248, a novel tyrosine kinase inhibitor targeting vascular endothelial growth factor and platelet-derived growth factor receptors: determination of a pharmacokinetic/pharmacodynamic relationship. *Clin Cancer Res,* 9**,** 327-37.

MEYER, R. D., MOHAMMADI, M. & RAHIMI, N. 2006. A single amino acid substitution in the activation loop defines the decoy characteristic of VEGFR-1/FLT-1. *J Biol Chem,* 281**,** 867-75.

MEYER, R. D., SRINIVASAN, S., SINGH, A. J., MAHONEY, J. E., GHARAHASSANLOU, K. R. & RAHIMI, N. 2011. PEST Motif Serine and Tyrosine Phosphorylation Controls Vascular Endothelial Growth Factor Receptor 2 Stability and Downregulation. *Mol Cell Biol,* 31**,** 2010-2025.

MIACZYNSKA, M., PELKMANS, L. & ZERIAL, M. 2004. Not just a sink: endosomes in control of signal transduction. *Curr Opin Cell Biol,* 16**,** 400-6.

MILLAUER, B., WIZIGMANN-VOOS, S., SCHNURCH, H., MARTINEZ, R., MOLLER, N. P., RISAU, W. & ULLRICH, A. 1993. High affinity VEGF binding and developmental

expression suggest Flk-1 as a major regulator of vasculogenesis and angiogenesis. *Cell,* 72**,** 835-46.

MITCHELL, H., CHOUDHURY, A., PAGANO, R. E. & LEOF, E. B. 2004. Ligand-dependent and -independent transforming growth factor-beta receptor recycling regulated by clathrin-mediated endocytosis and Rab11. *Mol Biol Cell,* 15**,** 4166-78.

MITTAR, S., ULYATT, C., HOWELL, G. J., BRUNS, A. F., ZACHARY, I., WALKER, J. H. & PONNAMBALAM, S. 2009. VEGFR1 receptor tyrosine kinase localization to the Golgi apparatus is calcium-dependent. *Exp Cell Res,* 315**,** 877-889.

MIZUNO, E., IURA, T., MUKAI, A., YOSHIMORI, T., KITAMURA, N. & KOMADA, M. 2005. Regulation of epidermal growth factor receptor down-regulation by UBPY-mediated deubiquitination at endosomes. *Mol Biol Cell,* 16**,** 5163-5174.

MIZUNO, E., KOBAYASHI, K., YAMAMOTO, A., KITAMURA, N. & KOMADA, M. 2006. A deubiquitinating enzyme UBPY regulates the level of protein ubiquitination on endosomes. *Traffic,* 7**,** 1017-31.

MOHRMANN, K. & VAN DER SLUIJS, P. 1999. Regulation of membrane transport through the endocytic pathway by rabGTPases. *Mol Membr Biol,* 16**,** 81-7.

MONIA, B. P., ECKER, D. J., JONNALAGADDA, S., MARSH, J., GOTLIB, L., BUTT, T. R. & CROOKE, S. T. 1989. Gene synthesis, expression, and processing of human ubiquitin carboxyl extension proteins. *J Biol Chem,* 264**,** 4093-103.

MORIN-BRUREAU, M., RIGAU, V. & LERNER-NATOLI, M. 2012. Why and how to target angiogenesis in focal epilepsies. *Epilepsia,* 53 Suppl 6**,** 64-8.

MUGHAL, N. A., RUSSELL, D. A., PONNAMBALAM, S. & HOMER-VANNIASINKAM, S. 2012. Gene therapy in the treatment of peripheral arterial disease. *Br J Surg,* 99**,** 6-15.

MUKHERJEE, S., TESSEMA, M. & WANDINGER-NESS, A. 2006. Vesicular trafficking of tyrosine kinase receptors and associated proteins in the regulation of signaling and vascular function. *Circ Res,* 98**,** 743-756.

MURDACA, J., TREINS, C., MONTHOUEL-KARTMANN, M. N., PONTIER-BRES, R., KUMAR, S., VAN OBBERGHEN, E. & GIORGETTI-PERALDI, S. 2004. Grb10 prevents Nedd4-mediated vascular endothelial growth factor receptor-2 degradation. *J Biol Chem,* 279**,** 26754-26761.

NAKAGAWA, T. 2007. Uncoupling of the VEGF-endothelial nitric oxide axis in diabetic nephropathy: an explanation for the paradoxical effects of VEGF in renal disease. *Am J Physiol Renal Physiol,* 292**,** F1665-72.

NANES, B. A., CHIASSON-MACKENZIE, C., LOWERY, A. M., ISHIYAMA, N., FAUNDEZ, V., IKURA, M., VINCENT, P. A. & KOWALCZYK, A. P. 2012. p120-

catenin binding masks an endocytic signal conserved in classical cadherins. *J Cell Biol,* 199**,** 365-380.

NILSSON, I., BAHRAM, F., LI, X., GUALANDI, L., KOCH, S., JARVIUS, M., SODERBERG, O., ANISIMOV, A., KHOLOVA, I., PYTOWSKI, B., BALDWIN, M., YLA-HERTTUALA, S., ALITALO, K., KREUGER, J. & CLAESSON-WELSH, L. 2010. VEGF receptor 2/-3 heterodimers detected in situ by proximity ligation on angiogenic sprouts. *EMBO J,* 29**,** 1377-88.

ODELL, A. F., HOLLSTEIN, M., PONNAMBALAM, S. & WALKER, J. H. 2012. A VE-cadherin-PAR3-alpha-catenin complex regulates the Golgi localization and activity of cytosolic phospholipase A(2)alpha in endothelial cells. *Mol Biol Cell,* 23**,** 1783-96.

OKSVOLD, M. P., SKARPEN, E., WIEROD, L., PAULSEN, R. E. & HUITFELDT, H. S. 2001. Re-localization of activated EGF receptor and its signal transducers to multivesicular compartments downstream of early endosomes in response to EGF. *Eur J Cell Biol,* 80**,** 285-94.

OLOFSSON, B., KORPELAINEN, E., PEPPER, M. S., MANDRIOTA, S. J., AASE, K., KUMAR, V., GUNJI, Y., JELTSCH, M. M., SHIBUYA, M., ALITALO, K. & ERIKSSON, U. 1998. Vascular endothelial growth factor B (VEGF-B) binds to VEGF receptor-1 and regulates plasminogen activator activity in endothelial cells. *Proc Natl Acad Sci U S A,* 95**,** 11709-14.

OLOFSSON, B., PAJUSOLA, K., VON EULER, G., CHILOV, D., ALITALO, K. & ERIKSSON, U. 1996. Genomic organization of the mouse and human genes for vascular endothelial growth factor B (VEGF-B) and characterization of a second splice isoform. *J Biol Chem,* 271**,** 19310-7.

OLSSON, A. K., DIMBERG, A., KREUGER, J. & CLAESSON-WELSH, L. 2006. VEGF receptor signalling - in control of vascular function. *Nat Rev Mol Cell Biol,* 7**,** 359-371.

ONAT, D., BRILLON, D., COLOMBO, P. C. & SCHMIDT, A. M. 2011. Human vascular endothelial cells: a model system for studying vascular inflammation in diabetes and atherosclerosis. *Curr Diab Rep,* 11**,** 193-202.

PAESLER, J., GEHRKE, I., POLL-WOLBECK, S. J. & KREUZER, K. A. 2012. Targeting the vascular endothelial growth factor in hematologic malignancies. *Euro J Haemat,* 89**,** 373-84.

PAJUSOLA, K., APRELIKOVA, O., ARMSTRONG, E., MORRIS, S. & ALITALO, K. 1993. Two human FLT4 receptor tyrosine kinase isoforms with distinct carboxy terminal tails are produced by alternative processing of primary transcripts. *Oncogene,* 8**,** 2931-7.

PAJUSOLA, K., APRELIKOVA, O., KORHONEN, J., KAIPAINEN, A., PERTOVAARA, L., ALITALO, R. & ALITALO, K. 1992. FLT4 receptor tyrosine kinase contains seven

immunoglobulin-like loops and is expressed in multiple human tissues and cell lines. *Cancer Res,* 52**,** 5738-43.

PAN, Q., CHATHERY, Y., WU, Y., RATHORE, N., TONG, R. K., PEALE, F., BAGRI, A., TESSIER-LAVIGNE, M., KOCH, A. W. & WATTS, R. J. 2007. Neuropilin-1 binds to VEGF121 and regulates endothelial cell migration and sprouting. *J Biol Chem,* 282**,** 24049-56.

PAN, S., WORLD, C. J., KOVACS, C. J. & BERK, B. C. 2009. Glucose 6-phosphate dehydrogenase is regulated through c-Src-mediated tyrosine phosphorylation in endothelial cells. *Arterioscler Thromb Vasc Biol,* 29**,** 895-901.

PELZER, C., KASSNER, I., MATENTZOGLU, K., SINGH, R. K., WOLLSCHEID, H. P., SCHEFFNER, M., SCHMIDTKE, G. & GROETTRUP, M. 2007. UBE1L2, a novel E1 enzyme specific for ubiquitin. *J Biol Chem,* 282**,** 23010-4.

PERRIN, R. M., KONOPATSKAYA, O., QIU, Y., HARPER, S., BATES, D. O. & CHURCHILL, A. J. 2005. Diabetic retinopathy is associated with a switch in splicing from anti- to pro-angiogenic isoforms of vascular endothelial growth factor. *Diabetologia,* 48**,** 2422-7.

PETRELLI, A., GILESTRO, G. F., LANZARDO, S., COMOGLIO, P. M., MIGONE, N. & GIORDANO, S. 2002. The endophilin-CIN85-Cbl complex mediates ligand-dependent downregulation of c-Met. *Nature,* 416**,** 187-90.

PHNG, L. K., POTENTE, M., LESLIE, J. D., BABBAGE, J., NYQVIST, D., LOBOV, I., ONDR, J. K., RAO, S., LANG, R. A., THURSTON, G. & GERHARDT, H. 2009. Nrarp coordinates endothelial Notch and Wnt signaling to control vessel density in angiogenesis. *Dev Cell,* 16**,** 70-82.

PICKART, C. M. 2001. Mechanisms underlying ubiquitination. *Annu Rev Biochem,* 70**,** 503-533.

PLOUET, J., MORO, F., BERTAGNOLLI, S., COLDEBOEUF, N., MAZARGUIL, H., CLAMENS, S. & BAYARD, F. 1997. Extracellular cleavage of the vascular endothelial growth factor 189-amino acid form by urokinase is required for its mitogenic effect. *J Biol Chem,* 272**,** 13390-6.

POLO, S., SIGISMUND, S., FARETTA, M., GUIDI, M., CAPUA, M. R., BOSSI, G., CHEN, H., DE CAMILLI, P. & DI FIORE, P. P. 2002. A single motif responsible for ubiquitin recognition and monoubiquitination in endocytic proteins. *Nature,* 416**,** 451-455.

PONNAMBALAM, S. & ALBERGHINA, M. 2011. Evolution of the VEGF-Regulated Vascular Network from a Neural Guidance System. *Mol Neurobiol,* 43**,** 192-206.

PONTING, C. P., CAI, Y. D. & BORK, P. 1997. The breast cancer gene product TSG101: A regulator of ubiquitination? *J Mol Med,* 75**,** 467-469.

QUINN, T. P., PETERS, K. G., DEVRIES, C., FERRARA, N. & WILLIAMS, L. T. 1993. Fetal liver kinase-1 is a receptor for vascular endothelial growth-factor and is selectively expressed in vascular endothelium. *Proc Natl Acad Sci U S A,* 90**,** 7533-7537.

RAHIMI, N., GOLDE, T. E. & MEYER, R. D. 2009. Identification of ligand-induced proteolytic cleavage and ectodomain shedding of VEGFR-1/FLT1 in leukemic cancer cells. *Cancer Res,* 69**,** 2607-14.

RAIBORG, C., BACHE, K. G., GILLOOLY, D. J., MADSHUSH, I. H., STANG, E. & STENMARK, H. 2002. Hrs sorts ubiquitinated proteins into clathrin-coated microdomains of early endosomes. *Nat Cell Biol,* 4**,** 394-398.

RAIKWAR, N. S., LIU, K. Z. & THOMAS, C. P. 2013. Protein kinase C regulates FLT1 abundance and stimulates its cleavage in vascular endothelial cells with the release of a soluble PlGF/VEGF antagonist. *Exp Cell Res,* 319**,** 2578-87.

RECHSTEINER, M. & ROGERS, S. W. 1996. PEST sequences and regulation by proteolysis. *Trends Biochem Sci,* 21**,** 267-271.

REICHERT, J. M. 2010. Antibodies to watch in 2010. *MAbs,* 2**,** 84-100.

REIHILL, J. A., EWART, M. A. & SALT, I. P. 2011. The role of AMP-activated protein kinase in the functional effects of vascular endothelial growth factor-A and -B in human aortic endothelial cells. *Vasc Cell,* 3**,** 9.

REILLY, J. F., MIZUKOSHI, E. & MAHER, P. A. 2004. Ligand dependent and independent internalization and nuclear translocation of fibroblast growth factor (FGF) receptor 1. *DNA Cell Biol,* 23**,** 538-48.

RIBATTI, D. & BAIGUERA, S. 2013. Phase II angiogenesis stimulators. *Expert Opin Investig Drugs,* 22**,** 1157-66.

ROBINSON, C. J. & STRINGER, S. E. 2001. The splice variants of vascular endothelial growth factor (VEGF) and their receptors. *J Cell Sci,* 114**,** 853-865.

RODMAN, J. S. & WANDINGER-NESS, A. 2000. Rab GTPases coordinate endocytosis - Commentary. *J Cell Sci,* 113**,** 183-192.

ROOSTERMAN, D., COTTRELL, G. S., SCHMIDLIN, F., STEINHOFF, M. & BUNNETT, N. W. 2004. Recycling and resensitization of the neurokinin 1 receptor. Influence of agonist concentration and Rab GTPases. *J Biol Chem,* 279**,** 30670-9.

ROSKOSKI, R., JR. 2007. Vascular endothelial growth factor (VEGF) signaling in tumor progression. *Crit Rev Oncol Hematol,* 62**,** 179-213.

ROW, P. E., PRIOR, I. A., MCCULLOUGH, J., CLAGUE, M. J. & URBE, S. 2006. The ubiquitin isopeptidase UBPY regulates endosomal ubiquitin dynamics and is essential for receptor down-regulation. *J Biol Chem,* 281**,** 12618-24.

RUAN, G. X. & KAZLAUSKAS, A. 2013. Lactate engages receptor tyrosine kinases Axl, Tie2, and vascular endothelial growth factor receptor 2 to activate phosphoinositide 3-kinase/Akt and promote angiogenesis. *J Biol Chem,* 288**,** 21161-72.

RUBIN, C., GUR, G. & YARDEN, Y. 2005. Negative regulation of receptor tyrosine kinases: unexpected links to c-Cbl and receptor ubiquitylation. *Cell Res,* 15**,** 66-71.

RUBIN, C., LITVAK, V., MEDVEDOVSKY, H., ZWANG, Y., LEV, S. & YARDEN, Y. 2003. Sprouty fine-tunes EGF signaling through interlinked positive and negative feedback loops. *Curr Biol,* 13**,** 297-307.

RUIZ DE ALMODOVAR, C., LAMBRECHTS, D., MAZZONE, M. & CARMELIET, P. 2009. Role and therapeutic potential of VEGF in the nervous system. *Physiol Rev,* 89**,** 607-48.

SAHARINEN, P., EKLUND, L., MIETTINEN, J., WIRKKALA, R., ANISIMOV, A., WINDERLICH, M., NOTTEBAUM, A., VESTWEBER, D., DEUTSCH, U., KOH, G. Y., OLSEN, B. R. & ALITALO, K. 2008. Angiopoietins assemble distinct Tie2 signalling complexes in endothelial cell-cell and cell-matrix contacts. *Nat Cell Biol,* 10**,** 527-37.

SANDILANDS, E., CANS, C., FINCHAM, V. J., BRUNTON, V. G., MELLOR, H., PRENDERGAST, G. C., NORMAN, J. C., SUPERTI-FURGA, G. & FRAME, M. C. 2004. RhoB and actin polymerization coordinate Src activation with endosome-mediated delivery to the membrane. *Dev Cell,* 7**,** 855-869.

SANTOS, C. R. & SCHULZE, A. 2012. Lipid metabolism in cancer. *FEBS J,* 279**,** 2610-23.

SANTOS, S. C. & DIAS, S. 2004. Internal and external autocrine VEGF/KDR loops regulate survival of subsets of acute leukemia through distinct signaling pathways. *Blood,* 103**,** 3883-9.

SASSO, F. C., TORELLA, D., CARBONARA, O., ELLISON, G. M., TORELLA, M., SCARDONE, M., MARRA, C., NASTI, R., MARFELLA, R., COZZOLINO, D., INDOLFI, C., COTRUFO, M., TORELLA, R. & SALVATORE, T. 2005. Increased vascular endothelial growth factor expression but impaired vascular endothelial growth factor receptor signaling in the myocardium of type 2 diabetic patients with chronic coronary heart disease. *J Am Coll Cardiol,* 46**,** 827-34.

SAWAMIPHAK, S., SEIDEL, S., ESSMANN, C. L., WILKINSON, G. A., PITULESCU, M. E., ACKER, T. & ACKER-PALMER, A. 2010. Ephrin-B2 regulates VEGFR2 function in developmental and tumour angiogenesis. *Nature,* 465**,** 487-U115.

SCHMIDT, M. H. H., DIKIC, I. & BOGLER, O. 2005. Src phosphorylation of Alix/AIP1 modulates its interaction with binding partners and antagonizes its activities. *J Biol Chem,* 280**,** 3414-3425.

SCHMIDT, M. H. H., HOELLER, D., YU, J. H., FURNARI, F. B., CAVENEE, W. K., DIKIC, I. & BOGLER, O. 2004. Alix/AIP1 antagonizes epidermal growth factor receptor downregulation by the Cbl-SETA/CIN85 complex. *Mol Cell Biol,* 24**,** 8981-8993.

SENNINO, B. & MCDONALD, D. M. 2012. Controlling escape from angiogenesis inhibitors. *Nat Rev Cancer,* 12**,** 699-709.

SHAIK, S., NUCERA, C., INUZUKA, H., GAO, D., GARNAAS, M., FRECHETTE, G., HARRIS, L., WAN, L., FUKUSHIMA, H., HUSAIN, A., NOSE, V., FADDA, G., SADOW, P. M., GOESSLING, W., NORTH, T., LAWLER, J. & WEI, W. 2012. SCF(beta-TRCP) suppresses angiogenesis and thyroid cancer cell migration by promoting ubiquitination and destruction of VEGF receptor 2. *J Exp Med,* 209**,** 1289-307.

SHALABY, F., ROSSANT, J., YAMAGUCHI, T. P., GERTSENSTEIN, M., WU, X. F., BREITMAN, M. L. & SCHUH, A. C. 1995. Failure of blood-island formation and vasculogenesis in Flk-1-deficient mice. *Nature,* 376**,** 62-6.

SHARMA, K., SHARMA, N. K. & ANAND, A. 2014. Why AMD is a disease of ageing and not of development: mechanisms and insights. *Front Aging Neurosci,* 6**,** 151.

SHIBUYA, M. 2001. Structure and function of VEGF/VEGF-receptor system involved in angiogenesis. *Cell Struct Func,* 26**,** 25-35.

SHIBUYA, M. 2006. Vascular endothelial growth factor receptor-1 (VEGFR-1/Flt-1): a dual regulator for angiogenesis. *Angiogenesis,* 9**,** 225-30; discussion 231.

SHIBUYA, M. 2010. Tyrosine Kinase Receptor Flt/VEGFR Family: Its Characterization Related to Angiogenesis and Cancer. *Genes Cancer,* 1**,** 1119-23.

SHIBUYA, M. 2014. VEGF-VEGFR Signals in Health and Disease. *Biomol Ther,* 22**,** 1-9.

SHIH, S. C., PRAG, G., FRANCIS, S. A., SUTANTO, M. A., HURLEY, J. H. & HICKE, L. 2003. A ubiquitin-binding motif required for intramolecular monoubiquitylation, the CUE domain. *EMBO J,* 22**,** 1273-1281.

SIGISMUND, S., ALGISI, V., NAPPO, G., CONTE, A., PASCOLUTTI, R., CUOMO, A., BONALDI, T., ARGENZIO, E., VERHOEF, L. G., MASPERO, E., BIANCHI, F., CAPUANI, F., CILIBERTO, A., POLO, S. & DI FIORE, P. P. 2013. Threshold-controlled ubiquitination of the EGFR directs receptor fate. *EMBO J,* 32**,** 2140-57.

SIGISMUND, S., WOELK, T., PURI, C., MASPERO, E., TACCHETTI, C., TRANSIDICO, P., DI FIORE, P. P. & POLO, S. 2005. Clathrin-independent endocytosis of ubiquitinated cargos. *Proc Natl Acad Sci U S A,* 102**,** 2760-2765.

SIMONS, M. 2005a. Angiogenesis, arteriogenesis, and diabetes: paradigm reassessed? *J Am Coll Cardiol,* 46**,** 835-7.

SIMONS, M. 2005b. Angiogenesis: where do we stand now? *Circulation,* 111**,** 1556-66.

SINGH, A. J., MEYER, R. D., BAND, H. & RAHIMI, N. 2005. The carboxyl terminus of VEGFR-2 is required for PKC-mediated down-regulation. *Mol Biol Cell,* 16**,** 2106-2118.

SINGH, A. J., MEYER, R. D., NAVRUZBEKOV, G., SHELKE, R., DUAN, L., BAND, H., LEEMAN, S. E. & RAHIMI, N. 2007. A critical role for the E3-ligase activity of c-CbI in VEGFR-2-mediated PLC gamma 1 activation and angiogenesis. *Proc Natl Acad Sci U S A,* 104**,** 5413-5418.

SMITH, G. A., FEARNLEY, G. W., ZANI, I. A., WHEATCROFT, S. B., TOMLINSON, D. C., HARRISON, M. A. & PONNAMBALAM, S. 2015. VEGFR2 trafficking, signaling and proteolysis is regulated by the ubiquitin isopeptidase USP8. *Traffic*.

SORKIN, A., KROLENKO, S., KUDRJAVTCEVA, N., LAZEBNIK, J., TESLENKO, L., SODERQUIST, A. M. & NIKOLSKY, N. 1991. Recycling of epidermal growth factor-receptor complexes in A431 cells: identification of dual pathways. *J Cell Biol,* 112**,** 55-63.

SORKIN, A., MCCLURE, M., HUANG, F. & CARTER, R. 2000. Interaction of EGF receptor and grb2 in living cells visualized by fluorescence resonance energy transfer (FRET) microscopy. *Curr Biol,* 10**,** 1395-8.

SORKIN, A. & VON ZASTROW, M. 2002. Signal transduction and endocytosis: close encounters of many kinds. *Nat Rev Mol Cell Biol,* 3**,** 600-14.

SOUBEYRAN, P., KOWANETZ, K., SZYMKIEWICZ, I., LANGDON, W. Y. & DIKIC, I. 2002. Cbl-CIN85-endophilin complex mediates ligand-induced downregulation of EGF receptors. *Nature,* 416**,** 183-187.

SRINIVASAN, S., MEYER, R. D., LUGO, R. & RAHIMI, N. 2013. Identification of PDCL3 as a novel chaperone protein involved in the generation of functional VEGF receptor 2. *J Biol Chem,* 288**,** 23171-81.

STACKER, S. A., STENVERS, K., CAESAR, C., VITALI, A., DOMAGALA, T., NICE, E., ROUFAIL, S., SIMPSON, R. J., MORITZ, R., KARPANEN, T., ALITALO, K. & ACHEN, M. G. 1999. Biosynthesis of vascular endothelial growth factor-D involves proteolytic processing which generates non-covalent homodimers. *J Biol Chem,* 274**,** 32127-36.

STENMARK, H. & OLKKONEN, V. M. 2001. The Rab GTPase family. *Genome Biol,* 2**,** 3007.

STERN, K. A., PLACE, T. L. & LILL, N. L. 2008. EGF and amphiregulin differentially regulate Cbl recruitment to endosomes and EGF receptor fate. *Biochem J,* 410**,** 585-594.

STERN, K. A., SMIT, G. D. V., PLACE, T. L., WINISTORFER, S., PIPER, R. C. & LILL, N. L. 2007. Epidermal growth factor receptor fate is controlled by Hrs tyrosine phosphorylation sites that regulate Hrs degradation. *Mol Cell Biol,* 27**,** 888-898.

STUTTFELD, E. & BALLMER-HOFER, K. 2009. Structure and function of VEGF receptors. *IUBMB Life,* 61**,** 915-22.

SUGAYA, K., ISHIHARA, Y. & INOUE, S. 2015. Analysis of a temperature-sensitive mutation in Uba1: Effects of the click reaction on subsequent immunolabeling of proteins involved in DNA replication. *FEBS Open Bio,* 5**,** 167-74.

SUN, Z., LI, X., MASSENA, S., KUTSCHERA, S., PADHAN, N., GUALANDI, L., SUNDVOLD-GJERSTAD, V., GUSTAFSSON, K., CHOY, W. W., ZANG, G., QUACH, M., JANSSON, L., PHILLIPSON, M., ABID, M. R., SPURKLAND, A. & CLAESSON-WELSH, L. 2012. VEGFR2 induces c-Src signaling and vascular permeability in vivo via the adaptor protein TSAd. *J Exp Med,* 209**,** 1363-1377.

TAKAHASHI, H. & SHIBUYA, M. 2005. The vascular endothelial growth factor (VEGF)/VEGF receptor system and its role under physiological and pathological conditions. *Clin Sci,* 109**,** 227-41.

TAKAHASHI, T. & SHIBUYA, M. 1997. The 230 kDa mature form of KDR/Flk-1 (VEGF receptor-2) activates the PLC-gamma pathway and partially induces mitotic signals in NIH3T3 fibroblasts. *Oncogene,* 14**,** 2079-89.

TAKAHASHI, T., YAMAGUCHI, S., CHIDA, K. & SHIBUYA, M. 2001. A single autophosphorylation site on KDR/Flk-1 is essential for VEGF-A-dependent activation of PLC-gamma and DNA synthesis in vascular endothelial cells. *EMBO J,* 20**,** 2768-78.

TAKAYAMA, Y., MAY, P., ANDERSON, R. G. W. & HERZ, J. 2005. Low density lipoprotein receptor-related protein 1 (LRP1) controls endocytosis and c-CBL-mediated ubiquitination of the platelet-derived growth factor receptor beta (PDGFR beta). *J Biol Chem,* 280**,** 18504-18510.

TAMMALI, R., REDDY, A. B., SRIVASTAVA, S. K. & RAMANA, K. V. 2011. Inhibition of aldose reductase prevents angiogenesis in vitro and in vivo. *Angiogenesis,* 14**,** 209-21.

TAN, X., THAPA, N., SUN, Y. & ANDERSON, R. A. 2015. A kinase-independent role for EGF receptor in autophagy initiation. *Cell,* 160**,** 145-60.

TANAKA, N. 1999. Possible Involvement of a Novel STAM-associated Molecule "AMSH" in Intracellular Signal Transduction Mediated by Cytokines. *J Biol Chem,* 274**,** 19129-19135.

TANG, W. H., MARTIN, K. A. & HWA, J. 2012. Aldose reductase, oxidative stress, and diabetic mellitus. *Front Pharmacol,* 3**,** 87.

TANOWITZ, M. & VON ZASTROW, M. 2002. Ubiquitination-independent trafficking of G protein-coupled receptors to lysosomes. *J Biol Chem,* 277**,** 50219-22.

TARALLO, V. & DE FALCO, S. 2015. The vascular endothelial growth factors and receptors family: Up to now the only target for anti-angiogenesis therapy. *Int J Biochem Cell Biol,* 64**,** 185-189.

TARALLO, V., VESCI, L., CAPASSO, O., ESPOSITO, M. T., RICCIONI, T., PASTORE, L., ORLANDI, A., PISANO, C. & DE FALCO, S. 2010. A placental growth factor variant unable to recognize vascular endothelial growth factor (VEGF) receptor-1 inhibits VEGF-dependent tumor angiogenesis via heterodimerization. *Cancer Res,* 70**,** 1804-13.

TCHAIKOVSKI, V., FELLBRICH, G. & WALTENBERGER, J. 2008. The molecular basis of VEGFR-1 signal transduction pathways in primary human monocytes. *Arterioscler Thromb Vasc Biol,* 28**,** 322-8.

TCHAIKOVSKI, V., OLIESLAGERS, S., BOHMER, F. D. & WALTENBERGER, J. 2009. Diabetes mellitus activates signal transduction pathways resulting in vascular endothelial growth factor resistance of human monocytes. *Circulation,* 120**,** 150-9.

TIEDE, C., TANG, A. A., DEACON, S. E., MANDAL, U., NETTLESHIP, J. E., OWEN, R. L., GEORGE, S. E., HARRISON, D. J., OWENS, R. J., TOMLINSON, D. C. & MCPHERSON, M. J. 2014. Adhiron: a stable and versatile peptide display scaffold for molecular recognition applications. *Protein Eng Des Sel,* 27**,** 145-55.

TRUJILLO, A., MCGEE, C. & COGLE, C. R. 2012. Angiogenesis in acute myeloid leukemia and opportunities for novel therapies. *J Oncol,* 2012**,** 128608.

TUGUES, S., KOCH, S., GUALANDI, L., LI, X. & CLAESSON-WELSH, L. 2011. Vascular endothelial growth factors and receptors: anti-angiogenic therapy in the treatment of cancer. *Mol Aspects Med,* 32**,** 88-111.

ULYATT, C., WALKER, J. & PONNAMBALAM, S. 2011. Hypoxia differentially regulates VEGFR1 and VEGFR2 levels and alters intracellular signaling and cell migration in endothelial cells. *Biochem Biophys Res Commun,* 404**,** 774-779.

UNGVARI, Z., SONNTAG, W. E. & CSISZAR, A. 2010. Mitochondria and aging in the vascular system. *J Mol Med,* 88**,** 1021-7.

URBE, S., SACHSE, M., ROW, P. E., PREISINGER, C., BARR, F. A., STROUS, G., KLUMPERMAN, J. & CLAGUE, M. J. 2003. The UIM domain of Hrs couples receptor sorting to vesicle formation. *J Cell Sci,* 116**,** 4169-4179.

VAISMAN, N., GOSPODAROWICZ, D. & NEUFELD, G. 1990. Characterization of the receptors for vascular endothelial growth factor. *J Biol Chem,* 265**,** 19461-6.

VAN DELFT, S., SCHUMACHER, C., HAGE, W., VERKLEIJ, A. J. & VAN BERGEN EN HENEGOUWEN, P. M. 1997. Association and colocalization of Eps15 with adaptor protein-2 and clathrin. *J Cell Biol,* 136**,** 811-21.

VAREY, A. H., RENNEL, E. S., QIU, Y., BEVAN, H. S., PERRIN, R. M., RAFFY, S., DIXON, A. R., PARASKEVA, C., ZACCHEO, O., HASSAN, A. B., HARPER, S. J. & BATES, D. O. 2008. VEGF 165 b, an antiangiogenic VEGF-A isoform, binds and inhibits bevacizumab treatment in experimental colorectal carcinoma: balance of pro-

and antiangiogenic VEGF-A isoforms has implications for therapy. *Br J Cancer,* 98**,** 1366-79.

VIEIRA, A. V., LAMAZE, C. & SCHMID, S. L. 1996. Control of EGF receptor signaling by clathrin-mediated endocytosis. *Science,* 274**,** 2086-9.

VINA-VILASECA, A. & SORKIN, A. 2010. Lysine 63-linked polyubiquitination of the dopamine transporter requires WW3 and WW4 domains of Nedd4-2 and UBE2D ubiquitin-conjugating enzymes. *J Biol Chem,* 285**,** 7645-56.

VIZAN, P., SANCHEZ-TENA, S., ALCARRAZ-VIZAN, G., SOLER, M., MESSEGUER, R., PUJOL, M. D., LEE, W. N. & CASCANTE, M. 2009. Characterization of the metabolic changes underlying growth factor angiogenic activation: identification of new potential therapeutic targets. *Carcinogenesis,* 30**,** 946-52.

VON ZASTROW, M. & SORKIN, A. 2007. Signaling on the endocytic pathway. *Curr Opin Cell Biol,* 19**,** 436-45.

WALCZAK, H., IWAI, K. & DIKIC, I. 2012. Generation and physiological roles of linear ubiquitin chains. *BMC Biol,* 10**,** 23.

WALDEN, H., PODGORSKI, M. S. & SCHULMAN, B. A. 2003. Insights into the ubiquitin transfer cascade from the structure of the activating enzyme for NEDD8. *Nature,* 422**,** 330-4.

WALTENBERGER, J. 2009. VEGF resistance as a molecular basis to explain the angiogenesis paradox in diabetes mellitus. *Biochem Soc Trans,* 37**,** 1167-70.

WALTENBERGER, J., CLAESSONWELSH, L., SIEGBAHN, A., SHIBUYA, M. & HELDIN, C. H. 1994. Differential signal-transduction properties of KDR and Flt1, 2 receptors for vascular endothelial growth-factor. *J Biol Chem,* 269**,** 26988-26995.

WANG, F., YAMAUCHI, M., MURAMATSU, M., OSAWA, T., TSUCHIDA, R. & SHIBUYA, M. 2011. RACK1 regulates VEGF/Flt1-mediated cell migration via activation of a PI3K/Akt pathway. *J Biol Chem,* 286**,** 9097-106.

WANG, L., CHEN, L., BENINCOSA, J., FORTNEY, J. & GIBSON, L. F. 2005. VEGF-induced phosphorylation of Bcl-2 influences B lineage leukemic cell response to apoptotic stimuli. *Leukemia,* 19**,** 344-53.

WANG, L., ZENG, H. Y., WANG, P., SOKER, S. & MUKHOPADHYAY, D. 2003. Neuropilin-1-mediated vascular permeability factor/vascular endothelial growth factor-dependent endothelial cell migration. *J Biol Chem,* 278**,** 48848-48860.

WANG, Y., HEILIG, K. O., MINTO, A. W., CHEN, S., XIANG, M., DEAN, D. A., GEIGER, R. C., CHANG, A., PRAVTCHEVA, D. D., SCHLIMME, M., DEB, D. K., WANG, Y. & HEILIG, C. W. 2010a. Nephron-deficient Fvb mice develop rapidly progressive renal failure and heavy albuminuria involving excess glomerular GLUT1 and VEGF. *Lab Invest,* 90**,** 83-97.

WANG, Y., NAKAYAMA, M., PITULESCU, M. E., SCHMIDT, T. S., BOCHENEK, M. L., SAKAKIBARA, A., ADAMS, S., DAVY, A., DEUTSCH, U., LUETHI, U., BARBERIS, A., BENJAMIN, L. E., MAEKINEN, T., NOBES, C. D. & ADAMS, R. H. 2010b. Ephrin-B2 controls VEGF-induced angiogenesis and lymphangiogenesis. *Nature,* 465**,** 483-U108.

WARREN, C. M., ZIYAD, S., BRIOT, A., DER, A. & IRUELA-ARISPE, M. L. 2014. A ligand-independent VEGFR2 signaling pathway limits angiogenic responses in diabetes. *Sci Sig,* 7**,** ra1.

WEI, X., SCHNEIDER, J. G., SHENOUDA, S. M., LEE, A., TOWLER, D. A., CHAKRAVARTHY, M. V., VITA, J. A. & SEMENKOVICH, C. F. 2011. De novo lipogenesis maintains vascular homeostasis through endothelial nitric-oxide synthase (eNOS) palmitoylation. *J Biol Chem,* 286**,** 2933-45.

WEIS, S., CUI, J. H., BARNES, L. & CHERESH, D. 2004. Endothelial barrier disruption by VEGF-mediated Src activity potentiates tumor cell extravasation and metastasis. *J Cell Biol,* 167**,** 223-229.

WERNER, G. S., RICHARTZ, B. M., HEINKE, S., FERRARI, M. & FIGULLA, H. R. 2003. Impaired acute collateral recruitment as a possible mechanism for increased cardiac adverse events in patients with diabetes mellitus. *Eur Heart J,* 24**,** 1134-42.

WIESMANN, C., FUH, G., CHRISTINGER, H. W., EIGENBROT, C., WELLS, J. A. & DE VOS, A. M. 1997. Crystal structure at 1.7 A resolution of VEGF in complex with domain 2 of the Flt-1 receptor. *Cell,* 91**,** 695-704.

WING, S. S. 2003. Deubiquitinating enzymes—the importance of driving in reverse along the ubiquitin–proteasome pathway. *Int J Biochem Cell Biol,* 35**,** 590-605.

WOODMAN, P. G. 2000. Biogenesis of the sorting endosome: the role of Rab5. *Traffic,* 1**,** 695-701.

WU, K., KOVACEV, J. & PAN, Z. Q. 2010. Priming and extending: a UbcH5/Cdc34 E2 handoff mechanism for polyubiquitination on a SCF substrate. *Mol Cell,* 37**,** 784-96.

XU, G. W., ALI, M., WOOD, T. E., WONG, D., MACLEAN, N., WANG, X., GRONDA, M., SKRTIC, M., LI, X., HURREN, R., MAO, X., VENKATESAN, M., BEHESHTI ZAVAREH, R., KETELA, T., REED, J. C., ROSE, D., MOFFAT, J., BATEY, R. A., DHE-PAGANON, S. & SCHIMMER, A. D. 2010. The ubiquitin-activating enzyme E1 as a therapeutic target for the treatment of leukemia and multiple myeloma. *Blood,* 115**,** 2251-9.

XU, W., LUKKARILA, J. L., DA SILVA, S. R., PAIVA, S. L., GUNNING, P. T. & SCHIMMER, A. D. 2013. Targeting the ubiquitin E1 as a novel anti-cancer strategy. *Curr Pharm Des,* 19**,** 3201-9.

YAMADA, K. H., NAKAJIMA, Y., GEYER, M., WARY, K. K., USHIO-FUKAI, M., KOMAROVA, Y. & MALIK, A. B. 2014. KIF13B regulates angiogenesis through Golgi to plasma membrane trafficking of VEGFR2. *J Cell Sci,* 127**,** 4518-30.

YANG, Y., KITAGAKI, J., DAI, R. M., TSAI, Y. C., LORICK, K. L., LUDWIG, R. L., PIERRE, S. A., JENSEN, J. P., DAVYDOV, I. V., OBEROI, P., LI, C. C., KENTEN, J. H., BEUTLER, J. A., VOUSDEN, K. H. & WEISSMAN, A. M. 2007. Inhibitors of ubiquitin-activating enzyme (E1), a new class of potential cancer therapeutics. *Cancer Res,* 67**,** 9472-81.

YEH, W. L., LIN, C. J. & FU, W. M. 2008. Enhancement of glucose transporter expression of brain endothelial cells by vascular endothelial growth factor derived from glioma exposed to hypoxia. *Mol Pharmacol,* 73**,** 170-7.

YU, Y., HULMES, J. D., HERLEY, M. T., WHITNEY, R. G., CRABB, J. W. & SATO, J. D. 2001. Direct identification of a major autophosphorylation site on vascular endothelial growth factor receptor Flt-1 that mediates phosphatidylinositol 3'-kinase binding. *Biochem J,* 358**,** 465-72.

ZACKSENHAUS, E. & SHEININ, R. 1990. Molecular cloning, primary structure and expression of the human X linked A1S9 gene cDNA which complements the ts A1S9 mouse L cell defect in DNA replication. *EMBO J,* 9**,** 2923-9.

ZECCHIN, A., PATTARINI, L., GUTIERREZ, M. I., MANO, M., MAI, A., VALENTE, S., MYERS, M. P., PANTANO, S. & GIACCA, M. 2014. Reversible acetylation regulates vascular endothelial growth factor receptor-2 activity. *J Mol Cell Biol,* 6**,** 116-27.

ZEIHER, A. M., DREXLER, H., SAURBIER, B. & JUST, H. 1993. Endothelium-mediated coronary blood flow modulation in humans. Effects of age, atherosclerosis, hypercholesterolemia, and hypertension. *J Clin Invest,* 92**,** 652-62.

ZHANG, L., ZHOU, F., HAN, W., SHEN, B., LUO, J., SHIBUYA, M. & HE, Y. 2010. VEGFR-3 ligand-binding and kinase activity are required for lymphangiogenesis but not for angiogenesis. *Cell Res,* 20**,** 1319-31.

ZHANG, S., CAO, Z., TIAN, H., SHEN, G., MA, Y., XIE, H., LIU, Y., ZHAO, C., DENG, S., YANG, Y., ZHENG, R., LI, W., ZHANG, N., LIU, S., WANG, W., DAI, L., SHI, S., CHENG, L., PAN, Y., FENG, S., ZHAO, X., DENG, H., YANG, S. & WEI, Y. 2011. SKLB1002, a novel potent inhibitor of VEGF receptor 2 signaling, inhibits angiogenesis and tumor growth in vivo. *Clin Cancer Res,* 17**,** 4439-50.

ZHANG, Y., ZHANG, Y., FURUMURA, M., ZHANG, Y., FURUMURA, M. & MORITA, E. 2008. Distinct signaling pathways confer different vascular responses to VEGF 121 and VEGF 165. *Growth Factors,* 26**,** 125-131.

APPENDIX A

PUBLICATIONS & CONFERENCE PROCEEDINGS

A.1. Accepted manuscripts

<u>**Smith GA**</u>, Fearnley GW, Wheatcroft SB, Tomlinson DC, Harrison MA, Ponnambalam S (2015) VEGFR2 signaling, trafficking and proteolysis is regulated by the ubiquitin isopeptidase USP8. *Traffic.* 17(1):53-65.

<u>**Smith GA**</u>, Fearnley GW, Wheatcroft SB, Tomlinson DC, Harrison MA, Ponnambalam S (2015) Vascular endothelial growth factor-mediated cellular responses require co-ordination of signal transduction, trafficking and proteolysis. *BioSci Reports* 35:e00253**.**

Karpov OA, Fearnley GW, <u>**Smith GA**</u>, Kankanala J, McPherson MJ, Tomlinson DC, Harrison MA, Ponnambalam S (2015) Receptor tyrosine kinase structure and function in health and disease. *AIMS Biophys* 2:476-5022.

<u>**Smith GA**</u>, Fearnley GW, Harrison MA, Tomlinson DC, Wheatcroft SB, Ponnambalam S (2015) Vascular endothelial growth factor and receptor function in health, metabolism and disease. *J Inherited Metab Dis* 38:753-763.

Fearnley GW, <u>**Smith GA**</u>, Odell AF, Latham AM, Wheatcroft SB, Harrison MA, Tomlinson DC, Ponnambalam S (2014) VEGF-A-stimulated signalling from endosomes in primary endothelial cells. *Methods Enzymol* 535:265-292.

Fearnley GW, <u>**Smith GA**</u>, Harrison MA, Wheatcroft SB, Tomlinson DC, Ponnambalam S (2013) The biochemistry of new blood vessel formation in health and disease. *OA Biochem* 1:5.

A.2. Manuscripts under revision

<u>**Smith GA**</u>, Fearnley GW, Wheatcroft SB, Tomlinson DC, Harrison MA, Ponnambalam S (2015) Basal VEGFR2 ubiquitination modulates signal transduction and endothelial function. **Under revision.**

<u>**Smith GA**</u>, Phillips C, Howell GJ, Muench SP, Ponnambalam S, Harrison MA (2015) Extracellular and luminal pH regulation by V-ATPase isoform expression and

targeting to the plasma membrane and endosomes. *J Biol Chem.* **Under revision.**

A.3. Manuscripts in preparation

<u>Smith GA</u>, Tiede C, Wilkinson J, Mandal U, Harrison MA, McPherson MJ, Tomlinson DC, Ponnambalam S (2015) Novel artificial binding proteins modulate VEGFR signal transduction and endothelial function. **In preparation.**

<u>Smith GA</u>, Tomlinson DC, Harrison MA, Ponnambalam S (2015) Ubiquitin-mediated regulation of the cellular response to vascular endothelial growth factors. **In preparation.**

<u>Smith GA</u>, Tomlinson DC, Harrison MA, Ponnambalam S (2015) E2 ubiquitin-conjugating enzymes regulate basal VEGFR2 turnover. **In preparation.**

Fearnley GW, Abdul Zani I, Yuldasheva N, **<u>Smith GA</u>**, Mughal NA, Homer-Vanniasinkam S, Tomlinson DC, Harrison, MA, Zachary IC, Kearney MT, Wheatcroft SB, Ponnambalam S (2015) VEGF-A isoform-specific signal transduction is modulated by VEGFR2 endocytosis. **Submitted.**

A.4. Poster presentations

<u>Smith GA</u>, Harrison MA, Tomlinson DC, Ponnambalam S (28-29th Sep 2015) VEGFR2 ubiquitination regulates trafficking, signalling, proteolysis and the endothelial response. *4th BHF Fellows Meeting*, Cambridge, UK. – **1st place poster prize.**

<u>Smith GA</u>, Harrison MA, Tomlinson DC, Ponnambalam S (15-18th Sep 2015) VEGFR2 ubiquitination regulates trafficking, signalling, proteolysis and the endothelial response. 78th *Harden Research Conference*, Winchester, UK.

<u>Smith GA</u>, Harrison MA, Tomlinson DC, Ponnambalam S (12th Sep 2014) VEGFR2 ubiquitination. *North of England Cell Biology Conference*, Leeds, UK.

<u>Smith GA</u>, Harrison MA, Tomlinson DC, Ponnambalam S (9-10th Apr 2014) VEGFR2 ubiquitination. *Postgraduate Symposium*, Leeds, UK.

<u>Smith GA</u>, Harrison MA, Tomlinson DC, Ponnambalam S (6-11th Jul 2014) VEGFR2 ubiquitination. *Gordon Research Conference*, Girona, Spain.

Smith GA, Harrison MA, Tomlinson DC, Ponnambalam S (20-21st Mar 2014) VEGFR2 ubiquitination. *MCRC Conference*, Leeds, UK.

Fearnley GW, **Smith GA**, Harrison MA, Wheatcroft SB, Tomlinson DC, Ponnambalam S (11th Sep 2013) Vascular endothelial growth factor A (VEGF-A) isoforms show differential regulation of the endothelial response. *North of England Cell Biology Conference*, Liverpool, UK.

Fearnley GW, **Smith GA**, Harrison MA, Wheatcroft SB, Tomlinson DC, Ponnambalam S (1-5th Sep 2013) Vascular endothelial growth factor A (VEGF-A) isoforms show differential regulation of the endothelial response. *Harden Research Conference*, Sheffield, UK.

A.5. Oral presentations

Role of ubiquitin-linked regulatory enzymes in signal transduction, trafficking and angiogenesis (7th Sept 2015). *North of England Cell Biology Conference*, York, UK.

VEGFR2 ubiquitination regulates signal transduction, trafficking and angiogenesis (7-8th Jul 2015). *Postgraduate Symposium,* Leeds, UK.

Session Chair:

North of England Cell Biology Conference (11th Sep 2013), Liverpool, UK.